1-1-2012

Design and analysis of a low-profile two-axis solar tracker with hybridized control

Laughlin Barker
Santa Clara University

Criselle Olaes
Santa Clara University

Joseph Valdez
Santa Clara University

Darcy Marumoto
Santa Clara University

SANTA CLARA UNIVERSITY

Department of Mechanical Engineering

Date: June 13, 2012

I HEREBY RECOMMEND THAT THE THESIS PREPARED
UNDER MY SUPERVISION BY:

Laughlin Barker, Criselle Olaes, Darcy Marumoto, and Joseph Valdez

ENTITLED:

Design and Analysis of a Low-Profile Two-axis Solar Tracker with Hybridized Control

BE ACCEPTED IN PARTIAL FULFILLMENT OF THE REQUIREMENTS
FOR THE DEGREE OF

BACHELOR OF SCIENCE
IN
MECHANICAL ENGINEERING

Dr. Hohyun Lee
THESIS ADVISOR

Dr. Drazen Fabris
CHAIRMAN OF MECHANICAL
ENGINEERING DEPARTMENT

Design and Analysis of a Low-Profile Two-axis Solar Tracker with Hybridized Control

By

Laughlin Barker, Criselle Olaes, Darcy Marumoto, and Joseph Valdez

THESIS

Submitted in Partial Fulfillment of the Requirements for the
Bachelor of Science Degree in
Mechanical Engineering in the School of Engineering
Santa Clara University, 2012

Santa Clara, California

Design and Analysis of a Low-Profile Two-axis Solar Tracker with Hybridized Control

Laughlin Barker, Criselle Olaes, Darcy Marumoto, and Joseph Valdez

Department of Mechanical Engineering
Santa Clara University
Santa Clara, California
2012

ABSTRACT

The adoption of solar power technologies throughout the world is increasing rapidly. Solar trackers are a necessary component in Concentrated Solar Power (CSP) applications and have also shown up to 46% per annum energy increase in photovoltaic (PV) panels when compared with fixed mounted panels. To resist wind forces, trackers typically incorporate heavy structural components and reinforced concrete foundations. Thus, the manufacture and installation of trackers is costly due to their size, weight, and careful consideration of geological conditions. This work presents a new solar tracker design for use with concentrating solar power and photovoltaic panels. The tracker is comprised of two coplanar perpendicular linear actuators and one linkage arm that can track the sun in two axes. A hybrid control strategy combines time and location based solar position estimates, with a two-axis misalignment sensor for a robust control strategy. Part cost is lowered by the low profile tracker geometry by allowing lighter structural and actuation components to combat gusty conditions, and installation costs are reduced by the wide footprint of the system, mitigating the need for deep foundations. A tracker prototype is built and tested for functionality and tracking accuracy. Testing shows an average mechanical pointing hysteresis of 0.05°. The tracker is outfitted with a parabolic mirror and blackbody receiving cavity, and in full sun reaches a steady-state temperature of 670 °C.

ACKNOWLEDGMENTS

The authors wish to thank Professor Hohyun Lee, graduate student Matthew Neber, and Professor Timothy Hight for the their technical guidance and support to complete this thesis. Also, Don MacCubbin, Calvin Sellers and Ursula Uys for their extensive aid and help in the machine shop to ensure that our model parts were manufactured accurately, precisely and completed on time. Additionally the EPA P3 Program, Willem and Maria Roelandts and the School of Engineering and the Undergraduate Travel Fund for their financial backing and support in this project. Finally, we would like to thank all of our friends and families for their dedication and support of our education at Santa Clara University.

Contents

List of Tables

List of Figures

List of Acronyms

AC	Alternating Current
ADC	Analog-to-Digital Converter
BJT	Bipolar Junction Transistor
CAD	Computer Aided Design
CSP	Concentrated Solar Power
DC	Direct Current
DNI	Direct Normal Irradiance
DOF	Degree of Freedom
EMF	Electromotive Force
EPA	Environmental Protection Agency
GHG	Greenhouse Gas
IC	Integrated Circuit
IDE	Integrated Development Environment
IO	Input/Output
MOS	MOSFET
MOSFET	Metal-Oxide-Semiconductor Field-Effect Transistor
PCB	Printed Circuit Board
PDS	Product Design Specification
PLC	Programmable Logic Control
PV	Photovoltaics
QFD	Quality Function Deployment
RTC	Real Time Clock

Chapter 1

Introduction

1.1 Background

In the face of global warming, growing social and economic inequality, and increasing energy prices, the need for affordable renewable energy has never been greater. In the developing world, electricity has been identified as "indispensable for certain activities such as lighting, refrigeration, and the running of household appliances, and cannot easily be replaced by other forms of energy" [15]. Access to affordable electricity is therefore critical in the process of human development. Here in the United States, sustainable power generation at the household level frees people from rising energy costs and reduces the reliance on power from conventional fossil fuel generating stations. Diversification of the nation's energy portfolio also has the added benefit of increasing overall energy security and reducing vulnerability to significant disruption of supply by natural or political forces.

At the residential scale, solar power is the most widely used and viable source of renewable energy. Distributed, small scale solar power generation has been proven to be not only technically feasible, but also economically sustainable for long term usage in both developed and developing countries [15]. In general, solar power production can be divided into two primary categories: PV and solar thermal. PV cells directly convert the sun's light energy into electricity, while solar thermal systems concentrate the sun's energy (typically through use of mirrors) to a single focal point where a working fluid is heated to run a mechanical compression cycle to produce electricity.

Although many people use PV panels on their rooftops, their power production is limited when installed at a fixed angle. Maximum energy is produced only when light hits the panel perpendicularly. When the sun is not perpendicular to the panel, power loss is proportional to the cosine of the angle of incidence (the angle formed from between the panel's normal vector and the vector pointing towards the sun). To maximize power production, solar trackers must be used to minimize the angular error throughout the day. Figure 1.1 shows the relationship between solar misalignment and power production for a fixed tilt PV system.

The sun's path in the sky changes over the course of the year, being highest and lowest in the sky during the summer and winter solstices (June 21 and December 21, respectively). Figure 1.2 shows the seasonal variation of the Sun's path. To fully track the Sun throughout the year, a tracking device must be capable of orientation to any degree between the highest and lowest paths.

Trackers can maximize power production for PV systems, but most existing PV systems

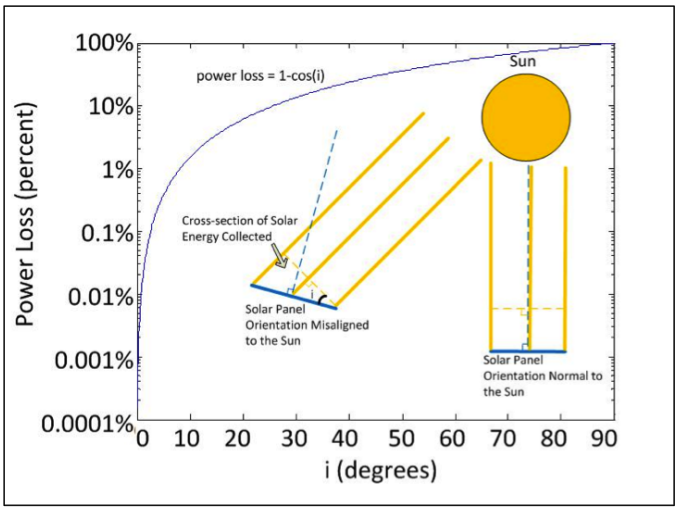

Figure 1.1: Power loss in relation to angle of misalignment.

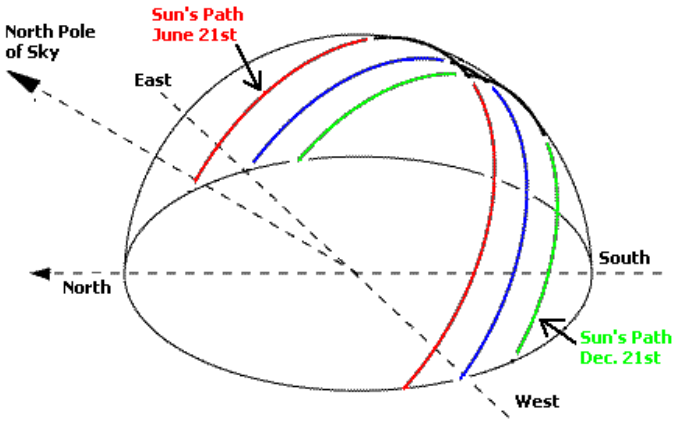

Figure 1.2: The sun appears to move from left to right and up and down above the horizon. This schematic shows the sun's motion for a particular day seen from the Northern Hemisphere [13].

can and most often do function without trackers. In contrast, CSP technologies necessitate the use of solar trackers. To function properly, CSP systems must concentrate the sun's light to a small point to achieve the necessary high temperatures. Directing the concentrated solar light requires that the lens or mirror be moved according to the position of the sun. Also with the use of trackers, care must be taken to avoid shading of adjacent trackers, and spacing needs to be optimized to ensure maximum power density for a given installation area.

One study showed that while tracking solutions can constitute up to 30% of total system cost, great potential exists to develop tracking technologies to reduce these costs [19]. Much of the trackers costs comes from the use of heavy-duty precision components and reinforced concrete foundations; these are believed to be necessary in order to achieve high pointing accuracies of heavy assemblies, while being resistant to wind loads.

Our prototype tracker aims to reduce cost by reducing the need for high precision parts and

concrete foundations. Through the use of a hybridized control system, high accuracy orientation is achieved with relatively low tolerance parts. Additionally, the tracker is built using many off-the-shelf parts, further reducing manufacturing costs.

1.2 Literature Review

Development and production of solar power technologies, especially PV, has increased by 627.26% percent over 10 years from 2000-2010 [11]. The price of PV has gone down drastically, from $10.34 per watt in 2000 to $6.95 per watt in 2010, a 32.79% decrease and as of today it is approximately $5.00 per watt. [11].

The amount of energy collected is based on the angle of incidence, θ, of light, with a higher angle producing less energy. Therefore, the maximum theoretical power gain of a tracking system compared to a that of a fixed system can be easily calculated. By integrating Equation 1.1 below, the total amount of energy produced can be calculated:

$$dW = ISdt \tag{1.1}$$

where dW is instantaneous power, I is constant solar insolation, and S is the effective collector area. The angular velocity of the sun can be assumed to be $\omega = \frac{2\pi}{T} = 7.27x10^{-5}rad/s$, where $T = 24h = 86400s$. When using a solar tracker, S will remain constant throughout the day as the receiving surface maintains its orthogonality to the sun. In the case of a fixed system however, the effective area is given by

$$S = S_0 \cos(\theta) \tag{1.2}$$

with S_0 being the surface area and θ the angle between the panels normal vector and the sun at any given time. By combining Equations 1.1 and 1.2 and integrating over the course of a day, the power generated by a fixed-tilt system can be estimated. Assuming a constant S (i.e. when used in concert with a tracking system) and integrated over the same period, a result is the production of 57% more energy. In reality insolation is not constant, and there are other compounding factors, but through these simplifying assumptions, it can be assumed that 57% is the upper bound for solar tracking energy gains.

Helwa et al studied the solar energy captured by different solar tracking systems. A fixed system with a 40° tilt angle, a one-axis tracker with a 33° tilt angle, a one-axis tracker with 6° tilt angle, and a dual-axis tracker were used in the experiments. The comparison curves amount the different systems showed an increase in annual radiation gain from the dual-axis, one-axis 33° tilt angle and one-axis 6° tilt angle of 30%, 18% and 11%, respectively [14]. Another study found that PV systems can generate up to 46% more energy using solar trackers than with fixed single systems [20].

Common characteristics of tracking systems (single or dual-axis) include: a single column

structure, open loop control, one or two moving motors, light sensing device, and an azimuth angle adjustment [18]. In analyzing existing solar tracking system designs, we have evaluated these characteristics based on their functionality and use. Structures that contain a single column produce a smaller sweep volume but require a stronger concrete foundation for support. As for the control mechanism, open loop control moves the tracker based on knowing the positions of the sun according to the latitude, longitude, date and time, while closed loop control moves the tracker based on sensory input. Each control strategy has its pros and cons. For instance, open loop control may not produce the desired accuracy and repeatability due to the the degradation of parts and installation misalignments. For solely closed loop control, the tracker may not function properly if the light intensity isn't strong enough. However if both are paired together, the flaws of one method can be corrected or compensated by the other.

The methods for changing the orientation of the system are classified as either passive or active tracking. Passive solar trackers rely on thermal expansion of a matter (usually Freon) or on shape memory alloys to provide actuation. One passive solar tracker designed by Clifford, which uses bimetallic strips to provide actuation, has the potential to increase solar panel efficiency by 23% [16]. Active trackers can be classified as microprocessors or other electronics to control positioning actuators. They can be based on either open or closed loop control strategies. Abdallah designed and constructed a 2-axis, open loop, programmable logic control (PLC controlled) sun-tracking system that showed an increase in total daily collection of about 43% [14]. He also found that the power consumption to drive motors and control systems was about 3% of daily power gained, making tracking system a viable solution.

1.3 Project Objectives

The objective of this project was to develop a prototype 2-axis tracking system for use with solar power generation systems. Motivations behind the design included:

- Reduced forces on critical members allowing for use of less robust and less expensive parts
- Base/mounting geometry capable of being installed without a concrete foundation
- Implementation of a control strategy to correct for tolerance buildup and installation misalignments

The prototype tracker was developed for use with a Brayton Cycle solar thermal generation system currently being developed by Dr. Hohyun Lee and graduate student, Matthew Neber. The tracker is a fully functional proof of concept and has been integrated with a parabolic mirror and prototype receiver used in the initial development of the Brayton Cycle receiver.

A full PDS can be found in Appendix F.3, but to be competitive with existing solar trackers, the following was set as design requirements:

- tracking accuracy of +/- 0.5°

- tracking power consumption of 20-40 Wh/day
- azimuthal rotation angle of +/- 90°
- elevation tilt angle 0-90°
- redundant and fail-safe control algorithm

Chapter 2

System-Level

2.1 System-Level Overview

The solar tracker prototype can be divided into three subsystems: the mechanical, electrical, and control. The mechanical system consists of the structural components that support the tracker and provide a means of actuation. This system dictates the range of the tracker and was designed to resist wind loading. The electrical system is comprised of the wiring and electronics used in controlling the tracker. Finally, the control system is defined as the microprocessor and source code that control the tracker.

The mechanical subsystem pictured in Figure 2.1 consists of the structure itself. From the base upwards, the structure consists of a flat wooden base, which will act as the mounting plane for the tracker whether it be the ground or rooftop. Mounted on the base are two linear actuators placed in a T-shaped configuration for dual-axis tracking and for distribution of the loads both statically and under wind loading. Attached to each linear actuator are shuttles which rotate about the lead screw in order to move the mounts to the proper location. These control the position of the tracker in order to obtain the proper orientation to the sun. Lastly, the parabolic dish or PV panel holder is mounted atop the linear actuator shuttles via linkages and an arm bar.

Figure 2.1: The items in the mechanical subsystem are circled in yellow

The electrical subsystem, circled in Figure 2.2, consists of a DC power supply, electrical

wiring to connect all the sensors and accompanying circuitry, limit switches, motors, and power switching electronics. All of the system wiring converges at the control box shown in Figure 2.3.

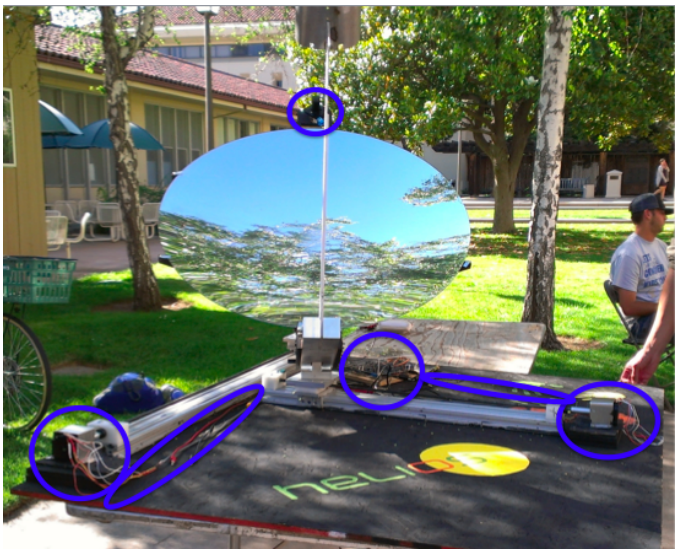

Figure 2.2: The items in the electrical subsystem are circled in blue

The control subsystem consists of the microcontroller and control code that are housed within the box circled in Figure 2.3. The control system ensures proper orientation of the tracker, and combines both open and closed loop control strategies. It is responsible for interpreting all the relevant input signals and commanding the motors in the appropriate manner.

Figure 2.3: The items in the control subsystem are circled in red

2.2 Customer Needs

To better understand the needs and desires of the end user, interviews were conducted with three different people. Joe Sugg is the Assistant Vice President of University Operations at Santa Clara University and recently oversaw the purchase a 1MW fixed-tilt PV array. Mark Freeman and Carlos Garcia are solar contractors that work in the industry. The results of those interviews are summarized in Table 2.1. The questions asked during the interview can be seen in the Appendix G.1 and their interpreted need can been seen in Appendix G.2.

Customer	Requirement	Importance
Joe Sugg	Price of the product is too expensive	High
	Reduce the amount of maintenance	High
	Interactive with end user	Medium
	Minimal monitoring from the end user	High
Mark Freeman	Meet government standards	High
	Product needs to be scalable to open the market, starting at the residential market	High
	Conversion of energy into electricity causes installation problems	Medium
	High price of system mainly due to high shipping costs	High
Carlos	Reduce the cost of expensive and permanent foundations	High
	Higher wind tolerances	High

Table 2.1: Summary of the needs of trackers coming from a range of customers from the end user to solar contractors to manufacturers.

Not surprisingly, affordability and ease of maintenance are of utmost importance to all parties. As a result, it is important to look at current designs and determine the main issues with solar trackers on the market in order to improve upon current designs. The main aspects that needed to be improved include: sweep volume, cost, reliability, and efficiency.

Interviews with solar contractors and manufacturing firms shed light on the elements that contribute to tracker cost. Their comments further corroborated the information presented in Kolb's heliostat reduction study [19]. Namely the cost of the tracker increases with weight, shipping costs (function of size and weight), extent of concrete foundation, and the amount of training needed to install the product.

From the interviews, we determined the essential needs of the customer and the relative importance of needs.

- Increase overall performance of the system
- Total price of the system
- Low operational power consumption

- Ability to handle adverse weather conditions
- Low maintenance and user friendly

The relative importance of needs for the product were considered as follows during the design process to ensure that the product produced would satisfy customer desires.

Design specifications of the tracker (shown in Appendix F.3), were based on a current dual axis solar tracker made by PV Trackers.

2.2.1 Commercial

In order for our tracker to be used in a commercial setting, the team needed to determine a way in which the tracker could be implemented with multiple panels or dishes. This includes determining the spacing between each unit to ensure the absence of shading issues and how each tracker would be controlled, whether it be collectively or independently.

2.2.2 Residential

In order for our tracker to be used in a residential setting, the team needed to determine the ideal location for the tracker to be implemented based on the limited area of the user and possible shading structures while meeting all of the other requirements.

2.3 User Scenario

The solar tracker designed is targeted for residential consumers in order to increase the power production of their current or future solar power generation system. The system will be easily implemented, negating the need for professional installation. Also, the system will be interactive to some degree by enabling the user to easily understand how the tracker is moving to follow the path of the sun and can determine how much power is being produced and consumed by the product through an interactive panel display.

2.4 Benchmarking

2.4.1 Current Trackers

Tracking systems have been around since the first megawatt-scale power station in Hisperia, Califorina in 1982. However, despite the push to transition to clean energy and make solar technologies more affordable, especially PV in the price per watt, there has not been significant advancements of tracking technologies at the residential scale. Currently, parts and installation of trackers cost up to 30% of the total system costs. Also, many people are not familiar with trackers and the benefits of their use due to their limited availability.

The trackers on the market today are used mainly in large scale applications. Solar fields are usually located in isolated areas where the mobility of the system is not an issue as it is in residential areas. For example, the latest project that has gone under way is in the Mojave Desert; it plans to power 85,000 homes using concentrated PV. Figure 2.4 depicts what the completed project should look like. These projects use advancing technologies that cannot be used at the residential scale because either the technology is not scalable or is too expensive.

Figure 2.4: The anticipated completed solar project located in the Mojave Desert [8]

2.4.1.1 MecaSolar MS-2 Tracker 10

Figure 2.5: MS-2 dual axis solar tracker for 13 kWp [9]

MecaSolar designs trackers for PV solar fields and has implemented their trackers (single and dual-axis) on every continent for a total of 343 MW installed. Their MS-2 Tracker 10 model has a V-shaped structure that is capable of holding up to 13.16 kWp. However, the tracker sits on a 7.5 m^3 foundation that does not require any excavation. Their design also includes a three phase motor which reduces losses in the wiring. Finally, their design consumes less than 100

kWh/year. Based on the installation and implementation of their design, there is a minimum of a 35% increase in energy production. The MS-2 Tracker 10 is pictured in Figure 2.5 and the data sheet can be seen in Appendix E.1.

2.4.1.2 OPEL Solar SF-20

Figure 2.6: SF-20 tracker used in a solar field [10]

OPEL Solar has developed single and dual-axis tracking systems for use in commercial and solar fields to increase power production up to 40%. The trackers have sold and deployed around the world for ten years and have a relatively easy installation (no welding). Although their system has a high level of accuracy (within +/- 0.1°), the installation requires a two-man team along with a concrete foundation. The SF-20 CPV is pictured in Figure 2.6 and the data sheet can be seen in Appendix E.2.

2.4.1.3 PV Trackers PVT 7.2 DX

PV Trackers mainly implements their solution in the United States and has only designed the PVT model but has made many upgrades. Due to their large basis in the United States, they design their system around power plants as a way to market their product. With their system, the tracker is made stationary through helical piles (done within 5 minutes) or concrete pier footing or pad foundations, which are minimally invasive. Through their design, it is believed that it reduces the cost by 33% and energy production of up to 40% based on site. The PVT 7.2 DX is pictured in Figure 2.7 and the data sheet can be seen in Appendix E.3.

Figure 2.7: PVT 7.2 DX tracker used in a solar field [12]

2.4.2 Benchmark Results

Based on the data collected from existing products on the market and potential in patents (more on patents in Chapter 8), it is evident that solar tracking technology needs improvement in order to be a viable solution at the residential scale. One of the major components of improvement is price. Price has a large effect to whether the consumer uses the technology or disregards it. The large price of trackers mainly comes from the excavation, concrete foundation, and expensive custom manufactured parts. Also, concentrated solar power technologies are more efficient than PV systems, but need trackers in order to produce electricity. Therefore we must improve on the tracking system in order to properly use the technology provided to us.

With the information gathered from current products and the customer needs, the ideal tracker can be designed and constructed. PV Trackers' PVT 7.2 DX is most similar to the product we wanted to design due to its minimal invasive foundation to support the structure. Also, many of the components are pre-made to ease installation, which allows the end user to possibly install the system if made at the residential scale. Finally, we wanted our design to be scalable, used at the residential or commercial level, which the PV Tracker design can also do (6.5 kW to 7.4 kW). Thus, this tracker will be used as a benchmark comparison to our design. The full comparison can be see in Appendix F.3.

2.5 System Layout

The system as previously mentioned is broken into three subsystems. Each of these systems interact with the others to accurately and precisely follow the sun. Figure 2.8 explains how each system communicates with each other. However, within each subsystem, there are other interactions that go on to translate the message to the other subsystems.

In the mechanical subsystem, the interactions between parts can be seen in Figure 2.9. It

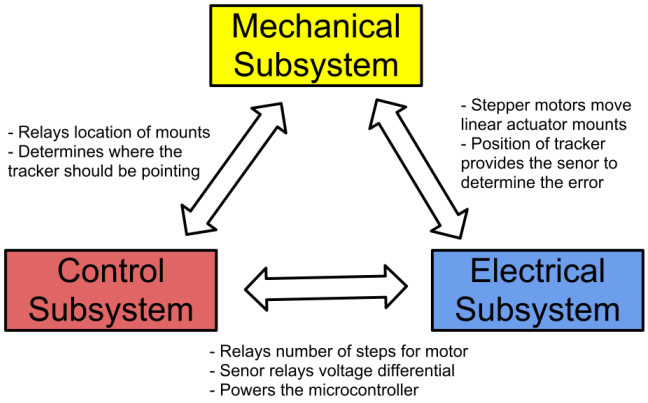

Figure 2.8: How each subsystem interacts with each other, with the inputs of one subsystem as an output from another

takes the outputs from the electrical subsystem to move the linear actuator mounts to its proper location, which places the parabolic dish or panel normal to the sun.

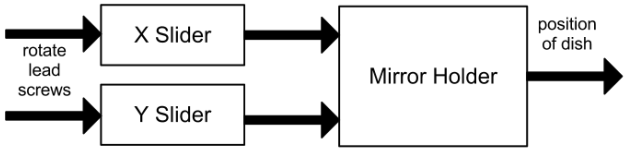

Figure 2.9: Mechanical subsystem interaction between parts

In the control subsystem, the interactions between the code and commands to the stepper motors can be seen in Figure 2.10. It takes the information from the Real Time Clock (RTC), user inputs (location), and the voltage differential, and calculates the most precise positioning of the linear actuator blocks. This is then translated into directing how many steps the motor must take when turning the lead screws for positioning the shuttle mounts.

In the electrical subsystem, the interactions between parts can be seen in Figure 2.11. This subsystem relays information between the mechanical and control subsystem and powers all of the components.

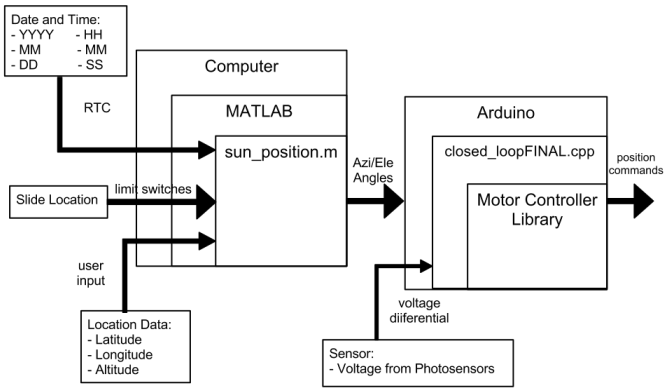

Figure 2.10: Control subsystem interaction between code and motors

2.6 System-Level Issues

2.6.1 System Options and Trade-Offs

In order to optimize the functionality of the tracker, the team needed to analyze the extent to which each feature affects the overall system. Certain design features will create synergies with other features or trade-offs in functionality. After conducting interviews and reviewing current designs and patents, the team created a prioritizing matrix of tracker features (seen in Figure 2.12) and Quality Function Deployment (QFD) (seen in Figure 2.13) based on the needs interpreted from the customers.

The most important feature the team decided on was the range of motion of the system. Without range of motion of the sun for most of the world, this product would be location specific and not have a wide range of benefits. The second most important feature was the sweep volume. With a smaller sweep volume, the system is compact and thus, can increase the power density. However, with a small sweep volume, there are certain design criteria which must be followed. Finally, the last two categories that must be taken into high consideration are cost and actuator force. Although cost was not as high of a priority, many of the design decisions made have synergies or trade-offs with cost. For example, a design with a small sweep volume usually has a trade-off with cost due to the large mast and concrete foundation that must be installed as well as expensive actuators to handle the high force. The team's initial designs and scoring based on the prioritizing matrix can be seen in Appendix F. After reviewing our own designs, we later decided that cost was a much more important factor than sweep volume since residential customers would only buy one system instead of a field of trackers and panels.

Other issues not considered in the prioritizing matrix or QFD that are key to the success of our design are the control system algorithm and actuation strategy. When we considered control algorithms, we discussed whether we should use an open loop or closed loop actuation strategy.

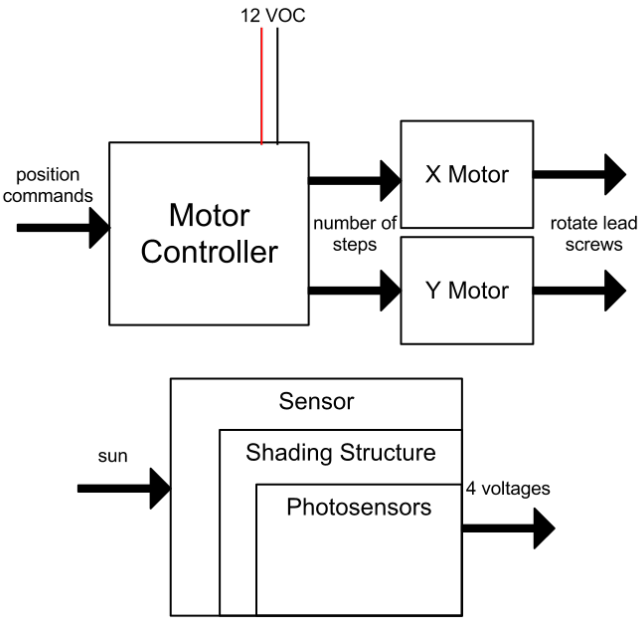

Figure 2.11: Electrical subsystem interaction between parts

An open loop system is easier to implement, but it does not account for any error created as a result of manufacturing tolerance. Thus, we opted to use a hybrid control system, an open loop and closed loop algorithm, which initially places the tracker to the theoretical position of the sun and then corrects itself to the brightest spot in the sky through dynamic feedback. This allowed us to avoid using high precision machined parts, which are expensive and time consuming to obtain. When we considered the type of actuation, we looked at hydraulics, linear actuators, stepper motors, and servo motors. The basis of our decision on the type of motor to use depended on the torque capacity, size, energy consumption, advantages at low speeds, and controllability. Although servo motors are simpler and much easier to use, the advantages of stepper motors matches the application of solar tracking appropriately due to its open loop control and the stability of holding its position when the system is not moving. The decision on the type of actuator also depended on the design of the system, since certain design only allows for one type of actuator.

2.7 Functional Analysis

2.7.1 Mechanical Subsystem

2.7.1.1 Mirror Holder Structure

The mirror holder subsystem, pictured in Figure 2.14, will be attached to the linear actuators in a way that encapsulates the sun's range of motion while keeping the parabolic dish stable.

PRIORITIZING MATRIX

CRITERIA	1	2	3	4	5	6	7	8	9	10	11	12	13	TOTAL	FACTOR
1 COST		0.5	0	1	1	0.5	0							3	3
2 BUILDING	0.5		0	0	0	0	0							0.5	0.5
3 RANGE OF MOTION	1	1		1	1	0.5	1							5.5	5.5
4 MOUNTING HARDWARE	0	1	0		0	0	0.5							1.5	1.5
5 CONTROL ALGORITHM	0	1	0	1		0	0							2	2
6 SWEEP VOLUME	0.5	1	0.5	1	1		1							5	5
7 ACTUATION FORCE	1	1	0	0.5	1	0								3.5	3.5

Figure 2.12: Prioritizing matrix to determine which feature in the design is most important. Each feature is then given a weighting to be used to rank the different ideas the team has.

Row #	Max Relationship Value in Row	Relative Weight	Weight / Importance	Quality Characteristics (a.k.a. "Functional Requirements" or "Hows") / Demanded Quality (a.k.a. "Customer Requirements" or "Whats")	# Machined Part	Actuation Strategy	Ground Mount	Mirror Mount	Tracker Angle Error	Range of Motion
1	9	25.0	8.0	Small Sweep Volume	▲	○	○	◎	▲	▲
2	9	12.5	4.0	Asthetically Pleasing	○	○	◎	◎	▲	▲
3	9	21.9	7.0	Low Cost	◎	◎	○	○	○	▲
4	9	18.8	6.0	Efficient	▲	◎	▲	▲	◎	◎
5	9	21.9	7.0	Reliability	◎	▲	○	○		

Figure 2.13: QFD based on the customer's interpreted needs and functional requirement. A triangle represents a weak relation, an empty circle represents a medium relation, a circle with a dot in the middle represents a strong relation and a blank box represents no relation between the two qualities.

The mirror holder also must house the sensor, which determines the error in the alignment to the sun.

2.7.1.2 Linear Actuators

The linear actuators and the mounts, pictured in Figure 2.15, support the mirror holder structure. The linear actuator mounts also must be able to move with the lead screw in order to to keep the dish oriented normal to the sun. This subsystem executes the commands delivered from the electrical subsystem from the control subsystem to position the dish.

2.7.2 Control Subsystem

2.7.2.1 Open Loop Control

The open loop control is operated by the sun's theoretical position in the sky based on a RTC, which uses the current date, time, latitude and longitude of the user. This subsystem directly

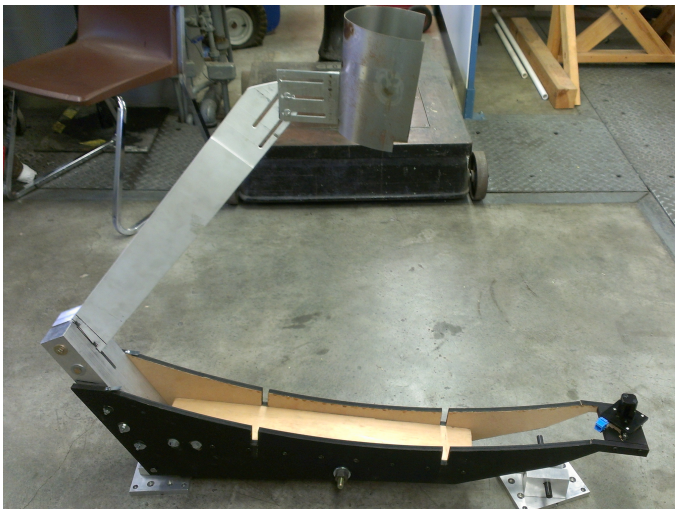

Figure 2.14: Parabolic mirror holder designed in Solidworks

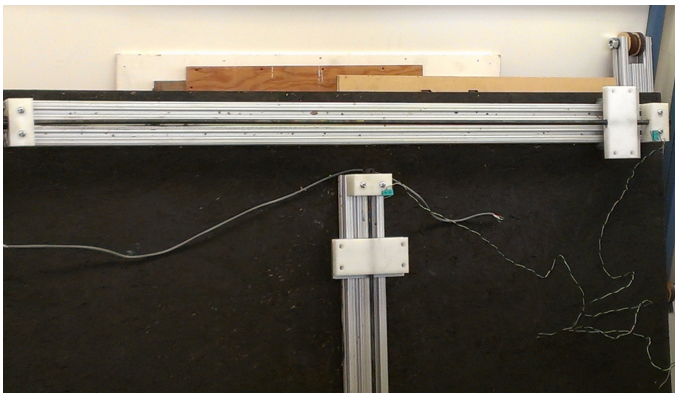

Figure 2.15: Linear actuators created from a lead screw and 80-20 aluminum extrusion

positions the panel or dish to where it predicts the sun to be. The actual position of the tracker and actual position of the sun are only aligned if the system is installed perfectly south and if the parts have not changed over time.

2.7.2.2 Closed Loop Control

Although open loop control seems to precisely orient the panel or dish normal to the sun, this alignment may be within a few degrees off target, in which case closed loop control takes over to ensure that the tracker is aligned normal to the brightest spot. From the error information the sensor gives the controller, the controller will then decide the amount of change in alignment to be made in order to correct the position. This allows the tracker to maintain normal alignment over a long period of time, even as parts degrade or if the installation is not perfect.

2.7.2.3 Stepper Motor Control

Based on the information gathered from open loop and closed loop control, the microcontroller calculates where the two mounts should be placed on the linear actuators to provide proper orientation. However, nothing is done unless the stepper motors receive a signal to move. The controller determines how many rotations each stepper motor must complete to achieve that position and relays that to the stepper motors to change the position of the two mounts.

2.7.3 Electrical Subsystem

2.7.3.1 Power

The power subsystem provides the power necessary for tracking. This involves the circuitry to distribute power to the controller and stepper motors. Because we were not able to attach a solar panel or a turbine on the receiver to use the power produced to track, our team used an external power source.

2.7.3.2 Sensor

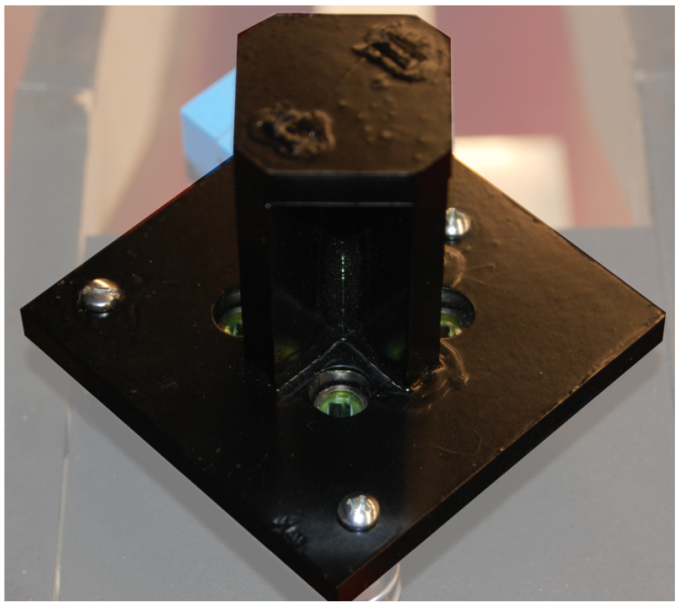

Figure 2.16: Senor to measure voltage differentials to determine the orientation error

The sensor subsystem, pictured in Figure 2.16, allows for real-time error analysis to correct the trackers position relative to the sun. The sensor, housed on the mirror structure, assesses whether the tracker is positioned normal to the sun. This is done through voltage differences determined from solar cells, located in the four compass directions, along with a shading structure. The information gathered is then sent to the controller, which decides whether or not the tracker's position needs to be corrected.

2.7.4 Inputs/Outputs

Each of the subsystems have their own requirements that must be met. However, because many of the subsystems are interlinked, they must work together for the project to succeed from the main inputs it receives. The inputs are the current date, time, latitude, longitude, and the error of the sun based on the sensor. Based on these inputs, the system will output the orientation of the dish or panel normal to the sun or brightest spot and place the tracker.

2.8 Team and Project Management

2.8.1 Project Challenges

There are many challenges and constraints that must be considered when attempting to develop a unique design for an "existing product". Particularly for a solar tracker, these issues range from minimizing the sweep volume, structural support, the design process, budgeting, and time management. In addition to these issues, other challenges arose from balancing course work given throughout the year and an advanced deadline in order to compete in the EPA P3 National Student Design Competition for Sustainability.

The challenges presented involved issues at the system and subsystem level. Although the sun's theoretical position can be determined without knowing the design of the tracker, the progress of the project is determined from the design process. With the chosen design of the tracker, the team could then move on and tackle the challenges at each subsystem level.

2.8.2 Budget

After determining that the proposed project is viable solution, the team estimated the total cost of the prototypes and scaled model to be constructed. From this estimate, the team sought out funding for the project through the the EPA P3 Competition Fund, School of Engineering, the Willem and Maria Roetlands Fund (through the Center of Science and Technology) and the Undergraduate Travel Fund for a total of $9650.00. The team spending and pending orders were placed in a document located on the serve and updated after every purchase to ensure that the team was within budget estimates. After project completion, the team was within budget with about $1,198.79 remaining. More on the budget can be seen in Chapter 7 and a full expense report can be seen in Appendix H.2.

2.8.3 Timeline

The course of this project occurred over the course of the 2011-2012 academic year and concluded with the annual Senior Design Conference. The project began with brainstorming preliminary designs to meet the project's initial objectives of reducing the sweep volume, costs, and distribution of force. From the chosen design, the scaled model of the tracker was manu-

factured and constructed from February to April with testing in April and May. A completed Gantt chart detailing the milestones made can be seen int he Appendix H.1.

2.8.4 Design Process

The design process used to design and construct this solar tracker was modeled after the Engineering Design Process. Since this project is a product that already exists in the market, the team first researched existing solutions and determined areas of improvement. Next, the team brainstormed different solutions that solve the current issues or improved other characteristics and determined whether or not developing another design was both within budget and competitive in the market. From there, the team developed preliminary designs which used the concepts formed from the solutions brainstormed, and a final design was chosen that addressed most of the issues concerning existing solutions on the market today. Based on the final design, a formal analysis was conducted to determine whether it met the project's objectives before construction took place.

2.8.5 Risks and Mitigations

In completing this project in a short period of time, there are many risks involved. The team was not able to assess each design fully and choose or implement a unique feature that may enhance functionality in another design. Thus, although the final product may be operational and novel, it may not be the best product that the team could have produced. Also, based on the scaled model, there may not have been a way to fully test the model other than through computer simulations.

2.8.6 Team Management

Throughout the course of the project design process, there were many issues in regards to time. Thus, the team had decided on a plan of action to take if any critical issues arose to ensure that the problem was dealt with in a timely manner. The team first developed a timeline where major milestones were listed to establish deadlines that needed to be met to have a successful project. Based on the upcoming milestones, work was divided based on the strength of each team member and was advised by the other team members throughout the process. To guarantee that each member was working on the project, the team met on a weekly basis to check the progress and ask for any help on their work. Also all work and resources were stored on a server, allowing each team member to have access to all of the project documents at any time. This helped the team work on different aspects of the project separately in order to make the most effective use of time.

Chapter 3

Mechanical System

3.1 Background

While developing a new and innovative solar tracking solution, the team addressed the issues of typical solar tracking designs. Wind is a major factor when designing a tracking solution because it dictates the strength of the structure holding the solar module. Solar trackers are expensive in part because of installation costs and the need for high strength components to withstand wind loading. Most trackers require construction of a large concrete base that penetrates the ground in order to make the tracker structurally stable. The concrete base reduces the bearing pressure on the soil and resists the tendency for the structure to rotate or lift up from the ground. However, concrete adds a significantly higher construction cost. A new low profile design that effectively reduces wind loading on the base was developed to eliminate the need for expensive high strength components and high installation costs. This low profile design is achieved through two linear actuators configured orthogonal to one another and on the same plane. The geometry of the dual axis tracking is described in section 3.2.1.

3.2 Subsystem Requirements

The development of the mechanical system involved designing around its ability to track the Sun, withstand high wind loads, and achieve high accuracy and precision with the design's actuation method. The position of the Sun can described in azimuth and elevation coordinates, where the azimuth angle, θ, describes the horizon angle from south and the elevation angle, ϕ, describes how high from the horizon the sun is. In order for the tracker to be effective, it must be able to track the sun when it is highest and lowest in the sky. These days are on June 21 (summer solstice) and December 21 (winter solstice), with the Sun's elevation varying depending on the location on the Earth. Several design considerations were developed to obtain the largest tracking range possible. The structure was also designed to reduce forces on critical parts by spreading out the load through two points of connection. This greatly reduces the cost of the linear actuators, allowing for less robust actuators to withstand the weight of the solar module and other external forces such as wind loads. The issue of friction between moving parts and joints was also addressed in order to reduce the torque requirements in the motors.

3.2.1 Range of Motion

The dual-axis movement is achieved through the positioning of the slides on the linear actuators. On the top of each slide is a rotating mechanism where the linkages are attached. By moving the slides along the actuators, the clevis mount mechanism rotates accordingly and the dish orientation is adjusted based on the desired azimuth and elevation angles. In Figure 3.1, the geometry of the yellow and red triangles determine where the slides need to be positioned in order to orient the dish to the proper azimuth and elevation angles. Equations 3.1 and 3.2 can be solved as a system to convert azimuth and elevation angles to corresponding x and y slide locations. Note that Equation 3.2, meaning it will have two solutions. It was found that the additive solution is in fact the correct solution. Derivations of Equations 3.1 and 3.2 can be found in Appendix D.1.

$$x = y \cos\theta \tag{3.1}$$

$$y^2 \sec^2\theta - 2y \sec\theta \cos\phi L_2 + (L_2^2 - L_1^2) = 0 \tag{3.2}$$

The angle θ is referenced off of a line pointing down the length of the y actuator (ideally pointing true south). Thus, if the desired azimuth angle is less than 180°(east of south), x will be positive, and likewise if the desired azimuth is greater than 180°(west of south) the sign of calculated x position must be negated.

With these equations of motion, a tracking range can be formulated based on the lengths of the actuators and lengths of the supports pictured in Figure 3.1. To determine if the tracker's geometry could actually follow the Sun's path, a MATLAB algorithm was created to see what type of azimuth/elevation solutions could be obtained with the particular geometry (see Appendix. The algorithm produced plots shown in Figure 3.2, with the black space representing the azimuth and elevation angle solutions the tracker can obtain with a particular geometry. Depending on the ratio of the linkage lengths L1 and L2, the tracking range can be varied and optimized.

With the low profile design, certain mechanical constraints reduced the range of motion of the tracker. In order to track the Sun at all points across the sky, the y actuator slide would have to cross over the x actuator. This would allow for tracking of the Sun at the beginning and end of the day. A mechanism would have to be designed in order to obtain this extra tracking range. However, constructing a scaled working prototype was made priority before further developing this aspect of the tracker.

3.2.2 Structural Stability

The structural aspect of the solar tracker consists of the clevis mounts, linkages, and a mirror holder. Clevis mounts (see Figure 3.5) were designed to mount a mirror structure to the linear

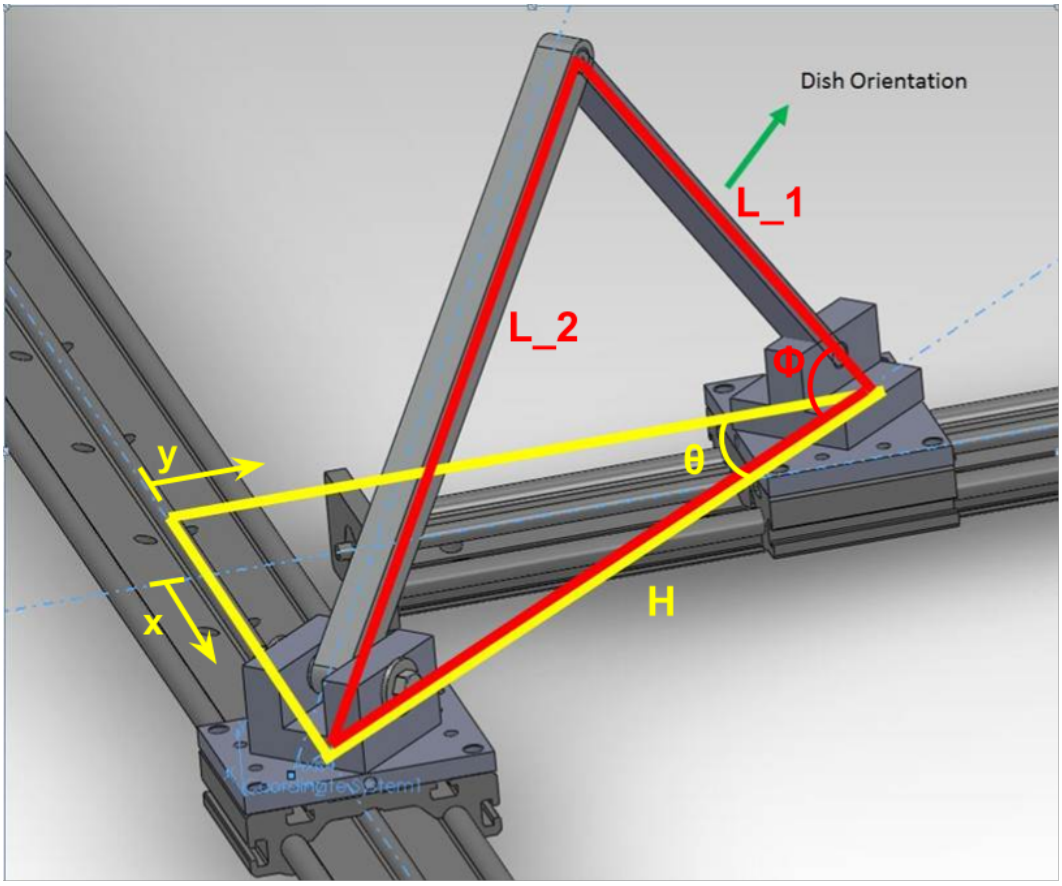

Figure 3.1: Triangles show how the dish is oriented through the geometric relationships of the actuator slides and linkages

actuators. The mounting point on the clevis was designed to sit as low as possible in order to reduce the moment induced on the linear actuator. Rigid clevis mounts and a connecting rod were designed to minimize play in the moving joints while being subject to wind loading. The structure must be able to support the weight of the solar module mounted on the tracker and also withstand high wind loads.

A mirror structure was developed with the purpose of holding a parabolic mirror and solar receiver. It needed to be strong enough to hold the weight of the receiver, which is approximately 14 kg. The weight of the structure must also be as light as possible in order to reduce the amount of energy used by the motors.

3.2.3 Accuracy

The solar tracker must be able to achieve high accuracy and precision when it is commanded to move to a certain position. Accuracy and precision for typical solar trackers on the market can vary depending on the application. Photovoltaics need not be as precise as concentrated solar power systems, because very small degrees of misalignment for PV do not significantly reduce

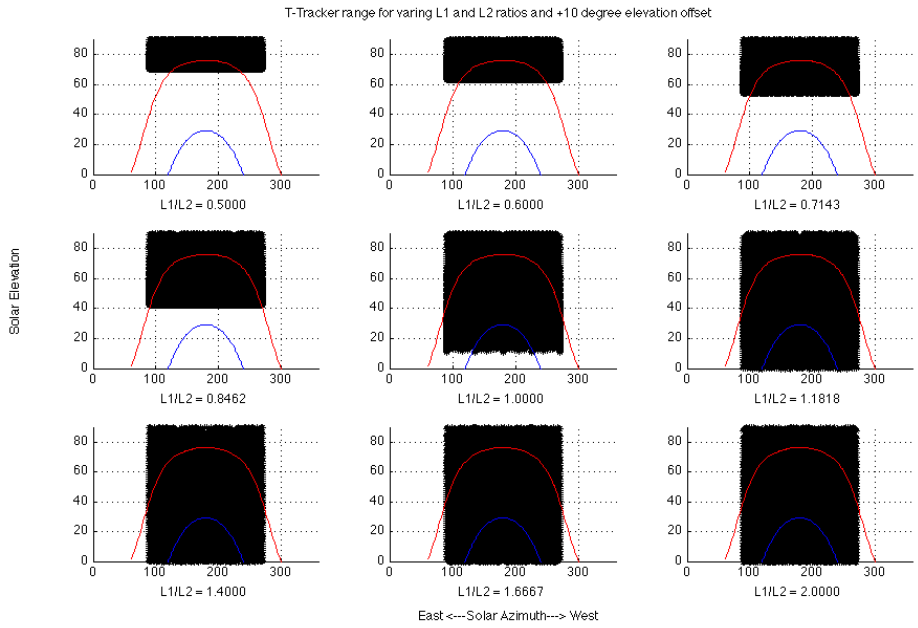

Figure 3.2: The geometry of the tracker can be varied in order to achieve the optimal tracking range (shown in black)

power production (5° only loses 2% of maximum power production). In order for our system to be cross-compatible with other solar technologies that benefit from tracking, the accuracy and precision must also meet the requirements of CSP.

The accuracy and precision of the solar tracker can be significantly affected by factors such as tolerance buildup in machined parts, backlash in gears, misalignment of the tracker with perfect south, and wind loading causing the structure to move. While these mechanical imperfections are inevitable, they can be compensated with closed loop control. The lead screw linear actuator design has many advantages that are desired in a solar tracker application. It can achieve high precision based on the pitch of the screw. Inexpensive low resolution stepper motors can therefore be used with high accuracy when coupled to a lead screw. For manufacturing, the tolerance fits on bearing, bushing, and shaft were kept at reasonable values so that they could be achieved with the machines available.

3.3 Design Options and Trade-Offs

While developing the solar tracker, many iterations were done on the design of critical parts such as the clevis mounts and linear actuator setup. For the clevis mount design, attention was placed on what bearings needed to be used and how to design it to be able to withstand external loads. Optimizing this design relied on reducing bending moments by designing the mounts with a low profile to attach to the actuators and also eliminating putting any screws in shear. It is good machine design practice to reduce any type of non-linear stresses and design

for linear stresses where applicable. The design of the tracking geometry had various options on setup, with each one giving a different tracking range. Being able to track the whole path of the Sun throughout the day would require a more robust design as stated in Section 3.2.1. Finding the optimal range while still maintaining a stable design proved to be the determining factor when designing the actuator geometry.

3.3.1 Tracker Geometry

For the low profile design based on two linear actuators, the linkage geometry could be varied in order to achieve the best tracking range. Lengths L1 and L2 are defined as the lengths seen in Figure 3.1. This minor adjustment allows the design to be scalable and use shorter actuators as the design is scaled up. As the scale of the design becomes larger, the actuators also become longer. This increase in length leads to higher costs for manufacturing bigger parts. Longer actuators can be minimized by adjusting the ratio of the L1 and L2. Adjusting this ratio varies both the tracking range and the stroke length requirement of the linear actuators.

3.3.2 Actuation

The actuation strategies were compared, with the pros and cons of each design setup according to cost and load requirements. Linear actuators can be either: ball screw, lead screw, or belt driven. Each have their own advantages and disadvantages, but all can achieve high accuracy. Due to price constraints and load carrying capacity, the lead screw method was decided upon. Lead screws can be easily designed for applications that require carrying large loads, precise and accurate linear motion, and large speed reduction with minimal parts. The low operating speed of the solar tracker eliminates the disadvantage of lower efficiency due to friction. Another advantage of lead screws is its ability to not be backdriven due to the friction between the screw and the nut. For solar tracking applications, this is desired because the tracker is more stable and less susceptible to misalignments.

3.3.3 Materials

For the prototype, typical engineering materials were used for construction. Aluminum 6061-T6 was used for construction of the clevis mounts. This material was chosen because of its reasonable price, machinability, light weight, and high yield stress. The function of the clevis mounts are to allow 2-DOF rotation of the linkages, while still maintaing structural rigidity. Because of the amount of machining required for the mounts, aluminum was a viable material to fabricate the mounts. Low carbon steel ground shafts were used at pin joints to withstand the shear stress at the clevis joints. Shaft diameters were sized based on load capacity and space requirements in order to account for magnified loading from the wind. Bronze flanged sleeve bearings were used at these joints to allow for lower friction at a lower cost than ball bearings. Steel thrust and roller needle bearings were used for their thin profile and high load carrying

capacity, while greatly reducing the friction between the rotating parts at an economical price. Bronze bushings were used in pinned joints instead of ball or roller bearings because of cost and simplicity. While the clevis mount bearings are mostly protected from the elements, the pinned joints are open to the environment. These bushings need zero maintenance and are very cheap to replace. While designing the linear actuators, economical materials were considered for their construction. Machined Delrin blocks were used to support the leadscrew at both ends instead of a ball bearing assembly. Delrin is still able to provide low friction for the leadscrew to rotate at a lower cost than a ball bearing assembly. Machining of these blocks is faster, because a bearing housing fit does not have to be accounted for.

3.4 Detailed Design Description

The design of the solar tracker started with a CAD Solidworks model. Parts that would be bought were imported into the CAD model from the company's online library, allowing for fast modeling. Material properties of all the parts were applied to obtain a calculated value for the weight of the entire tracker. In order to see any interferences of parts during operation, a motion study for the assembly was created. The motion of the tracker following the sun was simulated in Solidworks, which checked to see if any collisions occurred. If any did occur, the design of the assembly and individual parts could be modified to achieve the necessary clearance.

3.4.1 Geometry

The final geometry consists of the two custom linear actuators in a T-configuration without the overhang mechanism. An L1/L2 ratio of 1.1 was determined to have the best tracking range for Santa Clara. With the current configuration, the tracking range can be seen in Figure 3.3.

The tracking range is limited, since the actuator lengths had to be shortened in order for the system to be shipped to the EPA P3 Conference. The tracking range can be extended by increasing the length of the x actuator. This would allow the solar tracker to cover the entire range of the Sun's path.

3.4.2 Linear Actuators

The lead screw design was chosen because of its simplicity, high accuracy and precision, and its high load carrying capacity. The linear actuators in Figure 3.4 were designed and built with 8020 aluminum extrusion and 8020 teflon sliders. These parts were chosen, because they are commonly used in custom CNC machine applications, which also require high precision. The aluminum extrusion can be obtained at various lengths and can be assembled easily.

Mounted onto the sliders are Delrin blocks that are threaded to mate with the ACME lead screw. The ACME lead screw is supported by two acetal blocks at opposite ends of the actuator. The Delrin blocks provide low friction for the screw to rotate. The lead screw assembly is designed so that it only experiences uniaxial forces. If the screw is subject to

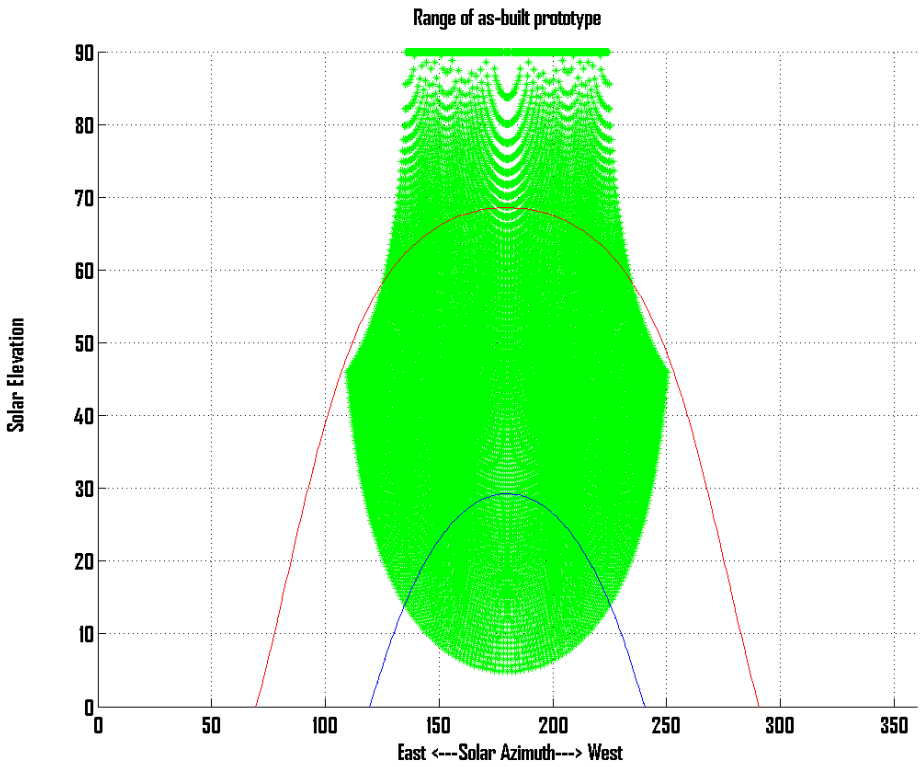

Figure 3.3: Tracking range of the final as-built prototype

bending moments, it has a higher chance of failure and lowers the precision of the system. The teflon slider is mounted to the aluminum extrusion so that it takes away any kind of bending moment on the lead screw and places it on itself. Stepper motors were sized based on the power screw torque equations (see Section 4). A spread sheet calculator was used to find the required torque to actuate the load from a 3/8"-12 lead screw (see Appendix D.2.)

3.4.3 Clevis Mounts

The purpose of the clevis mount is to provide 2-DOF rotation. The clevis pin joint allows for vertical angular motion and the thrust bearings allows for horizontal angular movement. It is an integral part of the mechanical system to have low friction and good structural stability. With the two clevis mounts mounted on the two linear actuators, the mirror structure can be attached to the tracker and have the degrees of freedom necessary to track the Sun. The mounts allow the movement of the x and y actuator slides to translate into azimuth and elevation angles.

The clevis mounts in Figure 3.5 are made of Aluminum 6061-T6. The mounts can be separated into two main parts: a top block and a bottom block. The clevis design allows for very little play and keeps a tight tolerance due to the compression of the channel. It also reduces the shear stress on the shaft, because the reaction force is split in half in the two supports. Needle bearings are used to allow for low friction movement between the two blocks. Low

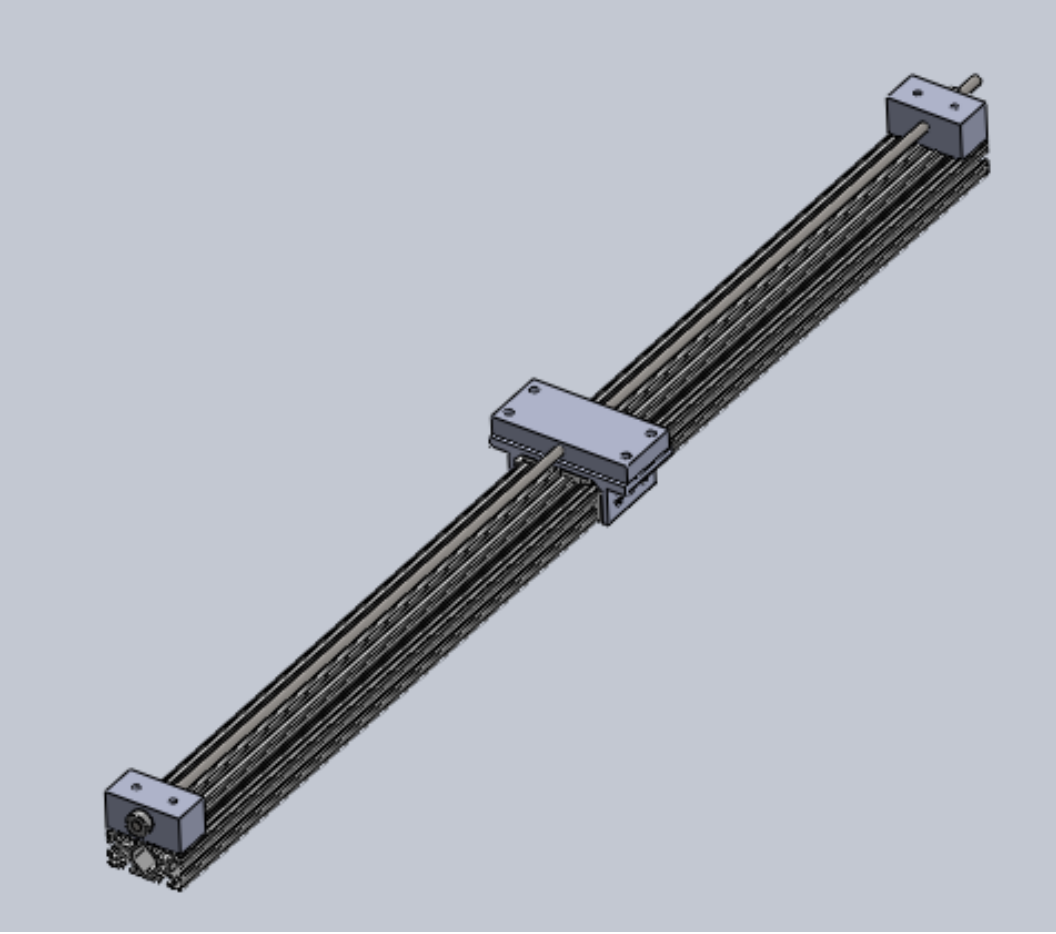

Figure 3.4: Custom lead screw linear actuator assembly

profile bearings were used because of the limited space and to allow the mount to create less of a bending moment on the actuator. A 1/2" diameter by 7/8" thick boss (see Figure 3.6) was machined in the aluminum in order to prevent any shear on the hex bolt holding the two blocks in compression. It experiences axial loads from the mirror structure and has a needle roller bearing mounted on it to reduce friction between the two blocks. The boss acts as a hollow shaft that carries all of the bending stress created from the moment of the mirror structure. The 1/4" bolt that holds the assembly together therefore does not experience shear or bending moments and is only loading in tension and compression. It sees tensile stress from the wind when the structure has a positive lift coefficient, and it sees compressive stress from the preloading of the bolt. The two thrust bearings allow the top block of the assembly to rotate independent of the bottom block with reduced friction. The needle roller design requires very little radial space, and for the radial loaded bearing, it leaves very little play on the shaft due to the roller length. Bearing shaft and housing tolerances were chosen using ISO standards for a typical press fit and shaft fit (see Appendix A.10). Due to the limitations of the milling machines used in the Santa Clara University Machine Shop, the maximum precision attainable was +/- 0.005". Because

the loading on the bearing can be considered static, creep was not a huge issue. These bearings are capable of carrying dynamic loads over 5000 lbs, making them an economical solution for solar tracking. For the pinned clevis joints, typical bronze oil bushings were used because of their cost, simplicity, and low profile design, while still reducing friction. Their tolerance (see Appendix A.9) allows a shaft to be inserted for a tight fit with no machining and little play.

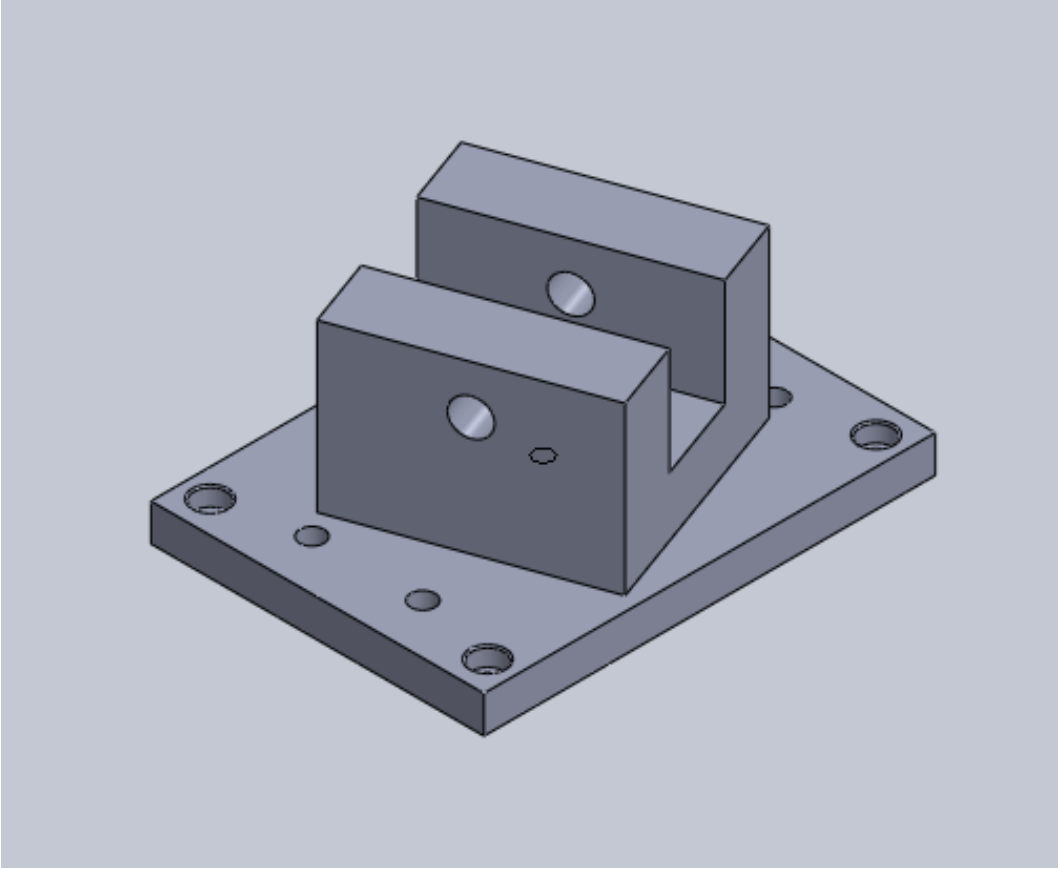

Figure 3.5: CAD as-built model of aluminum needle roller bearing clevis mount assembly

3.4.4 Mirror Support

The mirror support built in conjunction with the solar receiver was made primarily out of wood and aluminum 6061-T6. The wood was cut on a laser cutting CNC machine in order to match the curvature of the parabolic mirror. The four pieces that adhere to the curvature of the mirror give adequate support to be held in place. The advantage to this design is that it is lightweight, inexpensive, and can be rapidly built on the laser cutter. The hole pattern on the wood mirror support (see Appendix D.4) is for wood screws and bolts to attach the wood to the beam in compression. The compression of the focal couple aluminum blocks that lie in between the mirror support allow the focal arm to be clamped down and reduce the shear on the two bolts that attach the arm to the structure. The two blocks of aluminum support both the focal arm and receiver (see Figure 3.7). Since the focal arm sees mostly bending stress from the moment

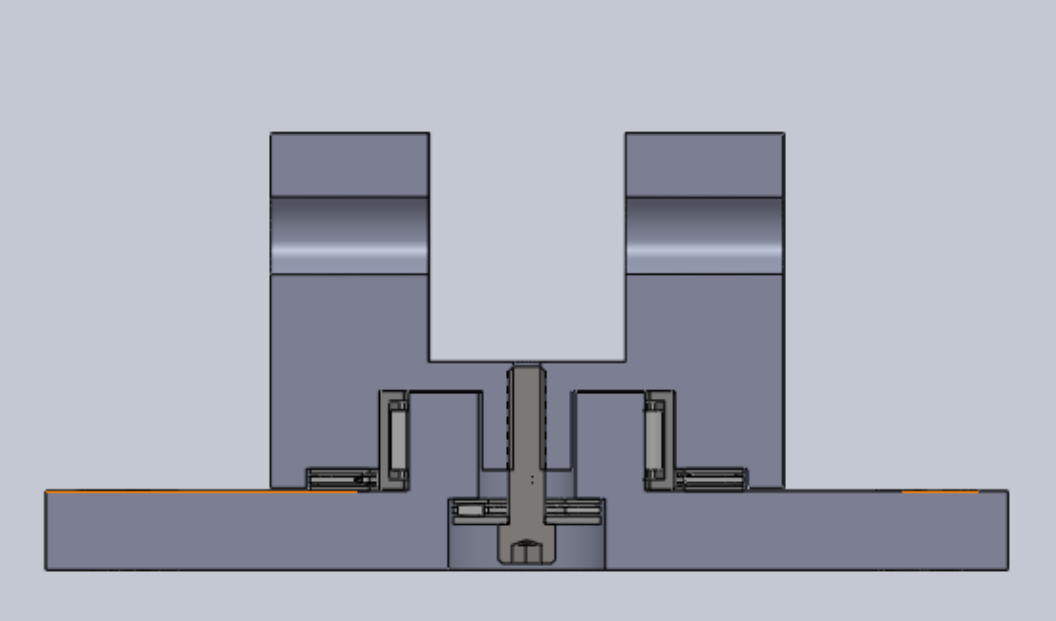

Figure 3.6: Section view of clevis mount assembly showing bearings and hex bolt

created by the receiver, it was designed to have minimal deflection with the height of the arm being much greater than the width. More design improvements could be made with the mirror support; however, it is out of the scope of the solar tracker aspect of the project. Additional analysis, such as a finite element analysis, could be done to verify the structural rigidity during adverse wind conditions. The hardware that allows for the mirror structure (clevis mounts and connecting linkage arm) to be attached to the tracker, however, went through a number of design revisions to increase structural rigidity.

3.5 Analysis

The analysis of the tracker consisted of wind load force calculations and testing of the accuracy and repeatability of the system. The wind load calculations were done in MATLAB (see Appendix B.4). These load calculations showed the reaction forces on the linear actuators with a constant wind load. From this analysis, one can see the performance gain of the low profile design over existing trackers, due to its ability to disperse the load through two points of connection. It also allowed us to see if our design would be able to withstand these external forces and if stronger parts were needed at areas of high stress. The wind load capacity of the tracker was compared to typical single pole tracker designs where there are high reaction forces on critical parts.

Another main design criteria of the tracker was to achieve high accuracy and repeatability. In order to compete with the performance of various trackers on the market today, a mechanical hysteresis and temperature response test were performed to show the performance of our design. The mechanical hysteresis test showed the level of high precision that the tracker can obtain,

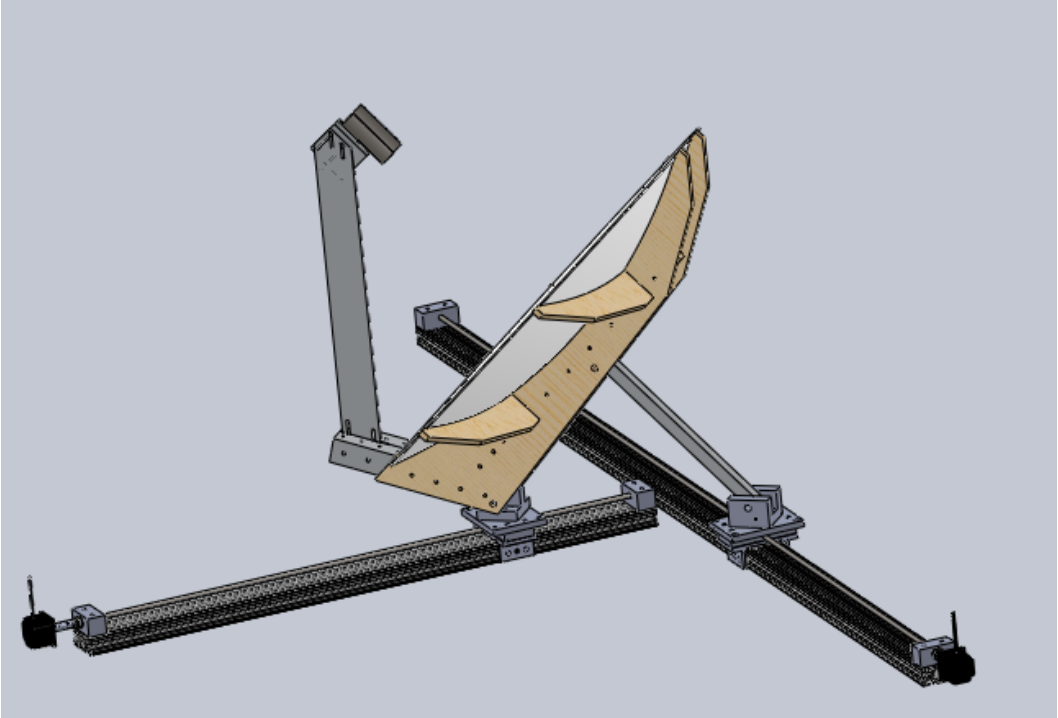

Figure 3.7: CAD model of tracker showing the entire assembly (mirror support, clevis mounts, and actuator assemblies

while the temperature response test showed how well the tracker can point at the Sun in order to keep a solar receiver at steady state temperature. Results from these experiments verified that our design and control system work to the high level of accuracy and repeatability needed for CSP systems by being able to focus the focal point into a small aperture.

3.5.1 Accuracy and Repeatability

The accuracy and repeatability of our system can be quantified by the results of the mechanical hysteresis test. The test was performed with a laser pointer mounted onto the structure. The experiment was based on positioning of the tracker orientation manually and cycling through various positions to measure the angular error in precision. The following results from the test are tabulated in the table below. These results show how precise the tracker points as it approaches the position from different paths. The tracker can therefore successfully orient itself precisely using open loop control. The closed loop control was analyzed through a temperature response test of a solar receiver. The temperature response can be seen in Figure 3.9, with a steady state temperature of about $690°C$. This temperature was successfully maintained over the course of about four hours with the hybridized control system (see Chapter 5). The verification of these tests show that the dynamics of the mechanical system can be successfully controlled and the actuation method has the capacity to be very precise when used in conjunction with CSP.

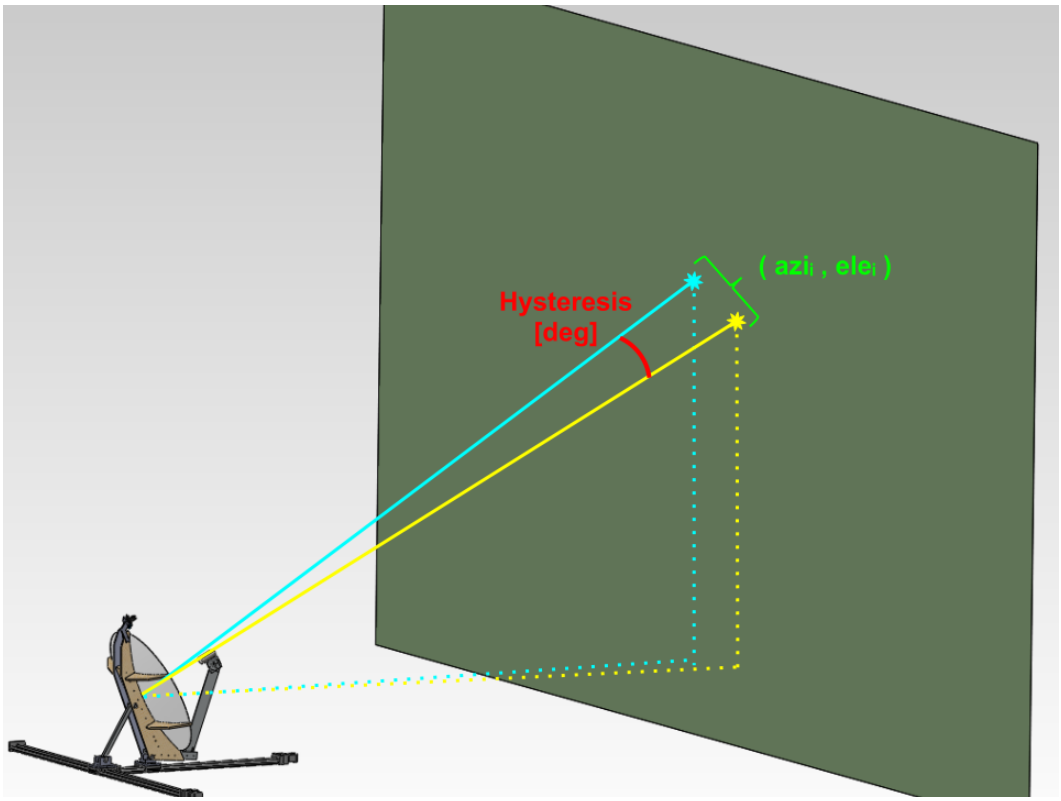

Figure 3.8: Experimental setup of the mechanical hysteresis test showing the resulting angular error

Hysteresis Results n=8	
Mean	0.05 °
Max	0.14 °
Standard deviation σ	0.05 °

Table 3.1: Results for mechanical hysteresis test

3.5.2 Loads

A force analysis was done using a mathematical model in MATLAB (see Appendix B). This model is able to calculate the reaction forces on the linear actuators. The analysis is set up by calculating the static load on the actuators from the weight of the mirror structure and by applying a 40 meters per second wind load coming from the south. The wind load is reduced to a resultant force focused at the center of pressure of the dish and is composed of the lift force. The results from this simulation can be seen in Figure 3.10. The maximum force on the system occurs on the back actuator when the dish is pointing straight into the wind. The point of comparison on the single pole design is at the base of the pole where the reaction force is very high due to the large bending moment the wind induces on the structure. Our tracker's low profile design and two points of connection experience much lower reaction forces, allowing for the use of less robust parts.

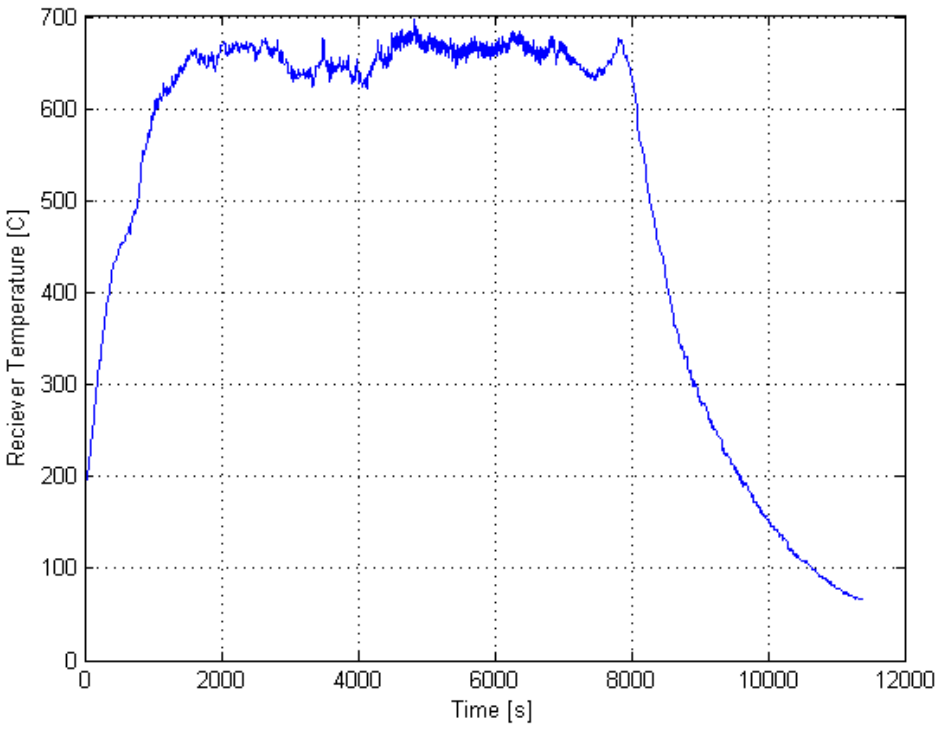

Figure 3.9: Temperature time response of the receiver

3.6 Results and Verification

The development of the mechanical system involved machine design, force analysis on critical parts, and analysis of the dynamics of the system. The clevis mount development went through various designs and utilized form synthesis principles. Designing for uniform stress patterns were used in the boss extrude on the bottom block of the clevis mount to remove shear and bending stress on the bolt that holds the assembly together. The clevis design proved to be structurally stable with very little play in areas where tolerance is an issue, such as the bearing housing and shaft fits. The testing of the mechanical precision was verified with the hysteresis experiment, and the system was shown to be controlled successfully with the temperature response test.

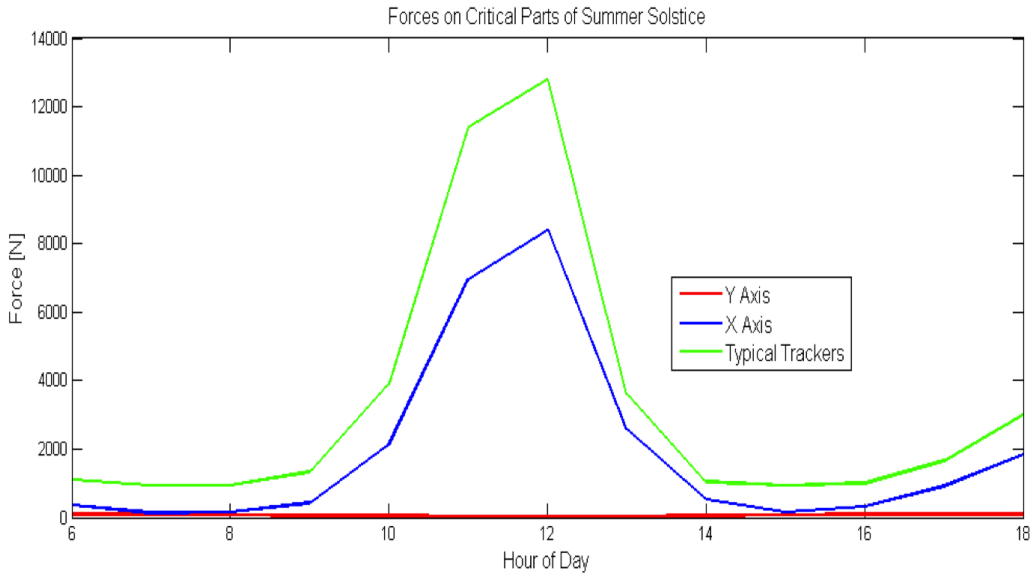

Figure 3.10: Reaction forces on linear actuators when subject to a 40 mph wind load compared to single pole design.

Chapter 4

Electrical System

4.1 Background

The electrical system of the tracker provides power for actuation as well as a means to sense the Sun's position relative to the tracker. Electrical components and actuators on solar trackers should be low power in order to maximize net power production from the solar energy system. It is also desirable for the electronics system to be power limited and low voltage (below 91 volts in California) [2]. Designing a system around low voltage not only reduces the risk of injury/fatality, but is subject to less regulation than standard higher voltage power systems.

The electrical system can be divided into three subsections: power/actuation, logic, and sensing. Each subsystem converges at a microcontroller, which is responsible for controlling the tracker based on various conditions and inputs.

4.2 Subsystem Requirements

4.2.1 Power Requirements

The power/switching components consist of motors and the switching components that provide current to those motors. The motor controller should be capable of controlling the motors in both forward and reverse operation (clockwise and counter-clockwise depending on orientation), and should consume as little power as possible. Motor controllers must also have sufficient EMF protection as they are driving an inductive load.

Motors are the principal source of actuation in the tracker, all positioning and movement in the system is derived from the rotation and torque provided by their shafts. The motors should meet the low voltage requirement, and the torque requirements of the mechanical system while consuming as little power as possible.

4.2.2 Sensing Requirements

Integrating a closed loop control system requires a sensor. The sensing system should provide information to the microcontroller about the orientation of the tracker relative to the sun. Signals from the sensor will therefore be used to not only determine if the tracker is oriented properly, but to what degree the tracker should adjust itself. Ideally, the sensor should have a linear behavior capable of detecting small differences in orientation. If a closed loop control system is to be used, it is also necessary to know the position of the linear actuators at any

given time.

4.2.3 Logic

The logic system is ultimately responsible for coordinating the movement of the tracker based on temporal conditions and sensory input. It should therefore have the ability to interpret date and time information, as well as current/voltage signals from the sensing system. In turn, it should be capable of controlling the motors.

4.3 Options and Trade-Offs

4.3.1 Motor Trade-Offs

In using leadscrew linear actuators, electric motors are the obvious choice to provide a rotational input, which by way of lead screw and slide is translated to horizontal displacement. Electric motors can be broken into two categories: AC motors and DC motors. AC motors are generally much larger and require expensive power electronics to control. Table 4.1 lists three of the most common types of DC electric motors with some of their pros and cons. There are naturally tradeoffs that come with each type of motor (the Brushed DC motor is relatively cheap, but contains consumable parts that eventually need to be replaced). Additionally, all but stepper motors are velocity control motors, meaning position of the shaft is controlled indirectly through a time integral and known motor transfer function. Utilizing a velocity control motor in a position control application requires combining the transfer function of the motor to that of the plant.

Motor Type	**Pros**	**Cons**	**Control**
Brushless DC	High Efficiency Long Lifespan Low Maintenance	Requires Controller Cost	Velocity
Brushed DC	Low Cost Simple speed control	Maintenance (brushes & commutator) Medium Lifespan	Velocity
Stepper	Precise Positioning High Holding Torque	Requires Controller Power consumption at standsitll	Position

Table 4.1: Pros and cons of several types of DC motors

While it is possible to derive a transfer function that describes the plant, it would be highly non-linear (as evidenced by the plant's non-linear equations of motion as shown in Equations 3.1 and 3.2). Controlling in position space is therefore desirable since no such transfer functions are necessary. Additionally, because the tracker moves slowly, it should be possible to dismiss plant and motor dynamics.

Stepper motors ("steppers" for short) operate based on the principles of Faraday's Law, just as all electric motors. Steppers have multiple fixed coils, and a rotating ferromagnetic shaft. By energizing a given coil, or set of coils, the shaft will orientate itself towards the energized coil; so long as that coil is energized, the shaft will resist any change in orientation–this is the motors holding torque. The first set of coils can be de-energized, and a set of adjacent coils can be energized to make the shaft move. This discrete movement is known as a step. Stepper motors are often classified by the number of steps in a single revolution of the shaft. The more steps a motor has, the more intermediate positions it has, higher positioning resolution.

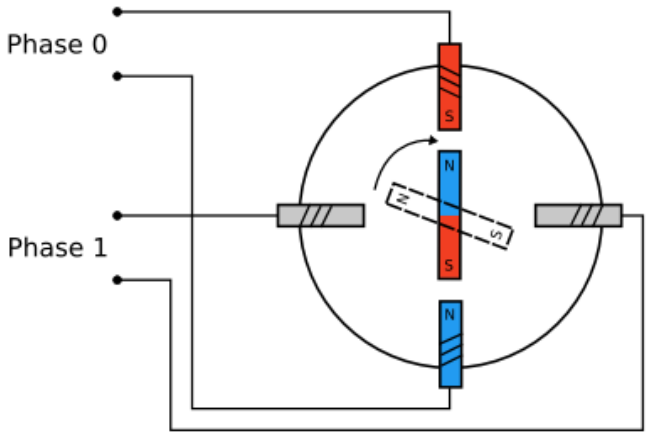

Figure 4.1: A simplified bipolar stepper motor diagram [3].

Stepper motors can be further broken down into two categories: bipolar and unipolar. Bipolar steppers are categorized by having four leads (corresponding to two sets of coils), where as unipolar stepper motors have more than four leads (and more than two sets of coils). Bipolar motors require a more complex switching circuitry as current must be able to move in either direction through a given coil. This need is mitigated in unipolar configurations through introduction of more coils and/or center-taps on existing coils. It is possible to use a unipolar motor in a bipolar setup by connecting coils in series or parallel.

A unipolar stepper motor's holding torque is increased with series and parallel combinations, because a larger number of total coils are energized at any given time. The differing responses of the series and parallel configurations are due to changes in the coils new effective resistance and inductance. Figure 4.2 shows the torque curves for a unipolar stepper motor in un-modified series, and parallel configurations. A changing of the effective coil resistance will also change the voltage and current requirements of the motors, which can in turn affect choice of motor controller.

The stepper motor chosen for the tracker application was the Lin Engineering 5718X-05E, capable of providing approximately 0.45 N-m of torque in a unipolar configuration. This motor was chosen because it was estimated that the linear actuators would require approximately 0.42 N-m of torque to actuate properly. With the motor configured in a bipolar configuration, it is

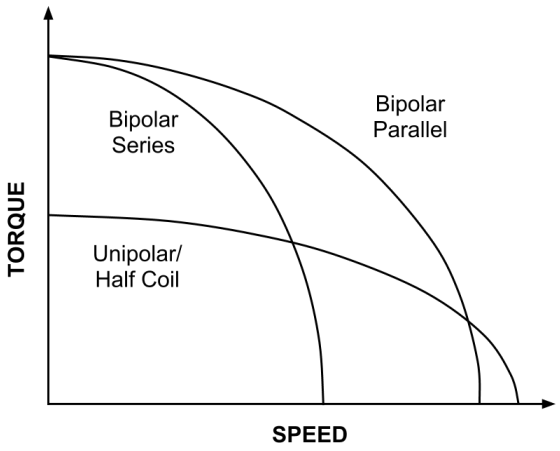

Figure 4.2: Generalized response of a unipolar stepper motor with motor windings in series & parallel configurations.

capable of providing 1.41 times its rated torque, affording the actuation system a safety factor of roughly 40%.

4.3.2 Motor Controller Trade-Offs

The motor controller is responsible for controlling current to the motors. The controller receives switching commands from the microcontroller, and using semiconductors (typically MOS or BJT transistors) controls the direction and duration of current flow into the motors' coils. To vary the direction of current flow in a motor application, H-Bridges are typically used. An H-Bridge consists of four switching components wired in a characteristic "H" shape with switching components on each leg and with the load straddling them. By switching diagonally opposite transisors simultaneously, the direction of current can be changed through the load as show in Figure 4.3.

Many hobby and professional grade stepper drivers are available for less than $100. Most drivers will accommodate two stepper motors and have full H-Bridges so bipolar motors can be used. Differentiation comes in their voltage and current ratings, micro stepping resolution (a method in which many smaller poles are induced by varying the voltage multiple coils simultaneously), efficiency, and maximum speed ratings. Control of the motor controller is typically handled through multiple digital logic connections.

The Adafruit Industries motor controller was the chosen motor controller. Based on two Texas Instruments L298D H-Bridge ICs, it is capable of driving two separate unipolar or bipolar stepper motors simultaneously. In addition, Adafruit driver is a "daughterboard" for the Arduino microcontroller, meaning the controller PCB mates with the Arduino's input/output pins. Lemor Fried, who designed the motor controller, also wrote extensive C libraries for the controller that are compatable with the Arduino Microcontroller.

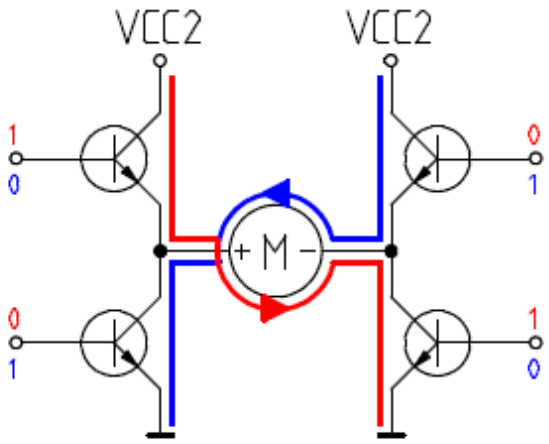

Figure 4.3: Direction of current through a load can be changed based on open/closing diagonally opposite switches [17]

4.3.3 Sensor Trade-Offs

For closed loop control, optical sensors must be used to provide feedback as to the trackers orientation relative to the Sun. Photodiodes and photoresistors are discrete components often used in optical sensing applications. A photoresistor changes resistance in response to changing light intensity, whereas a photodiode changes the amount of current flowing through it based on light intensity. Table 4.2 outlines some of the performance differences between a commercially available photodiode and resistor. Generally speaking, photodiodes have a larger range, and faster response time.

Device	Photoresistor	Photodiode
Part #	GL5528	BPW21R
Range	0 to 100 lux	0 to 10^6 lux
Response Time	55 mS	3 uS
Operating Temperature Range	-30 to 75 C	-40 to 125 C

Table 4.2: Optical sensor comparison

To create a meaningful output based on the Sun's position, additional circuitry is needed to translate a varying resistance or current into a voltage, which can be read by an ADC. Regardless of the sensor used, the accompanying circuitry should have a full scale output equal to that of the ADC's input.

4.3.4 Microcontroller Trade-Offs

The Arduino is a microcontroller prototyping platform built around the Atmel AVR series chips. The AVR chips are available in varying packages and system parameters and can be programmed in C and Assembly languages. The Arduino combines the Atmel AVR chips with

the necessary power regulation and serial communication and integrated ADC. Additionally, an IDE (Integrated Development Environment) exists for the Arduino, taking much of the work out of compiling and uploading code to the chip.

Arduino offers multiple prototyping platforms, but the two most common are based on the ATmega328 and ATmega2650. The chips differ primarily in their number of IO ports and amount of non-voliatle flash memory used for program storage.

As mentioned in Section 5.4.1 it is also necessary to have date and time information if the sun's azimuth and elevation is to be calculated. To keep accurate date and time information a low-power, battery operated clock must be employed. Real Time Clocks (RTC)are lower-power digital clocks used in computers and other electronics to keep date and time information even when the device is powered down. The Dallas 1307 is one such RTC, and is commonly found on computer motherboards. A single 3.3 volt coin-cell battery, can keep the clock powered for up to 15 years. The 1307 uses the I^2C protocol for serial communication.

4.4 Detailed Design Description

The Arduino Mega is based upon the ATmega2850 chip and was the microcontroller of choice in construction of the solar tracker. The Mega was chosen for its 16 analog inputs, 54 digital IO ports, and 256 KB of flash memory for program storage. Detailed specifications on the Arduino Mega can be found in Appendix A.1. The Adafruit Industries motor controller was selected based on earlier, smaller prototypes of the tracker, which also used smaller stepper motors. The L293D chips are capable of supplying 0.6 A maximum per phase, well below the needed 2 Amps for the larger stepper motors. By the time the current inadequacy of the motor controller was realized, the majority of the C code had already been written and tested, and made extensive use of the AFMotor and AccelStepper control libraries. Instead of having to find a new motor controller and modifying the source code for potentially different libraries, an additional H-Bridge circuit was built from power MOSFETs to handle the higher currents of the stepper motors.

The additional power switching circuit was built atop perfboard with screw down connectors to interface with motor leads and the motor controller. With the new power switching circuit, the Adafruit controller effectively only provides a switching signals. Figure 4.4 shows the completed quad H-Bridge circuit.

The photodiodes were mounted in the laser-cut sensor assembly shown in Figure 2.16 and Cat-5 ethernet jacks were used to provide connectivity to the electronics enclosure. To provide an output for the ADC, high precision 5k resistors were used to produce a voltage drop within the 0-5 volt range of the ADC. The optimal resistance of these resisters was found experimentally with the sensor assembly under full sun conditions. With the two photodiodes equally shaded by the shade structure, different resisters were inserted until a voltage drop of approximately 2.5 volts was achieved (corresponding to 0.5mA of current through the diode). The 2.5 volt

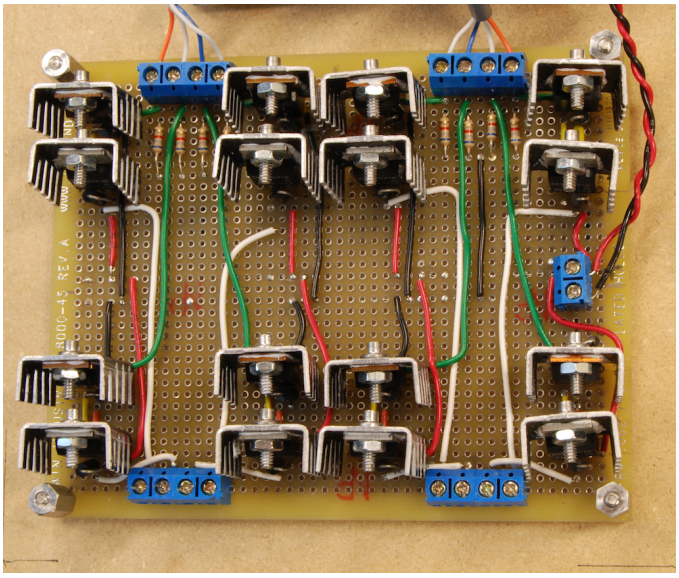

Figure 4.4: A quad H-Bridge constructed of power MOSFETs

target was chosen because it is the midpoint of the ADC, meaning there is equal room for the voltage to rise or fall without saturating or zeroing-out the ADC.

It was determined that position feedback for the linear actuators was unnecessary, since the motor controller and microcontroller could keep track of the motors current and desired position in memory (provided that no steps were skipped and no loss of power). For this to be an effective method, the stepper motors must first have a reference. A limit switch was installed at the end of each actuator. When depressed, a electrical signal is sent to the Arduino and a new datum point is set. One of the limit switches can be seen in Figure 4.5.

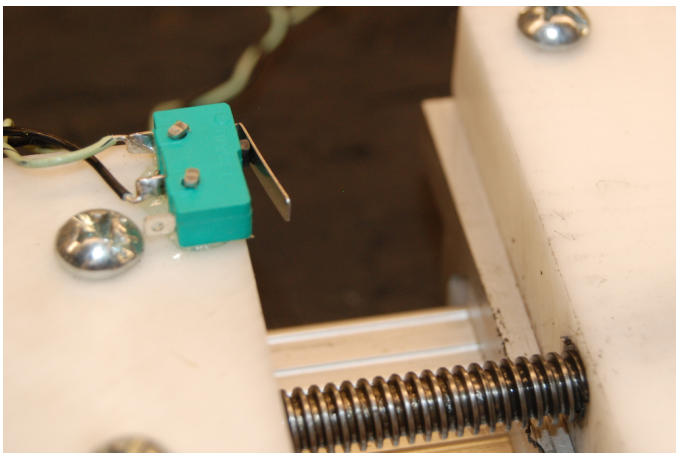

Figure 4.5: A limit switch used in setting the actuator datum upon startup

The Dallas 1307 RTC was soldered onto the circuit board that receives signals from the limit switches and optical sensors. A single ribbon carries the solar sensor voltages, limit switch lines, and the RTC data bus back to the microcontroller as seen in Figure 4.6.

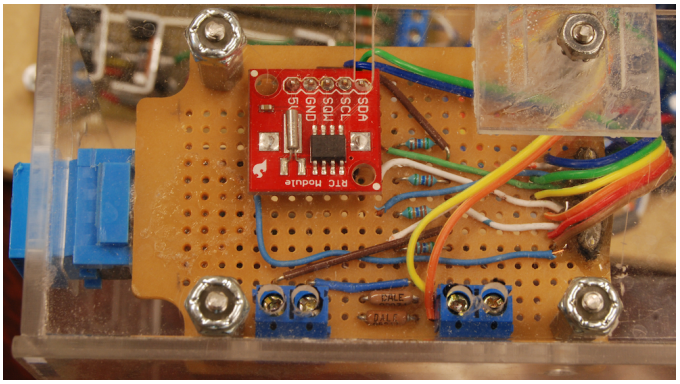

Figure 4.6: The RTC (in red) and resistor networks for the limit switches and optical sensor

4.5 Schematics

The new power H-Bridges were designed using the IRFZ44 and SMP20P10 N and P MOSFETs; their data sheets can be found in Appendices A.5 and A.4, respectively. The selected MOSFETs were chosen for their integrated back-EMF protection diodes and maximum 10 A rating (giving a safety factor of rougly 5 for the 2 A stepper motors). Each H-Bridge is built using two logic inverters, comprised of a P and N MOSFET in series. This configuration is called an inverter because when the gates are pulled low (to ground), the output is pulled high (to VDD), and vice versa. Figure 4.7 shows the schematic for a single inverter.

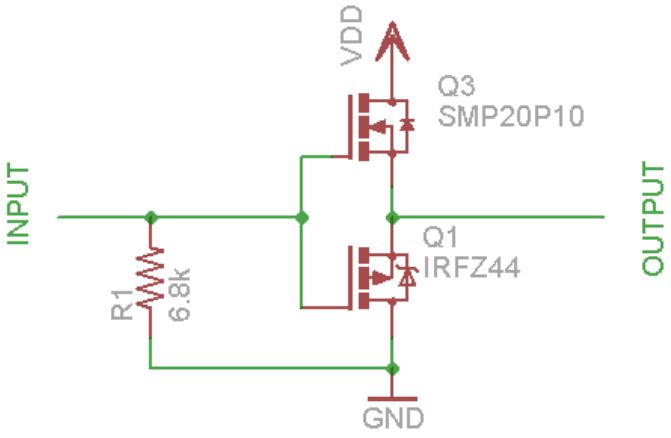

Figure 4.7: A logic inverter used in one half of an H-Bridge.

The 6.8k resistors between each pair of gates and ground serves to keep the gate voltage from floating. Without this resistor, both MOSFETs will open, resulting in an effective short to ground.

As stated in Section 4.4 the optical sensor is constructed from photodiodes and precision resistors. Optimal resistor values were determined experimentally and connected in series with the photodiodes. The high side of each resistor is connected to the Arduino's ADC to measure

the voltage drop across the resistor, which is determined by the current passing through the photodiode. Figure 4.8 shows the circuit diagram for the optical sensor and accompanying resistors. This configuration gives the Arduino four voltage measurements from which two voltage differentials can be calculated, one corresponding to 2-DOF.

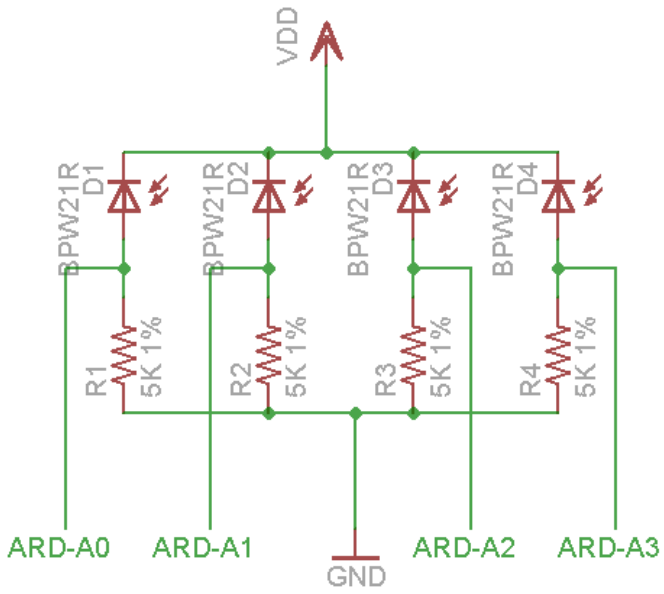

Figure 4.8: Optical sensor schematic.

4.6 Results and Verification

4.6.1 H-Bridge

Prior to soldering the H-Bridge to perfboard, the circuit was prototyped on a breadboard and tested with 1kHz square wave. Figure 4.9 shows the input and output waveform. The inverter circuit operated as intended, and soldering of the full quad H-Bridge circuit was completed. A break-in test was then conducted with the stepper motors in which they were commanded to rotate at 60 RPM for over two hours. The motors operated nominally, and while each power MOSFET was outfitted with a heat sink, no discernible temperature rise was noticed.

4.6.2 Optical Sensor

The optical sensor was mounted to a tripod and tested under full sun conditions. Voltage readings were taken from each resistor, and voltages from opposing Azimuth and Elevation resistors were subtracted to find their difference. The orientation of the sensor was adjusted until the two voltage differentials were approximately zero, indicating an equal amount of current flowing through each photodiode and correspondingly equal illuminance. The photo

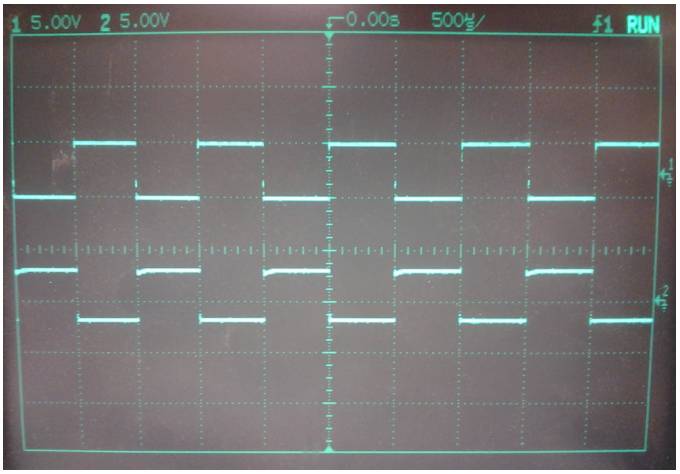

Figure 4.9: Test of MOS inverter circuit with 1kHz square wave

sensor was then inspected visually, and the shadow cast by the shade structure appeared to be casting an equally partial shadow across all four photo diodes.

Chapter 5

Control

5.1 Background

At the heart of the solar tracker is its control system. The control system is ultimately responsible for ensuring the tracker is pointed at the sun, ideally with a high level of accuracy and precision. Many methods of control exist for solar trackers, but the decided upon and designed system should strike the balance between robustness, cost, and accuracy.

5.2 Subsystem Requirements

5.2.1 Accuracy Requirements

As stated in Section 2.4, commercially available trackers typically have 1° pointing accuracies. To be competitive with existing trackers, and meet the accuracy set forth in the PDS the control algorithm must be capable of sub 0.5° control.

5.2.2 Communication Requirements

For debugging and development purposes, the system should have a means by which to output (display) information to a user. Serial communication capabilities are incorporated into most microcontrollers, and provide a convenient means for event based or periodic notification. Additionally, the system should be capable of communication with various sensors, integrated circuits, and electronics.

5.3 Design Options and Trade-Offs

5.3.1 Open versus Closed Loop Control

Solar trackers typically use either open or closed loop control. Open loop control is characterized by lack of feedback or sensory input about a system's current state. By contrast, closed loop control uses sensory information about a system's current state to make decisions or adjustments to the system.

Open loop control is typically cheaper than a closed loop system and is easier to implement. A simple open loop control for a solar tracker calculates the position of the sun (or approximate it from a look-up table) and then adjusts the tracker to said position. Such a system can be

simple and inexpensive, because there is no need for sensing electronics or development of control logic.

The primary downside to open loop control, however, is that the system has no way of knowing if its actually on target. Installation misalignment, erroneous time & date information, wear on mechanical parts, and mechanical backlash are a handful of possible sources of error that could result in misalignment with the Sun.

With closed loop control, such alignment errors can be effectively eliminated through sensory feedback. Closed loop systems are not without problems, however. Electrical sensors can be susceptible to noise, and there are scenarios when such a system could misalign the tracker significantly with the sun. A potential example of this might be with the passing of a cloud; it's conceivable that a cloud could pass overhead covering the sun (effectively eliminating DNI) so that the brightest spot in the sky becomes an area on the periphery of the cloud. With the sun exposed again, the tracker would spend time moving back into position to lock back onto the sun. Time spent moving the tracker into position is lost energy production and thus lost revenue.

5.3.2 Hybridized Control

Hybridized control combines open and closed loop control to create a more robust tracking solution. It was decided that such a control system was potentially advantageous in a solar tracking solution for a handful of reasons. By having two pieces of information–where the sun should be (open loop) and where the brightest point in the sky is (closed loop)–a more robust control algorithm could be designed.

5.3.3 Microcontroller Limitations

The computational limitations of a controller cannot be overlooked, especially when high accuracies are called for. The variation of C used on the Arduino uses multiple types of numerical variables, each with their own limitations. Floating point numbers are the only variable type that allow computation of decimal numbers. The Arduino's floating point numbers are stored as 32 bits of information and are limited by 6-7 decimal points of precision (not the same as digits to the right of of the decimal). While 6-7 decimal points of precision can provide high accuracy in some applications, non-linear computations (exponential and trigonometric operations for example) have the potential to. Furthermore, math operations with floating point numbers are more computationally intensive than those with integer numbers and can slow down a program loop.

5.4 Detailed Design Description

As designed, the control system is a hybrid control system, integrating both open and closed loop elements. RTC provides date and time information, which, when combined with latitude

and longitude of the tracker's location, the position of the sun can be calculated. The calculated position is treated as an estimation of the sun's true position and is used in coarse positioning of the tracker. Knowing the approximate location of the sun, the tracker will move towards the estimated location of the sun. Once the tracker is within an acceptable error limit (an acceptable angular error between the trackers position and the solar position estimation), the tracker switches to closed loop mode to provide accurate tracking of the sun.

By combining open and closed loop strategies, the tracker can position itself on the horizon, anticipating sunrise even when the sun is still below the horizon (open loop strategy). In closed loop mode, the estimated solar position is used as maximum deviation bound, meaning the tracker is free to orient itself to the brightest spot within the allowable deviation window. Figure 5.1 shows the high level control logic in flow chart form.

The closed loop positioning system provides large potential installation cost savings. A tracker misaligned from true South, and/or on an incline, can still track the sun without any need for code adjustment or configuration, reducing or potentially eliminating the need for expensive grading and concrete foundations. The final version of the hybrid control source code can be seen in Appendix B.

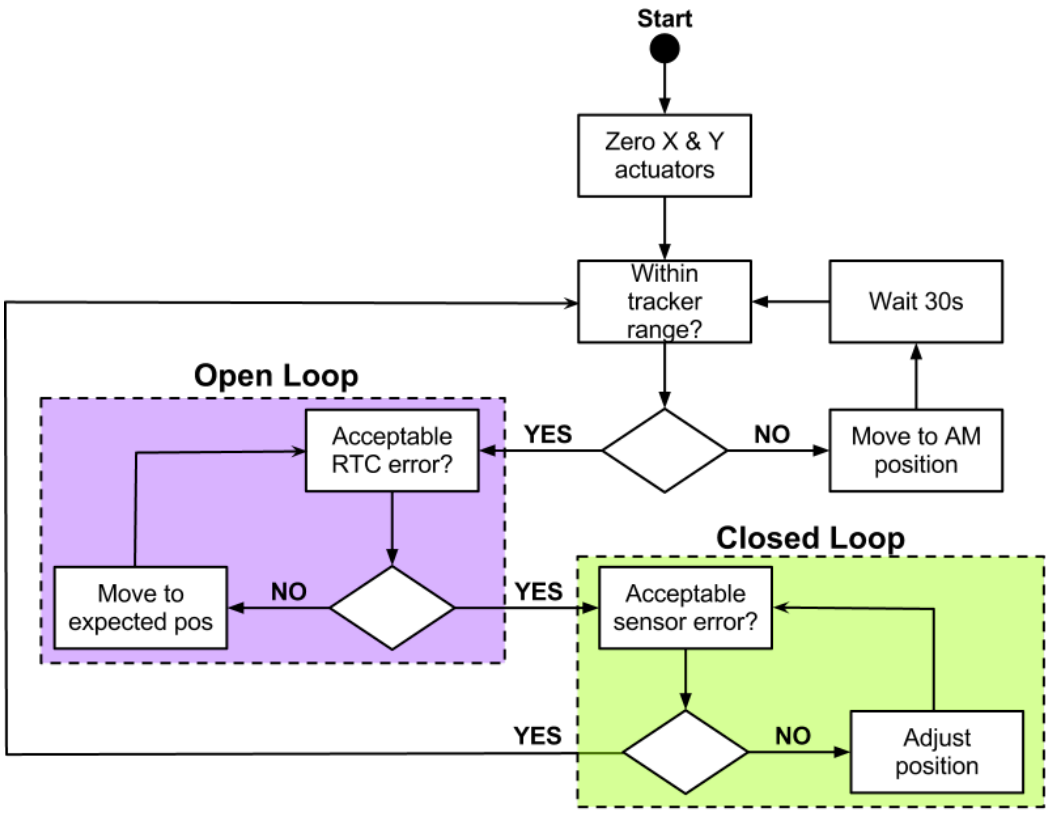

Figure 5.1: Logic flowchart for the final control algorithm

Use of PID control was briefly explored but quickly abandoned in light of the highly non-linear equations of motion (Equations 3.1 and 3.2). Various control methods exist for highly

non-linear systems such as fuzzy logic and adaptive control. It was decided that the dynamics of the system could be ignored because of the slow angular velocity of the Sun across the sky (the maximum possible angular velocity of the sun is 0.25°/m as shown in Section 1.2. Moreover, use of a lead screw to drive the actuator slides makes overshoot difficult as the forces needed to back-drive the lead screw are avoided through implementation of controlled stepper deceleration.

5.4.1 Solar Position Algorithm

Using date, time, and latitude and longitude information, the Sun can be calculated using the process and equations in Appendix D.3. The equations therein are arduous, and the high number of floating point number computations can significantly affect the speed of the Arduino's 16 Mhz processor.

Instead of implementing the equations exactly as outlined in Appendix D.3, an open-source implementation of those equations that uses multiple look-up tables was incorporated. The algorithm used in the code was written by Gabriel Miller of `www.cerebralmeltdown.com`. The code was released under the Creative Commons Attribution-Noncommerical-ShareAlike License [7].

5.4.2 Sensor Input

The Arduino ADC measures the voltages across the four precision resistors mentioned in Section 4.4. The 8-bit ADC values are converted to voltages, and opposing voltage values are subtracted from one another in the code. If both voltage differentials are zero, or approximately zero, the solar sensor is normal (or nearly normal) to the Sun. Through trial and error, a maximum allowable differential of 0.25 V was set. This means that when the voltage differential exceeds 0.25 V, the tracker will adjust itself in 0.25° increments until the differential is below the 0.25 V threshold.

It took several combinations of differential thresholds and movement increments to prevent the system from oscillating on a regular basis.

5.4.3 Stepper Motor Control

The stepper motors are controlled using the AccelStepper and AFMotor libraries written by Lemur Fried. Upon startup of the tracker, datum points are set on both actuators by running them until limit switches are hit at each end. Knowing the length of the actuators, lead of the threaded rod, and number of steps in a full rotation of the stepper motor, the zero point is set for each actuator.

The motor is then commanded to rotate the desired number of steps at a given speed. The motor will accelerate and decelerate automatically at a rate specified in the preamble of the code.

5.5 Analysis

Several tests were performed prior to full hybridized control testing. Calculation of the Sun's position using the open-source algorithm was compared to results provided by the US Navy Astronomical Applications Department [6]. Angles provided by the RTC and open-source solution were within 0.5° value provided by the Navy's calculation.

The Arduino implementation of the actuator space to azimuth/elevation space calculations was compared to the MATLAB version of the calculation (which utilizes double floating point precision numbers and thus, provides for significantly higher accuracy). Differences were negligible.

Finally, the tracker was setup in an open loop mode in which it was commanded to various azimuth and elevation angles using serial communication with a computer. The tracker was commanded to several different azimuth and elevation combinations, and the angles were verified approximately using a protractor.

With the combination of these three sets of tests, all positioning and open loop functions were verified. The last set of tests necessary to verify the tracker operated as intended was the full integration of sensing system.

Chapter 6

System Integration and Testing

Integrating the electrical, control, and mechanical aspects of the project required much coordination. Information about the mechanical system was needed, such as tracker geometry and torque requirements, in order to engineer the right electrical system and control system. In order to make best use of the limited time available for designing and building the solar tracker, the project was divided into mechanical, electrical, and computation systems. The mechanical system required a detailed CAD model and drawings for construction. The electrical system needed to be sized to provide enough electrical power to actuate the system. The control system was designed to have a certain desired accuracy. Building these systems separately required coordination for construction. In order for testing to be done on the tracker, the construction phase had to be executed in a timely manner. To make sure the system would operate as planned, the mechanical system design and construction was prioritized. The electrical and control aspects of the project were designed to be integrated with the mechanical system.

Before the final design for the tracker was chosen, the ability to control it needed to be evaluated. Because of the new design's unique geometry, the team had to see if it was possible to control it. Once the geometrical relationships in the design were evaluated and determined controllable, the design was chosen for further development and implementation. A smaller scale prototype was constructed to facilitate electrical and code testing (see Figure 6.1). These earlier phases of development relied upon rapid construction of the mechanical system, so that the large scale prototype could be developed further. This was made possible through use of readily available miniature linear actuators and CNC laser cut acrylic. The acrylic pieces were used to make the clevis mounts and linkages.

For the construction phase of the final large scale prototype, machining of the mechanical components was completed first. This included the clevis mounts which required the most development and fabrication time. About 60 man hours were needed to machine the clevis mounts on the milling machine. The mirror structure was developed and constructed by using a CNC machine to laser cut the wood structure. The linear actuators were originally ordered from PBC linear (see Appendix A Section A.8). Ordering of the shelf linear actuators manufactured by another company would reduce the man hours necessary for machining. The parts would also be more precise, since the company's manufacturing process is commercialized and has wider access to higher quality machines. However, the actuators did not arrive in time to be implemented into the solar tracker prototype. Custom made actuators were fabricated as a backup plan. Fabrication time was reduced by designing the actuators using 8020 aluminum extrusions, which are widely used in custom CNC machines. Once, the mechanical system was

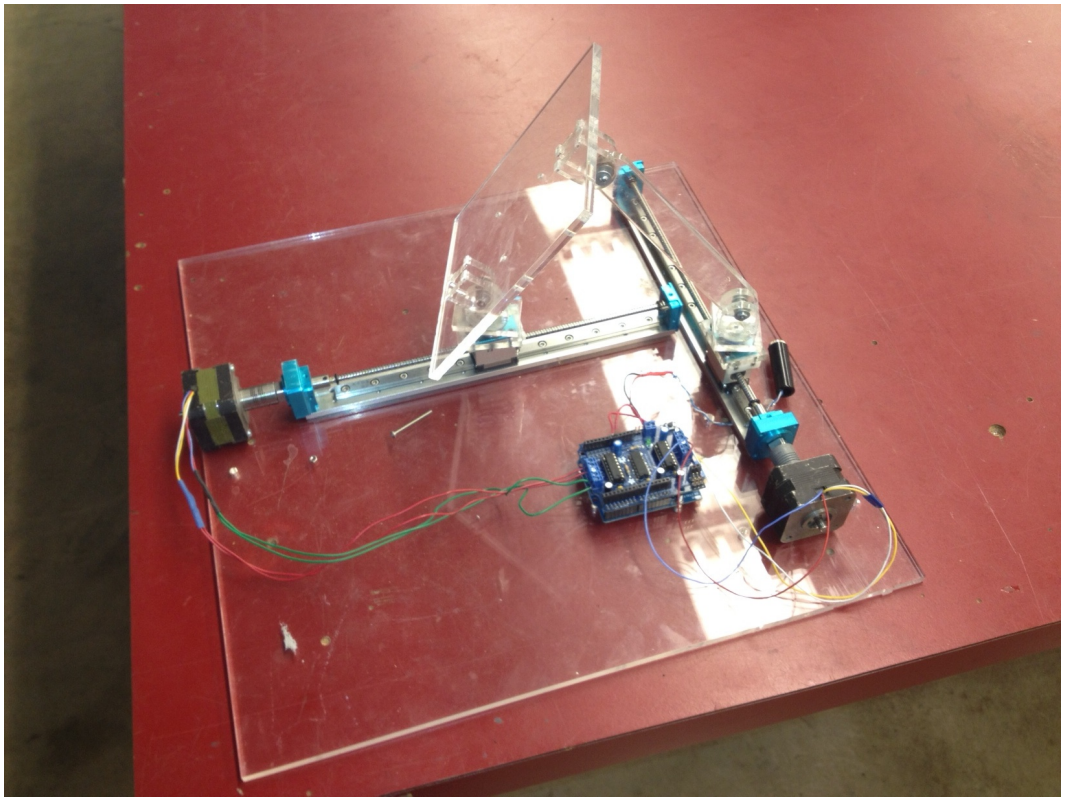

Figure 6.1: Small mock up of final design for testing the tracking control algorithm

finished with construction, testing of the electrical and control subsystems was performed.

While the manufacturing of the mechanical components was made a priority during the construction phase, the electrical components and control system algorithm were being developed in parallel with construction. Electrical components such as the Arduino electronics, custom h-bridge circuit, and photodiode sensor were designed in parallel with the other subsystems, so that testing could be done once the mechanical system was built. Electrical wiring diagrams were created (see Appendix C in order to make clear how the electrical system was integrated with the other subsytems. The control system was finalized after testing and debugged after being integrated into the other finalized mechanical and electrical systems. Once the systems were integrated through construction and code troubleshooting, the actual testing of accuracy and repeatability performance was conducted (see subsection 3.5.1).

Chapter 7

Cost Analysis

The estimated total cost of our current project prototype is shown in Table 7.1. Included are the total budget from funding, total cost of our system, and cost for each component. The cost per part is based on our current scaled prototype, while the business plan is based on a conservative production model. (Note: Table 7.1 does not include expenses on materials used for previous prototypes, as well as miscellaneous expenses including uniforms, shipping and handling, adhesives, etc.)

Our senior design project received three sources of funding: the Roelandts Grant through the Center for Science, Technology and Society; School of Engineering Grant from the Undergraduate Programs Senior Design Project Funds; and an undergraduate Travel Grant from the Research Office (listed respectively in Table 7.1). Although not shown above, most of our budget was spent not only on our final prototype design, but also on the previously iterated prototypes. There were also unforeseen expenses including shipping of the parts. In addition, Santa Clara University's Leavey School of Business student, Oliver Glenn, developed a business plan. Based on his research, the average cost of existing solar trackers on the market is about $2000, with installation costs of $4000, making the total system cost $6000. Currently, our solar tracker is priced at about $3000 with installation costs of $1500. Compared to the combined selling price and installation costs of existing designs, our tracker is a cheaper alternative by $1500. Thus, although our solar tracker is more costly as a unit, our design significantly reduces the total cost of the system plus installation. Moreover, the current cost of our solar tracker is an extremely conservative estimation. The selling price and break-even point does not fully take into account the lowered price per unit based on high manufacturing and production rates. Costs could further be reduced after contracting with a manufacturer. Having reduced the overall cost of the system for use at the residential scale, our system helps to make solar tracking technologies more available at the residential and consumer level. It serves as cheaper alternative whose function and use is in a manner comparable to existing solar trackers.

Total Budget	
Total Funding:	$6650.00
Willem P. Roelandts & Maria Constantino-Roelandts Grant (CSTS)	$3000.00
Undergraduate Programs Senior Design Project Funds	$1650.00
Undergraduate Research Office–Travel Grant	$2000.00
Cost per Part	
Total Cost:	$2913.97
Actuators	$1981.39
Mirror	$309.99
Mounting Hardware	$18.02
Arduino Mega & Motor Controller	$88.54
Ball Bearings & Shaft Coupling	$78.91
RTC, Cable, DIP Switches, Headers, Solar Cells, Accelerometer	$133.83
Aluminum Stock & HSC Components	$142.85
Aluminum Stock	$25.47
HSC & Motor Controller	$114.97
Misc (Screws, Bolts, Washers, etc.)	$20.00
Business Plan	
Selling Price	$3500.00
Break-Even Point (units)	87
Installation Costs	$1000.00
Cost of Unit and Installation	$4500.00

Table 7.1: Cost Analysis

Chapter 8

Patent Development

8.1 Invention Description

A low cost easily deployable solar tracking unit was conceived for concentrated solar power applications where a large and heavy dish concentrator must articulate to follow the sun's path throughout the sky. The benefits of the design were soon recognized to be applicable to photovoltaic panels as well with the unique feature that the panel may be positioned in a flat, low profile orientation. Existing trackers are mounted atop a tall structure to allow the tracking device to have sufficient ground clearance when tracking the sun at elevations relatively close to the horizon. This design fixes the base of the tracking device close to the ground for added stability and support in a lower cost and more easily deployable package.

8.1.1 Technical Features – Advantages & Uniqueness

The invention is comprised of two perpendicular and coplanar linear actuators. Together these two actuators control the azimuth and elevation of whatever device is mounted to the two moving pivot points. This configuration is believed to be new and previously unused. The advantage of this design is the ability to use off the shelf and low fidelity parts instead of manufacturing specifically to the application.

The tracker supports the device tracking the sun at two points for added structural stability over most other trackers, which typically attach at a single pivot point. However a large moving base is not necessary as with other trackers, which employ a two-mount point scheme. Figure 8.1 and Figure 8.2 illustrate the tracking system with a concentrated solar power apparatus mounted. A flat panel supporting a photovoltaic array may easily replace the solar collector, hence the versatility of this system. Note from Figure 8.2 that by extending the actuator attached to the base to its full length, the solar collector will lay down flat. The benefits include the ability to lay flat in adverse weather conditions, and the possibility to be applied to a roof mounting system for home power generation. This design includes all of the mentioned advantages and is still able to cover the entire range of the sun's movement (see Figure 8.3).

The most common two axis tracking systems currently in use are a single pole driven into the ground with a drive unit coupling the pole to the tracking unit. To install the pole, an auger must be used and can only be installed in climates where the soils will support a heavy post set in with cement. Installation requires considerable work from a civil engineering standpoint as the pressure distribution for a pole in the earth is complex even for simple lateral and axial loads from wind. The single drive unit rotates at the top of the pole about a central point. Multiple

sets of gears are used and must be capable of handling very large moments and loads. These gears are heavy duty pieces of equipment, and are often fitted with heavy counter balances. In contrast, our design requires only light anchoring into the ground due to its wide base and efficiently deals with moment loading from the geometry of the design.

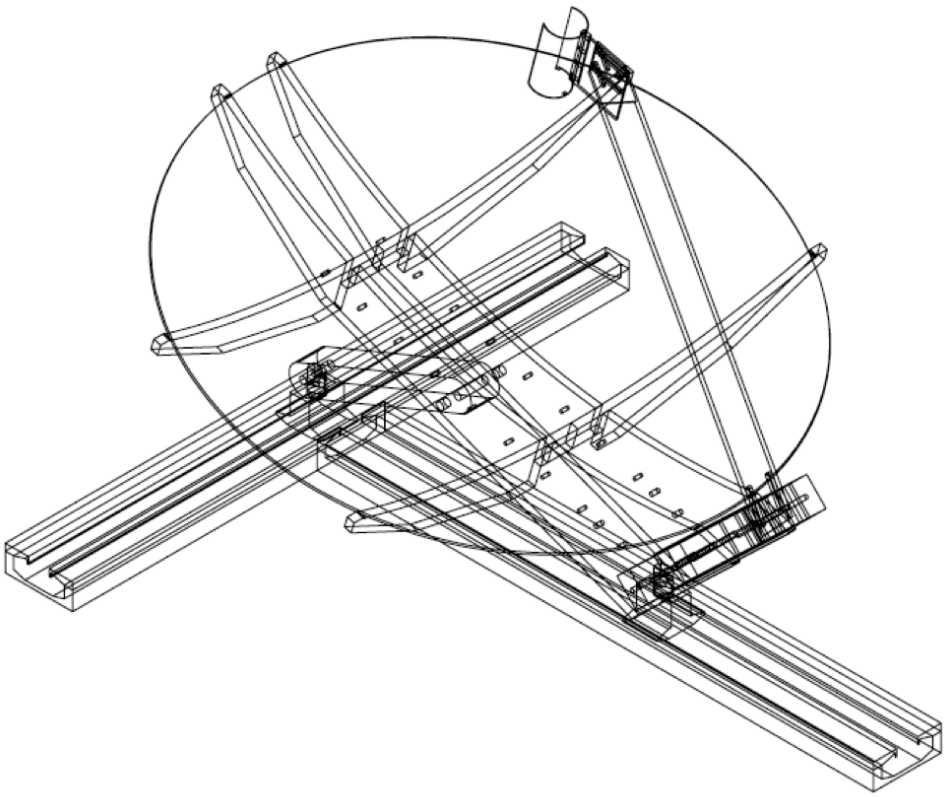

Figure 8.1: Overview of concentrated solar power tracking unit

8.1.2 Possible Variations & Modifications

One possible variation on the invention currently being investigated is the possibility of mounting multiple panels on a single unified grid system to be driven with a single pair of drive units (see Figure 8.4). The arrays would then be considered a single modular deployable unit driven by only one central location. This would save on cost by reducing the total number of components and save on power requirements to drive the system by reducing redundancies. The scale of this variation is as large as megawatt size photovoltaic arrays for utility scale power production.

8.1.3 Competing Technologies & Current Solutions

The solar tracker is a well-known device, which is essential for any concentrated solar power application and greatly improves performance of photovoltaic devices. This invention adds the

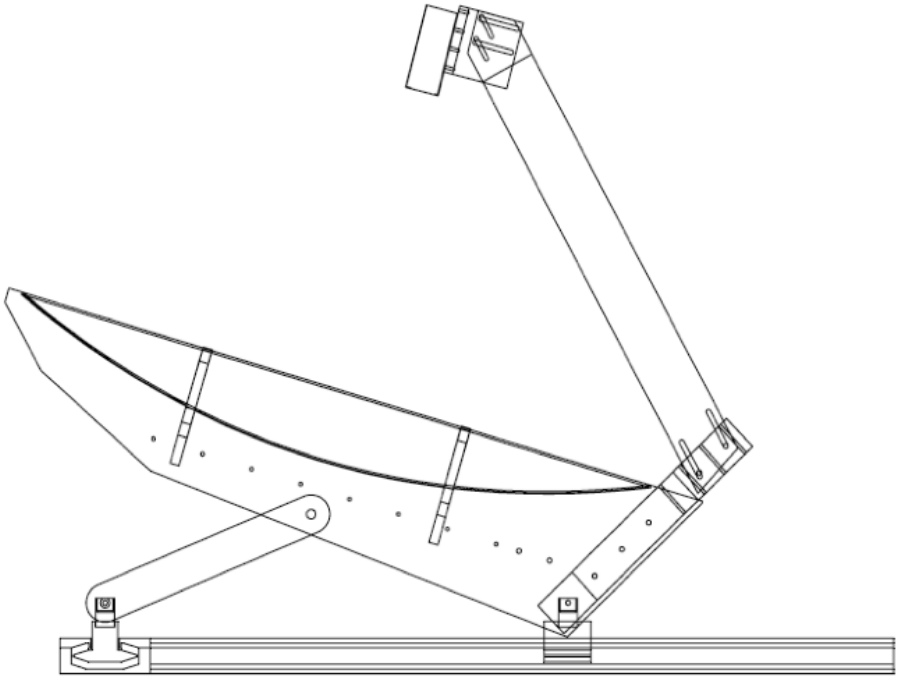

Figure 8.2: Side view of concentrated solar power unit

benefit of easily produced parts and fewer parts and a wide base that does not require an auger and cemented post for installation. Wind forces are currently an issue with mounting a tracking dish or PV panel atop a pole driven into the ground. In no case can such a system be regressed for self-preservation without disassembly and storage. The proposed design may autonomously lay down flat to strong winds. For photovoltaics specifically, this presents opportunity to have roof mount panels which track the Sun without adding any risk to the roof itself in adverse weather conditions. Patents for existing two axis trackers include US 7,884,279 B2; US 7,799,987 B1; US 2010/0282243 A1; US 2010/0024861 A1.

8.1.4 Commercialization Possibilities

Calculated designs exist for the concentrated solar power application, and a prototype has been fabricated for a lab scale concentrated solar power unit. A small mockup prototype has been built for proof of concept.

For concentrated solar power applications this system can be used on large-scale commercial and residential units as well as small-scale (lab scale) units. Large-scale units include dish collectors up to 100 square meters in collector area and are used primarily for renewable power generation. Small-scale (lab scale) units are solar collectors that can be easily stored in a room and transported to test sites. For photovoltaic applications the system offers the possibility to roof mount solar panels, which may track the sun. The system also provides more support to

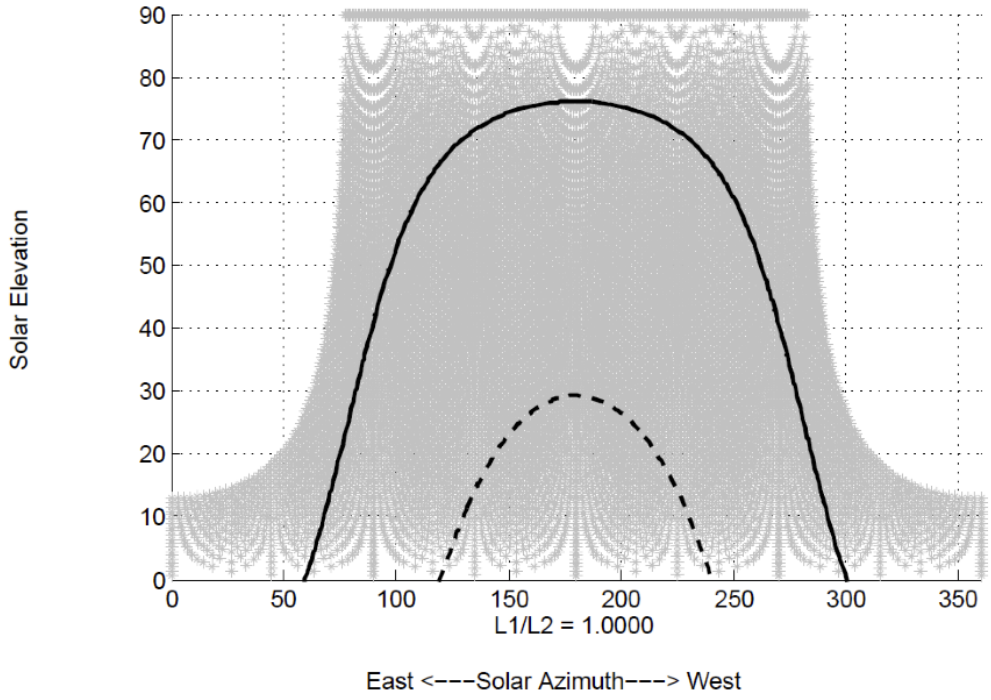

Figure 8.3: Coverage area of solar tracker. Shaded area represents all possible combinations of elevation and azimuths for a particular geometry. The solid line and dashed line represent the Sun's path at summer and winter solstices respectively

a photovoltaic module than any currently produced system and offers the ability to retract to a low profile flat position for adverse weather conditions.

8.1.5 Key Dates

- Date of initial idea: 7/25/2011
- Date of conception (when all the essential elements of an invention were formed in the inventors mind): 9/17/2011
- Date first reduced to practice (first successful demonstration of the invention): 2/5/2012
- Date and venue of first public disclosure (date and venue of proposal or manuscript submission, date and venue of conference presentation, date and venue of electronic or web postings): 4/21/2012
- Date and venue of any future public disclosures (date and venue of future, planned publications, conference presentations, etc.): 6/6/2012

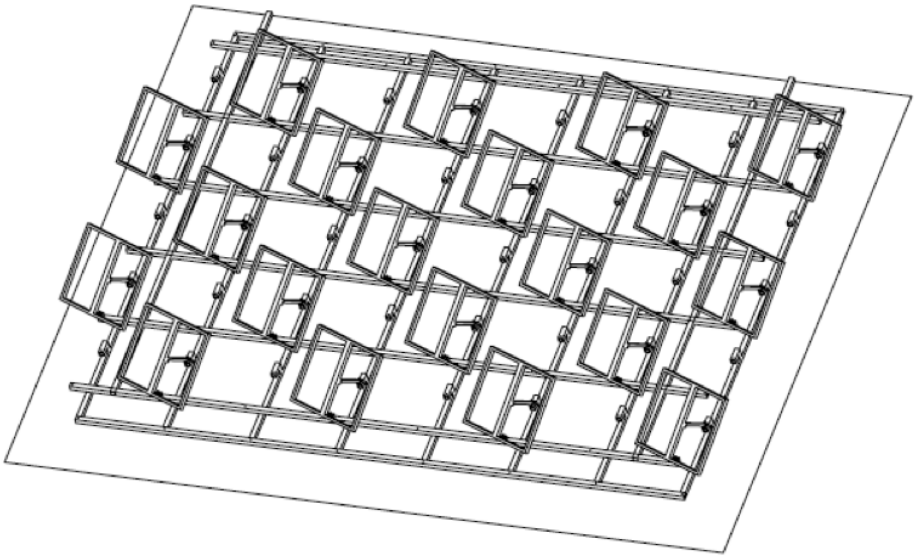

Figure 8.4: Possible roof array of solar panels on a unified grid system

8.2 Summary of Patent Classifications

The design of our solar tracker falls under several patent classification classes, which include but are not limited to: D13, 126, 194, 250, and 388 [4]. Generating electricity through use of the Brayton cycle, the solar tracker classifies under Class D13, which applies to equipment for production, distribution, or transformation of energy. Class 126 for stoves and furnaces applies because it generally includes any apparatus for the application of heat. Due to the control algorithm and use of the linear actuators, Class 194 for check-actuated control mechanisms applies. In addition, Class 250 applies to all radiant energy systems, including apparatus for using, generating, controlling, or detecting radiant energy. The motor control system classifies the tracking system under Class 388 for electricity: motor control systems.

8.3 Review of Recent Patents

Our team has devoted much time to researching existing products through patent searching and company inquiry. As in any design process, it was vital for us to discover what similar products have already been created. We looked at each design we found, both past inventions and currently used products, and evaluated the positive and negative aspects of each. Among the patented designs we found, all were similar in their purpose but varied slightly in their design. The existing solar trackers differed in size and used PV panels instead of concentrated solar dishes. We looked closely at the actuation types used in order to determine what would be best for our own design. In addition, existing designs all varied in base structure. We found that many possibilities existed for choosing the base depending on factors of stability

and movement of the solar tracker; the base could range from a single leg planted into stable ground to multiple legs for above ground stability. The following are brief reviews of selected patents found (see Summary of Patents in Appendix E.4 for more information).

8.3.1 Patent No.: US 7,884,279 B2

This two-axis tracker, capable of withstanding extreme weather conditions, uses a photovoltaic solar array and two actuators. The PV panel is mounted on a frame, which is connected to a base. Also connected to the base is a pivotal frame that allows one actuator to control the elevational movement and the other actuator to control the azimuthal movement of the solar array. The solar tracker may be raised or placed in a stowed position. This patented design is similar to our design in its use of two actuators that control both the elevation and azimuthal position of the panel. This design also keeps in mind the need to withstand adverse weather conditions. This design can be placed in a stowed position when not in use, while ours achieves a low profile by laying flat. In addition, this design was built in a way that makes shipping and transportation easy by collapsing the parts into a compact position.

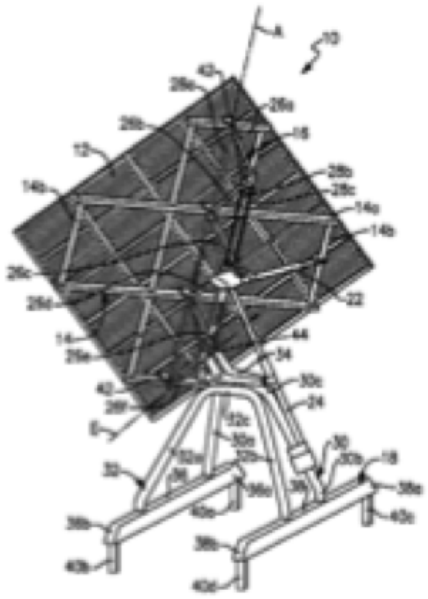

Figure 8.5: Patent No.: US 7,884,279 B2

8.3.2 Patent No.: US 7,799,987 B1

This is a unique design of a solar tracker that uses an elongated tube. Although held in a vertical position when not in use, the tube is made of material that serves as an easily bendable mounting surface support for photovoltaic panels. The solar tracker is able to bend by contraction and expansion. More specifically, it uses water to cause capillary action to control the growth or

shrinkage of the outer surface material. This design is extremely different from our design; it works much like a flower that follows the course of the sun throughout the day. The material, structure, and positioning method are all different from our design of a solar tracker. We noted this patented design as a unique idea. Although we did not incorporate much of its features into our own design, we did like its ease of shipping and transportation due to its simple structure.

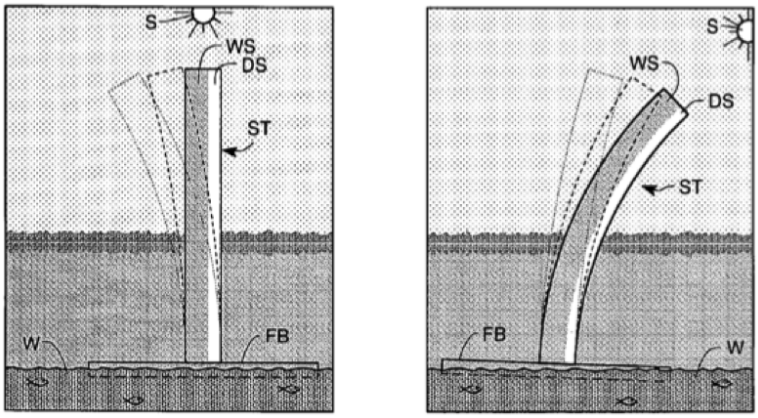

Figure 8.6: Patent No.: US 7,799,987 B1

8.3.3 Pub. No.: US 2010/0282243 A1

This invention is of a two axis solar tracker that uses stepper motors and lead screw actuators to move the entire structure (not just the panels). Having two degrees of freedom, this system focuses on structural support, reduced wind loading, easy maintenance, low cost, and less complexity. Our solar tracker design also uses stepper motors and lead screw actuators. Also, our system also focuses on having a stable foundation, reducing wind loading during adverse wind conditions, and reducing maintenance and cost. However, our design is different in that we use the two linear actuators as the base. Hence, our base does not move but the position of the solar panels or dish are controlled by moving the shuttles of the actuators.

8.3.4 Pub. No.: US 2010/0024861 A1

A unique design of a two axis solar tracker is shown in which the supporting system for the solar panels can move entirely around a circular track. A structure, which supports and rotates the panels, extends out to the running track and is kept on that track via small wheels. The structure rotates about a fixed central point. Based on this publication, our group considered having the structure rotate on a circular track. However, we decided to use two linear actuators instead in order to reduce sweep volume, the number of parts, and to achieve a low profile. Because of the T-configuration of the linear actuators, our design does not rotate about a fixed center point.

In addition to patent research, our team researched existing companies that design, sell,

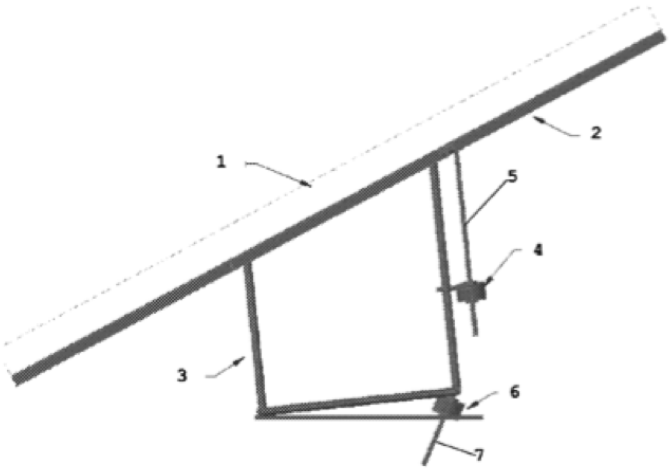

Figure 8.7: Publication No.: US 2010/0282243 A1

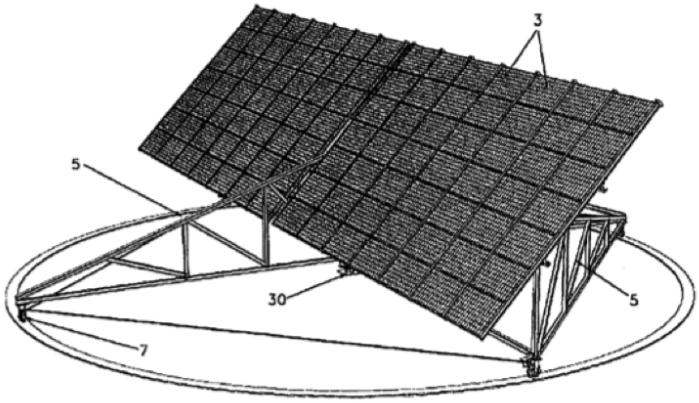

Figure 8.8: Publication No.: US 2010/0024861 A1

and install concentrated solar trackers. We found that most use PV panels instead of solar dishes. Several of the companies provide installation services for their products in residential and commercial areas. However, their product is still rather costly and not popular among residential communities. Since installation is expensive, their primary customers are businesses.

As a result, the information we gathered on existing products was used in determining what was necessary to include in our own product design. With the goal of generating more energy and lowering system cost, we hope that our design makes concentrated solar tracking more available to residential and commercial consumers.

8.4 Patent Application

After the reception of our product over the course of the year, at the EPA P3 National Sustainable Design Exposition, and at the Senior Design Conference, the team believed our design has

unique features which are patentable. On April 18, the team decided to file for a preliminary patent (61/635239) to ensure that the public disclosure deadlines were met for the conferences. In the patent application we claimed that our tracker has a low-profile and hybridized control which reduces the cost of the overall system. The patent application can be found in Appendix app:patent.

Chapter 9

Engineering Standards and Constraints

Santa Clara Universitys commitment to sustainability has had great importance in relation to the environmental responsibility of its students. We are constantly seeking ways to reduce our use of non-renewable resources and minimize pollution so as to ensure a brighter future for subsequent generations. As engineering students, our innovative approach to the design of our senior project is aimed at benefiting the globalizing world. This means focusing on an issue locally before moving onto a global outreach. However, with developing new technologies comes a need to evaluate the impact of our decisions. Not only must we consider the impacts of sustainability, environmental protection, economic, and social development, but we must also take into account manufacturability, and health and safety. In addition, it is also important to analyze the moral and ethical questions that may arise pertaining to each of these impacts. Thus, the evaluation of our project is not only based on its design and construction, but also impacts communities globally.

9.1 Manufacturability

We would like to increase the simplicity of our solar tracker design compared to other solutions by using readily available parts that can reduce the need for fabrication. Assembly and mass production are easily achieved through the use of off-the-shelf parts of commonly used/found materials. Only standard machining is required since the precision dimensions and tolerances of each part are not as critical as for custom made, high-precision parts.

Manufacturability of our product can be a fully automated process. However, starting manufacturing costs will be initially high due to the costs of buying all necessary materials to mass produce our product. If the process is fully automated, we still need to ensure that some degree of precision is maintained. In addition, since our product can be easily scaled up or down, the manufacturing process would change slightly due to the desired size set by the customers needs.

9.2 Social

Using solar energy technologies helps to solve the energy crisis by increasing renewable power production. Our small scale design can be used with both PV and CSP technologies. Photovoltaic panels are cheaper but CSP solar dishes allow for more energy to be generated within a smaller amount of operating space. No matter which technology is used, this solar tracker

design can be used by residents, commercial businesses, and schools. Multiple solar trackers can also be placed together to form an array in remote locations. These could be powered by only one set of motors instead of individual motors for each separate solar tracking unit. In addition, this solar tracker can be used in other countries located in regions of the world that receive a great amount of sunlight throughout the year. This could help to generate energy in locations were electricity is scarce.

9.3 Political

In recent years the government has played a major role in implementing laws that will aid in encouraging the use of renewable energy. Furthering the advancement of solar trackers will bring more interest for the government to encourage the use of solar tracking technology. In order to get a patent for the design and possibly place our product on the market, we must familiarize ourselves with the politics that control the outcome of the development of the product. The patent application process has many steps that are required in order to get exclusive rights to intellectual property. This process will determine whether or not the design is original and patentable.

There are also laws that can restrict our product from being used by both residential and commercial sectors. We must be able to prove our electrical and structural design can function safely and pass tests under a variety of conditions for it to be acceptable to sell on the market. There may be regulations that we must follow, especially in terms of installation. We must consider aesthetics, obstruction, safety concerns, community opinions, etc. In addition, a permit may be required before installation can take place. If the government supports the use of solar trackers in communities, government subsidies may be issued. This would help to encourage the use of solar trackers by both businesses and communities.

9.4 Economic

One main objective of our project is to lower the cost of our solar tracker in order to make it a more viable option for residential and commercial markets. Costs are reduced in three aspects: parts, installation, and shipping. Part costs are lowered by using off-the-shelf parts rather than custom made parts. Less part precision is needed in the tolerances of each of the individual components. Also, each part need not be as heavy or robust as in other existing trackers. Installation costs are lowered by lessening the number of steps required for proper installation. For many existing trackers in the market, the base commonly consists of a single pole driven into the ground. Installation requires ensuring the soil can support a heavy post set in with cement before actual installation work is done. In contrast, our solar tracker base consists of a flat wooden plane. The base can simply be bolted directly onto another flat plane, such as a rooftop or level ground. Shipping costs are also lowered in that our tracker consists

of components that are easy to disassemble and transport.

In order to put a successful solar tracker on the market, it is necessary to have a business plan on how the product can make a substantial profit. If we were to continue onto the manufacturing and selling of this product, a loan would be necessary to start the product development. Our team will speak with several manufacturing companies and work with one that is willing to accommodate. Once production is started, the units will most likely be sold to contractors, who will then sell it to customers. Currently, the cost of our system is valued at about $3000 with an estimated payback time of 3 years. The break-even point will be to sell 87 units. Our solar tracker installation costs are about $1500, which is roughly half the price of installation for other existing trackers. Our tracker will be appealing to customers due to the short and long term financial benefits. The increased efficiency of a customers solar energy technology will save them more money by not having to rely and buy as much electricity from the grid.

9.5 Environmental

As with any product that is made available to the market, the environmental impact of the product and all the processes involved must be considered. Focusing on the product itself, all of the materials used in the construction of our prototype are non-toxic, recyclable materials. Each component is made of common, standard materials, including wood, aluminum, and steel. These materials can be easily recycled and/or reused. At the beginning of the design process, our team decided upon using common, easy accessible materials for parts. The materials we chose to use for the different components of our final design are relatively easy to find and also easy to machine. This helps to lower costs by diverting our need to purchase expensive material parts and by requiring only simple machining that does not necessarily product high precision parts. Our material choices proved to be extremely beneficial. Not only did it make it easier to purchase the parts and machine them in the Machine Shop, but we can proudly say that our project supports and promotes sustainability.

Despite the advantages of our product, the energy required to make the product and distribute it to the public must also be taken into account. In other words, we must also look at the consequences that result from manufacturing as well as shipping and transportation of the solar tracker. Pollution from factories and transportation vehicles is inevitable. However, these negative impacts can be reduced. Our prototype was built with ease of shipping and transportation in mind. Having several components that are easy to assemble and disassemble allows for easier shipping and distribution. The parts used in our design are cheaper and lighter in weight, reducing shipping charges based on overall weight. Also, the parts can be easily shipped together as a disassembled unit or package, making transportation by aircraft and/or vehicle much easier when transporting multiple units in one load. In being mindful of having a low carbon footprint as a result of developing our product, it is desirable to lessen the embodied energy of the product design process. We believe that the success of our project is

dependent upon lessening the harmful impacts on the environment.

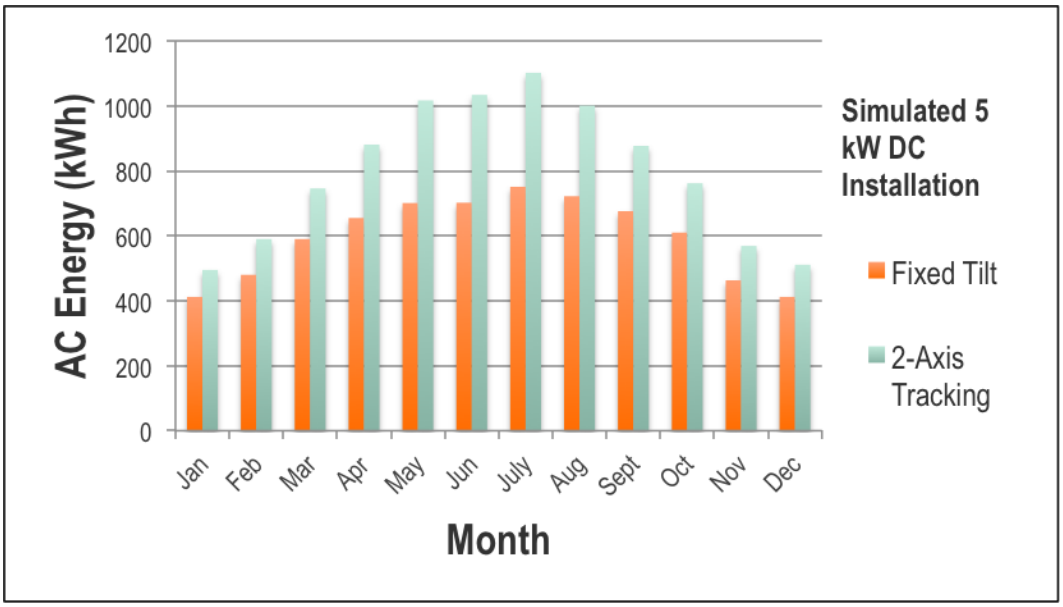

Figure 9.1: AC Energy recorded over the course of a year for fixed tilt and dual axis tracking [1]

9.6 Health & Safety

Before our product is placed on the market, health and safety must be addressed before the product is available to consumers. First, the solar tracker must be weather resistant and able to withstand and operate in different weather conditions. More specifically, it needs to be able to withstand high wind loads due to a factor of safety. Our current design can withstand wind loads of up to 90 mph and has a factor of safety of 2. The factor of safety for the final product should adhere to structural codes in order for it to be used by consumers. Second, for concentrated solar power, the receiver is able to reach high temperatures of up to 1700 K. This can be extremely dangerous and involves proper installation and care instructions for the users. Lastly, other smaller factors are of concern. These include taking into account the roof penetrations and the weight of the unit on the roof, protection of electrical wiring, and maintenance. Adherence to proper building code would have to be considered during design and construction of the final consumer product.

9.7 Sustainability

The scientific community has come to virtual consensus that global warming is real and that it is anthropogenic. The burning of fossil fuels are responsible for the emission of greenhouse gasses (GHG) that contribute to climate change. To reduce production of GHGs, sources of renewable

energy can replace the need for traditional fossil fuel for power generation. Additionally, fossil fuels are a finite resource and it is only a matter of time until we need to transition to a renewable energy economy. From this arose a desire to explore alternative energy options and to successfully use other sources of renewable energy to support our way of living. In an energy study conducted in 2010 (see Figure 9.2), it was found that renewable energy only makes up for 8% of the total U.S. energy consumption. Of that, solar power only accounts for 1% of the renewable energy consumption, which results in only a 0.8% contribution of solar power energy to the total U.S. consumption of energy. The sun serves as our most abundant source of renewable energy, and yet, solar power is not being utilized as much as it should. A growth in solar power technologies is much needed in order for solar power usage to be widespread. Improving upon solar tracking systems can lead to advancements that are beneficial for future generations.

For our design, all of the components are off-the-shelf parts that are made of long lasting, durable standard metals of aluminum and steel. The use of non-custom made parts lowers costs of production and manufacturing. With the exception of the bearings and the lead screws, little maintenance is required and parts are easy to repair or replace. The final product is expected to last about 10-20 years, and is beneficial to regions of the world that receive a considerable amount of sunlight throughout the year.

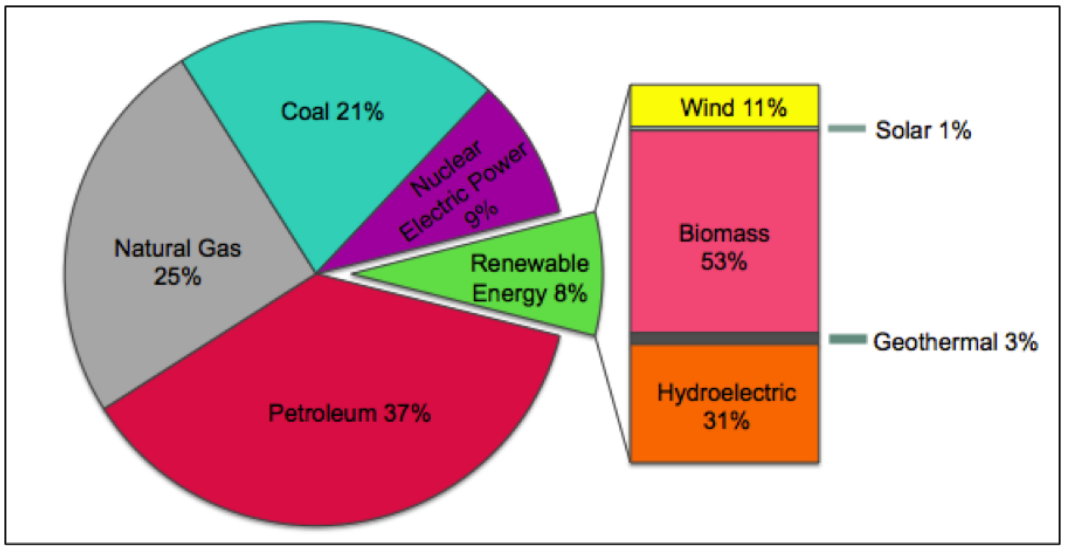

Figure 9.2: Energy Consumption in the U.S., 2010 [5]

Chapter 10

Conclusion

10.1 Summary

Solar thermal power generation is heavily dependent on solar tracking technologies. This is because high solar concentrations are needed to focus the suns energy to achieve the high temperatures necessary to operate a mechanical compression power generation system. To concentrate the suns light efficiently and direct it into a receiver, concentrating systems must maintain high-precision orientation toward the sun. Our goal was to design a solar tracker in which pointing accuracy and precision served as one of the primary design criterion.

Although we were not able to create the minimized sweep volume we desired, the unique geometry and T-shaped configuration of the linear actuators allowed us to achieve a low system profile. This is desirable during adverse weather conditions, as well as aesthetics. By enabling the system to lay completely flat relative to the plane it is held on, wind loads on the system are reduced during strong wind situations.

Using a hybrid open/closed loop control system, we were able to achieve high pointing accuracies typically associated with by expensive, precision-machined components, but at a fraction of the cost. Compounding misalignments, errors, and other mechanical deficiencies that would traditionally result in poor pointing accuracies can be compensated for through active error correction. This was achieved by using a set of photodiodes in a fabricated shaded structure to sense the actual position of the sun. The control system should operate with open loop control ensuring the tracker is pointing in approximately the right direction, and then allowing precise alignment to be handled through the closed loop system.

This design project promotes sustainability, an aspect highly valued by Santa Clara University. In the celebration of 100 years of Engineering at SCU, our project reflects the engineering excellence that is instilled in SCU students and engineering for the future. Our project aims to serve as a solution to the energy crisis faced by our generation by making the use of solar energy available to the greater public. From its simple beginnings to its fruitful end, the progress of our project has reflected the values Santa Clara University instills in its students.

10.2 Lessons Learned

Having experienced the entire product design process from start to finish, our senior design team has learned a great deal about the demands of developing a product. We did much research on existing solar tracking technologies. We also explored several alternatives for the components to

use in our final prototype design, including actuators, motors, and materials. We brainstormed many possible design ideas and analyzed which aspects of our designs we wanted to incorporate into the design of a prototype. Throughout the course of the school year, we designed and built two prototypes before finally building the final design. Not only did we have to use various software and machining equipment, but we also went through several design iterations after analysis and testing.

By experiencing the entire design process from start to finish, we learned several important lessons along the course of the year. We found that there are seemingly endless existing solutions in the market. A solution to a problem need not necessarily be solved with a completely innovative idea, but rather, can be comprised of a combination of existing ideas brought together successfully. In deciding upon an idea, we realized that any given product in general will focus on highlighting certain desired aspects. Not all great ideas can always be incorporated into one final product; there is always room for improvement. In addition, the design process requires several iterations of the product design. Through our experience, several CAD designs and prototypes were necessary in order to result in our finished product. Some issues or problems do not become apparent until the prototype is built and tested. It is difficult to fit an entire design process into the course of a school year, but we have successfully achieved the goals we had set for ourselves.

10.3 Future Work

After analysis and testing of our final prototype design, we have discovered several challenges and design improvements to address those challenges. If given more time and funding, our senior design team would design a new mirror holder that uses less material and is therefore lighter in weight. In order to achieve a larger range of tracking the suns movement, the design of an overhang is needed in which the y actuator slide would overlap and cross over the x actuator. With the linear actuators actually overlapping each other in the T-configuration, a wider range is attainable so that the entire course of the sun is tracked throughout a given day. We could also continue to reduce the cost by choosing different components that affect power consumption ie. DC motor/worm gear. In addition, design changes will be implemented to make the solar tracker a viable consumer product. This includes protecting the parts from various weather conditions in order to further reduce maintenance, as well as making installation and daily operation of the tracker user friendly. Other improvements will be addressed after a life cycle analysis has been conducted. When these design improvements have been incorporated into our design and tested, discussion with manufacturers will take place in order for our product to be mass produced and made available to the public.

Bibliography

[1] AC Energy Comparison Graph. http://rredc.nrel.gov/solar/calculators/PVWATTS.

[2] CA Department of Consumer Affairs. http://www.cslb.ca.gov/generalinformation/library/licensingclassifications/C-7LowVoltageSystems.asp.

[3] Motors and Control Systems for Precise Motion Control. http://www.1-core.com/library/auto/motion-control/figure1-stepper-motor.png.

[4] United States Patent and Trademark Office. http://www.uspto.gov/web/patents/classification/.

[5] US 2010 Energy Consumption. http://205.254.135.7/totalenergy/data/annual/perspectives.cfm.

[6] US Navy Astronomical Applications Department. http://aa.usno.navy.mil/data/docs/AltAz.php.

[7] Creative Commons Licence. http://creativecommons.org/licenses/by-nc-sa/3.0/us/, 2012.

[8] Geogrophy Blog. www.geographyblog.eu/wp/google-invests-168m-into-solar-project, June 2012.

[9] Meca Solar. http://www.civicsolar.com/product/meca-solar-ms-2, June 2012.

[10] Opel Solar. http://explow.com/cpv_video, June 2012.

[11] The open pv project. http://openpv.nrel.gov/, June 2012.

[12] Pv trackers. http://www.pvtrackers.com/, June 2012.

[13] Solar Tracker - Solar. http://www.reuk.co.uk/Solar-Tracker.htm, May 2012.

[14] Salah Abdallah and Salem Nijmeh. Two axes sun tracking system with plc control. *Energy Conversion and Management*, 45(11-12):1931–1939, July 2004.

[15] International Energy Agency. IEA World Energy Outlook 2004. Technical report, 2004.

[16] M.J. Clifford and D. Eastwood. Design of a novel passive solar tracker. *Solar Energy*, 77(3):269–280, September 2004.

[17] Eckhard Gosch. Control Motors with the L 293 D or SN754410 H-Bridge Driver. http://www.eckhard-gosch.de/en/articles.php?article_id=2.

[18] Shafee A.M.R.E. Shenawy E.T.E. Helwa N.H., Bahgat A. B. G. Maximum collectable solar energy by different solar tracking systems. *Energy Sources*, 22(1):22–34, January 2000.

[19] G.J. Kolb, S.A. Jones, M.W. Donnelly, D. Gorman, R. Thomas, R. Davenport, and R. Lumia. Heliostat cost reduction study. 2007.

[20] H. Mousazadeh, A. Keyhani, A. Javadi, H. Mobli, K. Abrinia, and A. Sharifi. A review of principle and sun-tracking methods for maximizing solar systems output. *Renewable and Sustainable Energy Reviews*, 13(8):1800–1818, 2009.

Appendix A

Data Sheets

A.1 Adruino Mega

The Arduino Mega 2560 is a microcontroller board based on the ATmega2560 (datasheet). It has 54 digital input/output pins (of which 14 can be used as PWM outputs), 16 analog inputs, 4 UARTs (hardware serial ports), a 16 MHz crystal oscillator, a USB connection, a power jack, an ICSP header, and a reset button. It contains everything needed to support the microcontroller; simply connect it to a computer with a USB cable or power it with a AC-to-DC adapter or battery to get started. The Mega is compatible with most shields designed for the Arduino Duemilanove or Diecimila.

Schematic & Reference Design

EAGLE files: arduino-mega2560-reference-design.zip

Schematic: arduino-mega2560-schematic.pdf

Summary

Microcontroller	ATmega2560
Operating Voltage	5V
Input Voltage (recommended)	7-12V
Input Voltage (limits)	6-20V
Digital I/O Pins	54 (of which 14 provide PWM output)
Analog Input Pins	16
DC Current per I/O Pin	40 mA
DC Current for 3.3V Pin	50 mA
Flash Memory	256 KB of which 8 KB used by bootloader
SRAM	8 KB
EEPROM	4 KB
Clock Speed	16 MHz

Power

The Arduino Mega can be powered via the USB connection or with an external power supply. The power source is selected automatically.

External (non-USB) power can come either from an AC-to-DC adapter (wall-wart) or battery. The adapter can be connected by plugging a 2.1mm center-positive plug into the board's power jack. Leads from a battery can be inserted in the Gnd and Vin pin headers of the POWER connector.

The board can operate on an external supply of 6 to 20 volts. If supplied with less than 7V, however, the 5V pin may supply less than five volts and the board may be unstable. If using more than 12V, the voltage regulator may overheat and damage the board. The recommended range is 7 to 12 volts.

The Mega2560 differs from all preceding boards in that it does not use the FTDI USB-to-serial driver chip. Instead, it features the Atmega8U2 programmed as a USB-to-serial converter.

The power pins are as follows:

- **VIN.** The input voltage to the Arduino board when it's using an external power source (as opposed to 5 volts from the USB connection or other regulated power source). You can supply voltage through this pin, or, if supplying voltage via the power jack, access it through this pin.

- **5V.** The regulated power supply used to power the microcontroller and other components on the board. This can come either from VIN via an on-board regulator, or be supplied by USB or another regulated 5V supply.

- **3V3.** A 3.3 volt supply generated by the on-board regulator. Maximum current draw is 50 mA.

- **GND.** Ground pins.

Memory

The ATmega2560 has 256 KB of flash memory for storing code (of which 8 KB is used for the bootloader), 8 KB of SRAM and 4 KB of EEPROM (which can be read and written with the EEPROM library).

Input and Output

Each of the 54 digital pins on the Mega can be used as an input or output, using pinMode(), digitalWrite(), and digitalRead() functions. They operate at 5 volts. Each pin can provide or receive a maximum of 40 mA and has an internal pull-up resistor (disconnected by default) of 20-50 kOhms. In addition, some pins have specialized functions:

- **Serial: 0 (RX) and 1 (TX); Serial 1: 19 (RX) and 18 (TX); Serial 2: 17 (RX) and 16 (TX); Serial 3: 15 (RX) and 14 (TX).** Used to receive (RX) and transmit (TX) TTL serial data. Pins 0 and 1 are also connected to the corresponding pins of the ATmega8U2 USB-to-TTL Serial chip.

- **External Interrupts: 2 (interrupt 0), 3 (interrupt 1), 18 (interrupt 5), 19 (interrupt 4), 20 (interrupt 3), and 21 (interrupt 2).** These pins can be configured to trigger an interrupt on a low value, a rising or falling edge, or a change in value. See the attachInterrupt() function for details.

- **PWM: 0 to 13.** Provide 8-bit PWM output with the analogWrite() function.

- **SPI: 50 (MISO), 51 (MOSI), 52 (SCK), 53 (SS).** These pins support SPI communication using the SPI library. The SPI pins are also broken out on the ICSP header, which is physically compatible with the Uno, Duemilanove and Diecimila.

- **LED: 13.** There is a built-in LED connected to digital pin 13. When the pin is HIGH value, the LED is on, when the pin is LOW, it's off.

- **I^2C: 20 (SDA) and 21 (SCL).** Support I^2C (TWI) communication using the Wire library (documentation on the Wiring website). Note that these pins are not in the same location as the I^2C pins on the Duemilanove or Diecimila.

The Mega2560 has 16 analog inputs, each of which provide 10 bits of resolution (i.e. 1024 different values). By default they measure from ground to 5 volts, though is it possible to change the upper end of their range using the AREF pin and analogReference() function.

There are a couple of other pins on the board:

- **AREF.** Reference voltage for the analog inputs. Used with analogReference().

- **Reset.** Bring this line LOW to reset the microcontroller. Typically used to add a reset button to shields which block the one on the board.

Communication

The Arduino Mega2560 has a number of facilities for communicating with a computer, another Arduino, or other microcontrollers. The ATmega2560 provides four hardware UARTs for TTL (5V) serial communication. An ATmega8U2 on the board channels one of these over USB and provides a virtual com port to software on the computer (Windows machines will need a .inf file, but OSX and Linux machines will recognize the board as a COM port automatically. The Arduino software includes a serial monitor which allows simple textual data to be sent to and from the board. The RX and TX LEDs on the board will flash when data is being transmitted via the ATmega8U2 chip and USB connection to the computer (but not for serial communication on pins 0 and 1).

A SoftwareSerial library allows for serial communication on any of the Mega2560's digital pins.

The ATmega2560 also supports I2C (TWI) and SPI communication. The Arduino software includes a Wire library to simplify use of the I2C bus; see the documentation on the Wiring website for details. For SPI communication, use the SPI library.

Programming

The Arduino Mega can be programmed with the Arduino software (download). For details, see the reference and tutorials.

The ATmega2560 on the Arduino Mega comes preburned with a bootloader that allows you to upload new code to it without the use of an external hardware programmer. It communicates using the original STK500 protocol (reference, C header files).

You can also bypass the bootloader and program the microcontroller through the ICSP (In-Circuit Serial Programming) header; see these instructions for details.

The ATmega8U2 firmware source code is available in the Arduino repository. The ATmega8U2 is loaded with a DFU bootloader, which can be activated by connecting the solder jumper on the back of the board (near the map of Italy) and then resetting the 8U2. You can then use Atmel's FLIP software (Windows) or the DFU programmer (Mac OS X and Linux) to load a new firmware. Or you can use the ISP header with an external programmer (overwriting the DFU bootloader). See this user-contributed tutorial for more information.

Automatic (Software) Reset

Rather then requiring a physical press of the reset button before an upload, the Arduino Mega2560 is designed in a way that allows it to be reset by software running on a connected computer. One of the hardware flow control lines (DTR) of the ATmega8U2 is connected to the reset line of the ATmega2560 via a 100 nanofarad capacitor. When this line is asserted (taken low), the reset line drops long enough to reset the chip. The Arduino software uses this capability to allow you to upload code by simply pressing the upload button in the Arduino environment. This means that the bootloader can

have a shorter timeout, as the lowering of DTR can be well-coordinated with the start of the upload.

This setup has other implications. When the Mega2560 is connected to either a computer running Mac OS X or Linux, it resets each time a connection is made to it from software (via USB). For the following half-second or so, the bootloader is running on the Mega2560. While it is programmed to ignore malformed data (i.e. anything besides an upload of new code), it will intercept the first few bytes of data sent to the board after a connection is opened. If a sketch running on the board receives one-time configuration or other data when it first starts, make sure that the software with which it communicates waits a second after opening the connection and before sending this data.

The Mega2560 contains a trace that can be cut to disable the auto-reset. The pads on either side of the trace can be soldered together to re-enable it. It's labeled "RESET-EN". You may also be able to disable the auto-reset by connecting a 110 ohm resistor from 5V to the reset line; see this forum thread for details.

USB Overcurrent Protection

The Arduino Mega2560 has a resettable polyfuse that protects your computer's USB ports from shorts and overcurrent. Although most computers provide their own internal protection, the fuse provides an extra layer of protection. If more than 500 mA is applied to the USB port, the fuse will automatically break the connection until the short or overload is removed.

Physical Characteristics and Shield Compatibility

The maximum length and width of the Mega2560 PCB are 4 and 2.1 inches respectively, with the USB connector and power jack extending beyond the former dimension. Three screw holes allow the board to be attached to a surface or case. Note that the distance between digital pins 7 and 8 is 160 mil (0.16"), not an even multiple of the 100 mil spacing of the other pins.

The Mega2560 is designed to be compatible with most shields designed for the Uno, Diecimila or Duemilanove. Digital pins 0 to 13 (and the adjacent AREF and GND pins), analog inputs 0 to 5, the power header, and ICSP header are all in equivalent locations. Further the main UART (serial port) is located on the same pins (0 and 1), as are external interrupts 0 and 1 (pins 2 and 3 respectively). SPI is available through the ICSP header on both the Mega2560 and Duemilanove / Diecimila. *Please note that I^2C is not located on the same pins on the Mega (20 and 21) as the Duemilanove / Diecimila (analog inputs 4 and 5).*

A.2 H-Bridge IC

SLRS008C – SEPTEMBER 1986 – REVISED NOVEMBER 2004

- **Featuring Unitrode L293 and L293D Products Now From Texas Instruments**
- **Wide Supply-Voltage Range: 4.5 V to 36 V**
- **Separate Input-Logic Supply**
- **Internal ESD Protection**
- **Thermal Shutdown**
- **High-Noise-Immunity Inputs**
- **Functionally Similar to SGS L293 and SGS L293D**
- **Output Current 1 A Per Channel (600 mA for L293D)**
- **Peak Output Current 2 A Per Channel (1.2 A for L293D)**
- **Output Clamp Diodes for Inductive Transient Suppression (L293D)**

L293 . . . N OR NE PACKAGE
L293D . . . NE PACKAGE
(TOP VIEW)

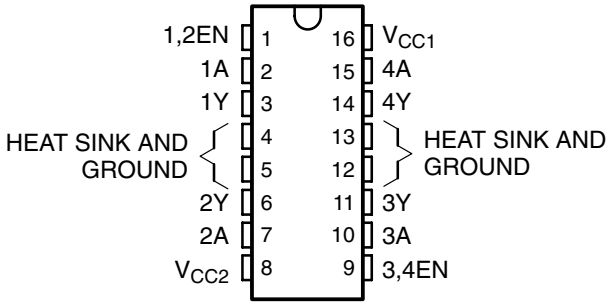

L293 . . . DWP PACKAGE
(TOP VIEW)

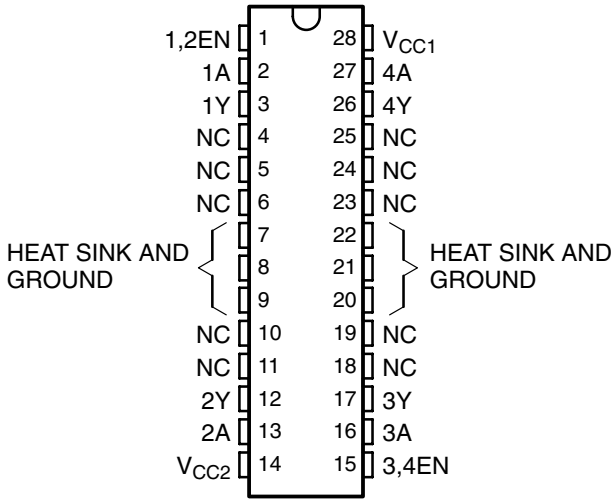

description/ordering information

The L293 and L293D are quadruple high-current half-H drivers. The L293 is designed to provide bidirectional drive currents of up to 1 A at voltages from 4.5 V to 36 V. The L293D is designed to provide bidirectional drive currents of up to 600-mA at voltages from 4.5 V to 36 V. Both devices are designed to drive inductive loads such as relays, solenoids, dc and bipolar stepping motors, as well as other high-current/high-voltage loads in positive-supply applications.

All inputs are TTL compatible. Each output is a complete totem-pole drive circuit, with a Darlington transistor sink and a pseudo-Darlington source. Drivers are enabled in pairs, with drivers 1 and 2 enabled by 1,2EN and drivers 3 and 4 enabled by 3,4EN. When an enable input is high, the associated drivers are enabled, and their outputs are active and in phase with their inputs. When the enable input is low, those drivers are disabled, and their outputs are off and in the high-impedance state. With the proper data inputs, each pair of drivers forms a full-H (or bridge) reversible drive suitable for solenoid or motor applications.

ORDERING INFORMATION

T_A	PACKAGE†		ORDERABLE PART NUMBER	TOP-SIDE MARKING
0 C to 70 C	HSOP (DWP)	Tube of 20	L293DWP	L293DWP
	PDIP (N)	Tube of 25	L293N	L293N
	PDIP (NE)	Tube of 25	L293NE	L293NE
		Tube of 25	L293DNE	L293DNE

† Package drawings, standard packing quantities, thermal data, symbolization, and PCB design guidelines are available at www.ti.com/sc/package.

description/ordering information (continued)

On the L293, external high-speed output clamp diodes should be used for inductive transient suppression.

A V_{CC1} terminal, separate from V_{CC2}, is provided for the logic inputs to minimize device power dissipation.

The L293and L293D are characterized for operation from 0 C to 70 C.

block diagram

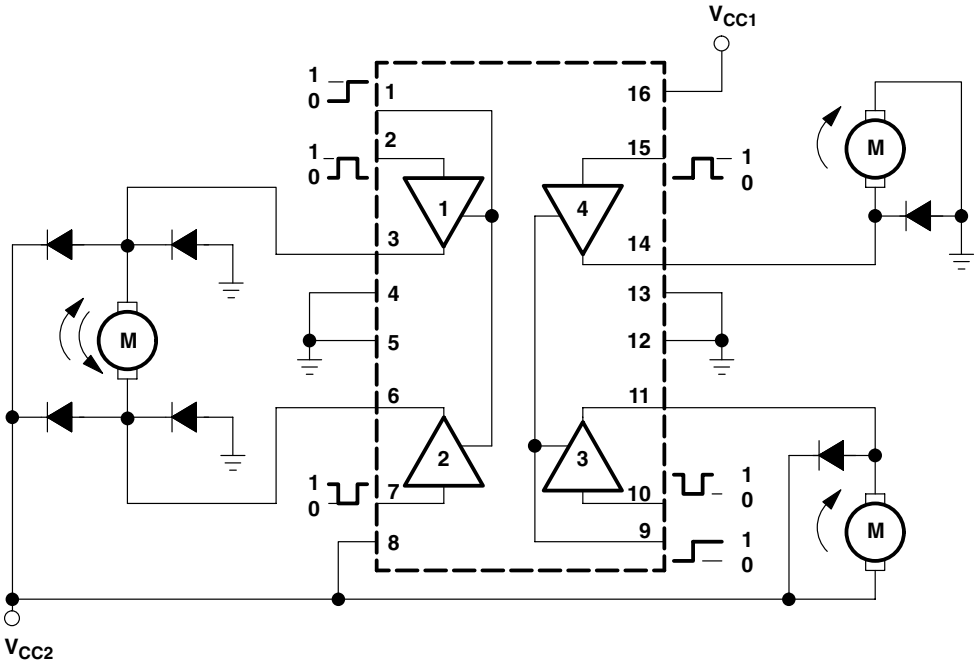

NOTE: Output diodes are internal in L293D.

FUNCTION TABLE
(each driver)

INPUTS†		OUTPUT
A	EN	Y
H	H	H
L	H	L
X	L	Z

H = high level, L = low level, X = irrelevant,
Z = high impedance (off)

† In the thermal shutdown mode, the output is in the high-impedance state, regardless of the input levels.

logic diagram

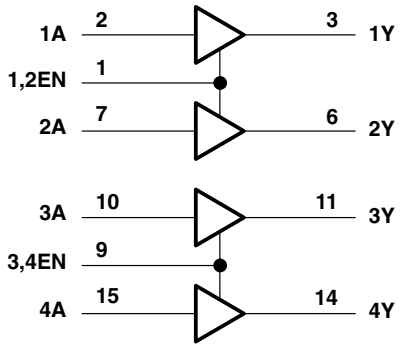

schematics of inputs and outputs (L293)

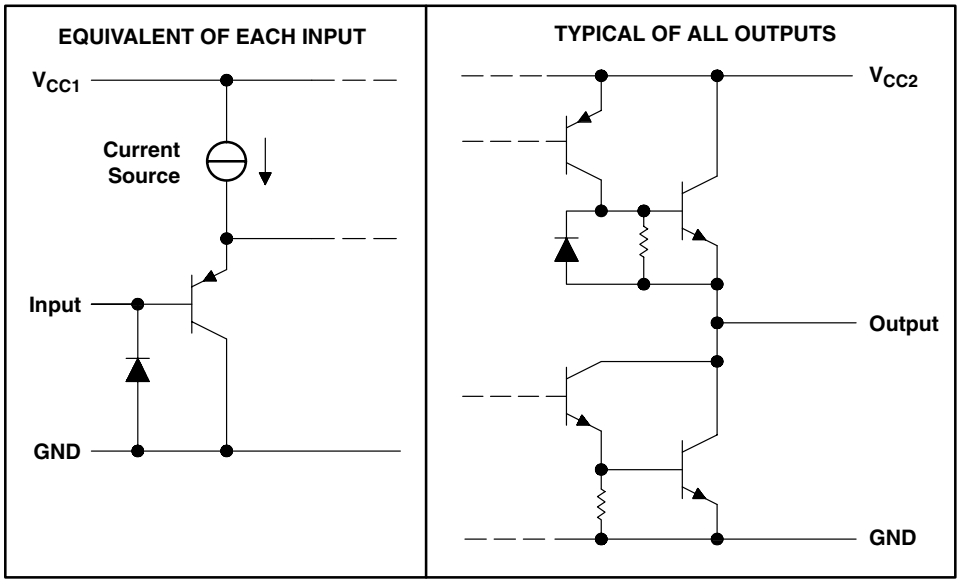

schematics of inputs and outputs (L293D)

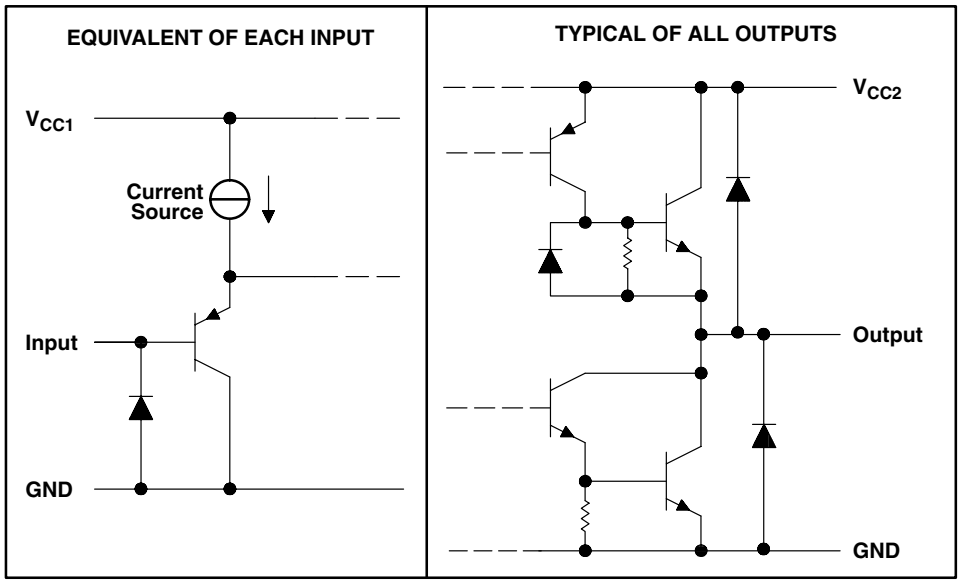

absolute maximum ratings over operating free-air temperature range (unless otherwise noted)†

Supply voltage, V_{CC1} (see Note 1) . . . . . 36 V
Output supply voltage, V_{CC2} . . . . . 36 V
Input voltage, V_I . . . . . 7 V
Output voltage range, V_O . . . . . –3 V to V_{CC2} + 3 V
Peak output current, I_O (nonrepetitive, t ≤ 5 ms): L293 . . . . . ±2 A
Peak output current, I_O (nonrepetitive, t ≤ 100 s): L293D . . . . . ±1.2 A
Continuous output current, I_O: L293 . . . . . ±1 A
Continuous output current, I_O: L293D . . . . . ±600 mA
Package thermal impedance, θ_{JA} (see Notes 2 and 3): DWP package . . . . . TBD C/W
N package . . . . . 67 C/W
NE package . . . . . TBD C/W
Maximum junction temperature, T_J . . . . . 150 C
Storage temperature range, T_{stg} . . . . . –65 C to 150 C

† Stresses beyond those listed under “absolute maximum ratings” may cause permanent damage to the device. These are stress ratings only, and functional operation of the device at these or any other conditions beyond those indicated under “recommended operating conditions” is not implied. Exposure to absolute-maximum-rated conditions for extended periods may affect device reliability.

NOTES: 1. All voltage values are with respect to the network ground terminal.
2. Maximum power dissipation is a function of $T_J(max)$, θ_{JA}, and T_A. The maximum allowable power dissipation at any allowable ambient temperature is $P_D = (T_J(max) – T_A)/\theta_{JA}$. Operating at the absolute maximum T_J of 150 C can affect reliability.
3. The package thermal impedance is calculated in accordance with JESD 51-7.

recommended operating conditions

			MIN	MAX	UNIT
	Supply voltage	V_{CC1}	4.5	7	V
		V_{CC2}	V_{CC1}	36	
V_{IH}	High-level input voltage	$V_{CC1} \le 7$ V	2.3	V_{CC1}	V
		$V_{CC1} \ge 7$ V	2.3	7	V
V_{IL}	Low-level output voltage		–0.3†	1.5	V
T_A	Operating free-air temperature		0	70	C

† The algebraic convention, in which the least positive (most negative) designated minimum, is used in this data sheet for logic voltage levels.

electrical characteristics, V_{CC1} = 5 V, V_{CC2} = 24 V, T_A = 25 C

PARAMETER			TEST CONDITIONS		MIN	TYP	MAX	UNIT
V_{OH}	High-level output voltage		L293: I_{OH} = –1 A L293D: I_{OH} = –0.6 A		V_{CC2} – 1.8	V_{CC2} – 1.4		V
V_{OL}	Low-level output voltage		L293: I_{OL} = 1 A L293D: I_{OL} = 0.6 A			1.2	1.8	V
V_{OKH}	High-level output clamp voltage		L293D: I_{OK} = –0.6 A			V_{CC2} + 1.3		V
V_{OKL}	Low-level output clamp voltage		L293D: I_{OK} = 0.6 A			1.3		V
I_{IH}	High-level input current	A	V_I = 7 V			0.2	100	A
		EN				0.2	10	
I_{IL}	Low-level input current	A	V_I = 0			–3	–10	A
		EN				–2	–100	
I_{CC1}	Logic supply current		I_O = 0	All outputs at high level		13	22	mA
				All outputs at low level		35	60	
				All outputs at high impedance		8	24	
I_{CC2}	Output supply current		I_O = 0	All outputs at high level		14	24	mA
				All outputs at low level		2	6	
				All outputs at high impedance		2	4	

switching characteristics, V_{CC1} = 5 V, V_{CC2} = 24 V, T_A = 25 C

PARAMETER		TEST CONDITIONS	L293NE, L293DNE			UNIT
			MIN	TYP	MAX	
t_{PLH}	Propagation delay time, low-to-high-level output from A input	C_L = 30 pF, See Figure 1		800		ns
t_{PHL}	Propagation delay time, high-to-low-level output from A input			400		ns
t_{TLH}	Transition time, low-to-high-level output			300		ns
t_{THL}	Transition time, high-to-low-level output			300		ns

switching characteristics, V_{CC1} = 5 V, V_{CC2} = 24 V, T_A = 25 C

PARAMETER		TEST CONDITIONS	L293DWP, L293N L293DN			UNIT
			MIN	TYP	MAX	
t_{PLH}	Propagation delay time, low-to-high-level output from A input	C_L = 30 pF, See Figure 1		750		ns
t_{PHL}	Propagation delay time, high-to-low-level output from A input			200		ns
t_{TLH}	Transition time, low-to-high-level output			100		ns
t_{THL}	Transition time, high-to-low-level output			350		ns

PARAMETER MEASUREMENT INFORMATION

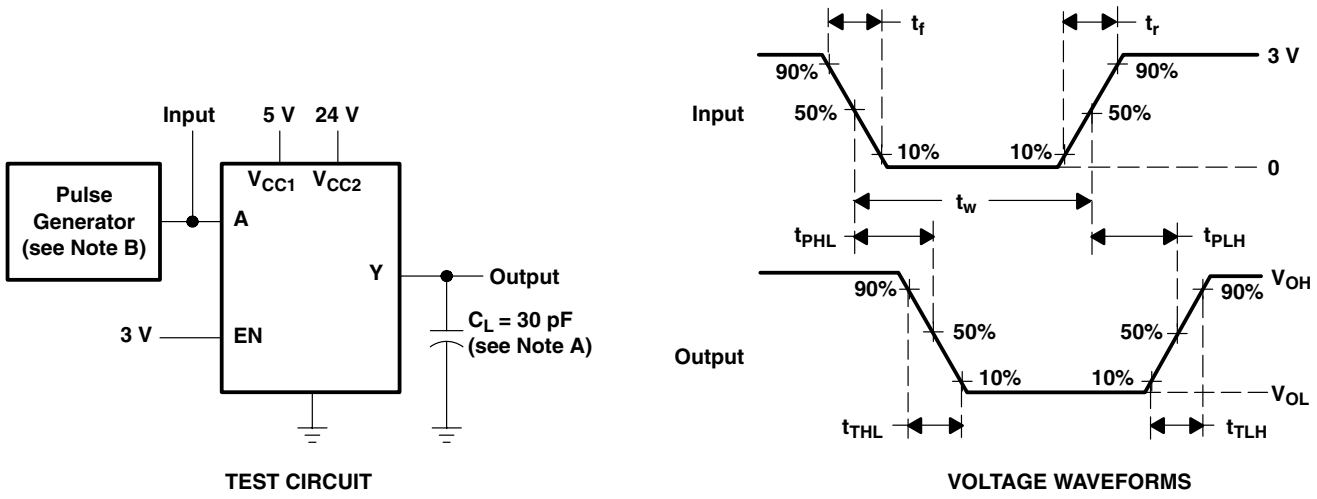

TEST CIRCUIT **VOLTAGE WAVEFORMS**

NOTES: A. C_L includes probe and jig capacitance.
B. The pulse generator has the following characteristics: $t_r \le 10$ ns, $t_f \le 10$ ns, $t_w = 10$ s, PRR = 5 kHz, $Z_O = 50\ \Omega$.

Figure 1. Test Circuit and Voltage Waveforms

APPLICATION INFORMATION

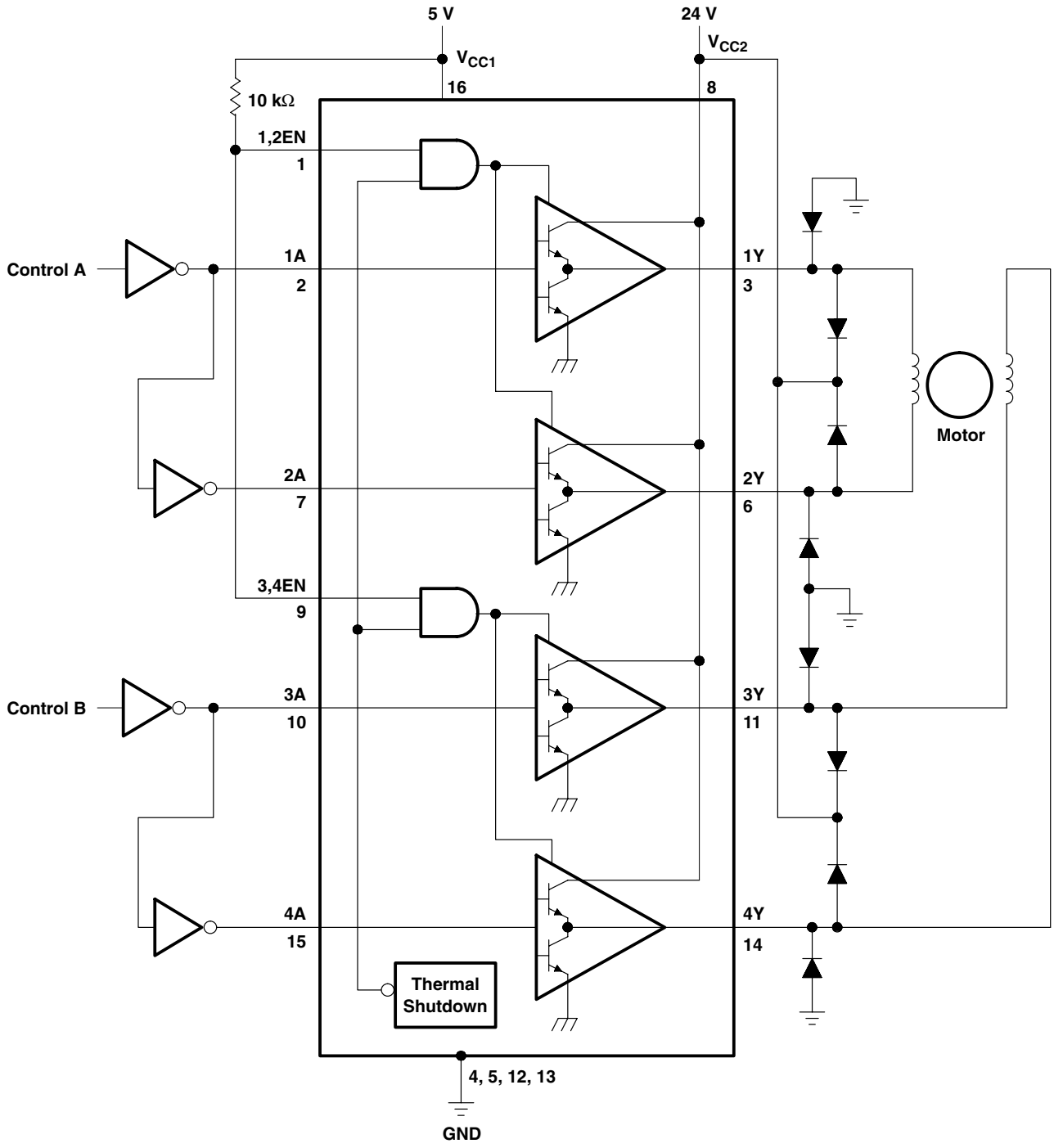

Figure 2. Two-Phase Motor Driver (L293)

APPLICATION INFORMATION

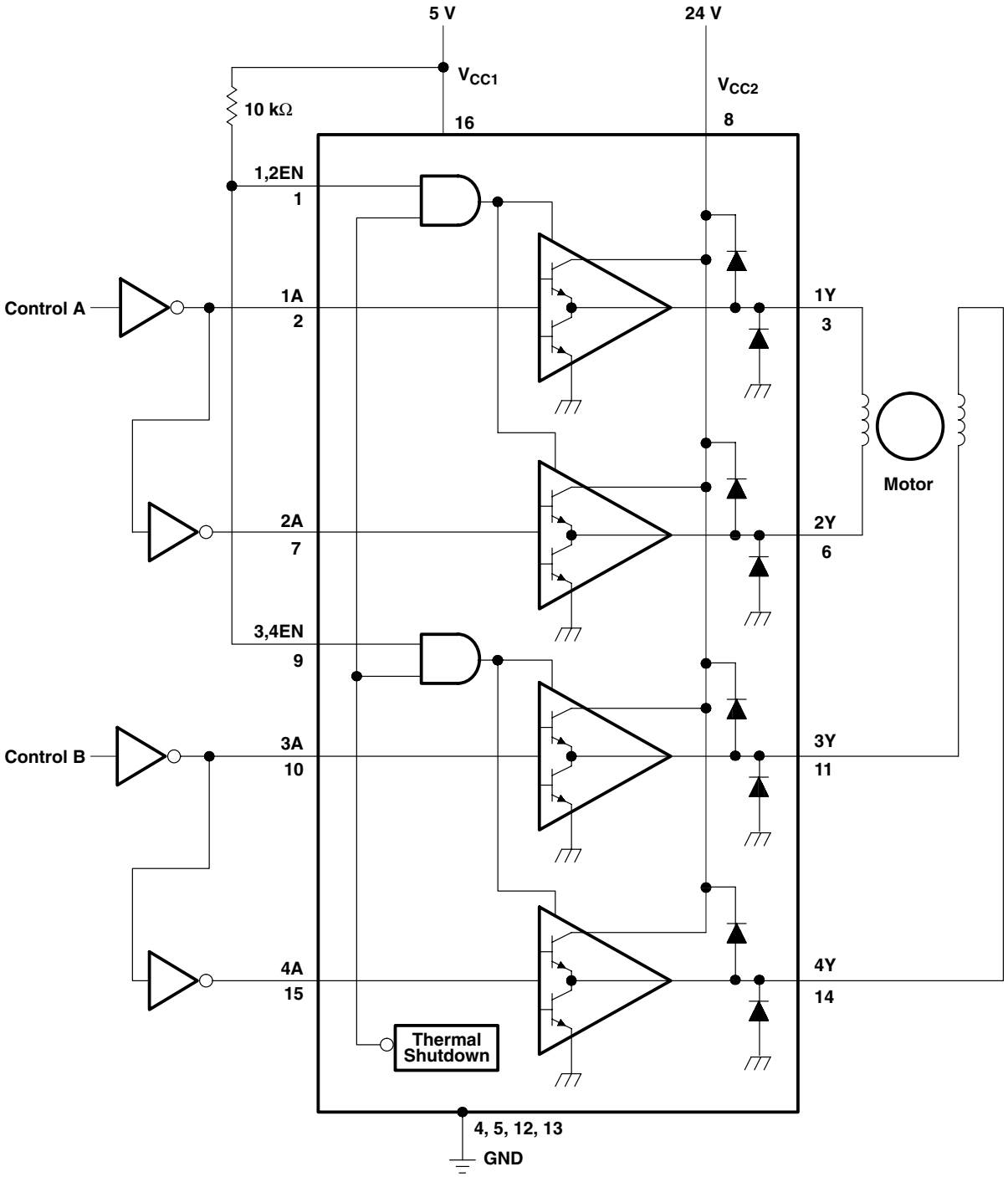

Figure 3. Two-Phase Motor Driver (L293D)

A.3 Stepper Motors

5718 HIGH TORQUE MOTOR

- High Torque
- Wide Selection of Windings
- *Can be Customized for:*
  - Maximum Torque *(see page 9)*
  - Cables & Assemblies *(see pages 21/70)*
  - Shafts *(see pages 21/69)*
  - Drivers & Controllers *(see page 99-108)*
  - Maximum Efficiency *(see page 12)*

SPECIFICATIONS

	Dimension "A" Max	Model #	Rated Current (Amps/Phase)	Holding Torque (oz-in)	Holding Torque (N-m)	Resistance (Ohms/Phase)	Inductance (mH/Phase)	Inertia (oz-in²)	Weight (Lbs.)	Number of Leads
BIPOLAR	1.74" 44.2 mm	5718X-01S	1.40	100.0	0.71	2.8	5.6	0.70	1.05	4
		5718X-01P	2.80	100.0	0.71	0.7	1.4	0.70	1.05	4
		5718X-05S	0.70	100.0	0.71	10.0	16.8	0.70	1.05	4
		5718X-05P	1.40	100.0	0.71	2.5	4.2	0.70	1.05	4
		5718X-15S	2.10	100.0	0.71	1.2	1.6	0.70	1.05	4
		5718X-15P	4.20	100.0	0.71	0.3	0.4	0.70	1.05	4
	2.22" 56.4 mm	5718M-02S	2.10	173.0	1.22	1.8	5.2	1.50	1.50	4
		5718M-02P	4.20	173.0	1.22	0.5	1.4	1.50	1.50	4
		5718M-04S	0.70	173.0	1.22	14.0	42.3	1.50	1.50	4
		5718M-04P	1.40	173.0	1.22	3.5	10.6	1.50	1.50	4
		5718M-05S	1.40	173.0	1.22	3.6	10.0	1.50	1.50	4
		5718M-05P	2.80	173.0	1.22	0.9	2.5	1.50	1.50	4
	3.1" 78.7 mm	5718L-01S	1.40	294.0	2.08	4.5	15.3	2.60	2.35	4
		5718L-01P	2.80	294.0	2.08	1.1	3.8	2.60	2.35	4
		5718L-03S	2.10	294.0	2.08	2.4	7.0	2.60	2.35	4
		5718L-03P	4.20	294.0	2.08	0.6	1.8	2.60	2.35	4
		5718L-04S	3.27	294.0	2.08	1.0	5.2	2.60	2.35	4
		5718L-04P	6.54	294.0	2.08	0.3	1.3	2.60	2.35	4

	Dimension "A" Max	Model #	Rated Current (Amps/Phase)	Holding Torque (oz-in)	Holding Torque (N-m)	Resistance (Ohms/Phase)	Inductance (mH/Phase)	Inertia (oz-in²)	Weight (Lbs.)	Number of Leads
UNIPOLAR	1.74" 44.2 mm	5718X-01	2.00	72.0	0.51	1.4	1.4	0.70	1.05	6
		5718X-05	1.00	72.0	0.51	5.0	4.2	0.70	1.05	6
		5718X-15	3.00	72.0	0.51	0.6	0.4	0.70	1.05	6
	2.22" 56.4 mm	5718M-02	3.00	130.0	0.92	0.9	1.4	1.50	1.50	6
		5718M-04	1.00	130.0	0.92	7.0	10.6	1.50	1.50	6
		5718M-05	2.00	130.0	0.92	1.8	2.5	1.50	1.50	6
	3.1" 78.2 mm	5718L-01	2.00	210.0	1.48	2.3	3.8	2.60	2.35	6
		5718L-03	3.00	210.0	1.48	1.2	1.8	2.60	2.35	6
		5718L-04	4.67	210.0	1.48	0.5	1.3	2.60	2.35	6

- Please complete our application data sheet on page 116 for different windings.
- Call Lin Engineering for additional bipolar torque curves.
- Performance, use, and appearance specifications of the products listed here are subject to change without notice.
- For operating temperatures, see page 114.
- All specifications are approximations. Please contact Lin Engineering for more details.

DIMENSIONS

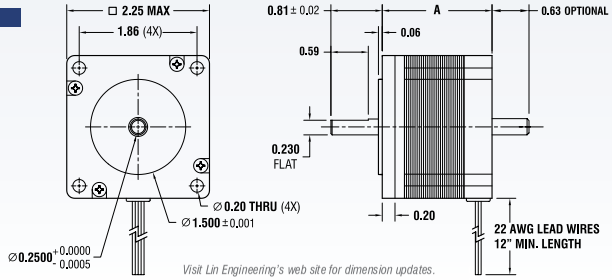

Visit Lin Engineering's web site for dimension updates.

TORQUE CURVES

5718X-01S 24VDC, 1,4 Amps/Phase, Bipolar Series, 1/2 Stepping
5718X-01P 24VDC, 2,8 Amps/Phase, Bipolar Parallel, 1/2 Stepping

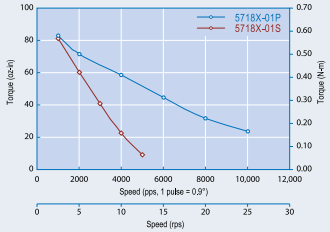

5718X-05S 24VDC, 0,7 Amps/Phase, Bipolar Series, 1/2 Stepping
5718X-05P 24VDC, 1,4 Amps/Phase, Bipolar Parallel, 1/2 Stepping

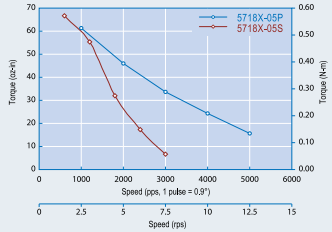

5718X-15S 24VDC, 2,1 Amps/Phase, Bipolar Series, 1/2 Stepping
5718X-15P 24VDC, 4,2 Amps/Phase, Bipolar Parallel, 1/2 Stepping

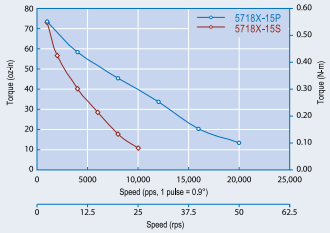

5718M-02S 24VDC, 2,1 Amps/Phase, Bipolar Series, 1/2 Stepping
5718M-02P 24VDC, 4,2 Amps/Phase, Bipolar Parallel, 1/2 Stepping

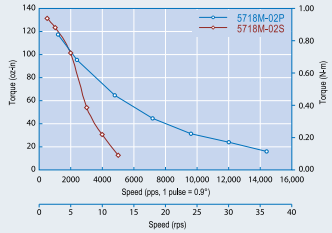

5718M-04S 24VDC, 0,7 Amps/Phase, Bipolar Series, 1/2 Stepping
5718M-04P 24VDC, 1,4 Amps/Phase, Bipolar Parallel, 1/2 Stepping

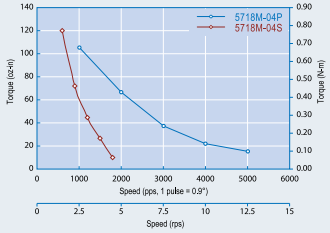

5718M-05S 24VDC, 1,4 Amps/Phase, Bipolar Series, 1/2 Stepping
5718M-05P 24VDC, 2,8 Amps/Phase, Bipolar Parallel, 1/2 Stepping

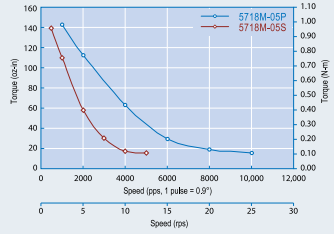

5718L-01S 24VDC, 1,4 Amps/Phase, Bipolar Series, 1/2 Stepping
5718L-01P 24VDC, 2,8 Amps/Phase, Bipolar Parallel, 1/2 Stepping

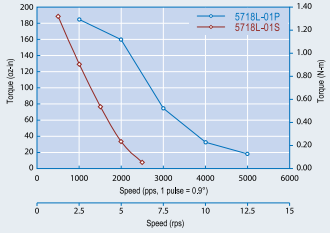

5718L-03S 24VDC, 2,1 Amps/Phase, Bipolar Series, 1/2 Stepping
5718L-03P 24VDC, 4,2 Amps/Phase, Bipolar Parallel, 1/2 Stepping

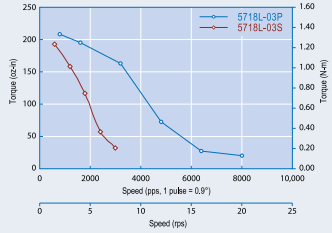

AVAILABLE OPTIONS

A.4 MOSFET (PNP)

P-Channel Enhancement-Mode Transistor

Product Summary

$V_{(BR)DSS}$ (V)	$r_{DS(on)}$ (Ω)	I_D (A)
–100	0.20	–20

TO-220AB

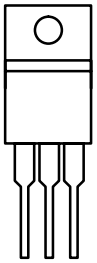

G D S

Drain Connected to Tab

Top View

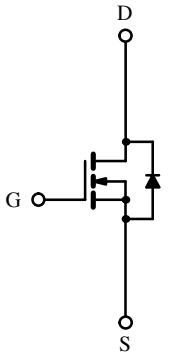

N-Channel MOSFET

Absolute Maximum Ratings (T_C = 25°C Unless Otherwise Noted)

Parameter		Symbol	Limit	Unit
Drain-Source Voltage		V_{DS}	–100	V
Gate-Source Voltage		V_{GS}	± 20	
Continuous Drain Current (T_J = 150°C)	T_C = 25°C	I_D	–20	A
	T_C = 100°C		–12	
Pulsed Drain Current		I_{DM}	–80	
Avalanche Current		I_{AR}	–20	
Repetitive Avalanche Energy[a]	L = 0.05 mH	E_{AR}	20	mJ
Maximum Power Dissipation	T_C = 25°C	P_D	125	W
	T_C = 100°C		50	
Operating Junction and Storage Temperature Range		T_J, T_{stg}	–55 to 150	°C
Lead Temperature ($^1/_{16}$" from case for 10 sec.)		T_L	300	

Thermal Resistance Ratings

Parameter	Symbol	Typical	Maximum	Unit
Maximum Junction-to-Ambient	R_{thJA}		80	°C/W
Maximum Junction-to-Case	R_{thJC}		1.0	
Case-to-Sink	R_{thCS}	1.0		

Notes:
a. Duty cycle ≤ 1%

Subsequent updates to this data sheet may be obtained via facsimile by calling Siliconix FaxBack, 1-408-970-5600. Please request FaxBack document #70287.

Specifications (T_J = 25°C Unless Otherwise Noted)

Parameter	Symbol	Test Condition	Limit			Unit
			Min	Typ[a]	Max	
Static						
Drain-Source Breakdown Voltage	$V_{(BR)DSS}$	V_{GS} = 0 V, I_D = –250 µA	–100			V
Gate Threshold Voltage	$V_{GS(th)}$	V_{DS} = V_{GS}, I_D = –250 µA	–2.0		–4.0	
Gate-Body Leakage	I_{GSS}	V_{DS} = 0 V, V_{GS} = ± 12 V			± 100	nA
Zero Gate Voltage Drain Current	I_{DSS}	V_{DS} = –80 V, V_{GS} = 0 V			–250	µA
		V_{DS} = –80 V, V_{GS} = 0 V, T_J = 125°C			–1000	
On-State Drain Current[b]	$I_{D(on)}$	V_{DS} = –10 V, V_{GS} = –10 V	–20			A
Drain-Source On-State Resistance[b]	$r_{DS(on)}$	V_{GS} = –10 V, I_D = –12 A		0.15	0.20	Ω
		V_{GS} = –10 V, I_D = –12 A, T_J = 125°C		0.24	0.30	
Forward Transconductance[b]	g_{fs}	V_{DS} = –15 V, I_D = –12 A	4.8	6.7		S
Dynamic						
Input Capacitance	C_{iss}	V_{GS} = 0 V, V_{DS} = –25 V, f = 1 MHz		1300		pF
Output Capacitance	C_{oss}			700		
Reverse Transfer Capacitance	C_{rss}			250		
Total Gate Charge[c]	Q_g	V_{DS} = –50 V, V_{GS} = –10 V, I_D = –20 A		47	60	nC
Gate-Source Charge[c]	Q_{gs}			10	18	
Gate-Drain Charge[c]	Q_{gd}			27	36	
Turn-On Delay Time[c]	$t_{d(on)}$	V_{DD} = –40 V, R_L = 2.1 Ω I_D ≃ –19 A, V_{GEN} = –10 V, R_G = 4.7 Ω		10	30	ns
Rise Time[c]	t_r			50	80	
Turn-Off Delay Time[c]	$t_{d(off)}$			25	80	
Fall Time[c]	t_f			15	60	
Source-Drain Diode Ratings and Characteristics						
Continuous Current	I_S				–20	A
Pulsed Current	I_{SM}				–80	
Diode Forward Voltage[b]	V_{SD}	I_F = –20 A, V_{GS} = 0 V			–1.7	V
Reverse Recovery Time	t_{rr}	I_F = –20 A, di/dt = 100 A/µs		150		ns
Reverse Recovery Charge	Q_{rr}			0.3		µC

Notes:
a. For design aid only; not subject to production testing.
b. Pulse test; pulse width ≤ 300 µs, duty cycle ≤ 2%.
c. Independent of operating temperature.

Typical Characteristics (25°C Unless Otherwise Noted)

Output Characteristics

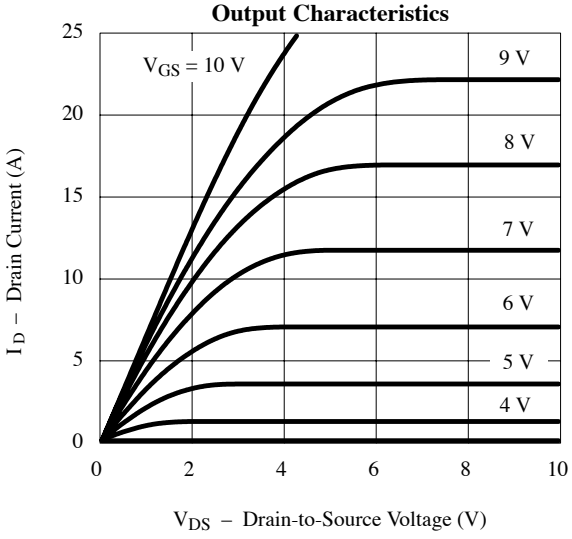

Transfer Characteristics

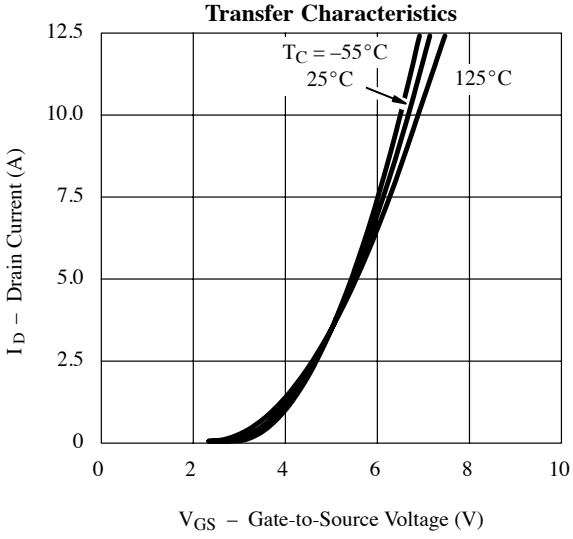

Transconductance

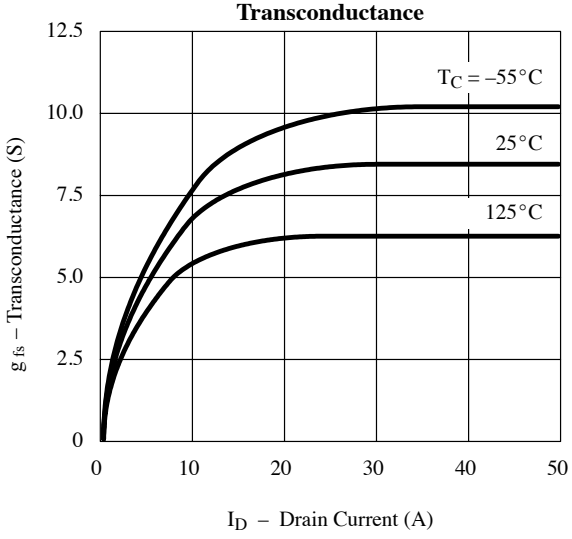

On-Resistance vs. Drain Current

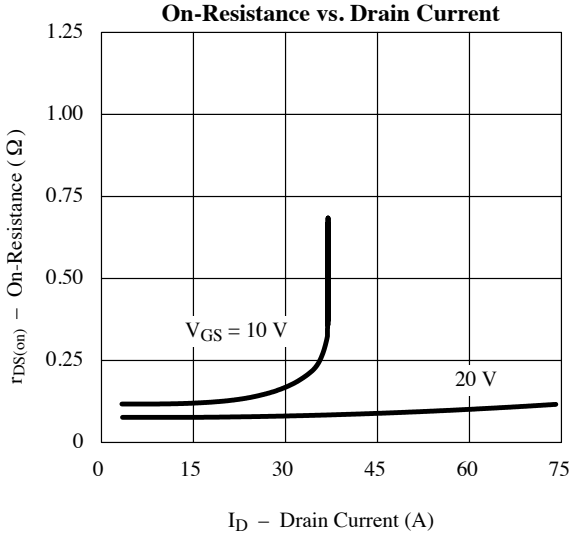

Capacitance

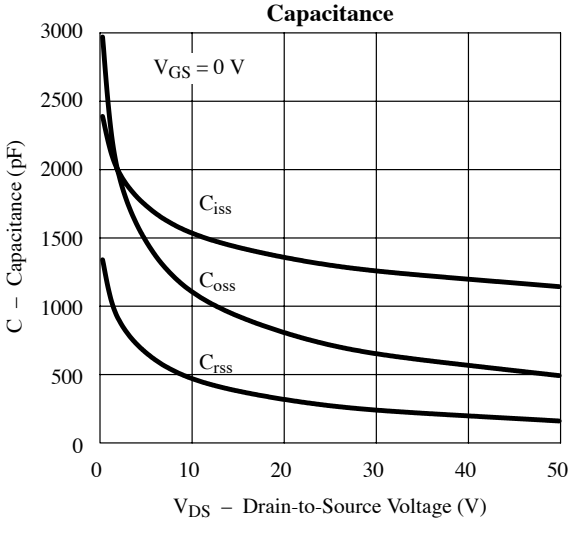

Gate Charge

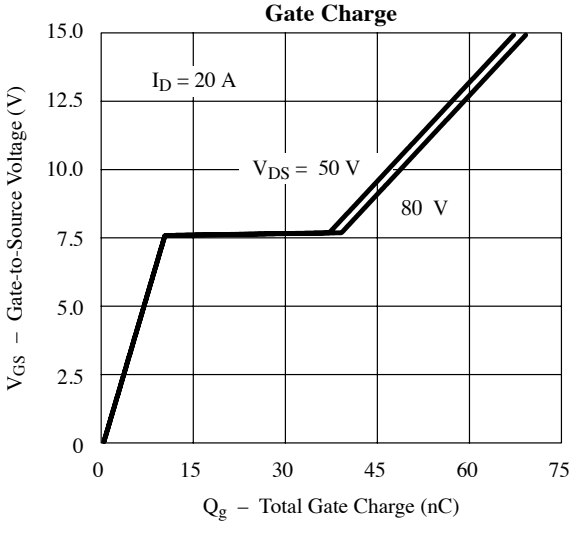

A.5 MOSFET (NPN)

FEATURES

- ♦ Avalanche Rugged Technology
- ♦ Rugged Gate Oxide Technology
- ♦ Lower Input Capacitance
- ♦ Improved Gate Charge
- ♦ Extended Safe Operating Area
- ♦ 175°C Operating Temperature
- ♦ Lower Leakage Current: 10μA (Max.) @ V_{DS} = 60V
- ♦ Lower $R_{DS(ON)}$: 0.020Ω (Typ.)

BV_{DSS} = 60 V

$R_{DS(on)}$ = 0.024Ω

I_D = 50 A

TO-220

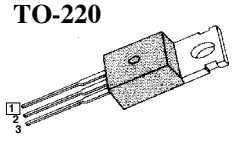

1.Gate 2. Drain 3. Source

Absolute Maximum Ratings

Symbol	Characteristic	Value	Units
V_{DSS}	Drain-to-Source Voltage	60	V
I_D	Continuous Drain Current (T_C=25°C)	50	A
	Continuous Drain Current (T_C=100°C)	35.4	
I_{DM}	Drain Current-Pulsed (1)	200	A
V_{GS}	Gate-to-Source Voltage	±20	V
E_{AS}	Single Pulsed Avalanche Energy (2)	857	mJ
I_{AR}	Avalanche Current (1)	50	A
E_{AR}	Repetitive Avalanche Energy (1)	12.6	mJ
dv/dt	Peak Diode Recovery dv/dt (3)	5.5	V/ns
P_D	Total Power Dissipation (T_C=25°C)	126	W
	Linear Derating Factor	0.84	W/°C
T_J , T_{STG}	Operating Junction and Storage Temperature Range	- 55 to +175	°C
T_L	Maximum Lead Temp. for Soldering Purposes, 1/8. from case for 5-seconds	300	

Thermal Resistance

Symbol	Characteristic	Typ.	Max.	Units
$R_{\theta JC}$	Junction-to-Case	--	1.19	°C/W
$R_{\theta CS}$	Case-to-Sink	0.5	--	
$R_{\theta JA}$	Junction-to-Ambient	--	62.5	

FAIRCHILD SEMICONDUCTOR™

Electrical Characteristics (T_C=25°C unless otherwise specified)

Symbol	Characteristic	Min.	Typ.	Max.	Units	Test Condition
BV_{DSS}	Drain-Source Breakdown Voltage	60	--	--	V	V_{GS}=0V,I_D=250μA
$\Delta BV/\Delta T_J$	Breakdown Voltage Temp. Coeff.	--	0.063	--	V/°C	I_D=250μA ***See Fig 7***
$V_{GS(th)}$	Gate Threshold Voltage	2.0	--	4.0	V	V_{DS}=5V,I_D=250μA
I_{GSS}	Gate-Source Leakage , Forward	--	--	100	nA	V_{GS}=20V
	Gate-Source Leakage , Reverse	--	--	-100		V_{GS}=-20V
I_{DSS}	Drain-to-Source Leakage Current	--	--	10	μA	V_{DS}=60V
		--	--	100		V_{DS}=48V,T_C=150°C
$R_{DS(on)}$	Static Drain-Source On-State Resistance	--	--	0.024	Ω	V_{GS}=10V,I_D=25A (4)
g_{fs}	Forward Transconductance	--	32.6	--	℧	V_{DS}=30V,I_D=25A (4)
C_{iss}	Input Capacitance	--	1770	2300	pF	V_{GS}=0V,V_{DS}=25V,f =1MHz ***See Fig 5***
C_{oss}	Output Capacitance	--	590	680		
C_{rss}	Reverse Transfer Capacitance	--	220	255		
$t_{d(on)}$	Turn-On Delay Time	--	20	40	ns	V_{DD}=30V,I_D=50A, R_G=9.1Ω ***See Fig 13*** (4) (5)
t_r	Rise Time	--	16	40		
$t_{d(off)}$	Turn-Off Delay Time	--	68	140		
t_f	Fall Time	--	70	140		
Q_g	Total Gate Charge	--	64	83	nC	V_{DS}=48V,V_{GS}=10V, I_D=50A ***See Fig 6 & Fig 12*** (4) (5)
Q_{gs}	Gate-Source Charge	--	12.3	--		
Q_{gd}	Gate-Drain (. Miller.) Charge	--	23.6	--		

Source-Drain Diode Ratings and Characteristics

Symbol	Characteristic	Min.	Typ.	Max.	Units	Test Condition
I_S	Continuous Source Current	--	--	50	A	Integral reverse pn-diode in the MOSFET
I_{SM}	Pulsed-Source Current (1)	--	--	200		
V_{SD}	Diode Forward Voltage (4)	--	--	1.8	V	T_J=25°C,I_S=50A,V_{GS}=0V
t_{rr}	Reverse Recovery Time	--	85	--	ns	T_J=25°C,I_F=50A
Q_{rr}	Reverse Recovery Charge	--	0.24	--	μC	di_F/dt=100A/μs (4)

Notes;

(1) Repetitive Rating: Pulse Width Limited by Maximum Junction Temperature

(2) L=0.4mH, I_{AS}=50A, V_{DD}=25V, R_G=27Ω, Starting T_J=25°C

(3) I_{SD} ≤ 50A, di/dt ≤ 350A/μs, V_{DD} ≤ BV_{DSS} , Starting T_J=25°C

(4) Pulse Test : Pulse Width = 250μs, Duty Cycle ≤ 2%

(5) Essentially Independent of Operating Temperature

Fig 1. Output Characteristics

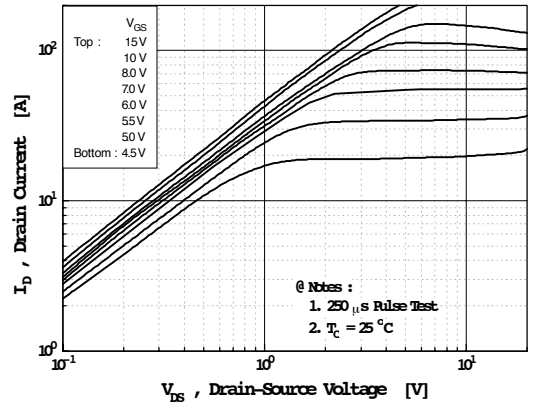

Fig 2. Transfer Characteristics

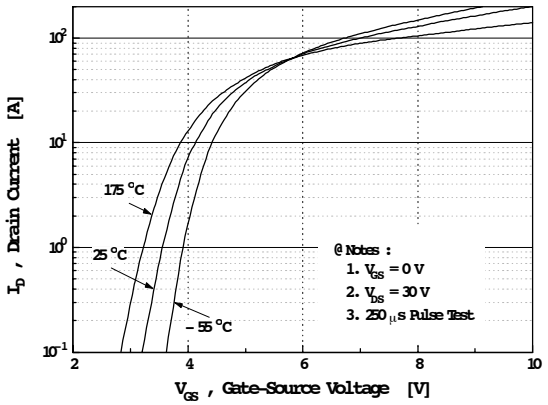

Fig 3. On-Resistance vs. Drain Current

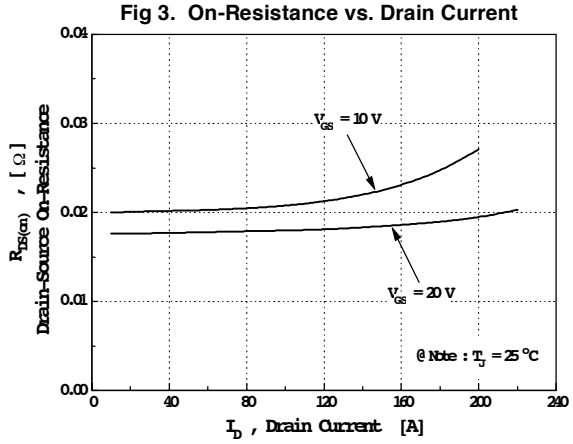

Fig 4. Source-Drain Diode Forward Voltage

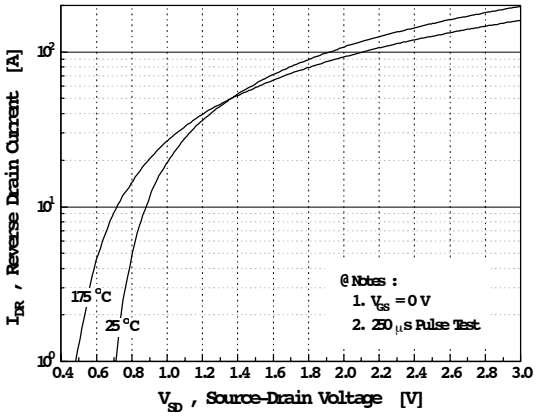

Fig 5. Capacitance vs. Drain-Source Voltage

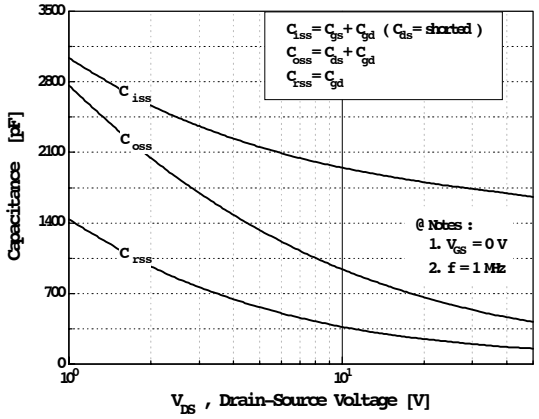

Fig 6. Gate Charge vs. Gate-Source Voltage

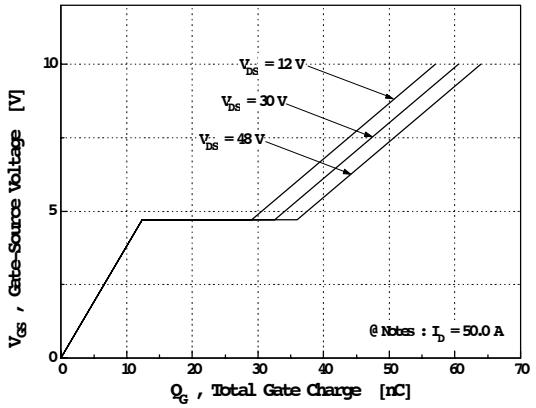

A.6 Photodiode

Silicon Photodiode

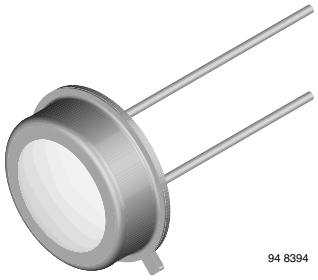

FEATURES

- Package type: leaded
- Package form: TO-5
- Dimensions (in mm): Ø 8.13
- Radiant sensitive area (in mm^2): 7.5
- High photo sensitivity
- Adapted to human eye responsivity
- Angle of half sensitivity: φ = ± 50°
- Hermetically sealed package
- Cathode connected to package
- Flat glass window
- Low dark current
- High shunt resistance
- High linearity
- Compliant to RoHS Directive 2002/95/EC and in accordance with WEEE 2002/96/EC

Pb-free

e4

RoHS COMPLIANT

DESCRIPTION

BPW21R is a planar Silicon PN photodiode in a hermetically sealed short TO-5 case, especially designed for high precision linear applications.

Due to its extremely high dark resistance, the short circuit photocurrent is linear over seven decades of illumination level.

On the other hand, there is a strictly logarithmic correlation between open circuit voltage and illumination over the same range.

The device is equipped with a flat glass window with built in color correction filter, giving an approximation to the spectral response of the human eye.

APPLICATIONS

- Sensor in exposure and color measuring purposes

PRODUCT SUMMARY			
COMPONENT	I_{ra} (µA)	φ (deg)	$\lambda_{0.5}$ (nm)
BPW21R	9	± 50	420 to 675

Note

- Test condition see table “Basic Characteristics”

ORDERING INFORMATION			
ORDERING CODE	PACKAGING	REMARKS	PACKAGE FORM
BPW21R	Bulk	MOQ: 500 pcs, 500 pcs/bulk	TO-5

Note

- MOQ: minimum order quantity

ABSOLUTE MAXIMUM RATINGS (T_{amb} = 25 °C, unless otherwise specified)				
PARAMETER	TEST CONDITION	SYMBOL	VALUE	UNIT
Reverse voltage		V_R	10	V
Power dissipation	$T_{amb} \leq 50$ °C	P_V	300	mW
Junction temperature		T_j	125	°C
Operating temperature range		T_{amb}	- 40 to + 125	°C
Storage temperature range		T_{stg}	- 40 to + 125	°C
Soldering temperature	t ≤ 5 s	T_{sd}	260	°C
Thermal resistance junction/ambient	Connected with Cu wire, 0.14 mm^2	R_{thJA}	250	K/W

BASIC CHARACTERISTICS (T_{amb} = 25 °C, unless otherwise specified)						
PARAMETER	**TEST CONDITION**	**SYMBOL**	**MIN.**	**TYP.**	**MAX.**	**UNIT**
Forward voltage	I_F = 50 mA	V_F		1.0	1.3	V
Breakdown voltage	I_R = 20 µA, E = 0	$V_{(BR)}$	10			V
Reverse dark current	V_R = 5 V, E = 0	I_{ro}		2	30	nA
Diode capacitance	V_R = 0 V, f = 1 MHz, E = 0	C_D		1.2		nF
	V_R = 5 V, f = 1 MHz, E = 0	C_D		400		pF
Dark resistance	V_R = 10 mV	R_D		38		GΩ
Open circuit voltage	E_A = 1 klx	V_o	280	450		mV
Temperature coefficient of V_o	E_A = 1 klx	TK_{Vo}		- 2		mV/K
Short circuit current	E_A = 1 klx	I_k	4.5	9		µA
Temperature coefficient of I_K	E_A = 1 klx	TK_{Ik}		- 0.05		%/K
Reverse light current	E_A = 1 klx, V_R = 5 V	I_{ra}	4.5	9		µA
Sensitivity	V_R = 5 V, E_A = 10^{-2} to 10^5 lx	S		9		nA/lx
Angle of half sensitivity		φ		± 50		deg
Wavelength of peak sensitivity		λ_p		565		nm
Range of spectral bandwidth		$\lambda_{0.5}$		420 to 675		nm
Rise time	V_R = 0 V, R_L = 1 kΩ, λ = 660 nm	t_r		3.1		µs
Fall time	V_R = 0 V, R_L = 1 kΩ, λ = 660 nm	t_f		3.0		µs

BASIC CHARACTERISTICS (T_{amb} = 25 °C, unless otherwise specified)

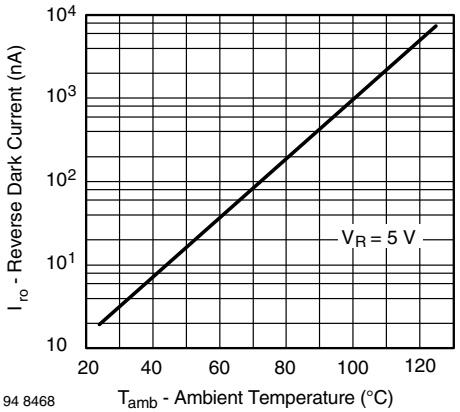

Fig. 1 - Reverse Dark Current vs. Ambient Temperature

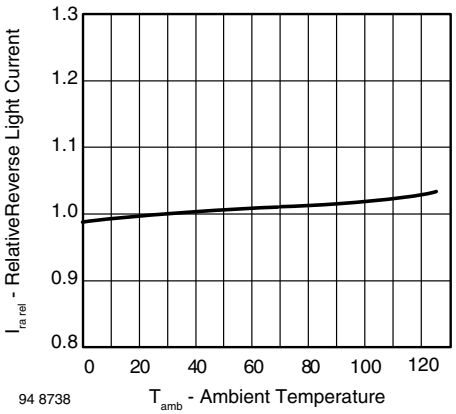

Fig. 2 - Relative Reverse Light Current vs. Ambient Temperature

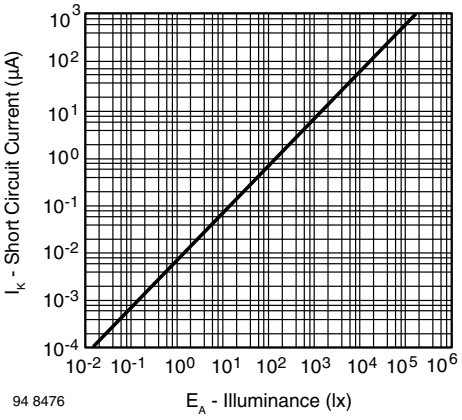

Fig. 3 - Short Circuit Current vs. Illuminance

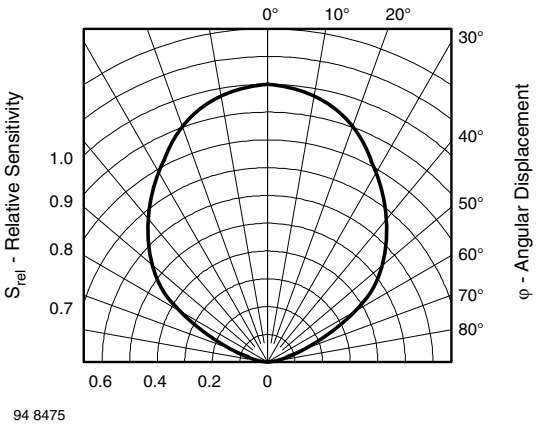

Fig. 6 - Relative Radiant Sensitivity vs. Angular Displacement

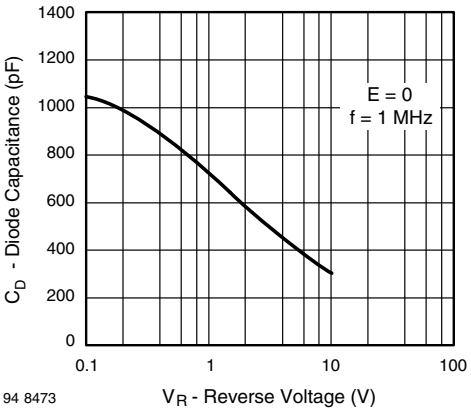

Fig. 4 - Diode Capacitance vs. Reverse Voltage

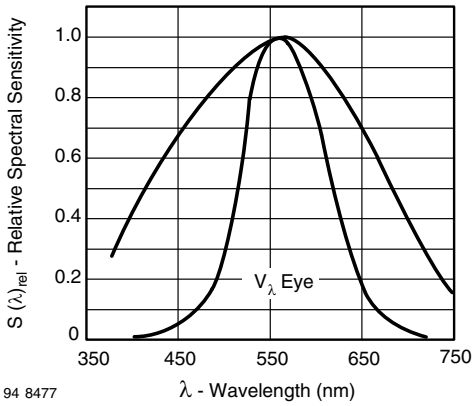

Fig. 5 - Relative Spectral Sensitivity vs. Wavelength

PACKAGE DIMENSIONS in millimeters

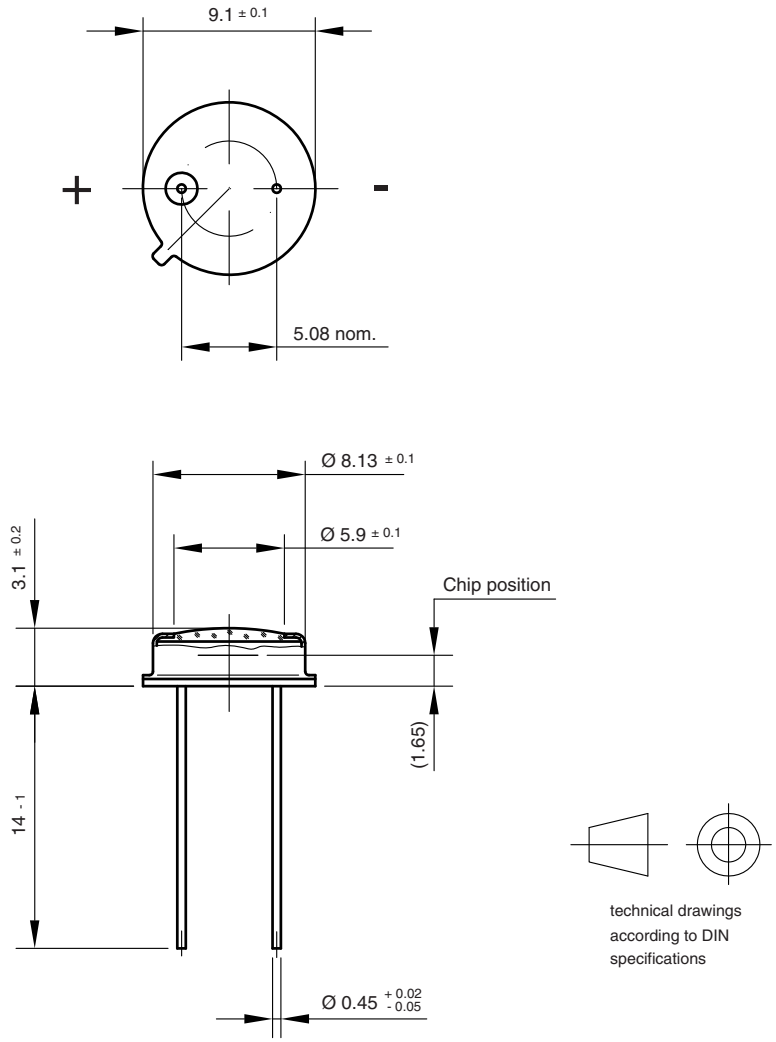

Drawing-No.: 6.511-5002.01-4
Issue:1; 01.07.96
96 12181

A.7 Real Time Clock

DS1307
64 x 8 Serial Real-Time Clock

www.maxim-ic.com

FEATURES

- Real-time clock (RTC) counts seconds, minutes, hours, date of the month, month, day of the week, and year with leap-year compensation valid up to 2100
- 56-byte, battery-backed, nonvolatile (NV) RAM for data storage
- Two-wire serial interface
- Programmable squarewave output signal
- Automatic power-fail detect and switch circuitry
- Consumes less than 500nA in battery backup mode with oscillator running
- Optional industrial temperature range: -40°C to +85°C
- Available in 8-pin DIP or SOIC
- Underwriters Laboratory (UL) recognized

ORDERING INFORMATION

DS1307	8-Pin DIP (300-mil)
DS1307Z	8-Pin SOIC (150-mil)
DS1307N	8-Pin DIP (Industrial)
DS1307ZN	8-Pin SOIC (Industrial)

PIN ASSIGNMENT

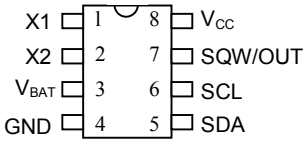

DS1307 8-Pin DIP (300-mil)

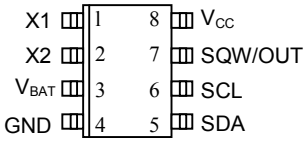

DS1307 8-Pin SOIC (150-mil)

PIN DESCRIPTION

V_{CC}	- Primary Power Supply
X1, X2	- 32.768kHz Crystal Connection
V_{BAT}	- +3V Battery Input
GND	- Ground
SDA	- Serial Data
SCL	- Serial Clock
SQW/OUT	- Square Wave/Output Driver

DESCRIPTION

The DS1307 Serial Real-Time Clock is a low-power, full binary-coded decimal (BCD) clock/calendar plus 56 bytes of NV SRAM. Address and data are transferred serially via a 2-wire, bi-directional bus. The clock/calendar provides seconds, minutes, hours, day, date, month, and year information. The end of the month date is automatically adjusted for months with fewer than 31 days, including corrections for leap year. The clock operates in either the 24-hour or 12-hour format with AM/PM indicator. The DS1307 has a built-in power sense circuit that detects power failures and automatically switches to the battery supply.

TYPICAL OPERATING CIRCUIT

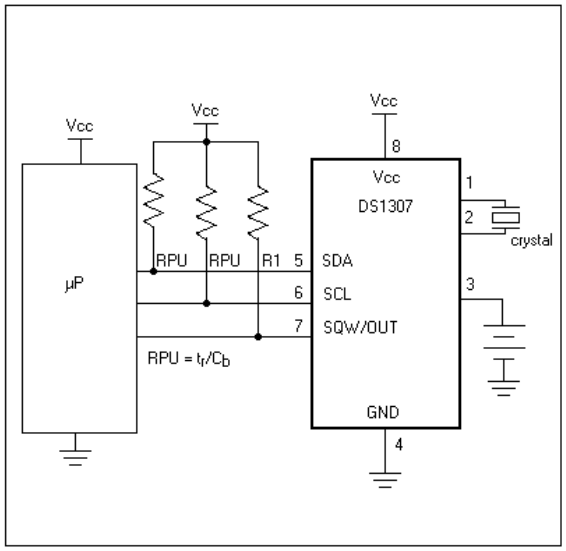

OPERATION

The DS1307 operates as a slave device on the serial bus. Access is obtained by implementing a START condition and providing a device identification code followed by a register address. Subsequent registers can be accessed sequentially until a STOP condition is executed. When V_{CC} falls below 1.25 x V_{BAT} the device terminates an access in progress and resets the device address counter. Inputs to the device will not be recognized at this time to prevent erroneous data from being written to the device from an out of tolerance system. When V_{CC} falls below V_{BAT} the device switches into a low-current battery backup mode. Upon power-up, the device switches from battery to V_{CC} when V_{CC} is greater than V_{BAT} + 0.2V and recognizes inputs when V_{CC} is greater than 1.25 x V_{BAT}. The block diagram in Figure 1 shows the main elements of the serial RTC.

DS1307 BLOCK DIAGRAM Figure 1

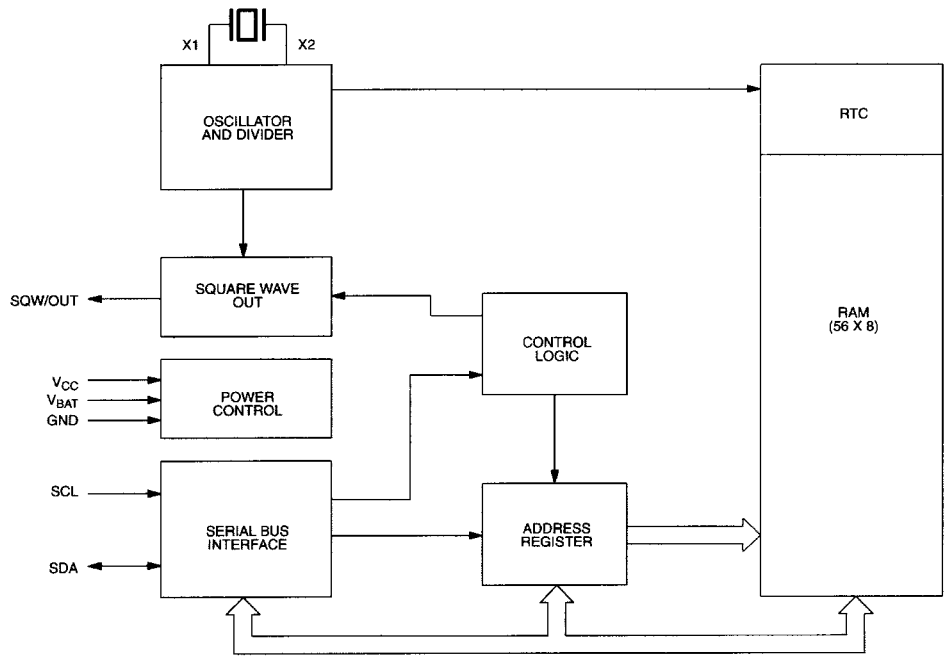

SIGNAL DESCRIPTIONS

V_{CC}, GND – DC power is provided to the device on these pins. V_{CC} is the +5V input. When 5V is applied within normal limits, the device is fully accessible and data can be written and read. When a 3V battery is connected to the device and V_{CC} is below 1.25 x V_{BAT}, reads and writes are inhibited. However, the timekeeping function continues unaffected by the lower input voltage. As V_{CC} falls below V_{BAT} the RAM and timekeeper are switched over to the external power supply (nominal 3.0V DC) at V_{BAT}.

V_{BAT} – Battery input for any standard 3V lithium cell or other energy source. Battery voltage must be held between 2.0V and 3.5V for proper operation. The nominal write protect trip point voltage at which access to the RTC and user RAM is denied is set by the internal circuitry as 1.25 x V_{BAT} nominal. A lithium battery with 48mAhr or greater will back up the DS1307 for more than 10 years in the absence of power at 25ºC. UL recognized to ensure against reverse charging current when used in conjunction with a lithium battery.

See "Conditions of Acceptability" at http://www.maxim-ic.com/TechSupport/QA/ntrl.htm**.**

SCL (Serial Clock Input) – SCL is used to synchronize data movement on the serial interface.

SDA (Serial Data Input/Output) – SDA is the input/output pin for the 2-wire serial interface. The SDA pin is open drain which requires an external pullup resistor.

SQW/OUT (Square Wave/Output Driver) – When enabled, the SQWE bit set to 1, the SQW/OUT pin outputs one of four square wave frequencies (1Hz, 4kHz, 8kHz, 32kHz). The SQW/OUT pin is open drain and requires an external pull-up resistor. SQW/OUT will operate with either Vcc or Vbat applied.

X1, X2 – Connections for a standard 32.768kHz quartz crystal. The internal oscillator circuitry is designed for operation with a crystal having a specified load capacitance (CL) of 12.5pF.

For more information on crystal selection and crystal layout considerations, please consult Application Note 58, "Crystal Considerations with Dallas Real-Time Clocks." The DS1307 can also be driven by an external 32.768kHz oscillator. In this configuration, the X1 pin is connected to the external oscillator signal and the X2 pin is floated.

RECOMMENDED LAYOUT FOR CRYSTAL

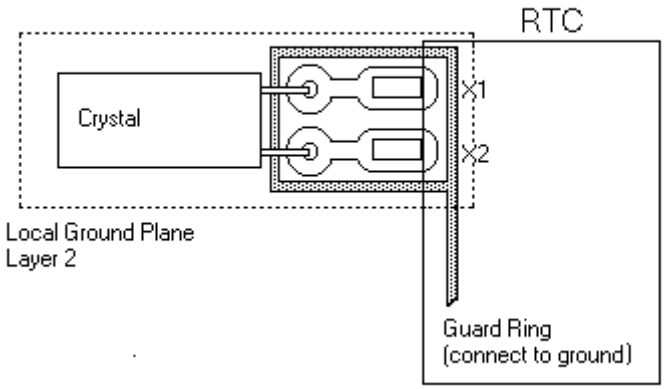

CLOCK ACCURACY

The accuracy of the clock is dependent upon the accuracy of the crystal and the accuracy of the match between the capacitive load of the oscillator circuit and the capacitive load for which the crystal was trimmed. Additional error will be added by crystal frequency drift caused by temperature shifts. External circuit noise coupled into the oscillator circuit may result in the clock running fast. See Application Note 58, "Crystal Considerations with Dallas Real-Time Clocks" for detailed information.

Please review Application Note 95, "Interfacing the DS1307 with a 8051-Compatible Microcontroller" for additional information.

RTC AND RAM ADDRESS MAP

The address map for the RTC and RAM registers of the DS1307 is shown in Figure 2. The RTC registers are located in address locations 00h to 07h. The RAM registers are located in address locations 08h to 3Fh. During a multi-byte access, when the address pointer reaches 3Fh, the end of RAM space, it wraps around to location 00h, the beginning of the clock space.

DS1307 ADDRESS MAP Figure 2

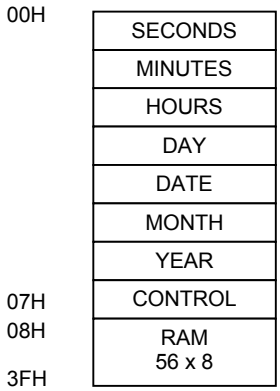

CLOCK AND CALENDAR

The time and calendar information is obtained by reading the appropriate register bytes. The RTC registers are illustrated in Figure 3. The time and calendar are set or initialized by writing the appropriate register bytes. The contents of the time and calendar registers are in the BCD format. Bit 7 of register 0 is the clock halt (CH) bit. When this bit is set to a 1, the oscillator is disabled. When cleared to a 0, the oscillator is enabled.

Please note that the initial power-on state of all registers is not defined. Therefore, it is important to enable the oscillator (CH bit = 0) during initial configuration.

The DS1307 can be run in either 12-hour or 24-hour mode. Bit 6 of the hours register is defined as the 12- or 24-hour mode select bit. When high, the 12-hour mode is selected. In the 12-hour mode, bit 5 is the AM/PM bit with logic high being PM. In the 24-hour mode, bit 5 is the second 10 hour bit (20-23 hours).

On a 2-wire START, the current time is transferred to a second set of registers. The time information is read from these secondary registers, while the clock may continue to run. This eliminates the need to re-read the registers in case of an update of the main registers during a read.

DS1307 TIMEKEEPER REGISTERS Figure 3

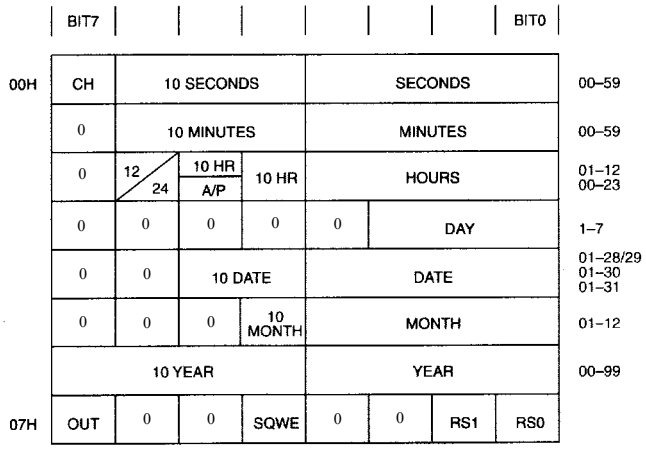

CONTROL REGISTER

The DS1307 control register is used to control the operation of the SQW/OUT pin.

BIT 7	BIT 6	BIT 5	BIT 4	BIT 3	BIT 2	BIT 1	BIT 0
OUT	0	0	SQWE	0	0	RS1	RS0

OUT (Output control): This bit controls the output level of the SQW/OUT pin when the square wave output is disabled. If SQWE = 0, the logic level on the SQW/OUT pin is 1 if OUT = 1 and is 0 if OUT = 0.

SQWE (Square Wave Enable): This bit, when set to a logic 1, will enable the oscillator output. The frequency of the square wave output depends upon the value of the RS0 and RS1 bits. With the square wave output set to 1Hz, the clock registers update on the falling edge of the square wave.

RS (Rate Select): These bits control the frequency of the square wave output when the square wave output has been enabled. Table 1 lists the square wave frequencies that can be selected with the RS bits.

SQUAREWAVE OUTPUT FREQUENCY Table 1

RS1	RS0	SQW OUTPUT FREQUENCY
0	0	1Hz
0	1	4.096kHz
1	0	8.192kHz
1	1	32.768kHz

2-WIRE SERIAL DATA BUS

The DS1307 supports a bi-directional, 2-wire bus and data transmission protocol. A device that sends data onto the bus is defined as a transmitter and a device receiving data as a receiver. The device that controls the message is called a master. The devices that are controlled by the master are referred to as slaves. The bus must be controlled by a master device that generates the serial clock (SCL), controls the bus access, and generates the START and STOP conditions. The DS1307 operates as a slave on the 2-wire bus. A typical bus configuration using this 2-wire protocol is show in Figure 4.

TYPICAL 2-WIRE BUS CONFIGURATION Figure 4

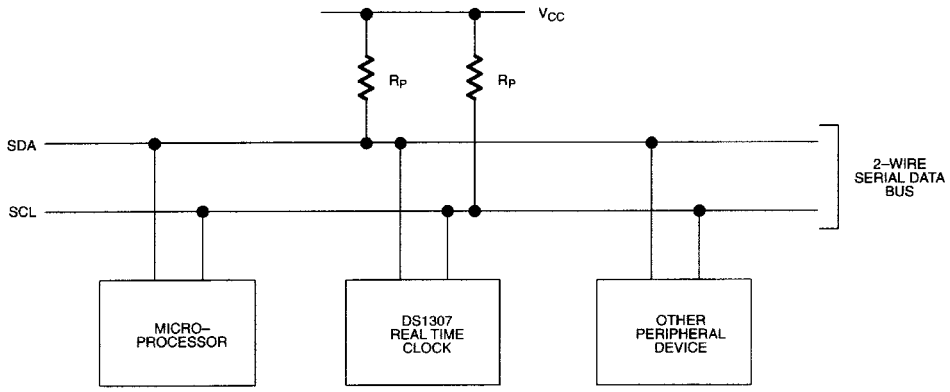

Figures 5, 6, and 7 detail how data is transferred on the 2-wire bus.

- Data transfer may be initiated only when the bus is not busy.
- During data transfer, the data line must remain stable whenever the clock line is HIGH. Changes in the data line while the clock line is high will be interpreted as control signals.

Accordingly, the following bus conditions have been defined:

Bus not busy: Both data and clock lines remain HIGH.

Start data transfer: A change in the state of the data line, from HIGH to LOW, while the clock is HIGH, defines a START condition.

Stop data transfer: A change in the state of the data line, from LOW to HIGH, while the clock line is HIGH, defines the STOP condition.

Data valid: The state of the data line represents valid data when, after a START condition, the data line is stable for the duration of the HIGH period of the clock signal. The data on the line must be changed during the LOW period of the clock signal. There is one clock pulse per bit of data.

Each data transfer is initiated with a START condition and terminated with a STOP condition. The number of data bytes transferred between START and STOP conditions is not limited, and is determined by the master device. The information is transferred byte-wise and each receiver acknowledges with a ninth bit. Within the 2-wire bus specifications a regular mode (100kHz clock rate) and a fast mode (400kHz clock rate) are defined. The DS1307 operates in the regular mode (100kHz) only.

Acknowledge: Each receiving device, when addressed, is obliged to generate an acknowledge after the reception of each byte. The master device must generate an extra clock pulse which is associated with this acknowledge bit.

A device that acknowledges must pull down the SDA line during the acknowledge clock pulse in such a way that the SDA line is stable LOW during the HIGH period of the acknowledge related clock pulse. Of course, setup and hold times must be taken into account. A master must signal an end of data to the slave by not generating an acknowledge bit on the last byte that has been clocked out of the slave. In this case, the slave must leave the data line HIGH to enable the master to generate the STOP condition.

DATA TRANSFER ON 2-WIRE SERIAL BUS Figure 5

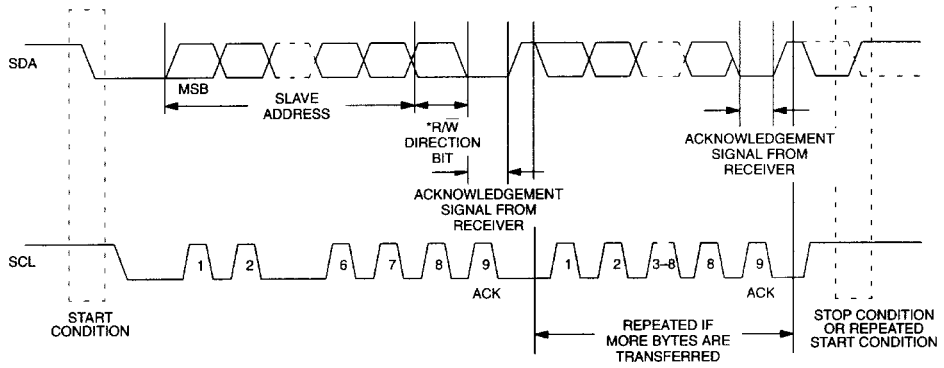

Depending upon the state of the R/$\overline{W}$ bit, two types of data transfer are possible:

1. **Data transfer from a master transmitter to a slave receiver.** The first byte transmitted by the master is the slave address. Next follows a number of data bytes. The slave returns an acknowledge bit after each received byte. Data is transferred with the most significant bit (MSB) first.

2. **Data transfer from a slave transmitter to a master receiver.** The first byte (the slave address) is transmitted by the master. The slave then returns an acknowledge bit. This is followed by the slave transmitting a number of data bytes. The master returns an acknowledge bit after all received bytes other than the last byte. At the end of the last received byte, a “not acknowledge” is returned.

The master device generates all of the serial clock pulses and the START and STOP conditions. A transfer is ended with a STOP condition or with a repeated START condition. Since a repeated START condition is also the beginning of the next serial transfer, the bus will not be released. Data is transferred with the most significant bit (MSB) first.

The DS1307 may operate in the following two modes:

1. **Slave receiver mode (DS1307 write mode):** Serial data and clock are received through SDA and SCL. After each byte is received an acknowledge bit is transmitted. START and STOP conditions are recognized as the beginning and end of a serial transfer. Address recognition is performed by hardware after reception of the slave address and *direction bit (See Figure 6). The address byte is the first byte received after the start condition is generated by the master. The address byte contains the 7 bit DS1307 address, which is 1101000, followed by the *direction bit ($R/\overline{W}$) which, for a write, is a 0. After receiving and decoding the address byte the device outputs an acknowledge on the SDA line. After the DS1307 acknowledges the slave address + write bit, the master transmits a register address to the DS1307 This will set the register pointer on the DS1307. The master will then begin transmitting each byte of data with the DS1307 acknowledging each byte received. The master will generate a stop condition to terminate the data write.

DATA WRITE – SLAVE RECEIVER MODE Figure 6

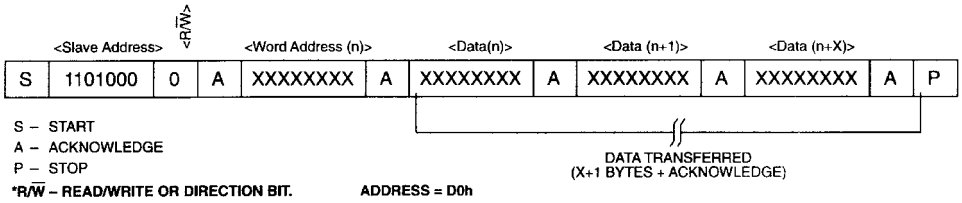

2. **Slave transmitter mode (DS1307 read mode):** The first byte is received and handled as in the slave receiver mode. However, in this mode, the *direction bit will indicate that the transfer direction is reversed. Serial data is transmitted on SDA by the DS1307 while the serial clock is input on SCL. START and STOP conditions are recognized as the beginning and end of a serial transfer (See Figure 7). The address byte is the first byte received after the start condition is generated by the master. The address byte contains the 7-bit DS1307 address, which is 1101000, followed by the *direction bit ($R/\overline{W}$) which, for a read, is a 1. After receiving and decoding the address byte the device inputs an acknowledge on the SDA line. The DS1307 then begins to transmit data starting with the register address pointed to by the register pointer. If the register pointer is not written to before the initiation of a read mode the first address that is read is the last one stored in the register pointer. The DS1307 must receive a "not acknowledge" to end a read.

DATA READ – SLAVE TRANSMITTER MODE Figure 7

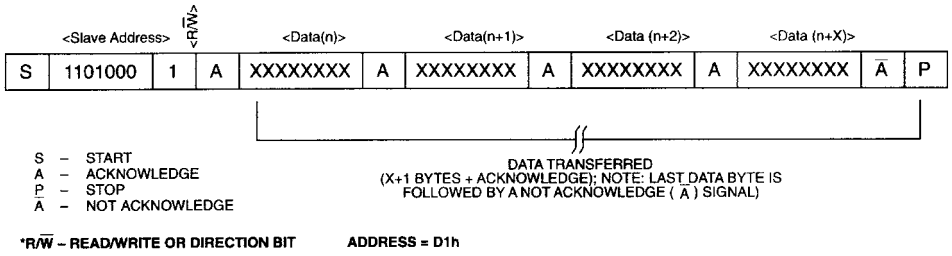

ABSOLUTE MAXIMUM RATINGS*

Voltage on Any Pin Relative to Ground	-0.5V to +7.0V
Storage Temperature	-55°C to +125°C
Soldering Temperature	260°C for 10 seconds DIP See JPC/JEDEC Standard J-STD-020A for Surface Mount Devices

* This is a stress rating only and functional operation of the device at these or any other conditions above those indicated in the operation sections of this specification is not implied. Exposure to absolute maximum rating conditions for extended periods of time may affect reliability.

Range	Temperature	V_{CC}
Commercial	0°C to +70°C	4.5V to 5.5V V_{CC1}
Industrial	-40°C to +85°C	4.5V to 5.5V V_{CC1}

RECOMMENDED DC OPERATING CONDITIONS

(Over the operating range*)

PARAMETER	SYMBOL	MIN	TYP	MAX	UNITS	NOTES
Supply Voltage	V_{CC}	4.5	5.0	5.5	V	
Logic 1	V_{IH}	2.2		V_{CC} + 0.3	V	
Logic 0	V_{IL}	-0.5		+0.8	V	
V_{BAT} Battery Voltage	V_{BAT}	2.0		3.5	V	

*Unless otherwise specified.

DC ELECTRICAL CHARACTERISTICS

(Over the operating range*)

PARAMETER	SYMBOL	MIN	TYP	MAX	UNITS	NOTES
Input Leakage (SCL)	I_{LI}			1	µA	
I/O Leakage (SDA & SQW/OUT)	I_{LO}			1	µA	
Logic 0 Output (I_{OL} = 5mA)	V_{OL}			0.4	V	
Active Supply Current	I_{CCA}			1.5	mA	7
Standby Current	I_{CCS}			200	µA	1
Battery Current (OSC ON); SQW/OUT OFF	I_{BAT1}		300	500	nA	2
Battery Current (OSC ON); SQW/OUT ON (32kHz)	I_{BAT2}		480	800	nA	
Power-Fail Voltage	V_{PF}	1.216 x V_{BAT}	1.25 x V_{BAT}	1.284 x V_{BAT}	V	8

*Unless otherwise specified.

AC ELECTRICAL CHARACTERISTICS

(Over the operating range*)

PARAMETER	SYMBOL	MIN	TYP	MAX	UNITS	NOTES
SCL Clock Frequency	f_{SCL}	0		100	kHz	
Bus Free Time Between a STOP and START Condition	t_{BUF}	4.7			µs	
Hold Time (Repeated) START Condition	$t_{HD:STA}$	4.0			µs	3
LOW Period of SCL Clock	t_{LOW}	4.7			µs	
HIGH Period of SCL Clock	t_{HIGH}	4.0			µs	
Set-up Time for a Repeated START Condition	$t_{SU:STA}$	4.7			µs	
Data Hold Time	$t_{HD:DAT}$	0			µs	4,5
Data Set-up Time	$t_{SU:DAT}$	250			ns	
Rise Time of Both SDA and SCL Signals	t_R			1000	ns	
Fall Time of Both SDA and SCL Signals	t_F			300	ns	
Set-up Time for STOP Condition	$t_{SU:STO}$	4.7			µs	
Capacitive Load for each Bus Line	C_B			400	pF	6
I/O Capacitance (T_A = 25ºC)	$C_{I/O}$		10		pF	
Crystal Specified Load Capacitance (T_A = 25ºC)			12.5		pF	

*Unless otherwise specified.

NOTES:

1. I_{CCS} specified with V_{CC} = 5.0V and SDA, SCL = 5.0V.
2. V_{CC} = 0V, V_{BAT} = 3V.
3. After this period, the first clock pulse is generated.
4. A device must internally provide a hold time of at least 300ns for the SDA signal (referred to the V_{IHMIN} of the SCL signal) in order to bridge the undefined region of the falling edge of SCL.
5. The maximum $t_{HD:DAT}$ has only to be met if the device does not stretch the LOW period (t_{LOW}) of the SCL signal.
6. C_B – Total capacitance of one bus line in pF.
7. I_{CCA} – SCL clocking at max frequency = 100kHz.
8. V_{PF} measured at V_{BAT} = 3.0V.

A.8 Linear Actuators

PRODUCT OVERVIEW

Based on proven Simplicity® linear bearing technology, the Uni-Guide contain Frelon GOLD® self-lubricating bearing material. This material results in no metal to metal contact, while dampening vibrations and shock loads. The Uni-Guide unique two-piece assembly eliminates tolerance stack up and the integrated lightweight packages can drop into existing applications making installation easy. Ideal for low cost automation, positioning tables and packaging equipment.

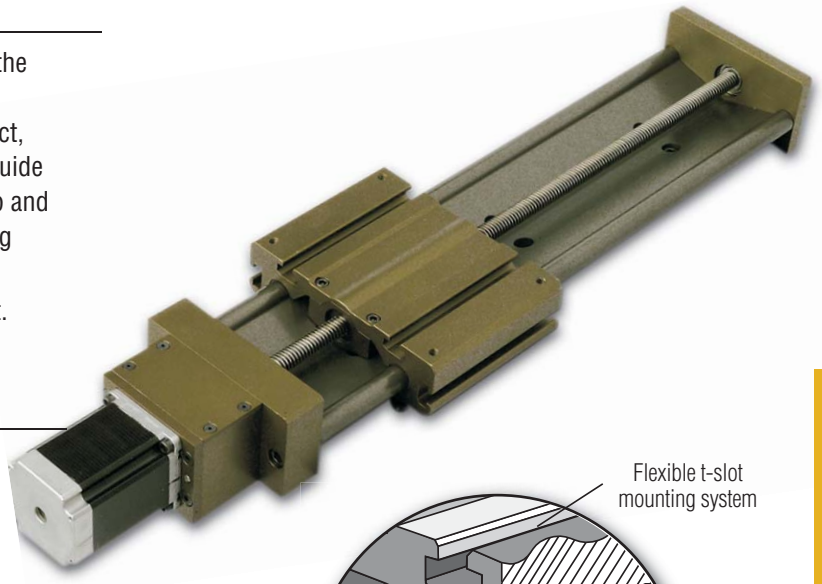

FEATURES & BENEFITS

- Two-piece assembly - lightweight and eliminates tolerance stack
- Self-lubricating - Frelon GOLD® provides low wear, low friction, and high strength
- Lengths up to 10' - butt-joinable for longer lenghts
- Mounting Flexibility
  - Pre-drilled rails
  - T-slots & mounting holes on carriages
  - Side or top mounting
- Easy drop in unit - no alignment needed
- Drive options
  - Ball
  - Lead screw (includes motor and drive)
  - Belt Driven
- Corrosion-Resistant - ideal in washdown environments
- Pre-engineered - ready to use

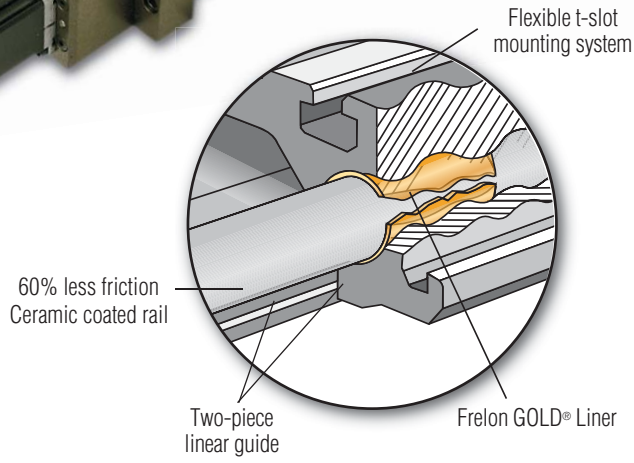

Uni-guide
MODULAR GUIDE SYSTEM

UNLIMITED DESIGN OPTIONS AND VERSATILITY.

ACCESSORIES*

- Hand Brake & Crank
- Vise Block
- Ratchet Pin
- Motor Mount
- End Block
- Pin Lock Clamp

APPLICATION EXAMPLES (Application examples require accessories. Contact manufacturer for availability)

Uni-Guide Ratchet

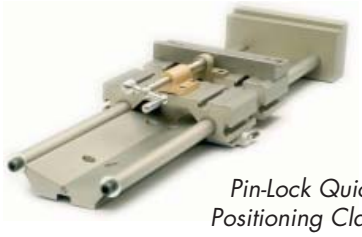

Pin-Lock Quick Positioning Clamp

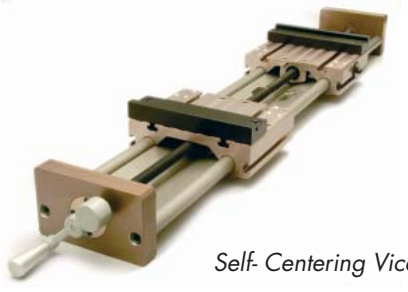

Self- Centering Vice

* Optional configurations and special carriages are available. Contact manfuracturer for availability.

STATIC LOADS WITH NO DRIVE MECHANISM

The numbers below are for guides only in a static condition. The drive mechanism selected (lead screw, ball screw, cylinder, etc.) becomes the limiting factor when calculating maximum load and speed capacities. The user is responsible for determining the maximum capacity for the complete system based on the manufacturer's data for their drive configuration.

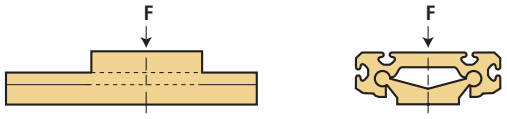

SIZE	F MAX LOAD (lbs.)	F MAX LOAD (N)
D075	500	2,224
D100	750	3,336
D125	1,000	4,448

SIZE	F MAX LOAD (lbs.)	F MAX LOAD (N)
D075	125	556
D100	190	845
D125	250	1,112

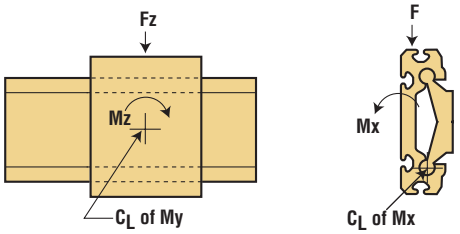

SIZE	F MAX LOAD (lbs.)	My (in./lbs.)	Mz (in./lbs.)	F MAX LOAD (N)	My (Nm)	Mz (Nm)
D075	250	340	350	1,112	38	40
D100	375	650	730	1,668	73	82
D125	500	1,200	1,225	2,224	136	138

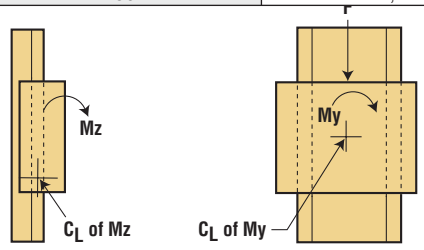

SIZE	My (in./lbs.)	Mx (in./lbs.)	My (Nm)	Mx (Nm)
D075	340	350	38	40
D100	650	730	73	82
D125	1,200	1,225	136	138

Designs must also operate within the following dynamic parameters:

- Maximum Loads (P) = from charts above
- Maximum Speed Dry (V) = 300 ft./min. (1.524 m/s)
- Maximum PV (pressure x velocity) = 20,000 (0.70 N/mm^2 x m/s)
- PV Example: Load = 85 psi
  Speed = 180 ft./min.
  PV = 85 x 180 = 15,300 PV

NOTE: Frelon GOLD® bearing material coefficient of friction is 0.125.

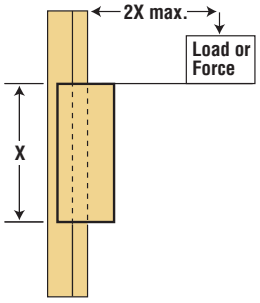

If the drive mechanism (lead screw, ball screw, cylinder, etc.) is centered on the carriage, the load may not exceed a 2:1 ratio to the length of the bearings or binding will occur.

ORDERING INFORMATION

D	L	M	100	A	CHB	–	xxx	P	M	–	X	# of Carriages

Series
D - Standard Uni-Guides

Carriage Options
No Entry - Standard Carriage
L - Extended Length Carriage

Mounting Hole Options
No Entry - Standard Inch Sizes
M - Metric Size Mounting Holes

Nominal Size
75mm, 100mm, 125mm
Based on mm from shaft center-to-center

Drive Options
No Entry - No Drive Mechanism
A - Right Hand Lead Screw with Standard Pitch
A1 - Right Hand Lead Screw with Optional Pitch (See pages 196-198 for specifications.)
Notes: Screw options require attaching collar.
Call the factory for other optional drive mechanisms.

Drive Mounting Options
No Entry - No Drive Mounting Options
H - Hand Crank
N - NEMA Standard Motor Mount (See pages 196-198 for specifications.)
HB - Handbrake (requires handcrank and screw)
CHB - Carriage Handbrake (not offered with screw driven options)

Overall Rail Length
"D" Series - enter length of rail in inches **xxx.xxx** (EX: 6" = 006.000)
"DM" Series - enter length of rail in mm **xxxx** (EX: 3500mm = 0350

Power and Control Options
No Entry - No Power Options
P - Standard Motor with Motor Mount, Programmable Drive, Cables and Software (must have "N" in Drive Mounting Option)
Note: Kits available for NEMA motor

Data Entry Option
No Entry - No Options
M - Optional MMI Keypad (Man-to-Machine Interface)

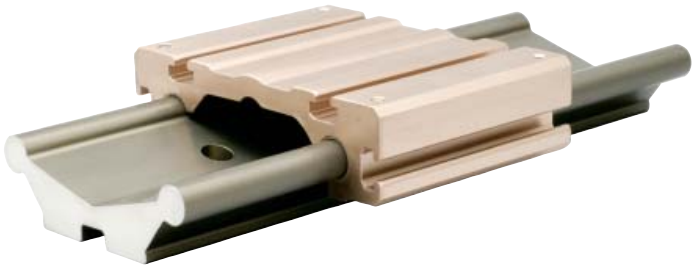

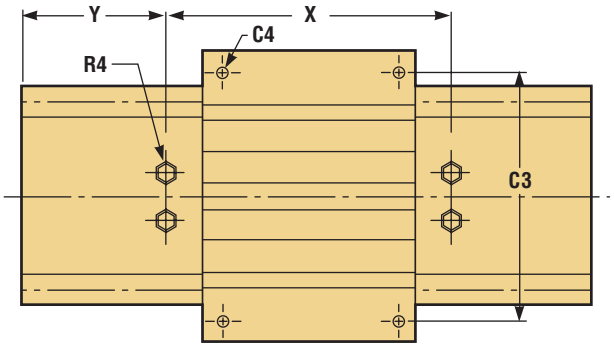

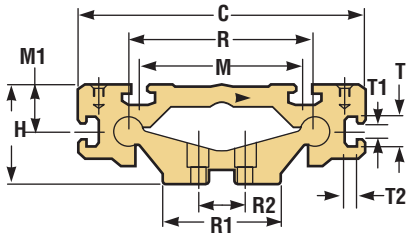

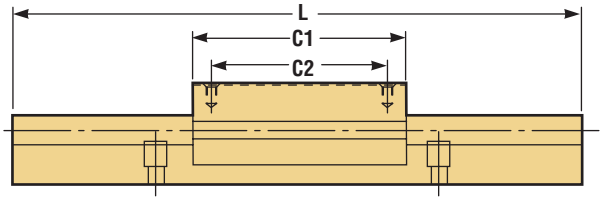

STANDARD INCH SERIES WITH NO DRIVE MECHANISM (inches)

PART NUMBER	R	R1	R2	X	R4 BOLT SIZE	Y	H	C	C1 STANDARD	C2 STANDARD	C1 EXTENDED	C2 EXTENDED	C3	C4 BOLT SIZE	M	M1	L MAX-FEET
D075-xxx	2.95	2	0.75	4	1/4	2	1.625	4.6	3.5	3	4.5	4	4	10-32	2.6	.819	
D100-xxx	3.94	2.6	1	6	5/16	3	2.125	6.1	4.5	3.75	6	5.25	5.25	1/4-20	3.5	1.02	12
D125-xxx	4.92	3.3	1.25		3/8	3	2.625	7.6	6	5.25	7.5	6.75	6.75	5/16-18	4.33	1.30	

CARRIAGE TYPES

PART NO.	DRILL	DEPTH	TAP	DEPTH
D075-xxx	.159	.534	10-32	.440
D100-xxx	.201	.750	1/4-20	.500
D125-xxx	.257		5/16-18	.625

T-SLOT INFORMATION (inches)

PART NO.	T	T1	T2
D075-xxx	.590	.256	.236
D100-xxx	.661	.319	.268
D125-xxx			

METRIC SERIES WITH NO DRIVE MECHANISM (mm)

PART NUMBER	R	R1	R2	X	R4 BOLT SIZE	Y	H	C	C1 STANDARD	C2 STANDARD	C1 EXTENDED	C2 EXTENDED	C3	C4 BOLT SIZE	M	M1	L MAX-FEET
DM075-xxx	75	51	20	120	M 6	60	41.3	117	85	73	110	98	105	M 5	66	16.5	
DM100-xxx	100	66	25	150	M 8	75	54	155	115	95	150	130	135	M 6	89	26	3.66m
DM125-xxx	125	84	30	200	M 10	100	66.7	193	150	130	190	170	175	M 8	110	33	

STANDARD LENGTHS CHART (inches)

PART NO.	8"	12"	16"	18"	20"	24"	28"	30"	32"	36"	40"	42"	48"
D075-xxx	X		X		X		X		X		X		
D100-xxx		X		X		X		X		X		X	X
D125-xxx													

T-SLOT INFORMATION (mm)

PART NO.	T	T1	T2
DM075-xxx	15.0	6.5	6.0
DM100-xxx	16.8	8.1	6.8
DM125-xxx			

RAIL Φ APPROXIMATE	
D075 =	.470 = 12mm
D100 =	.630 = 16mm
D125 =	.820 = 22mm

Straightness - ±.002"/ft

WEIGHTS

PART NO.	RAIL PER INCH (lbs.)	STANDARD CARRIAGE (lbs.)	EXTENDED CARRIAGE (lbs.)
D075-xxx	0.19	0.98	1.26
D100-xxx	0.32	2.12	2.82
D125-xxx	0.48	4.56	5.7

D100

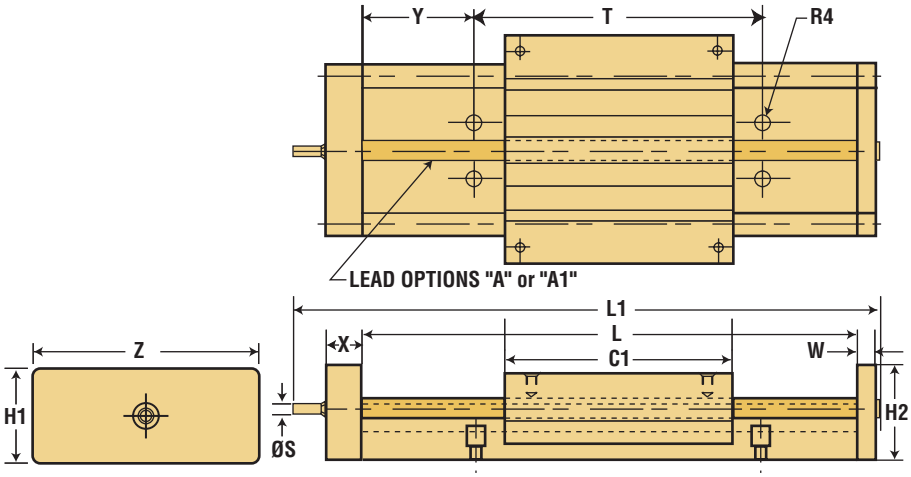

OPTIONAL HAND BRAKE

NOTE: available only with optional hand crank

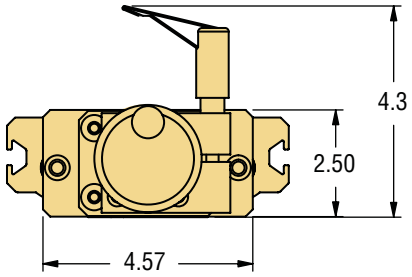

PART NO.	P	H
DO100AHB	2.31	1.75

PART NO.	STROKE (L-C1)	L	L1	C1	NOMINAL SCREW DIA.	STANDARD LEAD A	OPTIONAL LEAD A1	S	Y	T	R4	W	X	Z	H1	H2
D100xx-12	7.5	12	14.61	4.5	1/2	0.250	0.500	0.314	3	6	5/16	0.5	1	4.56	2.5	2.500
D100xx-18	13.5	18	20.61													
D100xx-24	19.5	24	26.61													
D100xx-30	25.5	30	32.61													
D100xx-48	25.5	30	32.61													

OPTIONAL HAND CRANK

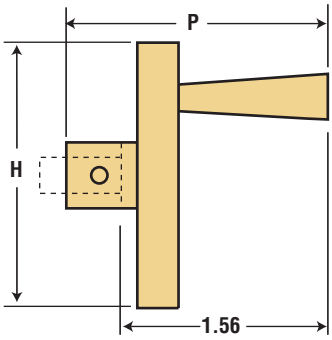

PART NO.	P	H
100H	2.31	2.25

*See order codes on page 199 to integrate.

OPTIONAL MOTOR MOUNT ATTACHMENT

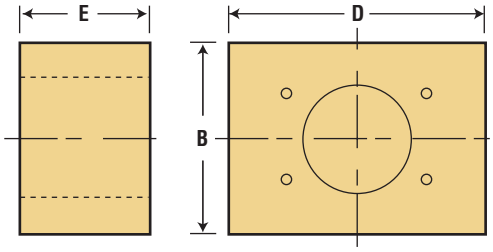

PART NO.	MOTOR MOUNT	B	E	D
100N	NEMA 23	2.5	1.81	3.25

LOAD & SPEED DATA FOR STANDARD LEAD SCREW DRIVEN (HORIZONTAL ORIENTATION)

D100A-xxx

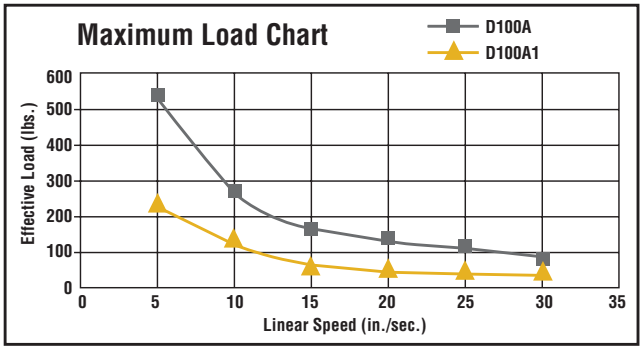

D100A-xxx

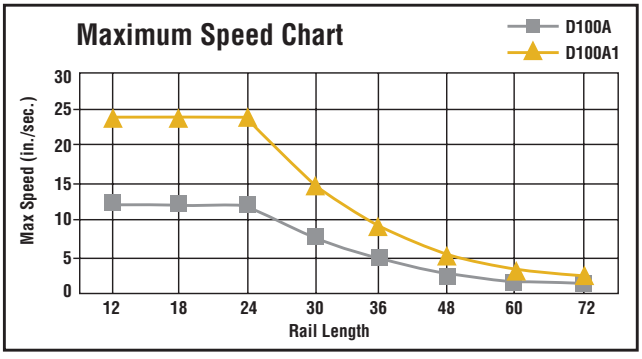

NOTE: Optional drives are available: ball screws, cylinders, linear motors, and belt drives.

DFG MODULAR GUIDE

- Self-lubricating- maintenance free
- Polymer inserts - smooth, replaceable, low cost
- Modular construction allow for multiple configurations
- Multiple carriage and rail sizes
- Industry standard interchangeable

**Not for resale or distribution inside the European Union.*

Materials:
POM polymer insert
Anodized aluminum rails
Chromate plated die cast carriage
Anodized aluminum carriage plate

Working Temperatures: -40C to 90C (-40F to 195F)
Coefficient of Friction: 0.1- 0.2
Maximum Velocity: 10 m/s (2000 fpm) for intermediate application and 8 m/s (1600 fpm) for continuous application
Maximum PV Value: 10,000 psi - fpm

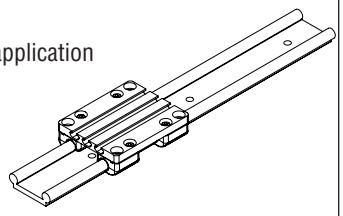

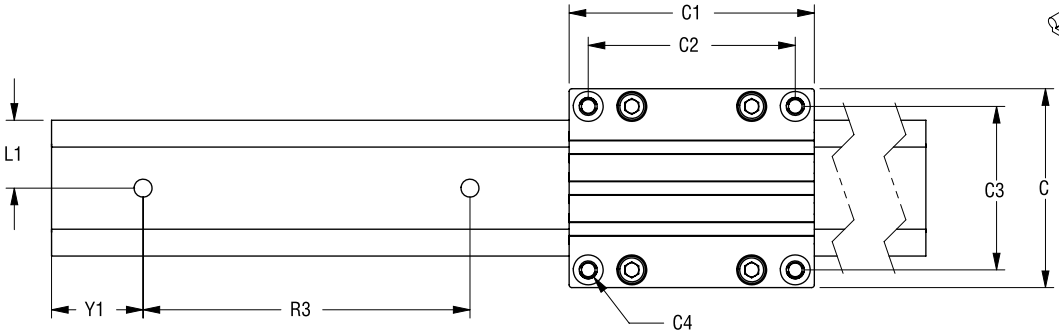

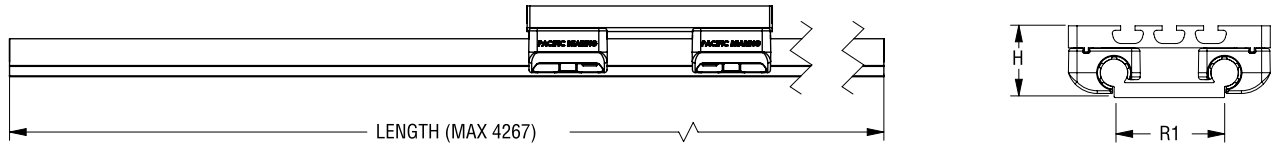

PART NUMBER	C (mm)	DIMENSIONAL INFORMATION C1 (mm)	C2 (mm)	C3 (mm)	C4 (mm)	H (mm)	L1 (mm)	R1 (mm)	R3 (mm)	R4 (mm)	Y (mm)	CARRIAGE WEIGHT (G)	RAIL WEIGHT (G/mm)	LOAD DATA Fy (N)	Fy (lbs.)	Fz (N)	Fz (lbs.)	Mx (N-m)	Mx (lbs.-in.)	My (N-m)	My (lbs.-in.)	Mz (N-m)	Mz (lbs.-in.)
DFG10CA-40A	73	100	87	60	M6	24	36.5	40	120	6.6	20	310	1.0	5039	1133	4031	1020	100	74	180	133	180	133
DFG10CA-40B	73	150	137	60	M6	24	36.5	40	120	6.6	20	370	1.0	5039	1133	4031	1020	100	74	305	225	305	225
DFG10CA-40C	107	200	187	60	M6	24	36.5	40	120	6.6	20	430	1.0	5039	1133	4031	1020	100	74	430	320	430	320
DFG10CA-80A	107	100	87	94	M6	24	53.5	80	120	6.6	20	360	1.4	5039	1133	4031	1020	184	136	180	132	180	132
DFG10CA-80B	107	150	137	94	M6	24	53.5	80	120	6.6	20	450	1.4	5039	1133	4031	1020	184	136	305	225	305	225
DFG10CA-80C	107	200	187	94	M6	24	53.5	80	120	6.6	20	530	1.4	5039	1133	4031	1020	184	136	430	320	430	320

NOTE: Apply a load reduction factor 0.25 on Fy rating if the system is used inverted.

ORDERING INFORMATION

EXAMPLE: DFG10-40A-0500-1

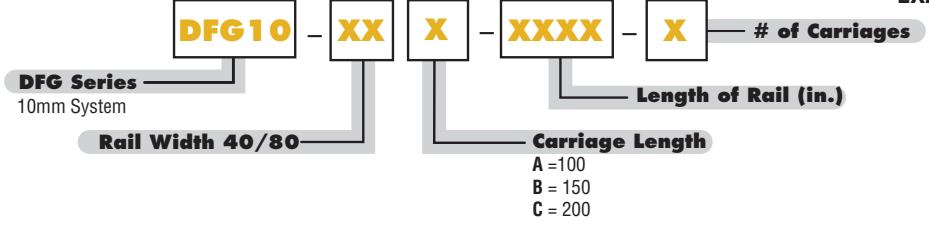

A.9 Bushings

Tolerances for Bronze Flanged Sleeve Bearings

SAE 841—6338K

For Shaft Dia.	OD	Tolerance for Shaft Dia.	OD Tolerance
3/16″	5/16″	+0.0010″ to +0.0020″	+0.0005″ to +0.0015″
1/4″	3/8″	+0.001″ to +0.002″	+0.002″ to +0.003″
5/16″	7/16″	+0.0010″ to +0.0020″	+0.0020″ to +0.003″
5/16″	9/16″	+0.0015″ to +0.0025″	+0.002″ to +0.003″
5/16″	5/8″	–0.001″ to +0.000″	+0.004″ to +0.005″
3/8″	1/2″	+0.0010″ to +0.0020″	+0.002″ to +0.003″
3/8″	5/8″	+0.001″ to +0.002″	+0.002″ to +0.003″
7/16″	9/16″	+0.0005″ to +0.0015″	+0.0015″ to +0.0025″
7/16″	5/8″	+0.0005″ to +0.0015″	+0.002″ to +0.003″
1/2″	5/8″	+0.001″ to +0.002″	+0.002″ to +0.003″
1/2″	3/4″	+0.001″ to +0.002″	+0.002″ to +0.003″
5/8″	3/4″	+0.000″ to +0.001″	+0.002″ to +0.003″
5/8″	7/8″	+0.001″ to +0.002″	+0.003″ to +0.004″
3/4″	7/8″	+0.001″ to +0.002″	+0.003″ to +0.004″
3/4″	1″	+0.001″ to +0.002″	+0.003″ to +0.004″
7/8″	1 1/8″	+0.001″ to +0.002″	+0.002″ to +0.003″
1″	1 1/4″	+0.000″ to +0.001″	+0.001″ to +0.002″
1 1/4″	1 1/2″	+0.0025″ to +0.0035″	+0.003″ to +0.004″
1 3/8″	1 5/8″	+0.001″ to +0.002″	+0.0015″ to +0.003″
1 1/2″	1 3/4″	+0.003″ to +0.004″	+0.0035″ to +0.005″
1 3/4″	2 1/4″	+0.0015″ to +0.003″	+0.003″ to +0.004″

Length	Tolerance
1/4″	±0.005″
3/8″	±0.005″
1/2″	±0.005″
5/8″	±0.005″
3/4″	±0.005″
1″	±0.005″
1 1/4″	±0.005″
1 1/2″	±0.005″
2 1/2″	±0.0075″

Graphite SAE 841—9440T

For Shaft Dia.	OD	Tolerance for Shaft Dia.	OD Tolerance
3/16″	5/16″	+0.001″ to +0.002″	+0.002″ to +0.003″
1/4″	3/8″	+0.001″ to +0.002″	+0.002″ to +0.003″
5/16″	7/16″	+0.001″ to +0.002″	+0.002″ to +0.003″
3/8″	1/2″	+0.001″ to +0.002″	+0.002″ to +0.003″
3/8″	5/8″	+0.001″ to +0.002″	+0.002″ to +0.003″
7/16″	9/16″	+0.001″ to +0.002″	+0.002″ to +0.003″
7/16″	5/8″	+0.001″ to +0.002″	+0.002″ to +0.003″
1/2″	5/8″	+0.001″ to +0.002″	+0.002″ to +0.003″
1/2″	3/4″	+0.001″ to +0.002″	+0.002″ to +0.003″
5/8″	3/4″	+0.001″ to +0.002″	+0.002″ to +0.003″
5/8″	7/8″	+0.001″ to +0.002″	+0.003″ to +0.004″
3/4″	7/8″	+0.001″ to +0.002″	+0.003″ to +0.004″
3/4″	1″	+0.001″ to +0.002″	+0.003″ to +0.004″
7/8″	1 1/8″	+0.001″ to +0.002″	+0.003″ to +0.004″
1″	1 1/4″	+0.002″ to +0.003″	+0.003″ to +0.004″
1 1/4″	1 1/2″	+0.0025″ to +0.0035″	+0.003″ to +0.004″
1 1/2″	1 3/4″	+0.003″ to +0.004″	+0.0035″ to +0.005″
1 3/4″	2 1/4″	+0.0025″ to +0.004″	+0.0035″ to +0.005″

Length	Tolerance
1/4″	±0.005″
3/8″	±0.005″
1/2″	±0.005″
5/8″	±0.005″
3/4″	±0.005″
1″	±0.005″
1 1/4″	±0.005″
1 1/2″	±0.0075″
2 1/2″	±0.0075″

(Continued on following page)

A.10 Bearings

7. Bearing Fits

7.1 Interference

For rolling bearings the bearing rings are fixed on the shaft or in the housing so that slip or movement does not occur between the mated surface during operation or under load. This relative movement (sometimes called creep) between the fitted surfaces of the bearing and the shaft or housing can occur in a radial direction, or in an axial direction, or in the direction of rotation. This creeping movment under load causes damage to the bearing rings, shaft or housing in the form of abrasive wear, fretting corrosion or friction crack. This, in turn, can also lead to abrasive particles getting into the bearing, which can cause vibration, excessive heat, and lowered rotational efficiency. To ensure that slip does not occur between the fitted surfaces of the bearing rings and the shaft or housing, the bearing is usually installed with an interference fit.

The most effective interference fit is called a tight fit (or shrink fit). The advantage of this “tight fit” for thin walled bearings is that it provides uniform load support over the entire ring circumference without any loss in load carrying capacity.

However, with a tight interference fit, ease of mounting and dismounting the bearings is lost; and when using a non-separable bearing as a non-fixing bearing, axial displacement is impossible.

7.2 Calculation of interference

1) Load and interference

The minimum required amount of interference for inner rings mounted on solid shafts when acted on by radial loads, is found by formula (7.1) and (7.2).

When $F_r \leq 0.3C_{or}$

$$\Delta_{dF} = 0.08\sqrt{\frac{d \bullet F_r}{B}} \cdots\cdots (7.1)$$

When $F_r > 0.3C_{or}$

$$\Delta_{dF} = 0.02\frac{F_r}{B} \cdots\cdots (7.2)$$

where,

Δ_{dF} : Required effective interference (for load) μm
d : Nominal bore diameter mm
B : Inner ring width mm
F_r : Radial load N
C_{or} : Basic static rated load N

2) Temperature rise and interference

To prevent loosening of the inner ring on steel shafts due to temperature increases (difference between bearing temperature and ambient temperature) caused by bearing rotation, an interference fit must be given. The required amount of interference can be found by formula (7.3).

$$\Delta_{dT} = 0.0015 \bullet d \bullet \Delta T \cdots\cdots (7.3)$$

where,

Δ_{dT} : Required effective interference (for temperature) μm
ΔT : Difference between bearing temperature and ambient temperature °C
d : Bearing bore diameter mm

3) Effective interference and apparent interference

The effective interference (the actual interference after fitting) is different from the apparent interference derived from the dimensions measured value. This difference is due to the roughness or slight variations of the mating surfaces, and this slight flattening of the uneven surfaces at the time of fitting is taken into consideration. The relation between the effective and apparent interference, which varies according to the finish given to the mating surfaces, is expressed by formula (7.4).

$$\Delta d_{eff} = \Delta d_f - G \cdots\cdots (7.4)$$

where,

Δd_{eff} : Effective interference μm
Δd_f : Apparent interference μm
G =1.0~2.5 μm for ground shaft
=5.0~7.0 μm for turned shaft

4) Maximum interference

When bearing rings are installed with an interference fit on shafts or housings, the tension or compression stress may occur. If the interference is too large, it may cause damage to the bearing rings and reduce the fatigue life of the bearing. For these reasons, the maximum amount of interference should be less than 1/1000 of the shaft diameter, or outside diameter.

7.3 Fit selection

Selection of the proper fit is generally based on the following factors: 1) the direction and nature of the bearing load, 2) whether the inner ring or outer ring rotates, 3) whether the load on the inner or outer ring rotates or not, 4) whether there is static load or direction indeterminate load or not. For bearings under rotating loads or direction indeterminate loads, a tight fit is recommended; but for static loads, a transition fit or loose fit should be sufficient (see Table 7.1).

The interference should be tighter for heavy bearing loads or vibration and shock load conditions. Also, a tighter than normal fit should be given when the bearing is installed on hollow shafts or in housings with thin walls, or housings made of light allows or plastic.

In applications where high rotational accuracy must be maintained, high precision bearings and high tolerance shafts and housings should be employed instead of a tighter interference fit to ensure bearing stability. High interference fits should be avoided if possible as they cause shaft or housing deformities to be induced into the bearing rings, and thus reduce bearing rotational accuracy.

Because mounting and dismounting become very difficult when both the inner ring and outer ring of a non-separable bearing (for example a deep groove ball bearing) are given tight interference fits, one or the other rings should be given a loose fit.

Table 7.1 Radial load and bearing fit

Bearing rotation and load	Illustration	Ring load	Fit
Inner ring : Rotating Outer ring : Stationary Load direction : Constant	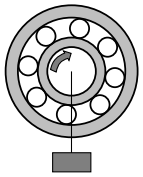 Static load	Rotating inner ring load	Inner ring : Tight fit
Inner ring : Stationary Outer ring : Rotating Load direction : Rotates with outer ring	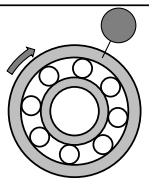 Unbalanced load	Static outer ring load	Outer ring : Loose fit
Inner ring : Stationary Outer ring : Rotating Load direction : Constant	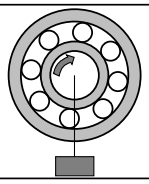 Static load	Static inner ring load	Inner ring : Loose fit
Inner ring : Rotating Outer ring : Stationary Load direction : Rotates with outer ring	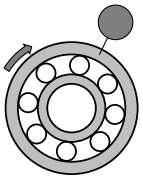 Unbalanced load	Rotating outer ring load	Outer ring : Tight fit

7.4 Recommended fits

Metric size standard dimension tolerances for bearing shaft diameters and housing bore diameters are governed by ISO 286 and JIS B 0401 (dimension tolerances and fits). Accordingly, bearing fits are determined by the precision (dimensional tolerance) of the shaft diameter and housing bore diameter. Widely used fits for various shaft and housing bore diameter tolerances, and bearing bore and outside diameters are shown in Fig. 7.1.

Generally-used, recommended fits relating to the primary factors of bearing shape, dimensions, and load conditions are listed in Tables 7.2 through 7.5. Table 7.6 gives the numerical values for housing and shaft fits.

The bore and outside diameter tolerances and tolerance ranges for inch and metric tapered roller bearings are different. Recommended fits and numerical values for inch tapered roller bearings are shown in Table 7.8. For special fits or applications, please consult NTN.

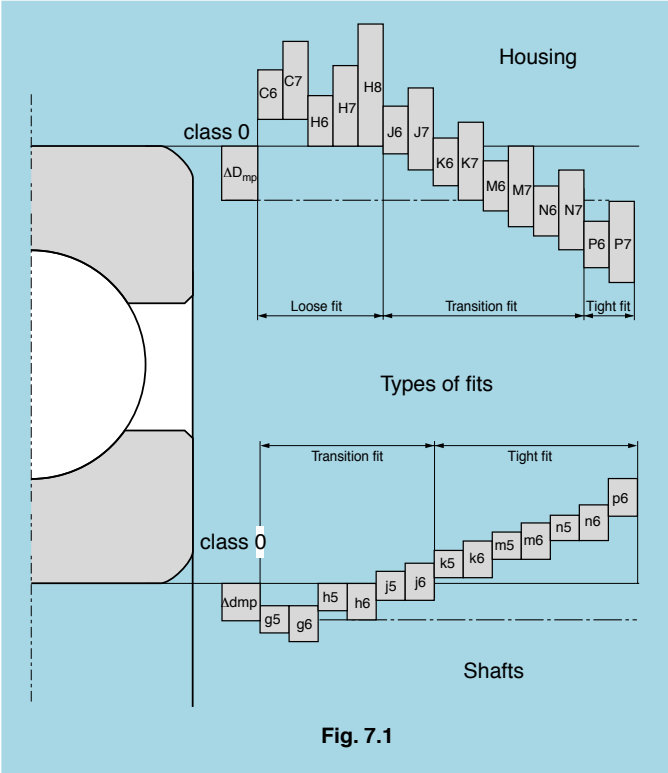

Fig. 7.1

Table 7.2 General standards for radial bearing fits (JIS class 0, 6, 6X)

Table 7.2 (1) Housing fits

Housing type	Load condition		Housing fits
Solid or split housing	Outer ring static load	All load conditions	H7
		Heat conducted through shaft	G7
Solid housing	Direction indeterminate load	Light to normal	JS7
		Normal to heavy load	K7
		Heavy shock load	M7
	Outer ring rotating load	Light or variable load	M7
		Normal to heavy load	N7
		Heavy load (thin wall housing) Heavy shock load	P7

Note: Fits apply to cast iron or steel housings. For light alloy housings, a tighter fit than listed is normally required.

Table 7.2 (2) Shaft fit

Bearing type	Load conditions		Ball bearings	Cylindrical and tapered roller bearings	Spherical roller bearings	Shaft fits
			Shaft diameter mm			
Cylindrical bore bearings	Rotating inner ring or indeterminate direction load	Light or fluctuating variable load	~ 18	—	—	h5
			18~100	~ 40	—	js6
			100~200	40~140	—	k6
			—	140~200	—	m6
		Normal to heavy load	~ 18	—	—	js5
			18~100	~ 40	~ 40	k5
			100~140	40~100	40~65	m5
			140~200	100~140	65~100	m6
			200~280	140~200	100~140	n6
			—	200~400	140~280	p6
			—	—	280~500	r6
		Very heavy or shock load	—	50~140	50~100	n6
			—	140~200	100~140	p6
			—	200~	140~	r6
	Static inner ring load	Inner ring axial displacement required	All shaft diameters			g6
		Easy axial displacement of inner ring not required	All shaft diameters			h6
Tapered bore bearings (With sleeve)	All load		All shaft diameters			h9/IT5

Note: 1. All values and fits listed are for solid steel shafts.
2. For radial bearings under axial loads, all shaft tolerance range classes are js6.
3. Load classifications are as follows:
LIght load: $P_r \leq 0.06\ C_r$
Normal load: $0.06\ C_r < P_r \leq 0.12\ C_r$
Heavy load: $P_r > 0.12\ C_r$

where,

P_r: Bearing equivalent load
C_r: Bearing basic dynamic load rating

Table 7.3 Solid type needle roller bearing fits

Table 7.3 (1) Shaft fit

Conditions			Shaft fits
Load type	Scale of load	Shaft diameter *d* mm	
Rotating inner ring or indeterminate direction load	Light load	~ 50	j5
	Normal load	~ 50	k5
		50~150	m5
		150~	m6
	Heavy load and shock load	~ 150	m6
		150~	n6
Static inner ring load	Medium & low speed revolution, light load	All sizes	g6
	General application	All sizes	h6
	When high rotation accuracy is required	All sizes	h5

Table 7.3 (2) Housing fit

Conditions		Housing fits
Static inner ring load	Normal to heavy load	J7
	Normal loads with split housings	H7
Outer ring rotating load	Light loads	M7
	Normal loads	N7
	Heavy and normal loads	P7
Direction indeterminate load	Light loads	J7
	Normal load	K7
	Very heavy or shock load	M7
High demands on running accuracy with light load		K6

Table 7.4 Standard fits for thrust bearings

Table 7.4 (1) Shaft fits

Load conditions		Shaft diameter	Shaft fits
“Pure” axial load (All thrust bearings)		All sizes	js6
Combined load: spherical roller thrust bearings	Static inner ring loads	All sizes	js6
	Inner ring rotating load or direction indeterminate	~200	k6
		200~400	m6
		400~	n6

Table 7.4 (2) Housing fits

Load conditions		Housing fits	Remarks
“Pure” axial load: All thrust bearings	When another bearing is used to support radial load	—	Clearance given between outer ring and housing
		H8	Accuracy required with thrust ball bearings
Combined load: spherical roller thrust bearings	Static outer ring load	H7	—
	Outer ring rotating load or direction indeterminate load	K7	Normal usage conditions
		M7	Relatively heavy

Table 7.5 Fits for electric motor bearings

Shaft or housing	Deep groove ball bearings			Cylindrical roller bearings		
	Shaft or housing bore diameter mm		Fits	Shaft or housing bore diameter mm		Fits
	over	incl.		over	incl.	
Shaft	—	18	j5	—	40	k5
	18	100	k5	40	160	m5
	100	160	m5	160	200	n5
Housing	All Sizes		H6 or J6	All sizes		H6 or J6

Table 7.6 Fitting values for radial bearings, Class 0

Table 7.6 (1) Shaft fit

Nominal bore diameter of bearing d (mm) over	incl.	Δ_{dmp} high	low	g5 bearing	shaft	g6 bearing	shaft	h5 bearing	shaft	h6 bearing	shaft	j5 bearing	shaft	js5 bearing	shaft	j6 bearing	shaft
3	6	0	–8	4T~9L		4T~12L		8T~5L		8T~8L		11T~2L		10.5T~2.5L		14T~2L	
6	10	0	–8	3T~11L		3T~14L		8T~6L		8T~9L		12T~2L		11T~3L		15T~2L	
10	18	0	–8	2T~14L		2T~17L		8T~8L		8T~11L		13T~3L		12T~4L		16T~3L	
18	30	0	–10	3T~16L		3T~20L		10T~9L		10T~13L		15T~4L		14.5T~4.5L		19T~4L	
30	50	0	–12	3T~20L		3T~25L		12T~11L		12T~16L		18T~5L		17.5T~5.5L		23T~5L	
50	80	0	–15	5T~23L		5T~29L		15T~13L		15T~19L		21T~7L		21.5T~6.5L		27T~7L	
80	120	0	–20	8T~27L		8T~34L		20T~15L		20T~22L		26T~9L		27.5T~7.5L		33T~9L	
120	140	0	–25	11T~32L		11T~39L		25T~18L		25T~25L		32T~11L		34T~9L		39T~11L	
140	160																
160	180																
180	200	0	–30	15T~35L		15T~44L		30T~20L		30T~29L		37T~13L		40T~10L		46T~13L	
200	225																
225	250																
250	280	0	–35	18T~40L		18T~49L		35T~23L		35T~32L		42T~16L		46.5T~11.5L		51T~16L	
280	315																
315	355	0	–40	22T~43L		22T~54L		40T~25L		40T~36L		47T~18L		52.5T~12.5L		58T~18L	
355	400																
400	450	0	–45	25T~47L		25T~60L		45T~27L		45T~40L		52T~20L		58.5T~13.5L		65T~20L	
450	500																

Table 7.6 (2) Housing fit

Nominal bore diameter of bearing D (mm) over	incl.	Δ_{dmp} high	low	G7 housing	bearing	H6 housing	bearing	H7 housing	bearing	J6 housing	bearing	J7 housing	bearing	Js7 housing	bearing	K6 housing	bearing
6	10	0	–8	5L~28L		0~17L		0~23L		4T~13L		7T~16L		7.5T~15.5L		7T~10L	
10	18	0	–8	6L~32L		0~19L		0~26L		5T~14L		8T~18L		9T~17L		9T~10L	
18	30	0	–9	7L~37L		0~22L		0~30L		5T~17L		9T~21L		10.5T~19.5L		11T~11L	
30	50	0	–11	9L~45L		0~27L		0~36L		6T~21L		11T~25L		12.5T~23.5L		13T~14L	
50	80	0	–13	10L~53L		0~32L		0~43L		6T~26L		12T~31L		15T~28L		15T~17L	
80	120	0	–15	12L~62L		0~37L		0~50L		6T~31L		13T~37L		17.5T~32.5L		18T~19L	
120	150	0	–18	14L~72L		0~43L		0-~58L		7T~36L		14T~44L		20T~38L		21T~22L	
150	180	0	–25	14L~79L		0~50L		0~65L		7T~43L		14T~51L		20T~45L		21T~29L	
180	250	0	–30	15L~91L		0~59L		0~76L		7T~52L		16T~60L		23T~53L		24T~35L	
250	315	0	–35	17L~104L		0~67L		0~87L		7T~60L		16T~71L		26T~61L		27T~40L	
315	400	0	–40	18L~115L		0~76L		0~97L		7T~69L		18T~79L		28.5T~68.5L		29T~47L	
400	500	0	–45	20L~128L		0~85		0~108		7T~78L		20T~88L		31.5T~76.5L		32T~53L	

Unit μm

js6		k5		k6		m5		m6		n6		p6		r6	
bearing	shaft	bearing	shaft	bearing	shaft	bearing	shaft	bearing	shaft	bearing	shaft	bearing	shaft	bearing	shaft
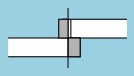		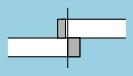		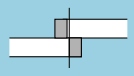		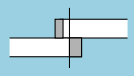		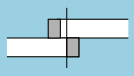		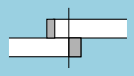		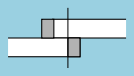		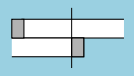	
12T~4L		14T~1T		17T~1T		17T~4T		20T~4T		24T~8T		28T~12T		—	
12.5T~4.5L		15T~1T		18T~1T		20T~6T		23T~6T		27T~10T		32T~15T		—	
13.5T~5.5L		17T~1T		20T~1T		23T~7T		26T~7T		31T~12T		37T~18T		—	
16.5T~6.5L		21T~2T		25T~2T		27T~8T		31T~8T		38T~15T		45T~22T		—	
20T~8L		25T~2T		30T~2T		32T~9T		37T~9T		45T~17T		54T~26T		—	
24.5T~9.5L		30T~2T		36T~2T		39T~11T		45T~11T		54T~20T		66T~32T		—	
31T~11L		38T~3T		45T~3T		48T~13T		55T~13T		65T~23T		79T~37T		—	
37.5T~12.5L		46T~3T		53T~3T		58T~15T		65T~15T		77T~27T		93T~43T		113T~63T 115T~65T 118T~68T	
44.5T~14.5T		54T~4T		63T~4T		67T~17T		76T~17T		90T~31T		109T~50T		136T~77T 139T~80T 143T~84T	
51T~16L		62T~4T		71T~4T		78T~20T		87T~20T		101T~34T		123T~56T		161T~94T 165T~98T	
58T~18L		69T~4T		80T~4T		86T~21T		97T~21T		113T~37T		138T~62T		184T~108T 190T~114T	
65T~20L		77T~5T		90T~4T		95T~23T		108T~23T		125T~40T		153T~68T		211T~126T 217T~132T	

Unit μm

K7		M7		N7		P7	
housing	bearing	housing	bearing	housing	bearing	housing	bearing
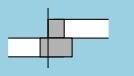		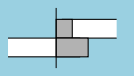		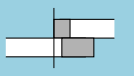		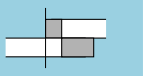	
10T~13L		15T~8L		19T~4L		24T~1T	
12T~14L		18T~8L		23T~3L		29T~3T	
15T~15L		21T~9L		28T~2L		35T~5T	
18T~18L		25T~11L		33T~3L		42T~6T	
21T~22L		30T~13L		39T~4L		51T~8T	
25T~25L		35T~15L		45T~5L		59T~9T	
28T~30L		40T~18L		52T~6L		68T~10T	
28T~37L		40T~25L		52T~13L		68T~3T	
33T~43L		46T~30L		60T~16L		79T~3T	
36T~51L		52T~35L		66T~21L		88T~1T	
40T~57L		57T~40L		73T~24L		98T~1T	
45T~63L		63T~45L		80T~28L		108T~0	

Table 7.7 Fits for inch series tapered roller bearing (ANSI class 4)

Unit μm
0.0001 inch

Table 7.7 (1) Fit with shaft

Load conditions		Shaft diameter d mm, inch over	incl.	Cone bore tolerance[2] Δ_{dS} high	low	Shaft tolerance high	low	Extreme fits[3] max	min
Rotating cone load	Normal loads, no shock	—	76.200	+13	0	+38	+26	38T~13T	
		—	3.0000	+5	0	+15	+10	15T~5T	
		76.200	304.800	+25	0	+64	+38	64T~13T	
		3.0000	12.0000	+10	0	+25	+15	25T~5T	
	Heavy loads or shock loads	—	76.200	+13	0	Use average tight cone fit of 0.5μm/mm, (0.0005 inch/inch) of cone bore, use a minimum fit of 25μm, 0.0010 inch tight.			
		—	3.0000	+5	0				
		76.200	304.800	+25	0				
		3.0000	12.0000	+10	0				
Stationary cone load	Cone axial displacement on shaft necessary[1]	—	76.200	+13	0	0	–13	0~26L	
		—	3.0000	+5	0	0	–5	0~10L	
		76.200	304.800	+25	0	0	–25	0~51L	
		3.0000	12.0000	+10	0	0	–10	0~20L	
	Cone axial displacement on shaft unnecessary	—	76.200	+13	0	+13	0	13T~13L	
		—	3.0000	+5	0	+5	0	5T~5L	
		76.200	304.800	+25	0	+25	0	25T~25L	
		3.0000	12.0000	+10	0	+10	0	10T~10L	

1) Applies only to ground shafts.
2) For bearings with negation deviation indicated in bearing tables, same fit applies.
3) T=tight, L=loose, d=cone bore, mm, inch
Note: For bearings higher than class 2, consult NTN.

Unit μm
0.0001 inch

Table 7.7 (2) Fit with housing

Load conditions		Housing bore diameter mm, inch over	incl.	Cup O.D. tolerance[1] high	low	Housing bore tolerance high	low	Extreme fits[2] max	min
Stationary cup load	Light and normal loads: cup easily axially displaceable	—	76.200	+25	0	+76	+50	25L~76L	
		—	3.0000	+10	0	+30	+20	10L~30L	
		76.200	127.000	+25	0	+76	+50	25L~76L	
		3.0000	5.0000	+10	0	+30	+20	10L~30L	
		127.000	304.800	+25	0	+76	+50	25L~76L	
		5.0000	12.0000	+10	0	+30	+20	10L~30L	
	Light and normal loads: cup axially adjustable	—	76.200	+25	0	+25	0	25T~25L	
		—	3.0000	+10	0	+10	0	10T~10L	
		76.200	127.000	+25	0	+25	0	25T~25L	
		3.0000	5.0000	+10	0	+10	0	10T~10L	
		127.000	304.800	+25	0	+51	0	25T~51L	
		5.0000	12.0000	+10	0	+20	0	10T~20L	
	Heavy loads: cup not axially displaceable	—	76.200	+25	0	–13	–39	64T~13T	
		—	3.0000	+10	0	–5	–15	25T~5T	
		76.200	127.000	+25	0	–25	–51	76T~25T	
		3.0000	5.0000	+10	0	–10	–20	30T~10T	
		127.000	304.800	+25	0	–25	–51	76T~25T	
		5.0000	12.0000	+10	0	–10	–20	30T~10T	
Rotating cup load	Cup not axially displaceable	—	76.200	+25	0	–13	–39	64T~13T	
		—	3.0000	+10	0	–5	–15	25T~5T	
		76.200	127.000	+25	0	–25	–51	76T~25T	
		3.0000	5.0000	+10	0	–10	–20	30T~10T	
		127.000	304.800	+25	0	–25	–51	76T~25T	
		5.0000	12.0000	+10	0	–10	–20	30T~10T	

1) For bearings with negation deviation indicated in bearing tables, same fit applies.
2) T=tight, L=loose
Note: For bearings higher than class 2, consult NTN.

Table 7.8 Fits for inch series tapered roller bearing (ANSI classes 3 and 0)

Unit μm
0.0001 inch

Table 7.8 (1) Fit with shaft

Load conditions		Shaft diameter mm, inch over	incl.	Cone bore[2] tolerance high	low	Shaft tolerance high	low	Extreme fits[3] max	min
Rotating cone load	precision machine tool spindles	—	304.800	+13	0	+31	+18	31T~5T	
		—	12.0000	+5	0	+12	+7	12T~2T	
	heavy loads, or high speed or shock	—	76.200	+13	0	Use minimum tight cone fit of 0.25μm/mm (0.00025 inch/inch) of cone bore.			
		—	3.0000	+5	0				
		76.200	304.800	+13	0				
		3.0000	12.0000	+5	0				
Stationary cone load	precision machine tool spindles	—	304.800	+13	0	+31	+18	31T~5T	
		—	12.0000	+5	0	+12	+7	36T~2T	

Note: Must be applied for maximum bore dia. 241.300mm (9.500 inch) in case of class 0 product.

Note 1) T=tight, L=loose
2) Must be applied for maximum cup OD 304.800mm (12.000 inch) case of class 0 product.

Unit μm
0.0001 inch

Table 7.8 (2) Fit with housing

Load conditions		Housing bore diameter mm, inch over	incl.	Cup O.D. tolerance high	low	Housing bore tolerance high	low	Extreme fits[2] max	min
Stationary cup load	Floating	—	152.400	+13	0	+38	+26	13L~38L	
		—	6.0000	+5	0	+15	+10	5L~15L	
		152.400	304.800	+13	0	+38	+26	13L~38L	
		6.0000	12.0000	+5	0	+15	+10	5L~14L	
	Clamped	—	152.400	+13	0	+25	+13	0~25L	
		—	6.0000	+5	0	+10	+5	0~10L	
		152.400	304.800	+13	0	+25	+13	0~25L	
		6.0000	12.0000	+5	0	+10	+5	0~10L	
	Adjustable	—	152.400	+13	0	+13	0	13T~13L	
		—	6.0000	+5	0	+5	0	5T~5L	
		152.400	304.800	+13	0	+25	0	13T~25L	
		6.0000	12.0000	+5	0	+10	0	5T~10L	
	Nonadjustable or in carriers	—	152.400	+13	0	0	–12	25T~0	
		—	6.0000	+5	0	0	–5	10T~0	
		152.400	304.800	+13	0	0	–25	38T~0	
		6.0000	12.0000	+5	0	0	–10	15~0	
Rotating cup load	Nonadjustable or in carriers	—	152.400	+13	0	–13	–25	38T~13T	
		—	6.0000	+5	0	–5	–10	15T~5T	
		152.400	304.800	+13	0	–13	–38	51T~13T	
		6.0000	12.0000	+5	0	–5	–15	20T~5T	

Note 1) T=tight, L=loose
2) Must be applied for maximum cup OD 304.800mm (12.000 inch) case of class 0 product.

A.11 Drawn Cup Needle Roller Bearings

Drawn cup needle roller bearings with open ends SCE2410 (Series SCE)

to ABMA 18.2 - 1982, inch sizes

The datasheet is only an overview of dimensions and basic load ratings of the selected product. Please always observe all the guidelines in these overview pages. Further information is given on many products under the menu item "Description". You can also order comprehensive information via the Catalogue ordering system (http://www.ina.de/content.ina.de/en/mediathek/library/library.jsp) or by telephone on +49 (91 32) 82 - 28 97.

F_w	1 1/2	inch	
F_w	38,1	mm	
D	1,875	inch	
D	47,625	mm	
C	0,625	inch	
C	15,875	mm	
m	0,119	lbs	Mass
m	54	g	Mass
C_r	5500	lbf	Basic dynamic load rating, radial
C_r	24400	N	Basic dynamic load rating, radial
C_{0r}	8200	lbf	Basic static load rating, radial
C_{0r}	36500	N	Basic static load rating, radial
n_G	6700	1/min	Limiting speed
n_B	4850	1/min	Reference speed

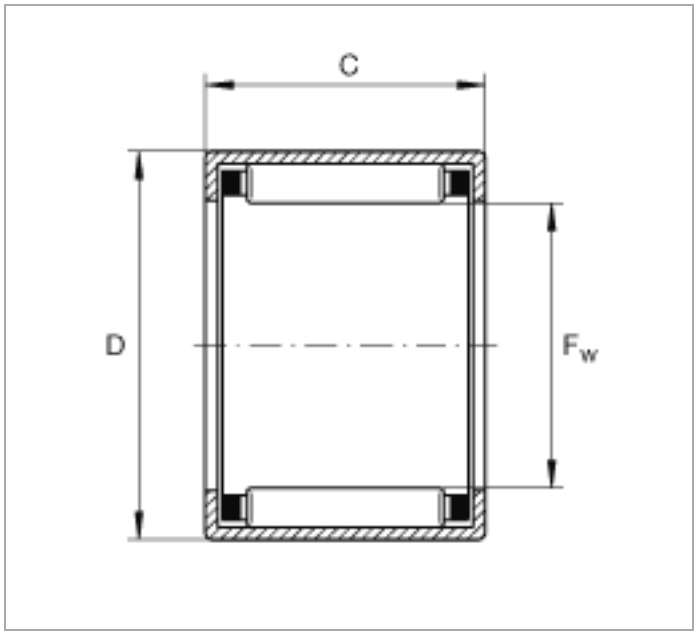
C
D
F_w

A.12 Axial Needle Roller Bearings (TC3244)

Axial needle roller bearings TC3244 (Series TC)

single direction, to ABMA 21.2 - 1988, suitable for combination with axial bearing washers TWA, inch sizes

The datasheet is only an overview of dimensions and basic load ratings of the selected product. Please always observe all the guidelines in these overview pages. Further information is given on many products under the menu item "Description". You can also order comprehensive information via the Catalogue ordering system (http://www.ina.de/content.ina.de/en/mediathek/library/library.jsp) or by telephone on +49 (91 32) 82 - 28 97.

D_{c1}	2	inch	
D_{c1}	50,8	mm	
D_c	2,75	inch	
D_c	69,85	mm	
D_w	0,078	inch	
D_w	1,984	mm	
E_a	2,661	inch	
E_a	67,6	mm	
E_b	2,071	inch	
E_b	52,6	mm	
m	0,033	lbs	Mass
m	0,015	kg	Mass
C_a	5620	lbf	Basic dynamic load rating, axial
C_a	25000	N	Basic dynamic load rating, axial
C_{0a}	32600	lbf	Basic static load rating, axial
C_{0a}	145000	N	Basic static load rating, axial
n_G	4100	1/min	Limiting speed

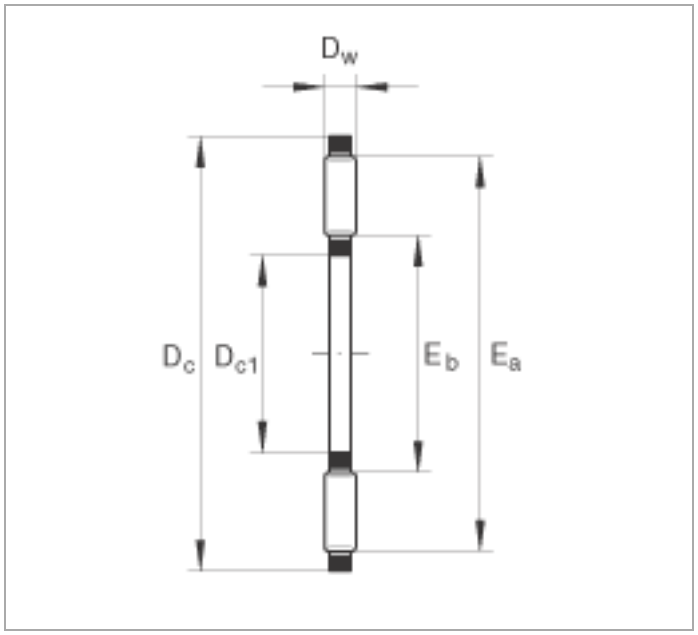
D_w
D_c
D_{c1}
E_b
E_a

A.13 Axial Needle Roller Bearings (TC815)

Axial needle roller bearings TC815 (Series TC)

single direction, to ABMA 21.2 - 1988, suitable for combination with axial bearing washers TWA, inch sizes

The datasheet is only an overview of dimensions and basic load ratings of the selected product. Please always observe all the guidelines in these overview pages. Further information is given on many products under the menu item "Description". You can also order comprehensive information via the Catalogue ordering system (http://www.ina.de/content.ina.de/en/mediathek/library/library.jsp) or by telephone on +49 (91 32) 82 - 28 97.

D_{c1}	1/2	inch	
D_{c1}	12,7	mm	
D_c	0,938	inch	
D_c	23,813	mm	
D_w	0,078	inch	
D_w	1,984	mm	
E_a	0,89	inch	
E_a	22,6	mm	
E_b	0,532	inch	
E_b	13,5	mm	
m	0,009	lbs	Mass
m	0,004	kg	Mass
C_a	1910	lbf	Basic dynamic load rating, axial
C_a	8500	N	Basic dynamic load rating, axial
C_{0a}	5300	lbf	Basic static load rating, axial
C_{0a}	23600	N	Basic static load rating, axial
n_G	15800	1/min	Limiting speed

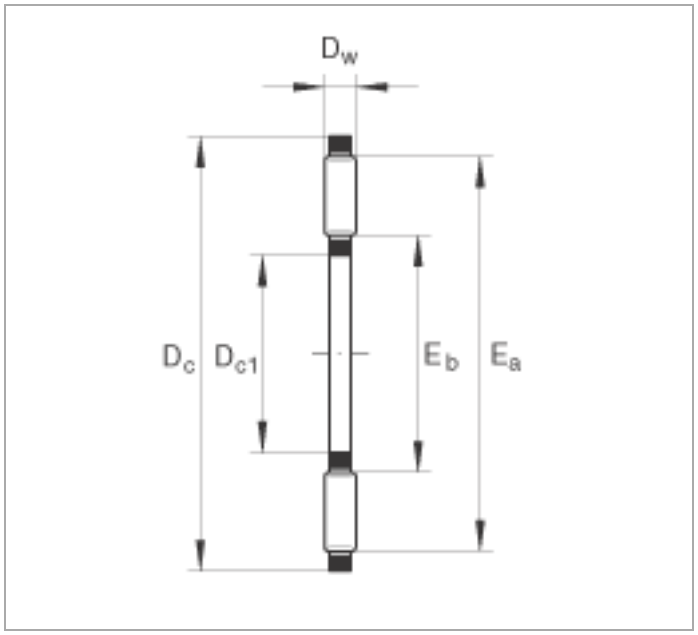
D_w
D_c
D_{c1}
E_b
E_a

A.14 80/20 Linear Bearings

80/20® Inc.
The Industrial Erector Set®
THE STANDARD

Double Flange Linear Bearings continued

DVD

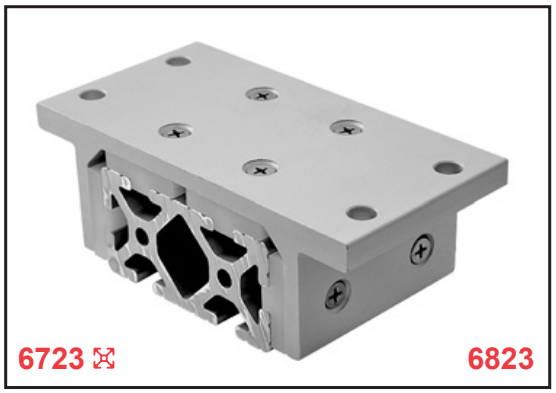

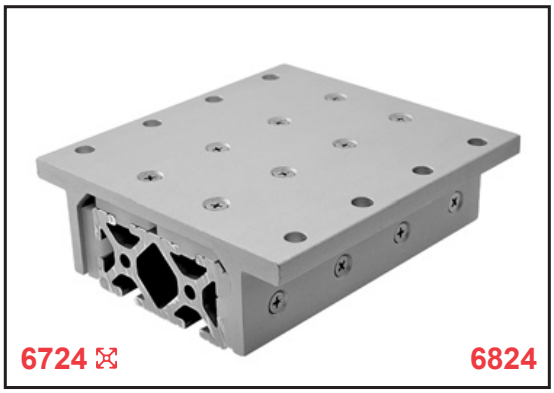

⊠ = 10 Series Compatible Part

- **Bearings include bearing pads, screws and shims**

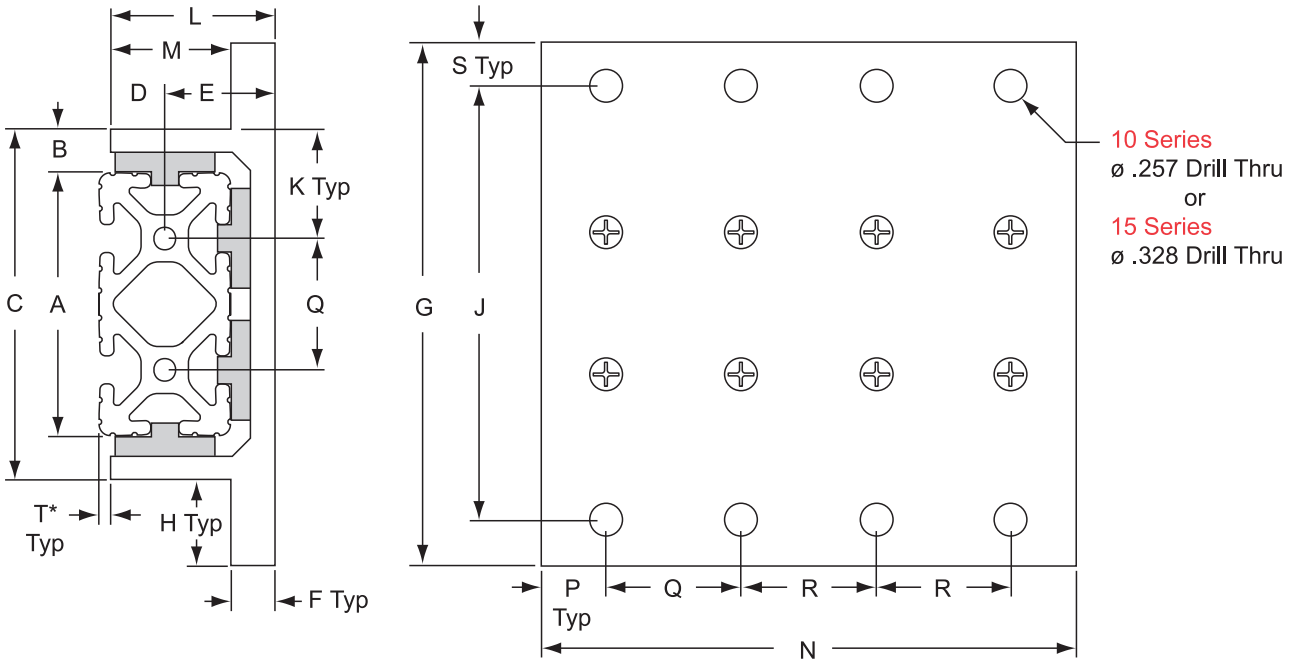

Part No.	A	B	C	D	E	F	G	H	J	K	L	M	N	P	Q	R	S	T*	Lbs.
6723 ⊠	2.000	.312	2.630	.406	.812	.312	3.937	.656	3.250	.812	1.218	.906	1.875	.437	1.000	—	.343	.094	.250
6423** ⊠	2.000	.312	2.630	.406	.812	.312	3.937	.656	3.250	.812	1.218	.906	1.875	.437	1.000	—	.343	.094	.250
6724 ⊠	2.000	.312	2.630	.406	.812	.312	3.937	.656	3.250	.812	1.218	.906	4.000	.500	1.000	1.000	.343	.094	.525
6424** ⊠	2.000	.312	2.630	.406	.812	.312	3.937	.656	3.250	.812	1.218	.906	4.000	.500	1.000	1.000	.343	.094	.525
6823	3.000	.500	4.000	.640	1.235	.375	5.500	.750	4.750	1.250	1.875	1.500	2.812	.656	1.500	—	.375	.125	.810
6523**	3.000	.500	4.000	.640	1.235	.375	5.500	.750	4.750	1.250	1.875	1.500	2.812	.656	1.500	—	.375	.125	.810
6824	3.000	.500	4.000	.640	1.235	.375	5.500	.750	4.750	1.250	1.875	1.500	6.000	.750	1.500	1.500	.375	.125	1.705
6524**	3.000	.500	4.000	.640	1.235	.375	5.500	.750	4.750	1.250	1.875	1.500	6.000	.750	1.500	1.500	.375	.125	1.705

*10 Series: Add 1.00" when using 2020 profile or 3.00" when using 2040 profile.
*15 Series: Add 1.50" when using 3030 profile or 4.50" when using 3060 profile.

** Brake Kit Ready Bearings are pre-drilled with brake holes, refer to page 527 for additional information.

A.15 80/20 T-Slotted Aluminum

1530 T-Slotted Profile - 15 Series

- Compatible with all 15 Series fasteners
- Six open T-slots for mounting accessories
- The center cavity can be pressurized up to 150 psi; refer to pages 451-453
- Ideal for machine guards, sound enclosures, work benches, displays and panel mount racks
- Compatibility Code*: 8-15

VIBRATION ** PROOF™

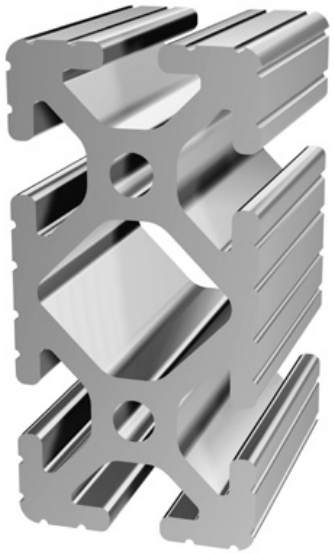

Part No.	1530
Material	6105-T5
Finish	Clear Anodized
Weight Per Foot	2.4209 Lbs.
Stock Length (+/- .125")	97" - Part No. 1530-97 145" - Part No. 1530-145 242" - Part No. 1530-242
Moment Of Inertia	IX=1.8042"⁴ IY=.4824"⁴
Estimated Area	2.0798 Sq. In.

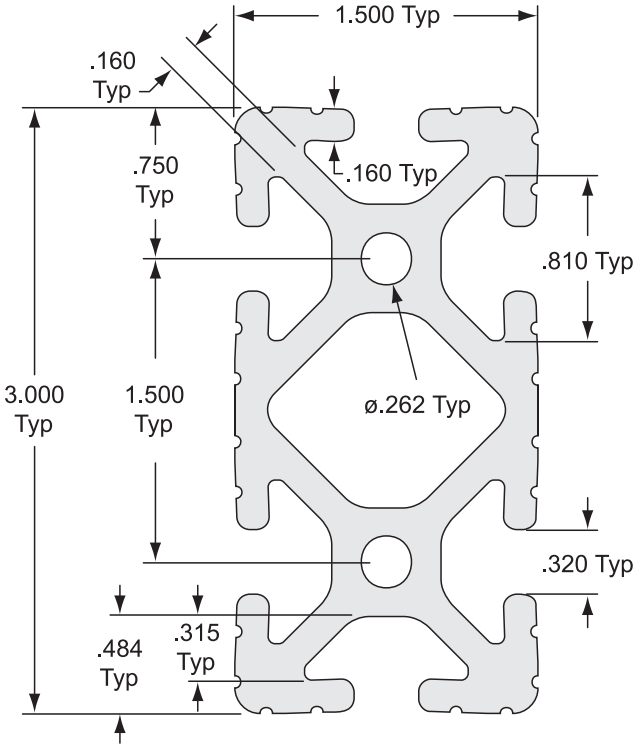

Quick Machining Reference

Machining Service	Service Number
Cut to Length	7020 (see page 563)
.295" Access Hole	7050 (see page 565)
Anchor Counterbore	7040 (see page 567)
Tap Profile End	7045 (see page 564)

* See Compatibility Code information on page 152.

** See 2° Drop-Lock information on page 150.

Pre-Cut Lengths

48" - Part No. 1530-48	72" - Part No. 1530-72

- Pre-cut, ready to ship
- Cut to our standard tolerance of +/- .015"
- One part number, one price (includes cut charge)

Appendix B

Source Code

B.1 Final Hybridized Control Source Code

```
/*
Arduino source code for Helios Solar Tracker.
Written by Laughlin Barker BSME & BS Environmental Studies '12

*/
#include <AccelStepper.h>
#include <AFMotor.h>
#include <Wire.h>
#include "RTClib.h"

RTC_DS1307 RTC;      //initialize RTC

//=======================================
//==============  CONSTANTS  =============
//=======================================
float latitude = 37.3477;      //SCU
float longitude = -121.9513;
//float timezone = -8;            //Timezone

float l1 = 16;        //in - L1 on mirror structure (back arm)
float l2 = 14.69;        //in - L2 on mirror structure

float pitch = 0.0833;    //in - leadscrew pitch (3/8 - 12 screw)
float starts = 1;        //# start
float lead = pitch*starts;  //in - lead of screw (distance traveled in 1 rotation)
float cartwidth = 4.5;        //in - width of cart on actuator
float lx = 47;              //in - length of x actuator space
float ly = 29.25;              //in - length of y actuator space

float stepper_resolution = 200;    //resolution of stepper

float xlims[2], ylims[2];    //x and y max/min in form [xmin, xmax], [ymin, ymax]
float args[2] = {180, 0};
long stepsx,stepsy;

float pi = 3.14159265;

//Logical holders for stepper zeroing
boolean xcal = 0;    //0 == FALSE i.e. not zeroed
boolean ycal = 0;
//=======================================
//=======================================


//=======================================
//============  GLOBAL VARS  ============
//=======================================
float azi = 0;
float ele = 0;          //open loop azi and ele
float x, y;             //open loop x and y
//====================
```

```
52
53
54 //================== MOTOR CONFIG STUFF ================
55 AF_Stepper motor1(200, 1); //X motor
56 AF_Stepper motor2(200, 2); //Y motor
57
58 void forwardstep1() {
59   motor1.onestep(FORWARD, DOUBLE);
60 }
61 void backwardstep1() {
62   motor1.onestep(BACKWARD, DOUBLE);
63 }
64
65 void forwardstep2() {
66   motor2.onestep(FORWARD, DOUBLE);
67 }
68 void backwardstep2() {
69   motor2.onestep(BACKWARD, DOUBLE);
70 }
71 // Motor shield has two motor ports, now we'll wrap them in an AccelStepper object
72 //AccelStepper stepper1(forwardstep1, backwardstep1);
73 AccelStepper stepper1(forwardstep1, backwardstep1);
74 AccelStepper stepper2(forwardstep2, backwardstep2);
75
76 int xcalpin = 19;
77 int ycalpin = 18;
78
79 void setup()
80 {
81     //setup steppers
82     stepper1.setMaxSpeed(300);    //steps/s
83     stepper1.setAcceleration(500);
84     stepper2.setMaxSpeed(300);
85     stepper2.setAcceleration(500);
86
87     //start serial
88     Serial.begin(115200);
89
90     //start 1-wire bus & RTC
91     Wire.begin();
92     RTC.begin();
93
94     //convert to rads
95     latitude = latitude * pi/180;
96
97     //uncomment if RTC is significantly off, upload, comment out, and then
   …
   re-reupload
98 //    RTC.adjust(DateTime(__DATE__, __TIME__));
99 }
100
101 char X_buffer[8];
```

```
102 float maxPOS = 32e3;
103 float setPointPOS, requestedPOS;
104 int j=1;
105 
106 long previousMillis = 0;
107 long interval = 5000;
108 
109 void loop() //begin main loop
110 {
111   DateTime now = RTC.now();
112   //if X and Y not calibrated, run motors until limit switch hit; will run on every
  … restart
113 //   Serial.println("Zeroing X Actuator");
114    while (xcal == 0){
115     stepper2.moveTo(-100000);
116     stepper2.run();
117     Serial.println("Calibarting X");
118 
119       if (digitalRead(xcalpin)==0){
120         xzero();
121       }
122 
123     }
124    while (ycal == 0){
125     stepper1.moveTo(-100000);
126     stepper1.run();
127     Serial.println("Calibarting Y");
128 
129       if (digitalRead(ycalpin)==0){
130         yzero();
131         Serial.println("Both actuators properly zeroed");
132         Serial.print(stepper2.currentPosition());
133         Serial.print(" , ");
134         Serial.print(stepper1.currentPosition());
135         azi = 246.9;
136         ele = 45.4;
137       }
138 
139     }
140 
141 //Serial input code...relic of Serial Positioning commands.
142 //Code taken from Instructables forum user
  … http://www.instructables.com/member/joachimp/
143 
144   //==========FOR X===========
145 if (Serial.available()){
146       //make sure we have all the data
147       delay(5);
148       //serial data is waiting, lets extract
149       int  i=0;
150       while(i<8){
```

```
151         X_buffer[i] = Serial.read();
152         //Serial.println(X_buffer[i]);
153         i++;
154       }
155 
156       //flush serial buffer of extra data>9999
157       Serial.flush();
158       //convert numeric string to int var
159       requestedPOS = atof(X_buffer);
160       //check for set point greater than maxPWR limit
161       if( requestedPOS < maxPOS){
162         //Buffer contains a safe value, copy out to setPointPWR
163         setPointPOS = requestedPOS;
164 //        Serial.print("Requested set point:");
165 //        Serial.println(setPointPOS);
166       }
167 
168       else{
169         Serial.println("'The #*$& is this?! The sun don't shine here!");
170         setPointPOS = 0; //
171       }
172       if (j>0){
173         Serial.print("Accepted AZI position:");
174         Serial.println(requestedPOS);
175         azi = setPointPOS;
176         //stepsx = setPointPOS;
177       }
178       else if (j<0){
179         Serial.print("Accepted ELE position:");
180         Serial.println(requestedPOS);
181         ele = setPointPOS;
182         //stepsy = setPointPOS;
183       }
184       j=-j;
185     }
186 
187 
188 
189  stepper1.run();
190  stepper2.run();
191 
192 
193      unsigned long currentMillis = millis();
194 
195   if(currentMillis - previousMillis > interval) {
196     // save the last time it went through this routine
197     previousMillis = currentMillis;
198 
199  //============================================================================
200  //                PERIODIC CALCULATIONS (not nec. every loop iteration)
201  //============================================================================
```

```
202
203     //get AZI and ELE of sun based on RTC
204     float azi_s = azi_func(latitude,longitude);
205     float ele_s = ele_func(latitude,longitude);
206
207     //instantaneous AZI and ELE of tracker
208     float azi_t = tracker_azi();
209     float ele_t = tracker_ele();
210
211     //tracker commanded position vars
212     float azi_t_command;
213     float ele_t_command;
214     long xcommand;
215     long ycommand;
216
217     //RTCerr = sqrt(a^2 + b^2)
218     float RTCerr = pow( (pow( (azi_s - azi_t) , 2) + pow( (ele_s - ele_t) , 2 ) ) ,
  … 0.5);
219
220     //if angular error ir greater than maxRTCerr, move tracker to sun orientation
221     float maxRTCerr = 3;        //degrees total error (sum of azi/ele error vectors)
222      if (RTCerr > maxRTCerr){
223
224       azi_t_command = azi_s;
225       ele_t_command = ele_s;
226       xcommand = x_step_pos(azi_t_command, ele_t_command);
227       ycommand = y_step_pos(azi_t_command, ele_t_command);
228       stepper1.moveTo(ycommand);
229       stepper2.moveTo(xcommand);
230
231       Serial.println("====================================");
232
233       Serial.println("OPEN-LOOP POSITIONING...");
234
235       Serial.println("====================================");
236      }
237
238      // Closed loop routine; only do it RTC error is within allowable limits
239      else if (RTCerr < maxRTCerr){
240
241       float EWcorr = senseEW();
242       float NScorr = senseNS();
243
244       azi_t_command = azi_t + EWcorr;
245       ele_t_command = ele_t + NScorr;
246
247       xcommand = x_step_pos(azi_t_command, ele_t_command);
248       ycommand = y_step_pos(azi_t_command, ele_t_command);
249       stepper1.moveTo(ycommand);
250       stepper2.moveTo(xcommand);
251
```

```
252         Serial.println("====================================");
253 
254         Serial.println("CLOSED LOOP MISALIGNMENT...CORRECTING");
255         Serial.print("Correcting ");
256         Serial.print(EWcorr);
257         Serial.println(" degrees West...");
258 
259         Serial.print("Correcting ");
260         Serial.print(NScorr);
261         Serial.println(" degrees North");
262 
263         Serial.println("====================================");
264       }
265 
266  long xcurrent = stepper2.currentPosition();
267  long ycurrent = stepper1.currentPosition();
268 
269  //=============================================================
270  //                PERIODIC SERIAL OUTPUT
271  //=============================================================
272 
273 //    Serial.println("Step pos: ");
274 //    Serial.print(xcurrent);
275 //    Serial.print(" , ");
276 //    Serial.println(ycurrent);
277 //    Serial.println(" ");
278 //
279 //    Serial.print("X,Y: ");
280 //    Serial.print(steps2disp(xcurrent));
281 //    Serial.print(" , ");
282 //    Serial.println(steps2disp(ycurrent));
283 //    Serial.println(" ");
284 
285     Serial.print("Date: ");
286     Serial.print(now.year(), DEC);
287     Serial.print('/');
288     Serial.print(now.month(), DEC);
289     Serial.print('/');
290     Serial.print(now.day(), DEC);
291     Serial.print(' ');
292     Serial.print(now.hour(), DEC);
293     Serial.print(':');
294     Serial.print(now.minute(), DEC);
295     Serial.print(':');
296     Serial.println(now.second(), DEC);
297     Serial.println(" ");
298 
299     Serial.print("Sun Pos: ");
300     Serial.print(azi_s);
301     Serial.print(" , ");
302     Serial.println(ele_s);
```

```
303     Serial.println(" ");
304
305     Serial.print("Tracker Pos: ");
306     Serial.print(tracker_azi());
307     Serial.print(" , ");
308     Serial.println(tracker_ele());
309     Serial.println("========================");
310
311
312   }
313
314 }
315
316
317
318
319 void xzero(){
320   Serial.println("Zeroing X actuator");
321   long tmppos = disp2steps(lx/2) - (cartwidth/2) * stepper_resolution / lead;
322   tmppos = -tmppos;
323    //calculating position based on screw and stepper info
324   stepper2.setCurrentPosition(tmppos);    //makes zero in the middle of the x
  … actuator when cart is at end...sneaky!
325   Serial.print("Current position: ");
326   Serial.println(stepper2.currentPosition());
327   stepsx = stepper2.currentPosition();
328   xcal = 1;
329 }
330
331 void yzero(){
332   Serial.println("Zeroing Y actuator");
333    //calculating position based on screw and stepper info
334   long tmppos = 8.75 * stepper_resolution / lead;
335   stepper1.setCurrentPosition(tmppos);    //makes zero in the middle of the x
  … actuator when cart is at end...sneaky!
336   Serial.print("Current position: ");
337   Serial.println(stepper1.currentPosition());
338   stepsy = stepper1.currentPosition();
339   ycal = 1;
340
341 }
342
343 long disp2steps(float disp){      //actuator displacement to steps
344   long steps = disp * stepper_resolution / pitch;    //will truncate; OK since 1
  … step = 0.00125" for .25 lead screw
345   return steps;
346 }
347
348 float steps2disp(long isteps){
349   float steps = (long)isteps;
350   float disp = steps/(stepper_resolution / pitch);
```

```
351   return disp;
352 }
353 
354 float tracker_azi(){
355   float x = steps2disp(stepper2.currentPosition());
356   float y = steps2disp(stepper1.currentPosition());
357   float azi = azi_pos(x, y, l1, l2, args);
358   return azi;
359 }
360 
361 float tracker_ele(){
362   float x = steps2disp(stepper2.currentPosition());
363   float y = steps2disp(stepper1.currentPosition());
364   float ele = ele_pos(x, y, l1, l2, args);
365   return ele;
366 }
367 
368 long x_step_pos(float azi, float ele){
369   float x = aziele2x(azi, ele, l1, l2, args);
370   long x_steps = disp2steps(x);
371   return x_steps;
372 }
373 
374 long y_step_pos(float azi, float ele){
375   float y = aziele2y(azi, ele, l1, l2, args);
376   long y_steps = disp2steps(y);
377   return y_steps;
378 }
379 
380 /// These functions convert given azimuth and elevation angles to X and Y
381 /// actuator positions for the low-profile T-Tracker solar tracker.
382 /// Copyright Team Helios 2012. Code written by Laughlin Barker BSME 2012.
383 ///
384 /// Input arguments are as follows:
385 
386 //   azi = azimuth of sun
387 //   ele = elevation of sun
388 //   l1 = l1 length of the tracker (riser arm)
389 //   l2 = l2 of the tracker (distance b/t two mirror mount/piviot points)
390 //   args = [Ori, offset]
391 //
392 //   (TRACKER TOP VIEW)
393 //         Oir = orientation of "T" of tracker (normally 180 deg)
394 //            ^
395 //            |
396 //            |
397 //            |
398 //            |   ^ +y
399 //            |   |
400 //            |  _|_
401 // ___________|___________
```

```
402 //
403 //            |----> +x
404
405 //=========   FIRST TO SOLVE FOR Y POSITION   ==========
406 float aziele2y(float azi, float ele, float l1, float l2, float args[2])
407 {
408 //convert to theta phi values
409 float theta = abs(azi - 180);
410 float phi = 90 - ele;
411
412 //a = sec(theta)^2
413 float a = pow((1/cos(theta*pi/180)),2);
414 //b = -2 * sec(theta) * cos(phi) * l2
415 float b = -2 * 1/cos(theta*pi/180) * cos(phi*pi/180) * l2;
416 //c = l2^2 - l1^2
417 float c = pow(l2,2) - pow(l1,2);
418
419 //additive solution to simple quadratic eqn
420 float y = (-b + pow((pow(b,2) - 4 * a * c),0.5)) / (2 * a);
421 return y;
422 }
423
424 float aziele2x(float azi, float ele, float l1, float l2, float args[2])
425 {
426 //convert to theta phi values
427 float theta = abs(azi - 180);
428 float phi = 90 - ele;
429
430 //a = sec(theta)^2
431 float a = pow((1/cos(theta*pi/180)),2);
432 //b = -2 * sec(theta) * cos(phi) * l2
433 float b = -2 * 1/cos(theta*pi/180) * cos(phi*pi/180) * l2;
434 //c = l2^2 - l1^2
435 float c = pow(l2,2) - pow(l1,2);
436
437 //additive solution to simple quadratic eqn
438 float y = (-b + pow((pow(b,2) - 4 * a * c),0.5)) / (2 * a);
439 float x = tan(theta*pi/180) * y;
440
441 if (azi<180){
442 x = x;
443 }
444 else{
445 x = -x;
446 }
447
448 return x;
449 }
450
451 //============================================================
452
```

```
453 float azi_pos(float x, float y, float l1, float l2, float args[]){
454
455  float theta = abs(atan(x/y))*180/pi;
456
457   if (x < 0){
458     azi = args[0] + theta;        //if x is negative azi angle of tracker is >180
  … deg
459   }
460   else if (x > 0){
461     azi = args[0] - theta;        // if x is positive azi angle of tracker is <180
  … deg
462   }
463   else if (x==0){
464     azi = args[0];
465   }
466   return azi;
467 }
468
469 float ele_pos(float x, float y, float l1, float l2, float args[]){
470
471    float h = pow( (pow(x,2) + pow(y,2)) ,0.5);
472    float phi = acos((pow(l1,2) - pow(h,2) - pow(l2,2))/(-2 * h *l2))*180/pi;
473    float  ele = 90 -  phi;
474     return ele;
475 }
476
477 // Function responsible for reading solar sensor, decideding
478 // if corrective action is necessary, and in what direction(s).
479
480
481
482 float senseEW()
483 {
484   //Error of arbitrary ADC value. Will likely require iterative calibration as there
  … is no direct
485   //transfer function from sensor output to sensor alignment. PLC essentially...
486   int maxerror = 50;
487
488   //degrees by which tracker will be corrected
489   float corrFactor = 0.25;
490
491   //  -255     -maxerror         0        maxerror           255
492   // E/N<-----------(acceptable error interval)------------->W/S
493
494   int east = analogRead(A2);
495   int west = analogRead(A3);
496
497   int EWerror = east - west;
498
499  // E-W Corrections
500 if (EWerror >= maxerror)
```

```
 {
  //Indicate correct to East
corrFactor = -corrFactor;
 }
 else if (EWerror <= -maxerror)
 {
   //Indicate correct to West
corrFactor = corrFactor;
 }
 else
 {
   //Do nothing
corrFactor = 0;
 }
 return corrFactor;

}


float senseNS()
{

  int maxerror = 50;

  //degrees by which tracker will be corrected
  float corrFactor = 0.25;

  int north = analogRead(A0);
  int south = analogRead(A1);

  int NSerror = north - south;

    // N-S Corrections
if (NSerror >= maxerror)
 {
  //Correct to North
   corrFactor = corrFactor;
 }
 else if (NSerror <= -maxerror)
 {
   //Correct to South
   corrFactor = -corrFactor;
 }
 else
 {
   //Do nothing
   corrFactor = 0;
 }
 return corrFactor;

}
```

```
552
553 //Set Time Zone
554 float timezone = -7;
555
556 float azi_func(float latitude, float longitude){
557
558   //Get time from the RTC
559 DateTime now = RTC.now();
560
561 float month2 = now.month();
562 float day = now.day();
563 float hour2 = now.hour();
564 float  minute2 = now.minute();
565
566 /*
567 Begin solar position code written by Gabriel Miller http://www.cerebralmeltdown.com
568 Modifications made by Laughlin Barker.
569 Implimented and modified with permission under Creative Commons Licence.
570 */
571
572 ////////////////////////////////////////////////////////
573 //MISC. VARIABLES
574 ////////////////////////////////////////////////////////
575   float altitude;
576   float azimuth;
577   float delta;
578   float h;
579   float northOrSouth = 0;
580 ////////////////////////////////////////////////////////
581 //END MISC. VARIABLES
582 ////////////////////////////////////////////////////////
583
584   //START OF THE CODE THAT CALCULATES THE POSITION OF THE SUN
585   float n = daynum(month2) + day;//NUMBER OF DAYS SINCE THE START OF THE YEAR.
586   delta = .409279 * sin(2 * pi * ((284 + n)/365.25));//SUN'S DECLINATION.
587   day = dayToArrayNum(day);//TAKES THE CURRENT DAY OF THE MONTH AND CHANGES IT TO A
  … LOOK UP VALUE ON THE HOUR ANGLE TABLE.
588   h = (FindH(day,month2)) + longitude + (timezone * -1 * 15);//FINDS THE NOON HOUR
  … ANGLE ON THE TABLE AND MODIFIES IT FOR THE USER'S OWN LOCATION AND TIME ZONE.
589   h = ((((hour2 + minute2/60) - 12) * 15) + h)*pi/180;//FURTHER MODIFIES THE NOON
  … HOUR ANGLE OF THE CURRENT DAY AND TURNS IT INTO THE HOUR ANGLE FOR THE CURRENT HOUR
  … AND MINUTE.
590   azimuth = ((atan2((sin(h)),((cos(h) * sin(latitude)) - tan(delta) *
  … cos(latitude)))) + (northOrSouth*pi/180)) *180/pi + 180;//FINDS THE SUN'S AZIMUTH.
591   //END OF THE CODE THAT CALCULATES THE POSITION OF THE SUN
592 return azimuth;
593 }
594
595 float ele_func(float latitude, float longitude){
596
597   //Get time from the RTC
```

```
598 DateTime now = RTC.now();
599
600 float month2 = now.month();
601 float day = now.day();
602 float hour2 = now.hour();
603 float  minute2 = now.minute();
604
605 ////SET TIME AND DATE HERE//////////////
606 // float month2 = 2;
607 // float day = 20;
608 // float hour2 = 9;//Use 24hr clock (ex: 1:00pm = 13:00) and don't use daylight
  … saving time.
609 // float minute2 = 0;
610 ////END SET TIME AND DATE //////////////
611
612
613 //MISC. VARIABLES
614   float altitude;
615   float azimuth;
616   float delta;
617   float h;
618   float northOrSouth = 0;
619 ////////////////////////////////////////////////////////
620 //END MISC. VARIABLES
621 ////////////////////////////////////////////////////////
622   //START OF THE CODE THAT CALCULATES THE POSITION OF THE SUN
623   float n = daynum(month2) + day;//NUMBER OF DAYS SINCE THE START OF THE YEAR.
624   delta = .409279 * sin(2 * pi * ((284 + n)/365.25));//SUN'S DECLINATION.
625   day = dayToArrayNum(day);//TAKES THE CURRENT DAY OF THE MONTH AND CHANGES IT TO A
  … LOOK UP VALUE ON THE HOUR ANGLE TABLE.
626   h = (FindH(day,month2)) + longitude + (timezone * -1 * 15);//FINDS THE NOON HOUR
  … ANGLE ON THE TABLE AND MODIFIES IT FOR THE USER'S OWN LOCATION AND TIME ZONE.
627   h = ((((hour2 + minute2/60) - 12) * 15) + h)*pi/180;//FURTHER MODIFIES THE NOON
  … HOUR ANGLE OF THE CURRENT DAY AND TURNS IT INTO THE HOUR ANGLE FOR THE CURRENT HOUR
  … AND MINUTE.
628   altitude = (asin(sin(latitude) * sin(delta) + cos(latitude) * cos(delta) *
  … cos(h)))*180/pi;//FINDS THE SUN'S ALTITUDE.
629   //END OF THE CODE THAT CALCULATES THE POSITION OF THE SUN
630 return altitude;
631 }
632
633 //THIS CODE TURNS THE MONTH INTO THE NUMBER OF DAYS SINCE JANUARY 1ST.
634 //ITS ONLY PURPOSE IS FOR CALCULATING DELTA (DECLINATION), AND IS NOT USED IN THE
  … HOUR ANGLE TABLE OR ANYWHERE ELSE.
635   float daynum(float month){
636    float day;
637    if (month == 1){day=0;}
638    if (month == 2){day=31;}
639    if (month == 3){day=59;}
640    if (month == 4){day=90;}
641    if (month == 5){day=120;}
```

```
642    if (month == 6){day=151;}
643    if (month == 7){day=181;}
644    if (month == 8){day=212;}
645    if (month == 9){day=243;}
646    if (month == 10){day=273;}
647    if (month == 11){day=304;}
648    if (month == 12){day=334;}
649    return day;
650   }
651
652 //THIS CODE TAKES THE DAY OF THE MONTH AND DOES ONE OF THREE THINGS: ADDS A DAY,
  … SUBTRACTS A DAY, OR
653 //DOES NOTHING. THIS IS DONE SO THAT LESS VALUES ARE REQUIRED FOR THE NOON HOUR
  … ANGLE TABLE BELOW.
654 int dayToArrayNum(int day){
655     if ((day == 1) || (day == 2) || (day == 3)){day = 0;}
656     if ((day == 4) || (day == 5) || (day == 6)){day = 1;}
657     if ((day == 7) || (day == 8) || (day == 9)){day = 2;}
658     if ((day == 10) || (day == 11) || (day == 12)){day = 3;}
659     if ((day == 13) || (day == 14) || (day == 15)){day = 4;}
660     if ((day == 16) || (day == 17) || (day == 18)){day = 5;}
661     if ((day == 19) || (day == 20) || (day == 21)){day = 6;}
662     if ((day == 22) || (day == 23) || (day == 24)){day = 7;}
663     if ((day == 25) || (day == 26) || (day == 27)){day = 8;}
664     if ((day == 28) || (day == 29) || (day == 30) || (day == 31)){day = 9;}
665   return day;
666 }
667
668 ////////////////////////////////////////////////////////////
669 //HERE IS THE TABLE OF NOON HOUR ANGLE VALUES. THESE VALUES GIVE THE HOUR ANGLE, IN
  … DEGREES, OF THE SUN AT NOON (NOT SOLAR NOON)
670 //WHERE LONGITUDE = 0. DAYS ARE SKIPPED TO SAVE SPACE, WHICH IS WHY THERE ARE NOT
  … 365 NUMBERS IN THIS TABLE.
671 float FindH(int day, int month){
672 float h;
673
674 if (month == 1){
675     float h_Array[10]={
676     -1.038,-1.379,-1.703,-2.007,-2.289,-2.546,-2.776,-2.978,-3.151,-3.294,};
677     h = h_Array[day];}
678
679 if (month == 2){
680     float h_Array[10]={
681     -3.437,-3.508,-3.55,-3.561,-3.545,-3.501,-3.43,-3.336,-3.219,-3.081,};
682     h = h_Array[day];}
683
684 if (month == 3){
685     float h_Array[10]={
686     -2.924,-2.751,-2.563,-2.363,-2.153,-1.936,-1.713,-1.487,-1.26,-1.035,};
687     h = h_Array[day];}
688
```

```
689 if (month == 4){
690     float h_Array[10]={
691     -0.74,-0.527,-0.322,-0.127,0.055,0.224,0.376,0.512,0.63,0.728,};
692     h = h_Array[day];}
693 
694 if (month == 5){
695     float h_Array[10]={
696     0.806,0.863,0.898,0.913,0.906,0.878,0.829,0.761,0.675,0.571,};
697     h = h_Array[day];}
698 
699 if (month == 6){
700     float h_Array[10]={
701     0.41,0.275,0.128,-0.026,-0.186,-0.349,-0.512,-0.673,-0.829,-0.977,};
702     h = h_Array[day];}
703 
704 if (month == 7){
705     float h_Array[10]={
706     -1.159,-1.281,-1.387,-1.477,-1.547,-1.598,-1.628,-1.636,-1.622,-1.585,};
707     h = h_Array[day];}
708 
709 if (month == 8){
710     float h_Array[10]={
711     -1.525,-1.442,-1.338,-1.212,-1.065,-0.9,-0.716,-0.515,-0.299,-0.07,};
712     h = h_Array[day];}
713 
714 if (month == 9){
715     float h_Array[10]={
716     0.253,0.506,0.766,1.03,1.298,1.565,1.831,2.092,2.347,2.593,};
717     h = h_Array[day];}
718 
719 if (month == 10){
720     float h_Array[10]={
721     2.828,3.05,3.256,3.444,3.613,3.759,3.882,3.979,4.049,4.091,};
722     h = h_Array[day];}
723 
724 if (month == 11){
725     float h_Array[10]={
726     4.1,4.071,4.01,3.918,3.794,3.638,3.452,3.236,2.992,2.722,};
727     h = h_Array[day];}
728 
729 if (month == 12){
730     float h_Array[10]={
731     2.325,2.004,1.665,1.312,0.948,0.578,0.205,-0.167,-0.534,-0.893,};
732     h = h_Array[day];}
733 
734 return h;
735       }
736 ////////////////////////////////////////////////////////////
737 
738 //End of code written by Gabriel Miller with modifications by Laughlin Barker.
739 
```

B.2 Azimuth and Elevation Angles to x and y Position of Linear Actuator Slides

```
function [x,y] = aziele2xy(azi,ele,l1,l2,xlims,ylims,args)

%% This function converts given azimuth and elevation angles to X and Y
%% actuator positions for the low-profile T-Tracker solar tracker.
%% Copyright Team Helios 2012. Code written by Laughlin Barker BSME 2012.
%%
%% Input arguments are as follows:
%
%   azi = azimuth of sun
%   ele = elevation of sun
%   l1 = l1 length of the tracker (riser arm)
%   l2 = l2 of the tracker (distance b/t two mirror mount/piviot points)
%   xlims = [xmin, xmax] min and max of X shuttle piviot point
%   ylims = [ymin, ymax] min and max of Y shuttle piviot point
%   args = [Ori, offset]

%   (TRACKER TOP VIEW)
%         Oir = orientation of "T" of tracker (normally 180 deg)
%            ^
%            |
%            |
%            |
%            |   ^ +y
%            |   |
%            |  _|_
% ___________|___________
%
%            |----> +x

error(nargchk(4,7,nargin,'string'));

if nargin == 4
    args = [180 0];
    xlims = [-1e6 1e6];
    ylims = [0 1e6];
end

% Convert to theta and phi coordoinate system
theta = abs(azi - 180);
phi = 90 - ele;

a = secd(theta).^2;
b = -2 * secd(theta) .* cosd(phi) .* l2;
c = l2^2 - l1^2;

y = (-b + (b.^2 - 4*a*c).^.5) ./ (2*a);
x = tand(theta) .* y;

if azi<180
    x = x;
else
    x = -x;
end

if y<ylims(1)
```

```
    disp('Warning!!, Y min of your actuator was exceeded (elevation angle is
too low)');
elseif y>ylims(2)
    disp('Warning!!, Y max of your actuator was exceeded (elevation angle too
large)');
elseif x<xlims(1) | x>xlims(2)
    disp('Warning!! X max/min of your actuator was exceeded (azimuth out of
range)');
end
```

B.3 x and y Position of Linear Actuator Slides to θ and ϕ

```
function [azi,ele] = xy2thetaphi(x,y,l1,l2,xlims,ylims,args)
%%
%%  This function converts X and Y actuator locations to azimuth and
%%  elevation angles for the low-profile T-Tracker solar tracker.
%%  Copyright Team Helios 2012. Code written by Laughlin Barker BSME 2012.
%%
%%  x and y may be row or string vectors.
%%
%%  Input arguments are as follows:
%%
%   x = distance along x actuator
%   y = distance along y actuator
%   l1 = l1 of the tracker (riser arm)
%   l2 = l2 of the tracker (distance between two mirror mount points
%   xlims = [xmin, xmax] min and max of X shuttle piviot point
%   ylims = [ymin, ymax] min and max of Y shuttle piviot point
%   args = [Ori, offset (angle)]

%    (TRACKER TOP VIEW)
%         Oir = orientation of "T" of tracker (normally 180 deg)
%            ^
%            |
%            |
%            |
%            |   ^ +y
%            |   |
%            |  _|_
% ___________|_____________
%
%            |----> +x



error(nargchk(4,7,nargin,'string'));

% If no additional input arguments are supplied, assume a true south
% orientation and zero angular offset
if nargin == 4
    args = [180 0];
    xlims = [-1e6 1e6];
    ylims = [0 1e6];
end

% Math to compute intermediate theta and phi angles which are added or
% subtracted to get azimuth and elevation angles.
theta = abs(atand(x./y));
H = (x.^2 + y.^2).^.5;
phi = acosd((l1^2 - H.^2 - l2^2) ./ (-2 * H * l2));
theta


if x<0
    xsign = 'neg';
elseif x>0
    xsign = 'pos';
```

```
else
    xsign = 'zero';
end

if y<0
    ysin = 'neg'
else
    ysin = 'pos'
end


Ori = args(1);

switch xsign
    case 'neg'
        azi = Ori + theta;
    case 'pos'
        azi = Ori - theta;
    case 'zero'
        azi = Ori;
end

if y<0 && x<0
    azi = Ori + 90 + theta;
elseif y<0 && x>0
    azi = theta + (Ori - 180);
end

if y<ylims(1)
    disp('Warning!!, Y min of your actuator was exceeded (elevation angle is
too low)');
elseif y>ylims(2)
    disp('Warning!!, Y max of your actuator was exceeded (elevation angle too
large)');
elseif x<xlims(1) | x>xlims(2)
    disp('Warning!! X max/min of your actuator was exceeded (azimuth out of
range)');
end

Orientation = args(1)
offset = args(2)
ele = 90 - (phi+offset);
```

B.4 Force Calculation Source Code

```
% Tracker input args
l1 = 5.53;
l2 = 4.95;
% End tracker input args

% Location input args.
location.altitude = 10;
location.longitude = -121.952;
location.latitude = 37.3414;        % For SCU
% End location input args

aziJun = [];
zenJun = [];
aziDec = [];
zenDec = [];
timespan = 1:23;

%fixed time args
time.year = 2012;
time.UTC = -8;              %for PST
%end fixed time args

%%%
time.month = 6;
time.day = 21;              %summer solstice
%%%

% This will cycle through one full day at above defined location.
for hour = 1:23;
    time.hour = hour;       %for loop cant run on structured var
    for min = 30;
        time.min = min;
        for sec = 30;

            time.sec = sec;
            sun = sun_position(time,location);
            aziJun= [aziJun, sun.azimuth];
            zenJun = [zenJun, sun.zenith];
        end
    end
end

%%%
time.month = 12;
time.day = 21;              %winter solstice
%%%

for hour = 1:23;
    time.hour = hour;
    for min = 30;
        time.min = min;
        for sec = 30;

            time.sec = sec;
            sun = sun_position(time,location);
```

```
            aziDec= [aziDec, sun.azimuth];
            zenDec = [zenDec, sun.zenith];

        end
    end
end

%convert zenith to elevation
eleJun = 90 - zenJun;
eleDec = 90 - zenDec;

%convert elevation to radians
eleJunr = eleJun*(pi/180);
eleDecr = eleDec*(pi/180);

%convert azimuth to radians
aziJunr = (aziJun*pi/180);
aziDecr = (aziDec*pi/180);

%weight of dish + structure
wm=40;
%distance between x axis arm and center of gravity
d1=8.285;
%distance between y axis joint and center+gravity
d2=9.714;
%elevation angle
phi=eleJunr';
%azimuth angle
theta=pi/2+aziJunr';

%reaction forces to support the regular structure
Fdz=wm;
Fdp=62.428*pi*.5^2*3.5; %7.85 g/cm^3 for steel
Fdzt=Fdz+Fdp;
Fdztt(1:23)=Fdz+Fdp;
Fdztx=Fdztt';
A=(2/3*35*3.*cos(theta)+1/2*pi*(35/2)^2.*sin(theta));
P=0.004*40^2;   %Wind at 40 MPH
Cd=1.1*sin(theta)
Fdy=A.*P.*Cd;
FdT=sqrt((Fdy.^2)+(Fdztx.^2)).*4.4482216152605;

%reaction forces to support the our structure
F1=wm.*d2.*sin(pi/2-phi)/(d1+d2);
F2=(wm./cos(phi))-F1;
F1x=F1.*sin(phi).*sin(theta);
F1y=F1.*sin(phi).*cos(theta);
F1z=F1.*cos(phi);
F2x=F2.*sin(phi).*sin(theta);
F2y=F2.*sin(phi).*cos(theta);
F2z=F2.*cos(phi);
Fytc=[F2x;F2y;F2z];
%Wind from Directly South
A=2/3*35*3.*cos(theta)+1/2*pi*(35/2)^2.*sin(theta);
P=.00256*40^2;   %Wind at 40 MPH
```

```
Cd=1.1*sin(theta);
Fw=A.*P.*Cd;
%F1y=F1y-Fw;
F2y=F2y+Fw;
%reaction forces on the joint to support structure
Fxtrx=-F1x;
Fxtry=-F1y;
Fxtrz=-F1z;
Fytrx=-F2x;
Fytry=-F2y;
Fytrz=-F2z;
%weight of joint
mj=0.27;
%length of joint (inches)
lj=3;
ljx=lj.*sin(phi).*sin(theta);
ljy=lj.*sin(phi).*cos(theta);
ljz=lj.*cos(phi);
%force to support joint
Fxtjx=-Fxtrx+0;
Fxtjy=-Fxtry+0;
Fxtjz=-Fxtrz+mj;
Fytjx=-Fytrx+0;
Fytjy=-Fytry+0;
Fytjz=-Fytrz+mj;
%moments around joint
Mxtjx=-ljz.*Fxtry+ljy.*Fxtrz+(ljy./2)*-mj;
Mxtjy=ljz.*Fxtrx+(-ljx).*Fxtrz+(-ljx./2)*-mj;
Mxtjz=-ljy.*Fxtrx+ljx.*Fxtry;
Mytjx=-ljz.*Fytry+ljy.*Fytrz+ljy*-mj;
Mytjy=ljz.*Fytrx+(-ljx).*Fytrz+(-ljx)*-mj;
Mytjz=-ljy.*Fytrx+ljx.*Fytry;
%reaction forces/moments on arm of joint to slider
Fxtjrx=-Fxtjx;
Fxtjry=-Fxtjy;
Fxtjrz=-Fxtjz;
Fytjrx=-Fytjx;
Fytjry=-Fytjy;
Fytjrz=-Fytjz;
Mxtjrx=-Mxtjx;
Mxtjry=-Mxtjy;
Mxtjrz=-Mxtjz;
Mytjrx=-Mytjx;
Mytjry=-Mytjy;
Mytjrz=-Mytjz;
%mass of arm
ma=5.22;
%length of arm
la=19.8;
lax=la.*sin(phi).*sin(theta);
lay=la.*sin(phi).*cos(theta);
laz=la.*cos(phi);
%forces/moment to support arm
Fxtax=-Fxtjrx+0;
Fxtay=-Fxtjry+0;
Fxtaz=-Fxtjrz+mj;
Mxtax=-ljz.*Fxtjry+ljy.*Fxtjrz+ljy./2*(-ma)+Mxtjx;
```

```
Mxtay=ljz.*Fxtjrx-ljx.*Fxtjrz-ljx./2*(-ma)+Mxtjy;
Mxtaz=-ljy.*Fxtjrx+ljx.*Fxtjry+Mxtjz;
%reaction force on slider from arm
Fxtarx=-Fxtax;
Fxtary=-Fxtay;
Fxtarz=-Fxtaz;
Mxtarx=-Mxtax;
Mxtary=-Mxtay;
Mxtarz=-Mxtaz;
%forces/moments to support the slider
Fxsx=-Fxtarx+0;
Fxsy=-Fxtary+0;
Fxsz=-Fxtarz+mj;
Fysx=-Fytjrx+0;
Fysy=-Fytjry+0;
Fysz=-Fytjrz+mj;
lc=[0 -3 0;3 0 0;0 0 0];
Mxsx=-3*Fxtary+0+Mxtarx;
Mxsy=3*Fxtarx+0+Mxtary;
Mxsz=0+0+Mxtarz;
Mysx=-3.*Fytjry+0+Mytjrx;
Mysy=3.*Fxtjrx+0+Mytjry;
Mysz=0+0+Mxtjrz;
Fxsx=(Fxsx)';
Fxsy=(Fxsy)';
Fxsz=(Fxsz)';
%Total Force on X Slider
FxT=sqrt((Fxsx.^2)+(Fxsy.^2)+(Fxsz.^2))*4.4482216152605;
%Total Force on Y Slider
FyT=sqrt((Fysx.^2)+(Fysy.^2)+(Fysz.^2))*4.4482216152605;
figure
plot(timespan,FxT,'r');
hold on;
plot(timespan,FyT,'b');
plot(timespan,FdT,'g');
xlabel('Time of Day');
ylabel('Force [N]');
title({'Forces on Critical Parts of Summer Solstice'});
legend('Y Axis','X Axis','Typical Trackers');
```

Appendix C

Schematics

C.1 Functional Electrical System Schematic

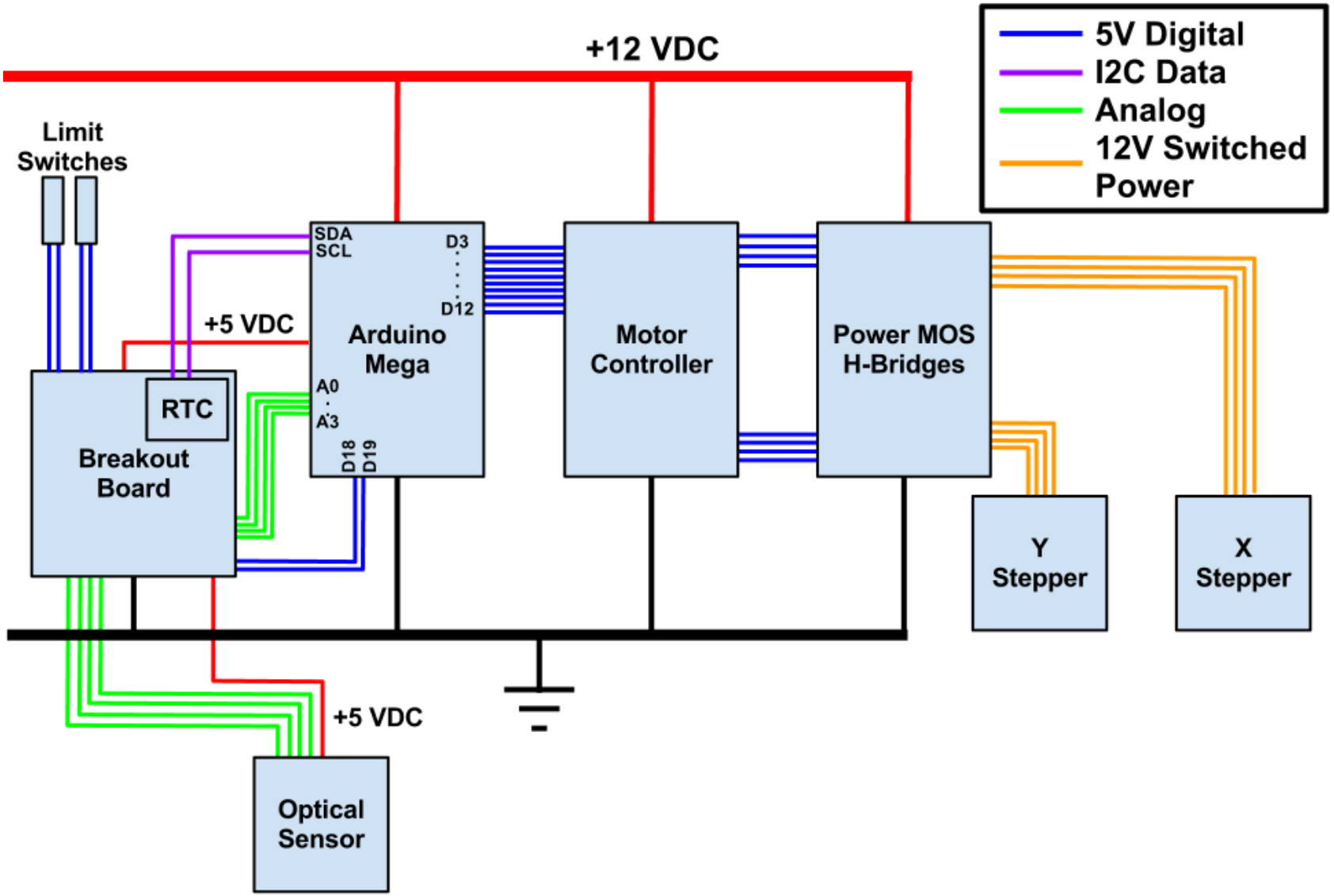
+12 VDC
5V Digital
I2C Data
Analog
12V Switched Power
Limit Switches
SDA
SCL
D3
D12
Arduino Mega
+5 VDC
A0
A3
D18
D19
RTC
Breakout Board
Motor Controller
Power MOS H-Bridges
Y Stepper
X Stepper
+5 VDC
Optical Sensor

C.2 Double H-Bridge Schematic

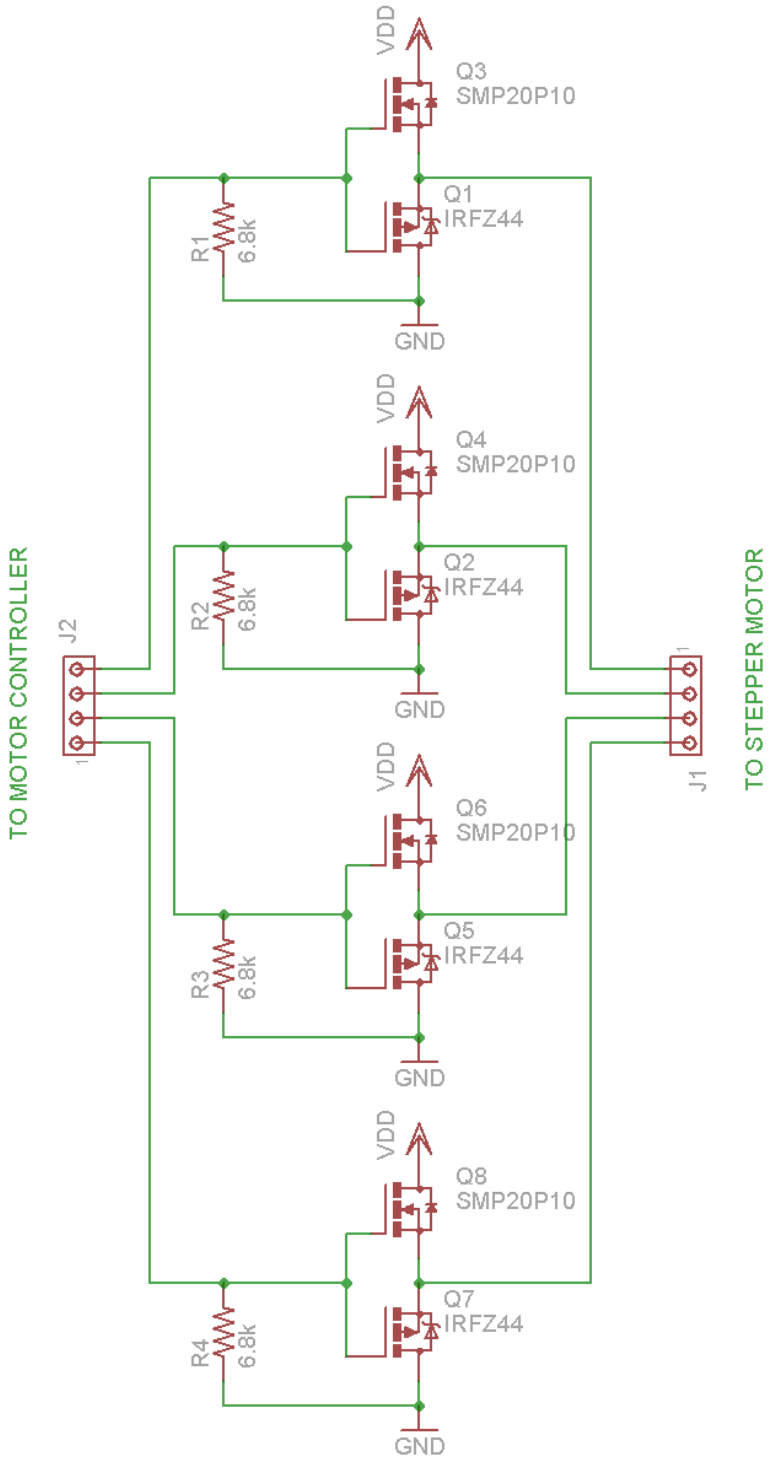

C.3 Arduino Mega 2560 Reference Design

Arduino™ Mega 2560 Reference Design

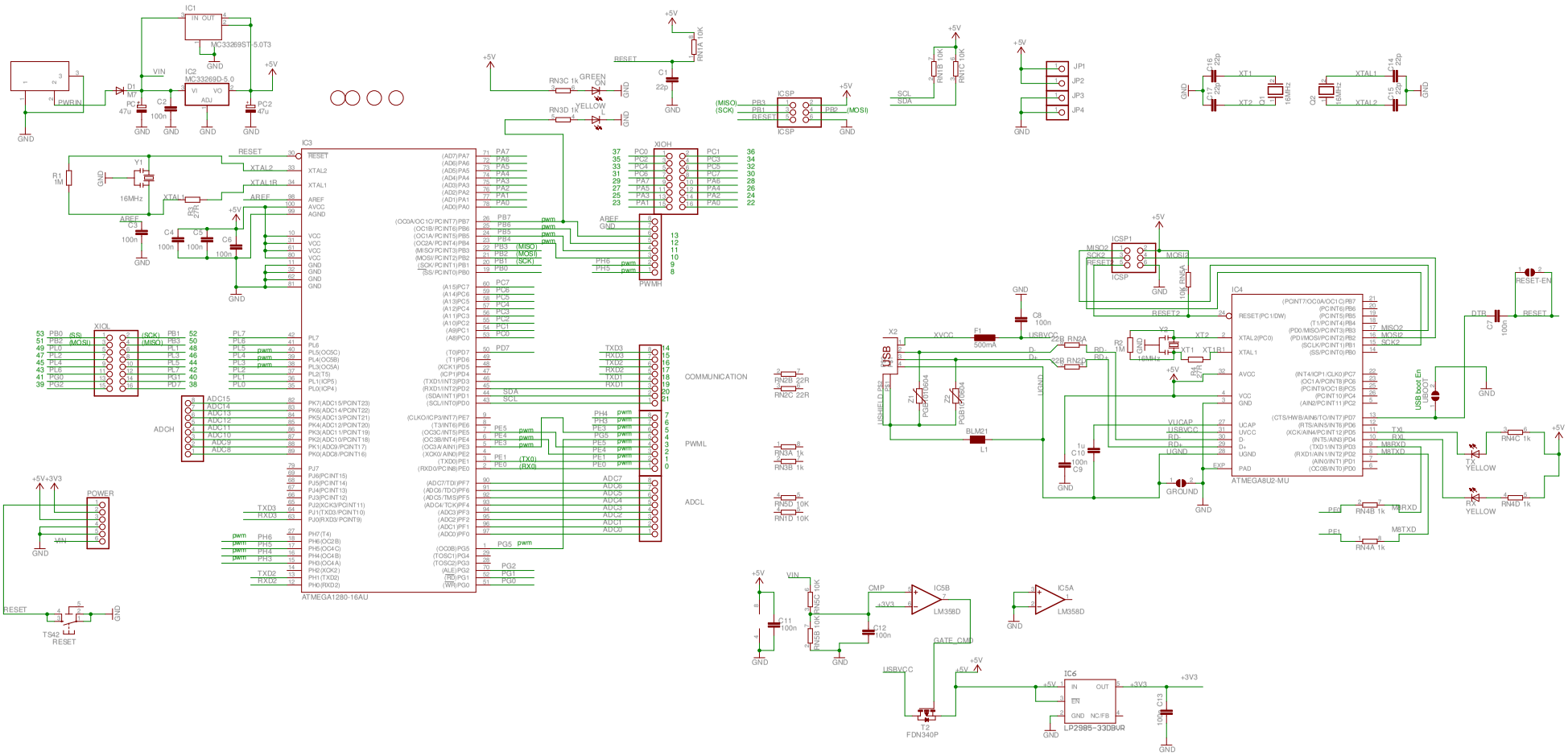

C.4 Controller Circuit Layout

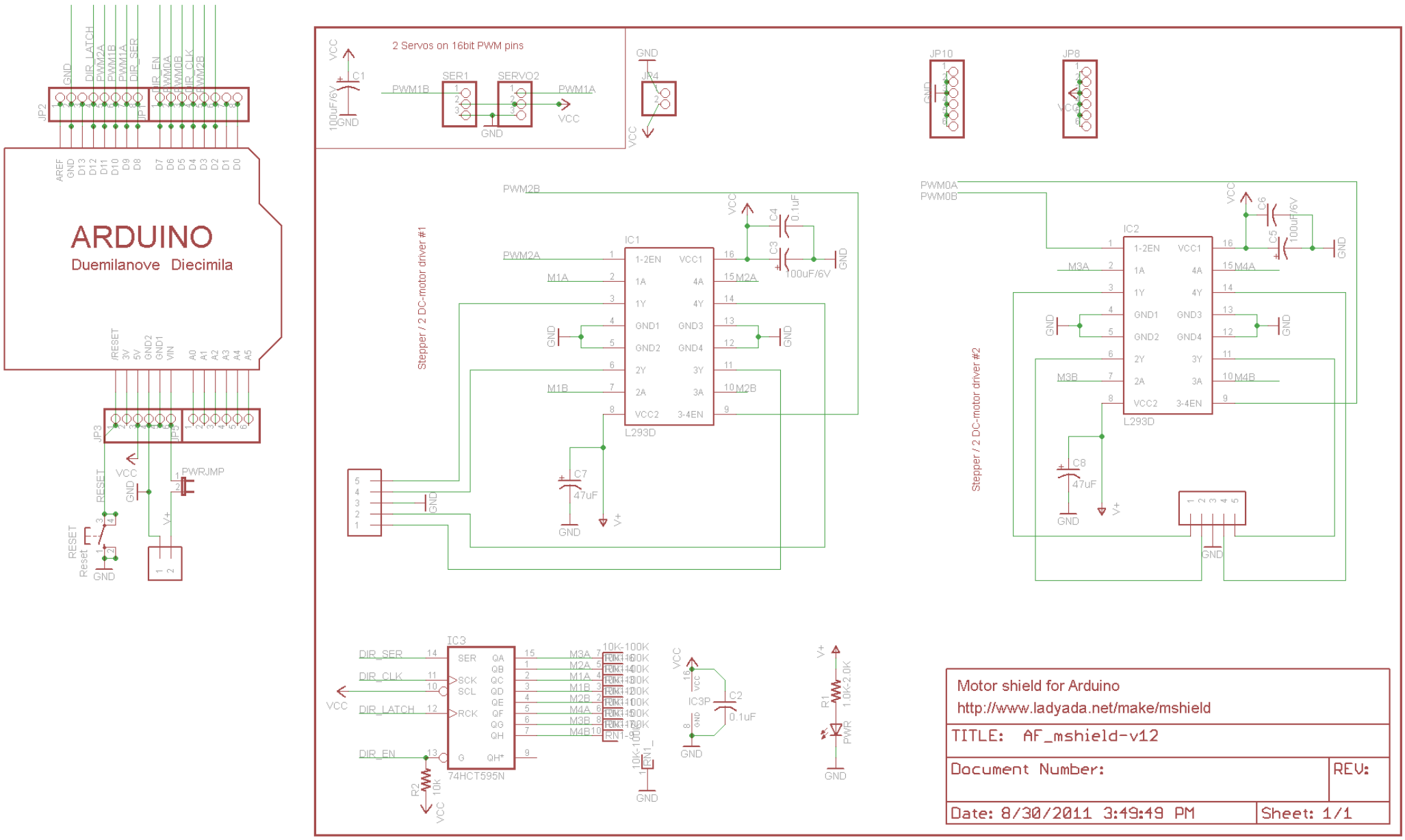
ARDUINO
Duemilanove Diecimila
2 Servos on 16bit PWM pins
Stepper / 2 DC-motor driver #1
Stepper / 2 DC-motor driver #2
L293D
74HCT595N
Motor shield for Arduino
http://www.ladyada.net/make/mshield
TITLE: AF_mshield-v12
Document Number:
REV:
Date: 8/30/2011 3:49:49 PM
Sheet: 1/1

Appendix D

Sketches and Calculations

D.1 Actuator space to azimuth-elevation space conversions

TOP VIEW

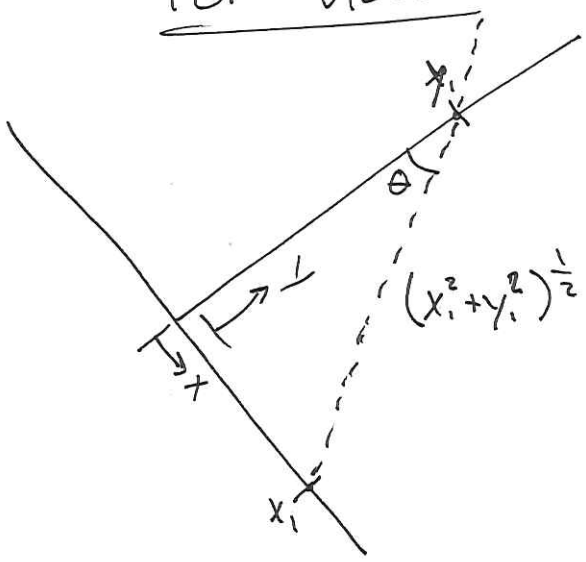

$\theta = \tan^{-1}\left(\frac{X_1}{Y_1}\right)$

$X = y\tan\theta$

2/5/12

LAUGHLIN BARGER

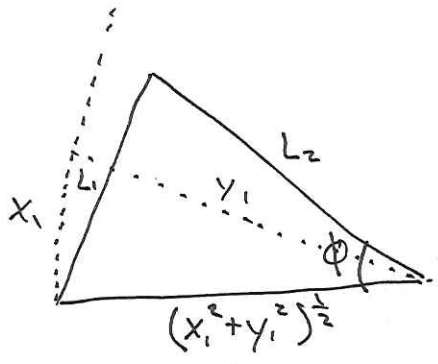

$=$
H

$$L_1^2 = H^2 + L_2^2 - 2HL_2\cos\phi$$

$$L_1^2 - H^2 - L_2^2 = -2HL_2\cos\phi$$

$$\cos\phi = \frac{L_1^2 - H^2 - L_2^2}{-2HL_2} \qquad H = (X_1^2+Y_1^2)^{\frac{1}{2}}$$

$$\cos\phi = \frac{L_1^2 - (x^2+y^2) - L_2^2}{-2(X_1^2+Y_1^2)^{\frac{1}{2}}L_2} \qquad X = y\tan\theta$$

$$\cos\phi = \frac{L_1^2 - ((y\tan\theta)^2+y^2) - L_2^2}{-2((y\tan\theta)^2+y^2)^{\frac{1}{2}}L_2}$$

$$\cos\phi = \frac{L_1^2 - (y^2(\tan^2\theta + 1)) - L_2^2}{-2\left(y^2(\tan^2\theta+1)\right)^{\frac{1}{2}} L_2} \qquad \tan^2\theta + 1 = \sec^2\theta$$

$$\cos\phi = \frac{L_1^2 - y^2\sec^2\theta - L_2^2}{-2\left(y^2\sec^2\theta\right)^{\frac{1}{2}} L_2}$$

$$\cos\phi = \frac{L_1^2 - y^2\sec^2\theta - L_2^2}{-2y\sec\theta L_2}$$

$$-2y\sec\theta L_2 = L_1^2 - y^2\sec^2\theta - L_2^2$$

$$y^2\sec^2\theta - y\,2\sec\theta\overset{\cos\phi}{\wedge}L_2 + (L_2^2 - L_1^2) = 0 \leftarrow \text{QUADRATIC!}$$

$$a = \sec^2\theta$$

$$b = -2\sec\theta\cos\phi L_2$$

$$c = L_2^2 - L_1^2$$

$$y = \frac{-b \pm \sqrt{b^2 - 4ac}}{2a}$$

D.2 ACME Lead Screw Torque Calculator

Click here for instructions on how to use this spreadsheet.

Click here to learn more about this spreadsheet.

Module 5-1
Torques required to operate a power screw.

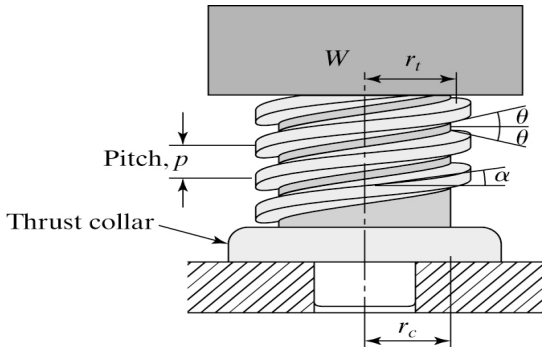

W =	1000	lbf	Load to be lifted
N_t =	4.00		Number of threads
p =	0.20	in.	Pitch of the screw
r_t =	0.45	in.	Screw pitch radius
θ =	14.50	degrees	Thread angle
r_c =	1.00	in.	Mean collar radius
μ_1 =	0.12		Coefficient of thread friction
μ_2 =	0.12		Coefficent of collar friction

Intermediate values computed:

L =	0.8	in.	Lead of screw
α =	15.80	degrees	Helix angle
θ_n =	13.97	degrees	Normal thread angle

Results found:

T_{raise} =	**309.6**	**in. lbf**	**Raising torque (Eqn. 12a)**
T_{lower} =	**50.7**	**in. lbf**	**Lowering Torque (Eqn. 14)**

If the lowering torque is negative, the system is overhauling. When this **happens, a means must be provided to lock the system in place.**

D.3 Solar Position Algorithm

Converting RA and DEC to ALT and AZ

[Root]

Contents

Overview

[Top]

"Today, the latitude and longitude lines govern with more authority than I could have imagined forty odd years ago, for they stay fixed as the world changes its configuration underneath them - with continents adrift across a widening sea, and national boundaries repeatedly redrawn by war or peace"

-Dava Sobel *Longitude*

This page is concerned with astronomical calculations. You will find out how to calculate the *Azimuth* (AZ) and *Altitude* (ALT) of an object in the sky if you know the date, time (UT) and the location of your observing site together with the *Right Ascension* (RA) and *Declination* (DEC) of the object. You do not actually need to calculate positions these days - there are lots of computer programs which will do the work for you - but calculating a position at least once may give a better insight into how the coordinate systems work. I tend to reflect on the sheer hard labour involved before the invention of calculators and computers!

As a concrete example, I shall calculate the ALT and AZ of the Messier object M13 for 10th August 1998 at 2310 hrs UT, for Birmingham UK. The RA and DEC of M13 are given as;

```
RA  = 16 h 41.7 min
DEC = 36 d 28   min
```

according to *The Cambridge Star Atlas*, and my old school atlas gives the latitude and longitude of Birmingham UK as;

```
LAT = 52 d 30 min North
LONG = 1 d 55 min West
```

We will need these figures in decimal form, along with the time;

```
RA   = 16 h 41.7 min      = 16 + 41.7/60 = 16.695      hrs
DEC  = 36 d 28   min      = 36 + 28/60   = 36.466667   degs
Time = 2310 hrs           = 23 + 10/60   = 23.166667   hrs
LAT  = 52 d 30 min North  = 52 + 30/60   = 52.5        degs
LONG =  1 d 55 min West   = -(1 + 55/60) = -1.9166667 degs
```

It is a good idea to keep all the decimal places in the figures until the calculation is complete, then round off later on. Notice how Longitudes west are counted as *negative*, and East counted as positive. We will also need the RA in degrees, not hours. Just multiply the hours figure by 15;

```
RA  = 16.695 * 15 = 250.425 degrees
```

In order to calculate the ALT and AZ of the comet for a given time and place, we need to calculate the *Local Siderial Time* (LST), and then work out the *Hour Angle* (HA) of the object. Then we can use some standard formulas from spherical trigonometry to transform the HA and DEC to the ALT and AZ.

If you are not sure what RA and DEC are, or about coordinate systems in general, then the following links might be useful;

- Sky and Telescope Backyard Astronomer series - Celestial Coordinates
- Sky and Telescope Backyard Astronomer series - About Time
- A series of lecture notes, from constellations to RA and DEC

I would strongly recommend the book by Peter Duffett-Smith (see Books section below) for further information and calculations, including precession.

Calculator notes

[Top]

A cheap basic scientific calculator is all that is needed for these calculations - although a programmable calculator can cut the work down if you want to calculate a whole series of positions. A spreadsheet allows you to prepare a list of positions of the object for each hour throughout the day.

When putting numbers into formulas, you must remember;

- I use '*' to represent multiply, and '/' to show divide. This means that the formulas can be copied straight into a spreadsheet, and the names changed to cell references.
- Multiplication (or division) is 'done before' addition (or subtraction) so that 3 + 4 *5 is 3 + 20 = 23, *not* 35! Scientific calculators have been programmed with the rules of precedence.
- Brackets are used to make sure certain results get calculated first, so (3+4) * 5 *does* give 35. Scientific calculators have brackets buttons.
- Most scientific calculators understand these rules of precedence, so if you type (999 - 994) /

(100 - 98) into your calculator and press the '=' or 'EXE' key, then you *should* get 2.5 as the answer.
- 50 / (2 * 5) is 5, not 125!
- the trigonometric functions usually work in degrees on calculators, but in *radians* on spreadsheets and in programming languages such as BASIC.
- To convert from degrees to radians, use `degs*3.14159265358979/180`, where `degs` is the angle in degrees.
- To convert from radians to degrees, use `rads*180/3.14159265358979`, where `rads` is the angle in Radians.

Days before J2000

[Top]

Many things (including the siderial time) are measured from a fundamental epoch or date. For most modern astronomical purposes, the reference date is J2000, which corresponds to 1200 hrs UT on Jan 1st 2000 AD, and you can use the table below to find how many days have gone by since J2000 for any date for the next 20 years or so.

```
Calculating the days from J2000
-------------------------------

The tables below can be used to calculate the number of days and
the fraction of a day since the epoch J2000. If you need the
number of Julian centuaries, then just divide the 'day number'
by 36525.
```

Table A — Days to beginning of month

Month	Normal year	Leap year
Jan	0	0
Feb	31	31
Mar	59	60
Apr	90	91
May	120	121
Jun	151	152
Jul	181	182
Aug	212	213
Sep	243	244
Oct	273	274
Nov	304	305
Dec	334	335

Table B — Days since J2000 to beginning of each year

Year	Days	Year	Days
1998	-731.5	2010	3651.5
1999	-366.5	2011	4016.5
2000	-1.5	2012	4381.5
2001	364.5	2013	4747.5
2002	729.5	2014	5112.5
2003	1094.5	2015	5477.5
2004	1459.5	2016	5842.5
2005	1825.5	2017	6208.5
2006	2190.5	2018	6573.5
2007	2555.5	2019	6938.5
2008	2920.5	2020	7303.5
2009	3286.5	2021	7669.5

```
Worked Example

To find the number of days from J2000.0 for 2310 hrs UT on
1998 August 10th, do the following;

1. divide the number of minutes by 60 to obtain the decimal
fraction of an hour, here 10/60 = 0.1666667
```

```
2. add this to the hours, then divide the total by 24 to obtain
the decimal fraction of the day, here 23.166667/24 = 0.9652778
This is the first number used below

3. find from table A the number of days to the beginning of
August from the start of the year, here 212 days

4. write down the day number within the month, here 10 above

5. find from table B the days since J2000.0 to the beginning of
the year, here -731.5

6. add these four numbers.

For the date above;

   0.9652778 + 212 + 10 - 731.5 = -508.53472 days from J2000.0

Note that dates which fall before J2000.0 will have negative day
numbers. Keep the negative sign in any calculations.

Exercise

What is the day number for 15:30 UT, 4th April 2008?
I got 3016.1458 days since J2000.0
```

Local Siderial Time

[Top]

Suppose you have a sunny morning. Put a stick in the ground, and watch the shadow. The shadow will get shorter and shorter - and then start to get longer and longer. The time corresponding to the shortest shadow is your local noon. We reckon a Solar day as (roughly) the mean time between two local noons, and we call this 24 hours of time.

The stars keep a day which is about 4 minutes shorter than the Solar day. This is because during one day, the Earth moves in its orbit around the Sun, so the Sun has to travel a bit further to reach the next day's noon. The stars do not have to travel that bit further to catch up - so the siderial day is shorter.

We need to be able to tell time by the stars, and the siderial time can be calculated from a formula which involves the number of days from the epoch J2000. An approximate version of the formula is;

```
LST = 100.46 + 0.985647 * d + long + 15*UT

      d    is the days from J2000, including the fraction of
           a day
      UT   is the universal time in decimal hours
      long is your longitude in decimal degrees, East positive.

Add or subtract multiples of 360 to bring LST in range 0 to 360
degrees.
```

and this formula gives your local siderial time in *degrees*. You can divide by 15 to get your local

siderial time in hours, but often we leave the figure in degrees. The approximation is within 0.3 seconds of time for dates within 100 years of J2000.

Worked Example for LST

```
Find the local siderial time for 2310 UT, 10th August 1998
at Birmingham UK (longitude 1 degree 55 minutes west).

I know that UT = 23.166667
             d = -508.53472 (last section)
          long = -1.9166667  (West counts as negative)

so

LST = 100.46 + 0.985647 * d + long + 15*UT
    = 100.46 + 0.985647 * -508.53472 - 1.9166667 + 15 * 23.166667
    = -55.192383 degrees
    = 304.80762 degrees

note how we added 360 to LST to bring the number into the range
0 to 360 degrees.
```

Hour Angle

[Top]

We can build in the Earth's rotation by replacing the RA by the Hour Angle. The HA of an object increases with siderial time, but the declination stays the same, as the DEC measures the angle from the Earth's equator. We calculate the HA in degrees, so that we can take sines and cosines later.

```
HA = LST - RA

If HA negative, then add 360 to bring in range 0 to 360
RA must be in degrees.
```

As you can see, the HA of the first point of Aries (where RA is 0) is just the LST expressed in degrees.

Worked example of HA

```
 RA = 250.425 degs
LST = 304.80762

HA = LST - RA
   = 304.80762 - 250.425
   = 54.382617 degs

HA is in correct range, so leave the number
```

HA and DEC to ALT and AZ

[Top]

Now we have the RA, DEC and HA for the object, and the Latitude (LAT) of the observing site, the following formulas will give us the ALT and AZ of the object at the current LST.

```
sin(ALT) = sin(DEC)*sin(LAT)+cos(DEC)*cos(LAT)*cos(HA)

ALT = asin(ALT)

                sin(DEC) - sin(ALT)*sin(LAT)
cos(A)   =   ---------------------------------
                    cos(ALT)*cos(LAT)

A = acos(A)

If sin(HA) is negative, then AZ = A, otherwise
AZ = 360 - A
```

Worked example of HA and DEC to ALT and AZ

I find it a good idea to use the calculator to find the values of the sines and cosines of the numbers needed first, then calculate the formulas. I record calculations step by step, which makes mistakes easier to find.

```
HA  =  54.382617
DEC =  36.466667 degrees
LAT =  52.5 degrees (North, so positive)

sin(DEC) = 0.5943550  cos(DEC) = 0.8042028
sin(LAT) = 0.7933533  cos(LAT) = 0.6087614
sin(HA)  is positive  cos(HA)  = 0.5823696

putting the values above into the first formula gives

sin(ALT) = sin(DEC)*sin(LAT)+cos(DEC)*cos(LAT)*cos(HA)

sin(ALT) = 0.5943550 * 0.7933533 + 0.8042028 * 0.6087614 * 0.5823696
         = 0.4715335 + 0.2851093
         = 0.7566428

ALT = 49.169122 degrees

cos(ALT) = 0.6538285

Putting values into the second formula below gives

             sin(DEC) - sin(ALT)*sin(LAT)
cos(A)   = ---------------------------------
                   cos(ALT)*cos(LAT)

           0.5943550 - 0.7566428 * 0.7933533
cos(A)   = ---------------------------------
                   0.6538285 * 0.6087614

          -0.0059301
         = -----------
            0.3980256
```

D.4 Detailed Assembly and Part Drawings

Project	Solar Tracker '12													
As-Built	Friday, May 18, 2012													
Subsystem	Component Description	Part #	# of items	B/M/O[1]	Vendor	Cost / part	Responsible person	Man-hours[2]	Des	Proc	Build (ea)	Assm	Order or start date	Receive or finish date
Clevis Mounts														
	Bottom Block	MMA-1	2	M	Metal Supermarkets	$30	Criselle,Laughlin	39	15	0	8		1-Feb	30-Mar
	Needle Sleeve Bearing	5909K43	2	B	Mcmaster	$15	Joe	0	0	0	0		1-Feb	30-Mar
	Washer	5909K56	4	B	McMaster	$0.50	Joe	0	0	0	0		1-Feb	30-Mar
	Top Block	MMA-2A	1	M	Metal Supermarkets	$25	Criselle,Laughlin	31	15	0	8		1-Feb	30-Mar
	Top Block Single	MMA-2B	1	M	Metal Supermarkets	$25	Criselle,Laughlin	31	15	0	8		1-Feb	30-Mar
	Needle Roller Bearing	5905K29	2	B	Mcmaster	$5	Joe	0	0	0	0		1-Feb	30-Mar
	Socket cap screw 1/4"-20 x 3/4"	90128A245	2	B	Mcmaster	$0.50	Joe	0	0	0	0		1-Feb	30-Mar
	Washer	98032A489	2	B	Mcmaster	$0.50	Joe	0	0	0	0		1-Feb	30-Mar
	Washer	5909K44	2	B	Mcmaster	$0.50	Joe	0	0	0	0		1-Feb	30-Mar
	Needle Roller Bearing	5909K31	2	B	Mcmaster	$5	Joe	0	0	0	0		1-Feb	30-Mar
	Clevis Mount Assembly	1	2	M			Criselle,Laughlin, Darcy,Joe	40	15	0	24	1	1-Feb	30-Mar
	Sub System Totals					**$117**		**141**						
Mirror Support														
	Wood MirrorTripodSupport1	MHA-1	2	M	Home Depot	$8	Joe	13	10	0	1		1-Feb	30-Mar
	FocalArm	MHA-2	2	M	Metal Supermarkets	$30	Joe	34	10	0	8		1-Feb	30-Mar
	Base_couple	MHA-3	1	M	Metal Supermarkets	$30	Joe	20	10	0	5		1-Feb	30-Mar
	focalmountcouple	MHA-4	1	M	Metal Supermarkets	$15	Joe	20	10	0	5		1-Feb	30-Mar
	SampleHolder	MHA-5	1	M	Mcmaster	$10	Joe	4	2	0	1		1-Feb	30-Mar
	Mirror1	MHA-6	1	M	Green Power Science	$350	Joe	0	0	0	0		1-Feb	30-Mar
	Wood MirrorTripodSupport2	MHA-7	2	M	Home Depot	$8	Joe	13	10	0	1		1-Feb	30-Mar
	Wood Beam	MHA-8	1	M	Home Depot	$5	Joe	3	1	0	1		1-Feb	30-Mar
	base_couple2	MHA-9	1	M	Metal Supermarkets	$30	Joe	20	10	0	5		1-Feb	30-Mar
	Linkage Arm	MHA-10	1	M	Metal Supermarkets	$25	Joe	6	2	0	2		1-Feb	30-Mar
	Grade 5 bolts 1/4"-20 x 5"	91247A562	6	B	Mcmaster	$0.50	Joe	0	0	0	0		1-Feb	30-Mar
	Grade 5 hex nuts 1/4"-20	95462A029	6	B	Mcmaster	$1	Joe	0	0	0	0		1-Feb	30-Mar
	Flat Washer 1/4" Screw Size	93852A102	6	B	Mcmaster	$0.25	Joe	0	0	0	0		1-Feb	30-Mar
	Wood Screws No. 6	90095A414	16	B	Mcmaster	$0.25	Joe	0	0	0	0		1-Feb	30-Mar
	Mirror Support Assembly	2	1	M					10	0		1	1-Feb	30-Mar
	Sub System Totals					**$76**		**53**						
Linear Actuators														
	Lead screw	93410A916	1	B	Mcmaster	$10	Sam, Mary	2	2	0			1-Feb	30-Mar
	80/20 Aluminum Extrusion	47065T159	1	B	Mcmaster	$100	Sam, Mary	0.5	0.5	0			1-Feb	30-Mar
	Lead screw endblocks	LAA-1	2	M	Mcmaster	$30	Jose, Clem	1	1	0			1-Feb	30-Mar
	Lead screw collar	LAA-2	2	M	Mcmaster	$30	Jose, Clem	0.5	0.5	0			1-Feb	30-Mar
	Shaft Collar	6435K13	1	B	Mcmaster	$25	Jose, Clem	2	2	0			1-Feb	30-Mar
	Teflon slide	8020-6523	1	B	Mcmaster	$100	Vita, Louise	0.2	0.2	0			1-Feb	30-Mar
	end-feed fasteners	47065T97	8	B	Pedal Power	$5	Vita, Louise	0.3	0.3	0			1-Feb	30-Mar
	Linear Actuator Assembly	3	2	M			Sam, Mary	6	3	0		3	1-Feb	30-Mar
	Sub System Totals					**$395**		**12.5**		.				
Solar Sensor														
	Sensor Base	SEN-1	1	M	TAP Plastics	$3	Sam, Mary	2	1	0	1		1-Feb	30-Mar
	Shade Hat	SEN-2	1	M	TAP Plastics	$3	Sam, Mary	2	1	0	1		1-Feb	30-Mar
	Sensor Mast	SEN-3	1	M	TAP Plastics	$3	Jose, Clem	2	1	0	1		1-Feb	30-Mar
	Vishay Photodiodes	bpw21r	4	B	HSC	$10	Jose, Clem	0	0	0	0		1-Feb	30-Mar
	Belkin cat5 female connector	R6D011	1	B	HSC	$5	Jose, Clem	0	0	0	0		1-Feb	30-Mar
	Solar Sensor Assembly	4	1	M			Sam, Mary	5	2	0	1	2	1-Feb	30-Mar
	Sub System Totals					**$54**		**11**		.				
Project Totals						**$642**		**205.0**	**149.5**	**0**	**123**	**7**		

[1] B = bought, M = made by you, O = made by others
[2] Total team hours in design, procurement, manufacture, and assembly

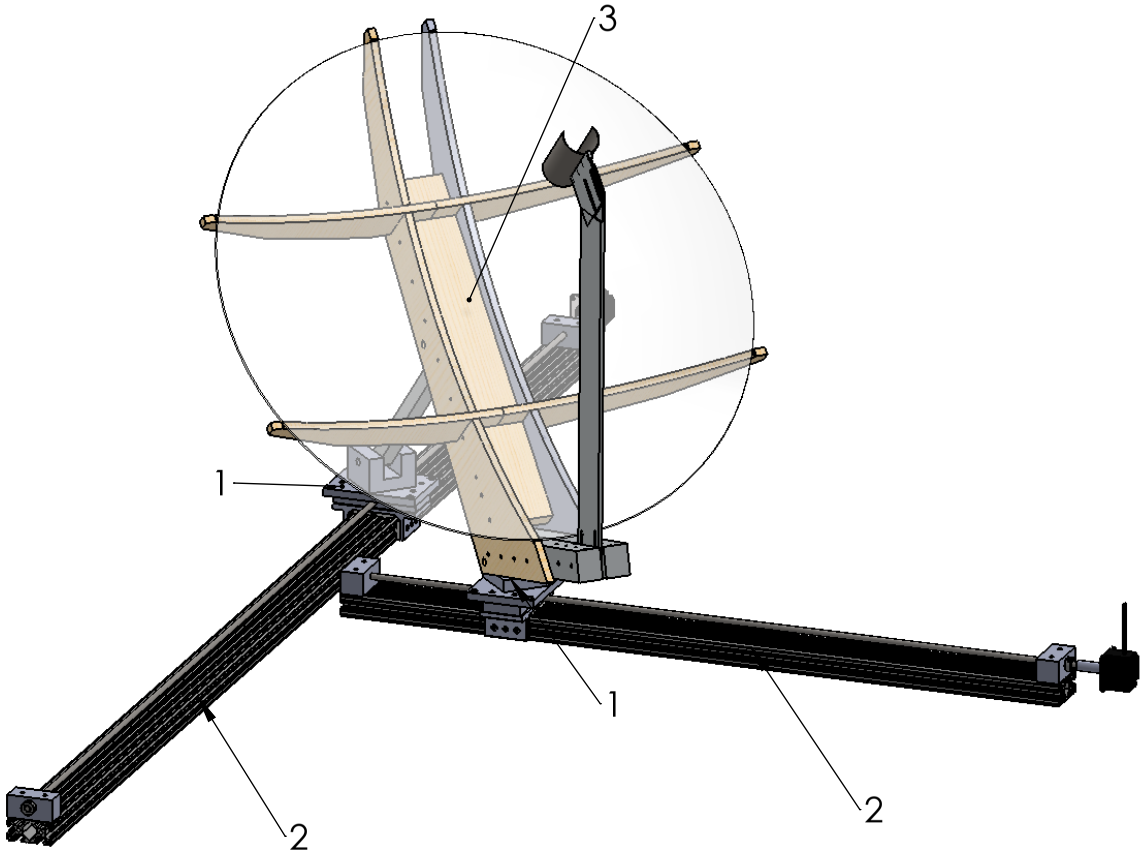

Sub-Assemblies:
1.mirror mounts
2.linear actuators
3.mirror structure

SolidWorks Student Edition.
For Academic Use Only.

TEAM HELIOS

TITLE: Solar Tracker Final

SANTA CLARA UNIVERSITY
SCHOOL OF ENGINEERING

DRAWN BY: Joseph Valdez

REV

SCALE: none

Date: 6/8/12

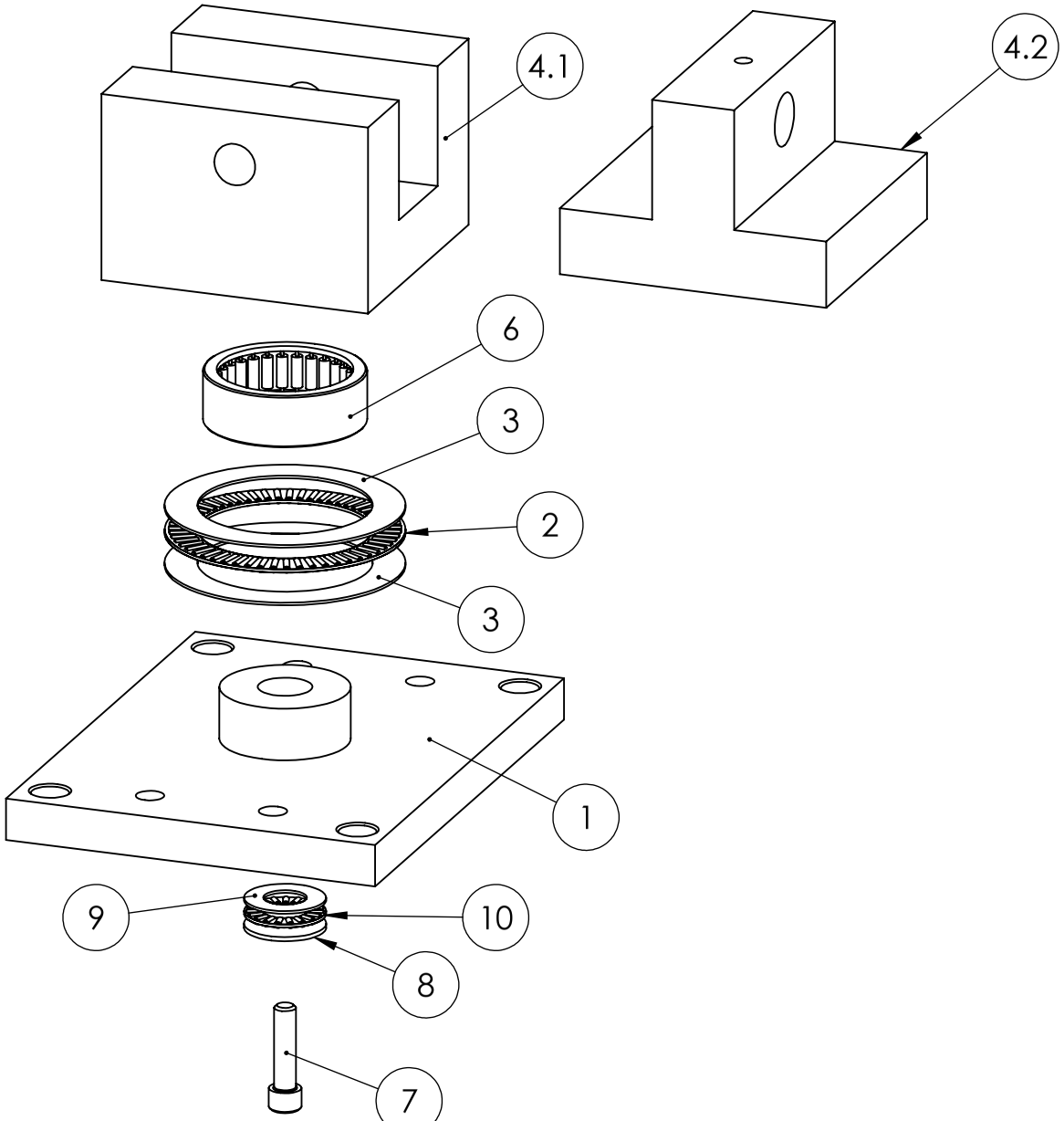

ITEM NO.	PART NUMBER	DESCRIPTION	QTY.
1	MMA-1	Aluminum block	1
2	5909K43	Needle sleeve bearing	1
3	5909K56	Washer	2
4.1	MMA-2A	Aluminum block	1
4.2	MMA-2B	Aluminum block	
6	5905K29	Needle roller bearing	1
7	90128A245	Socket cap screw 1/4"-20-3/4	1
8	98032A489	Washer	1
9	5909K44	Washer	1
10	5909K31	Needle roller bearing	1

TEAM HELIOS

TITLE: Mirror Mount Assembly

SANTA CLARA UNIVERSITY
SCHOOL OF ENGINEERING

DRAWN BY: Joseph Valdez

REV

SCALE:none | Date: 3/21/12

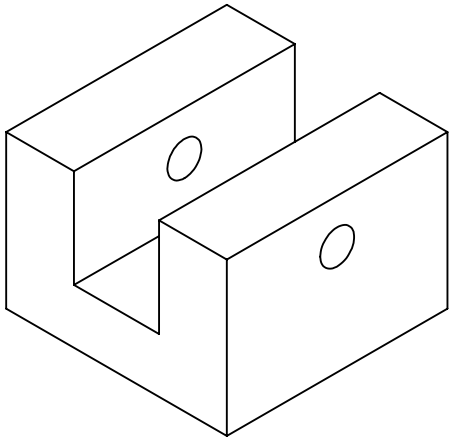

Sheet Note:
-Units: inches
-tolerance: +/- 0.005
-Material: Aluminum 6061 T6

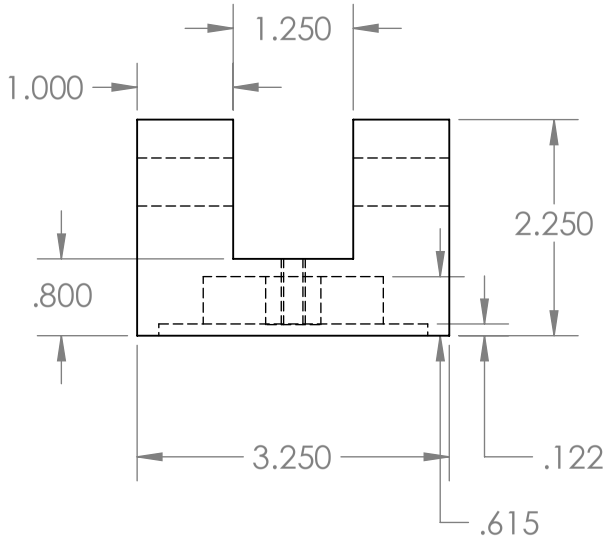

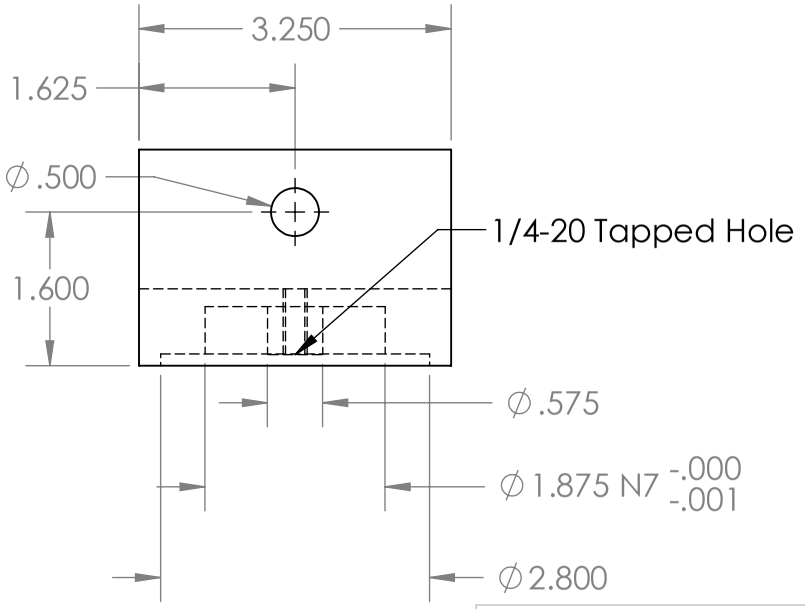

SolidWorks Student Edition.
For Academic Use Only.

TEAM HELIOS

TITLE: top block

SANTA CLARA UNIVERSITY
SCHOOL OF ENGINEERING

DRAWN BY: Joseph Valdez

REV

SCALE: 1:2 | Date: 6/5/12 | PART No: MMA-2A

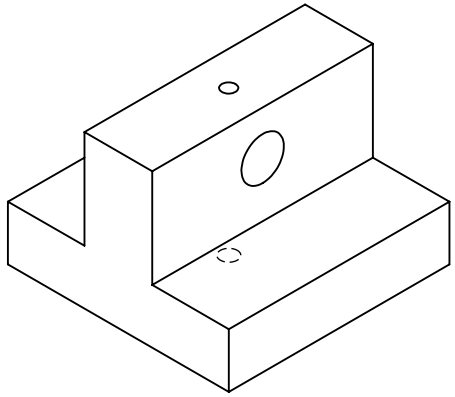

Sheet Note:
-Units: inches
-tolerance: +/- 0.005
-Material: Aluminum 6061 T6

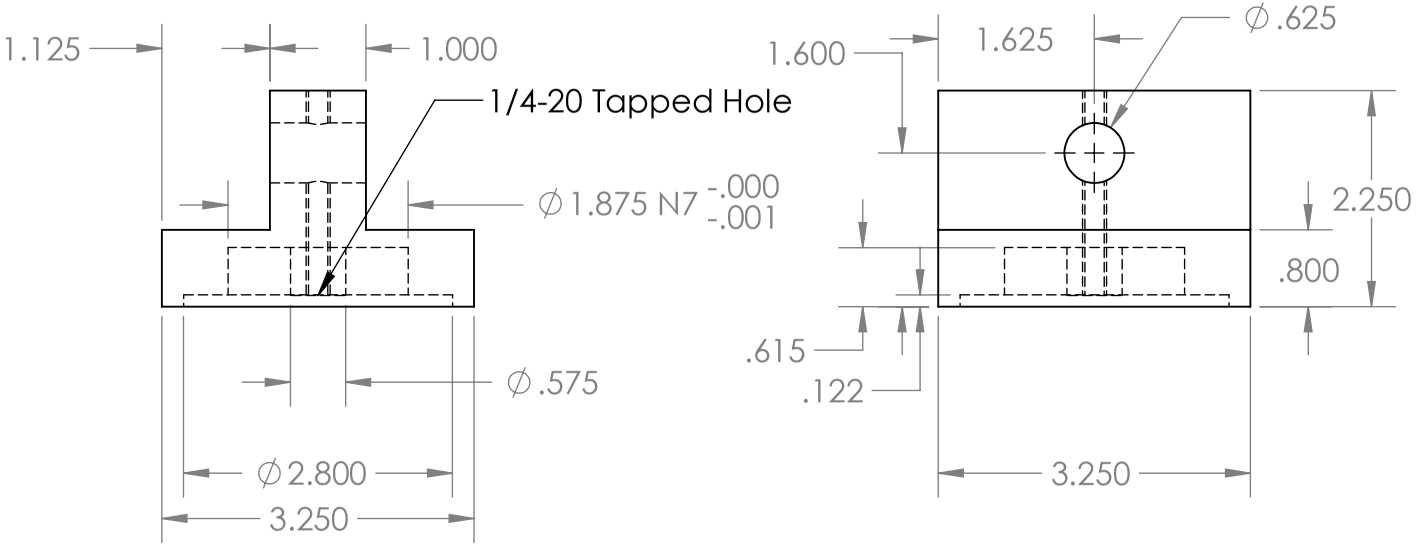

SolidWorks Student Edition.
For Academic Use Only.

TEAM HELIOS

TITLE: top block single

SANTA CLARA UNIVERSITY
SCHOOL OF ENGINEERING

DRAWN BY: Joseph Valdez

REV

SCALE: 1:2 | Date: 6/5/12 | PART No: MMA-2B

Sheet Notes:
-Units: inches
-tolerance: +/- 0.005"
-Material: Aluminum 6061 T6

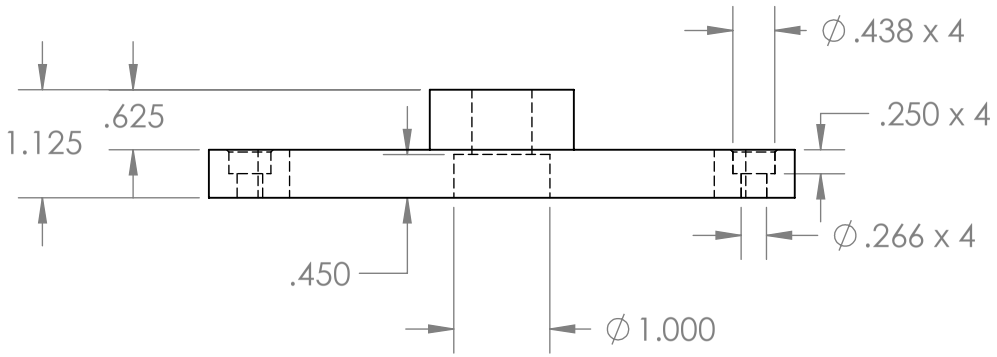

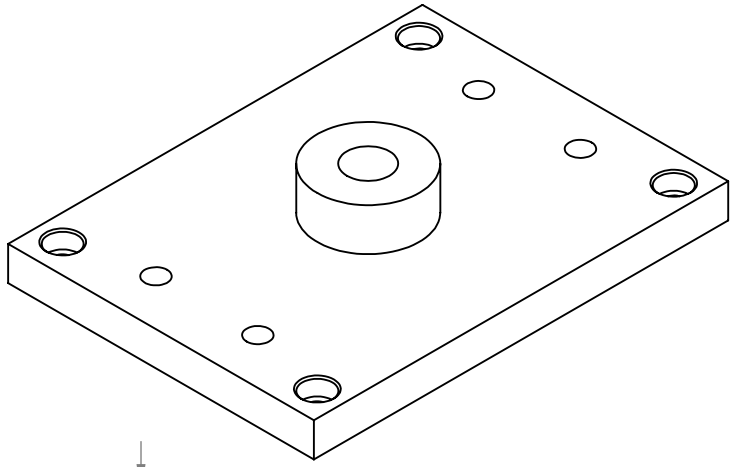

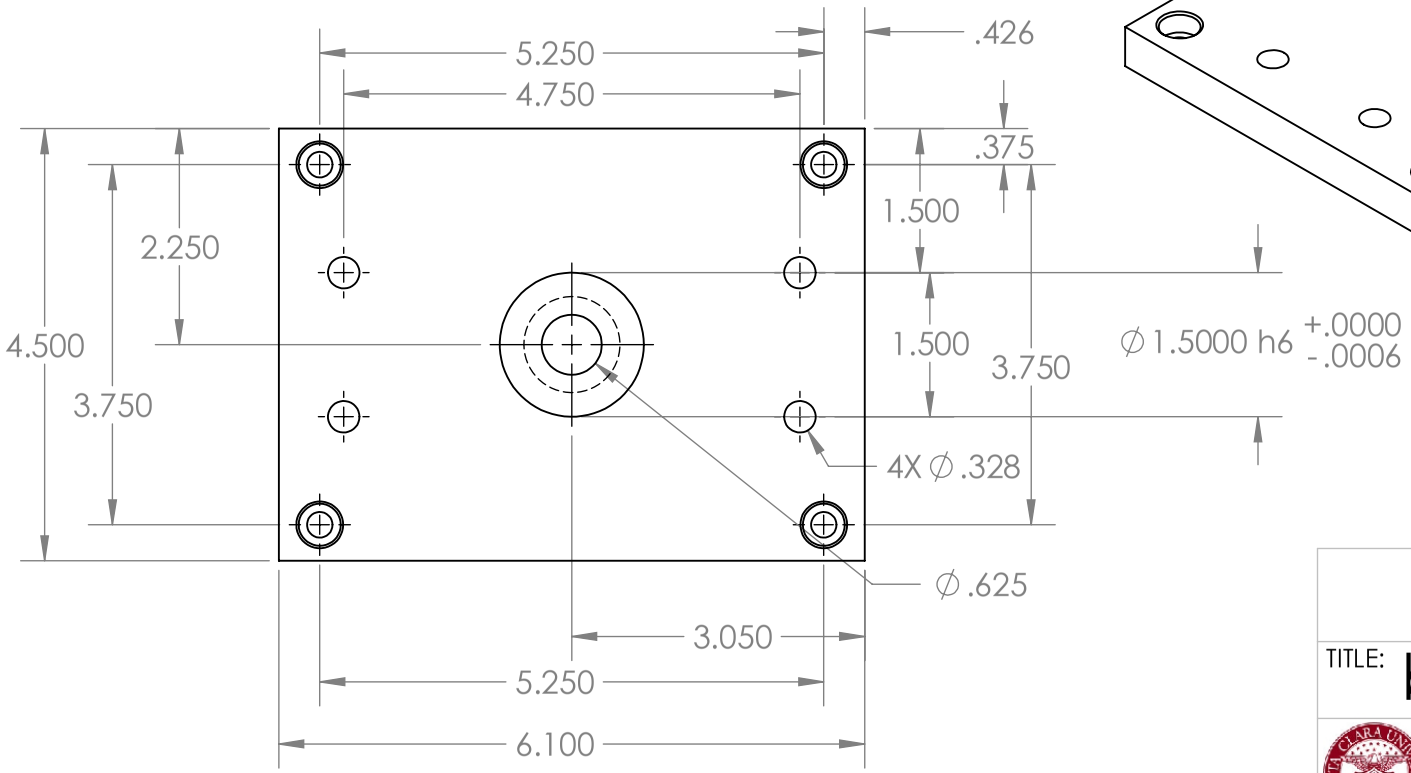

SolidWorks Student Edition.
For Academic Use Only.

TEAM HELIOS

TITLE: bottom block

SANTA CLARA UNIVERSITY
SCHOOL OF ENGINEERING

DRAWN BY: Joseph Valdez

REV

SCALE: 1:2 | Date: 6/5/12 | PART No: 1

Sheet Notes:
A. Secured with (2) 1/4"-20 x 2" machine screws and end-feed fasteners.
B. Secured with (4) 5/16"- 18 x 1-3/4" machine screws, washers, and nuts.

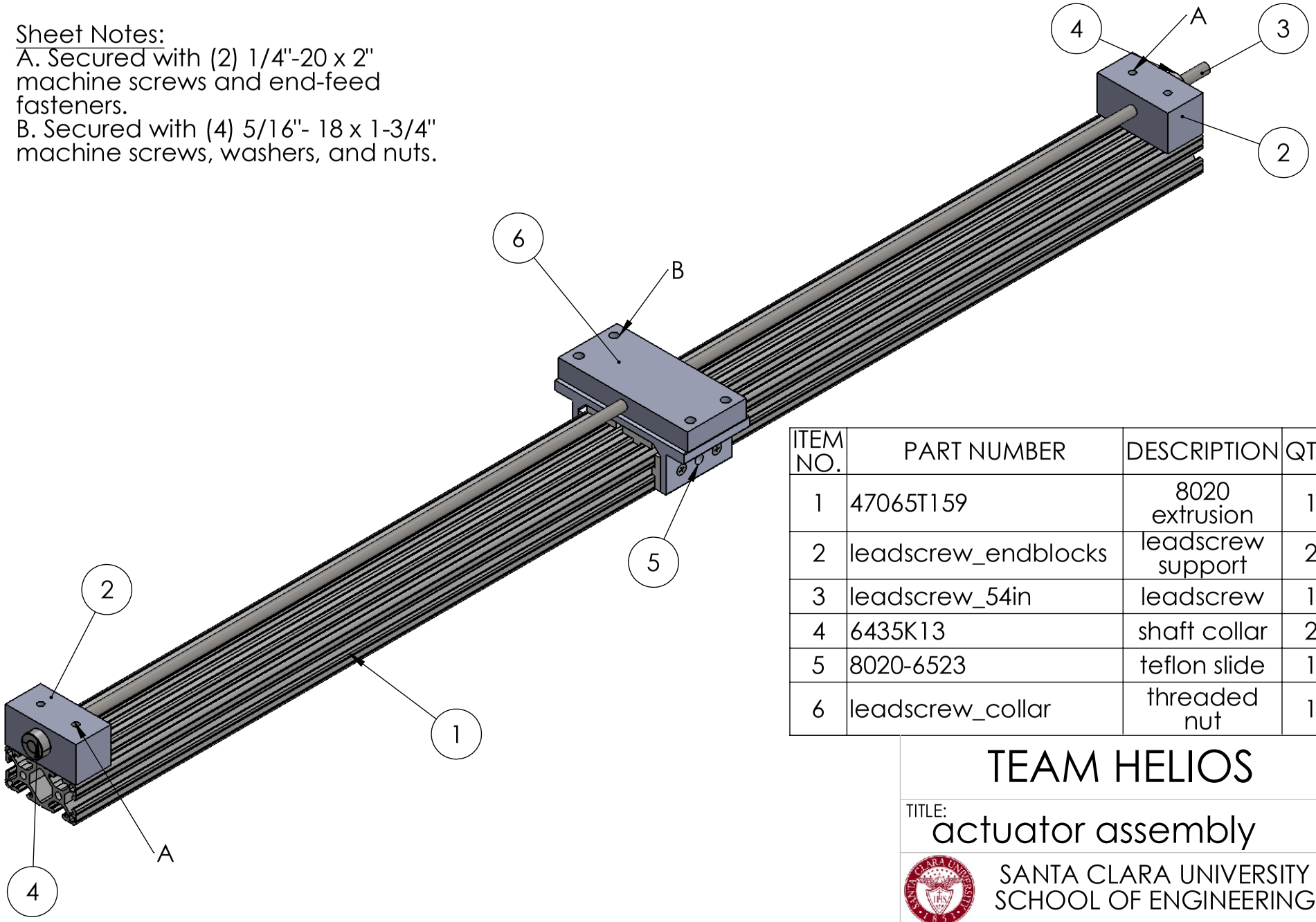

ITEM NO.	PART NUMBER	DESCRIPTION	QTY.
1	47065T159	8020 extrusion	1
2	leadscrew_endblocks	leadscrew support	2
3	leadscrew_54in	leadscrew	1
4	6435K13	shaft collar	2
5	8020-6523	teflon slide	1
6	leadscrew_collar	threaded nut	1

SolidWorks Student Edition.
For Academic Use Only.

TEAM HELIOS

TITLE:
actuator assembly

SANTA CLARA UNIVERSITY
SCHOOL OF ENGINEERING

DRAWN BY:
Joseph Valdez

REV

SCALE: none | Date: 6/8/12

Sheet Notes:
-units:inches
-material: delrin
-tolerance: ±0.005

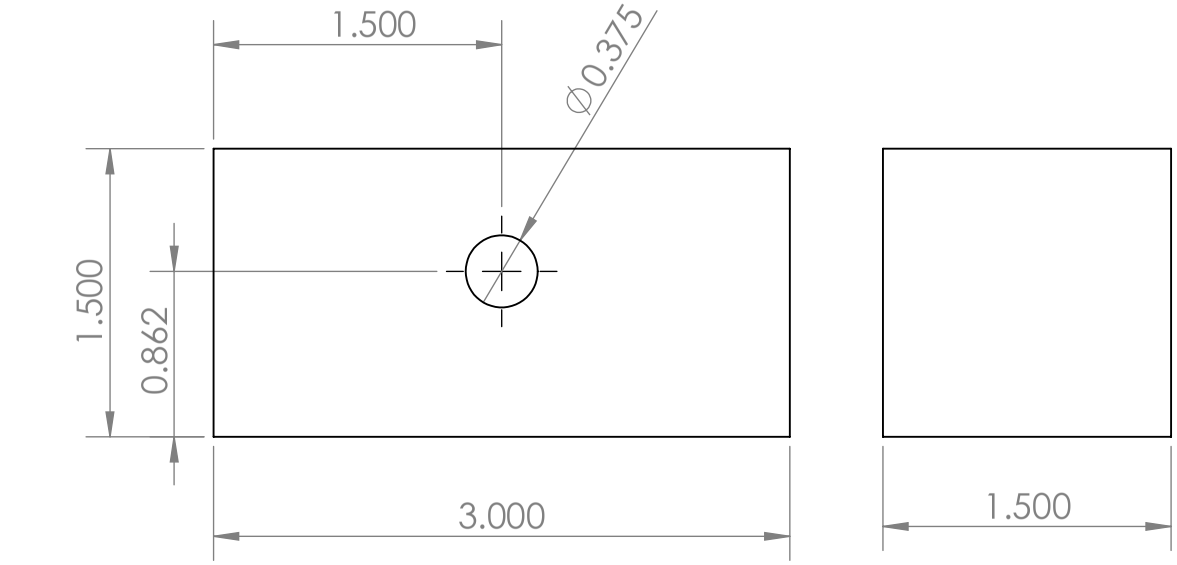

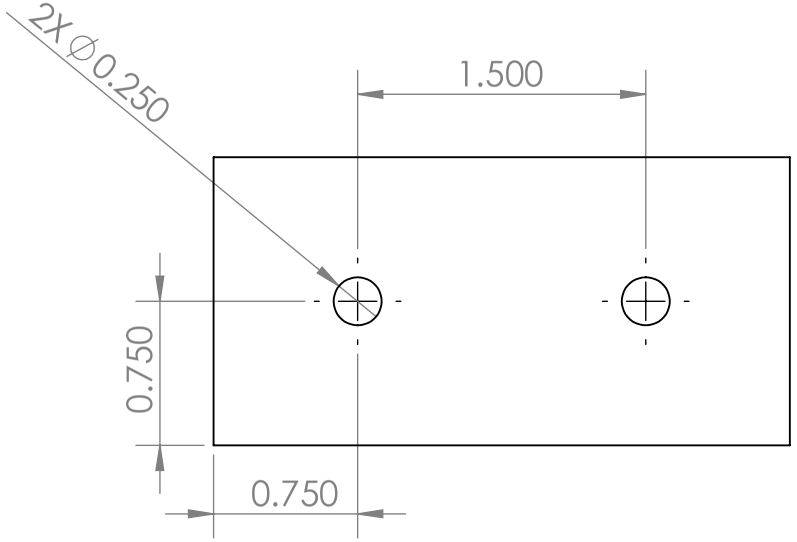

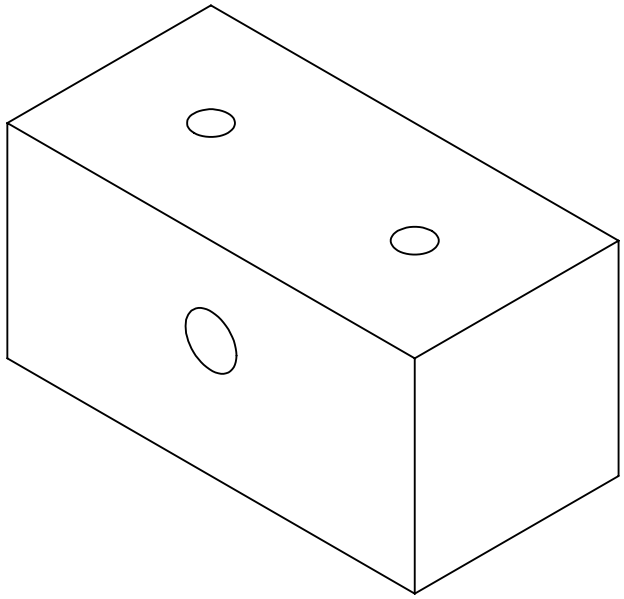

SolidWorks Student Edition.
For Academic Use Only.

TEAM HELIOS

TITLE: Leadscrew support

SANTA CLARA UNIVERSITY
SCHOOL OF ENGINEERING

DRAWN BY: Joseph Valdez

REV

SCALE: 1:1 | Date: 6/8/12 | PART No: LAA-1

Sheet Notes:
-Units: inches
-Material: Delrin
-Tolerance: ±0.005

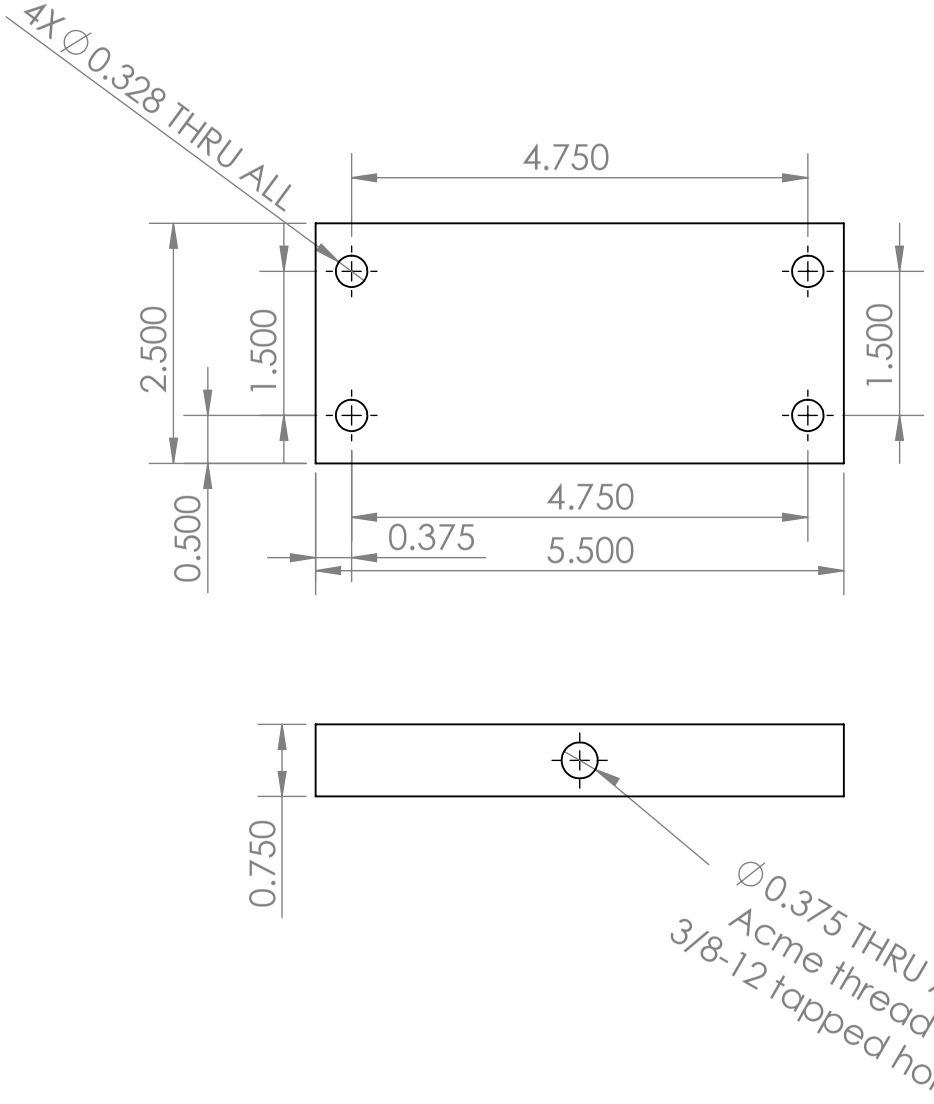

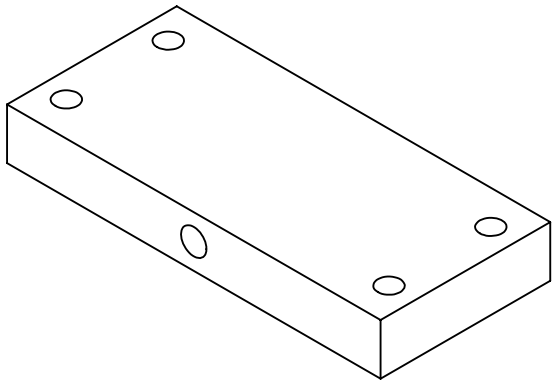

SolidWorks Student Edition.
For Academic Use Only.

TEAM HELIOS

TITLE: Leadscrew Collar

SANTA CLARA UNIVERSITY
SCHOOL OF ENGINEERING

DRAWN BY: Joseph Valdez

REV

SCALE: 1:2 | Date: 6/8/12 | PART No: LAA-2

Sheet Notes:
-units: inches
-material: Black oxide steel

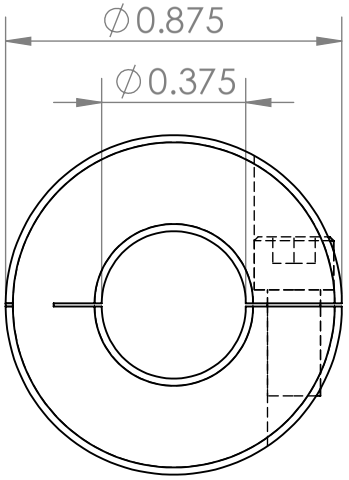

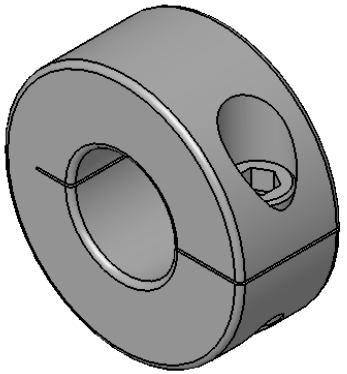

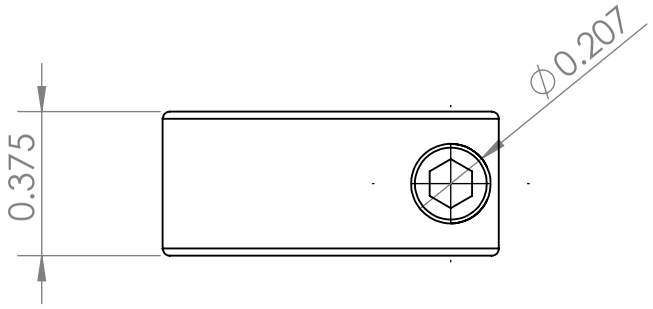

SolidWorks Student Edition.
For Academic Use Only.

TEAM HELIOS

TITLE: Shaft Collar

SANTA CLARA UNIVERSITY
SCHOOL OF ENGINEERING

DRAWN BY: Joseph Valdez

REV

SCALE: 2:1 | Date: 6/8/12 | PART No: 6435K13

Sheet Notes:
-units: inches
-material: Aluminum 6061 T6
-tolerance: ±0.005

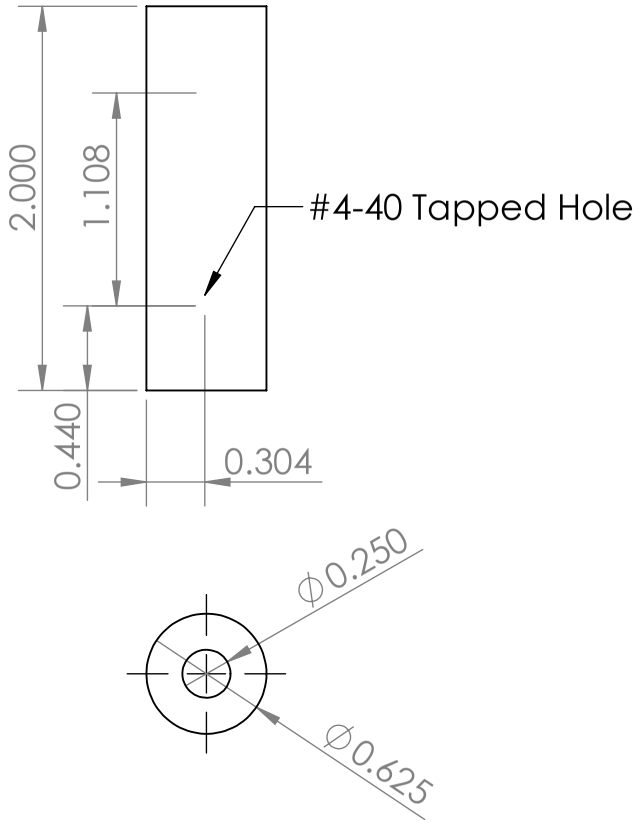

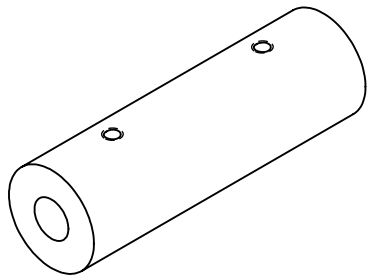

SolidWorks Student Edition.
For Academic Use Only.

TEAM HELIOS	
TITLE: shaft collar	
SANTA CLARA UNIVERSITY SCHOOL OF ENGINEERING	
DRAWN BY: Joseph Valdez	REV
SCALE: 1:1	Date: 6/8/12

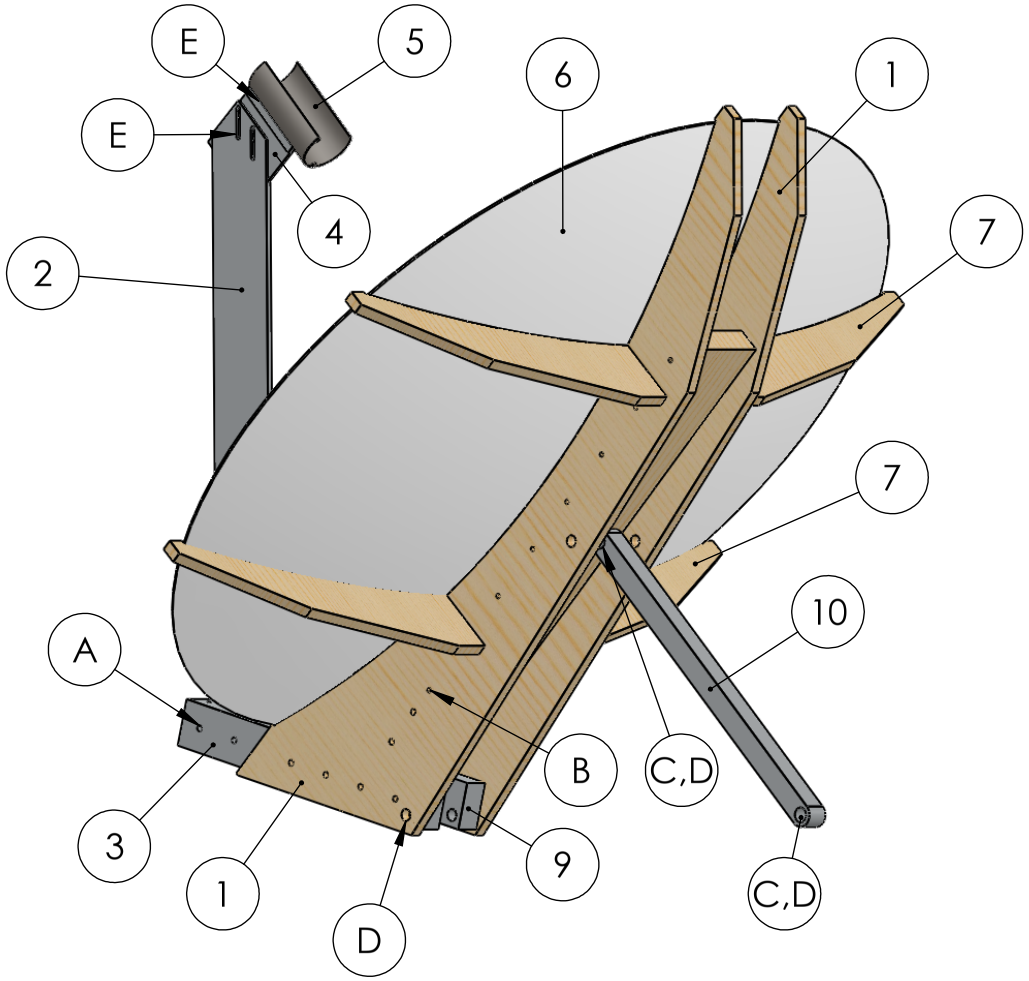

Sheet Notes:

A. (TYP 6) Grade 5 1/4"-20 bolts thru holes with washers and nuts

B. (TYP 16) No. 6 wood screws attaching MHA-1 to MHA-8

C. (TYP 2) ∅1/2" ID flanged bronze bushings press fit aluminum 5/8" thru hole

D. ∅1/2" x 6" steel shaft thru clevis joint

E. (TYP 2) #10-32 button head screw

ITEM NO.	PART NUMBER	DESCRIPTION	QTY.
1	MHA-1	Mirror Support	2
2	MHA-2	Focal Arm	1
3	MHA-3	base couple	1
4	MHA-4	focal mount	1
5	MHA-5	Sample Holder	1
6	MHA-6	Arcylic mirror	1
7	MHA-7	Mirror Support	2
8	MHA-8	Wood 2X4	1
9	MHA-9	base couple	1
10	MHA-10	Linkage arm	1
11	*91247A562	Grade 5 bolts	8
12	*90095A414	Wood screws	16
13	*95462A029	Hex nuts	8
14	*93852A102	flat washers	8
15	*1886K22	steel shaft	3
16	*6338K417	bronze bushing	4

*pins, fasteners, and bushings not shown

SolidWorks Student Edition.
For Academic Use Only.

TEAM HELIOS

TITLE: Mirror Holder Assembly

SANTA CLARA UNIVERSITY
SCHOOL OF ENGINEERING

DRAWN BY: Joseph Valdez

REV

SCALE: none

Date: 3/21/12

Sheet Notes:
-Units: inches
-Material: 0.5" thick Wood (MDF)
-Will be cut on laser CNC machine
-Diameter of laser: 0.013"

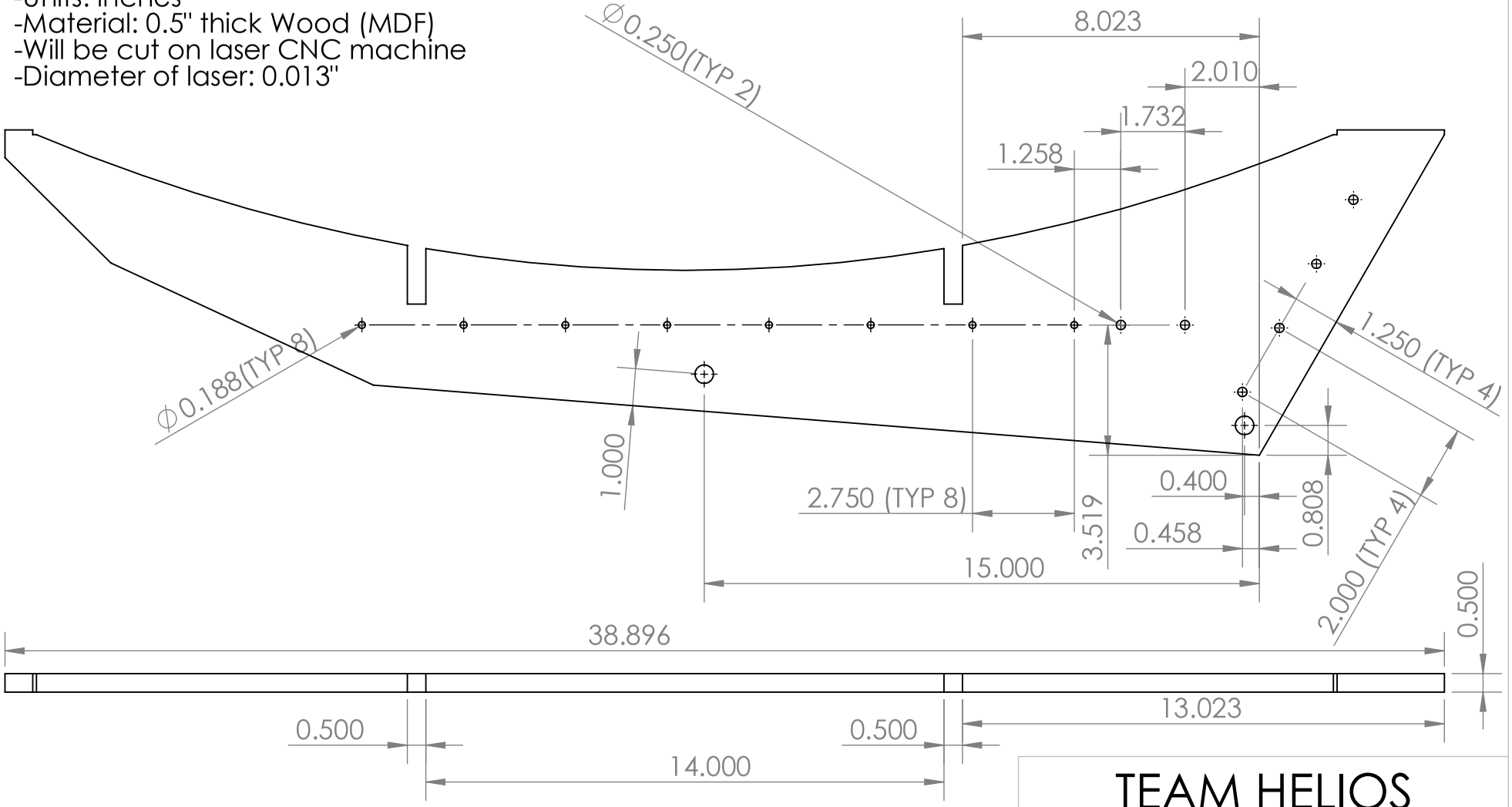

SolidWorks Student Edition.
For Academic Use Only.

TEAM HELIOS

TITLE: MirrorTripod Support1

SANTA CLARA UNIVERSITY
SCHOOL OF ENGINEERING

DRAWN BY: Joseph Valdez

REV

SCALE: 1:4 | Date: 6/5/12 | PART No: MHA-1

Sheet Notes:
-Material: 0.5" thick Wood (MDF)
-Will be cut on laser CNC machine
-Diameter of laser: 0.013"

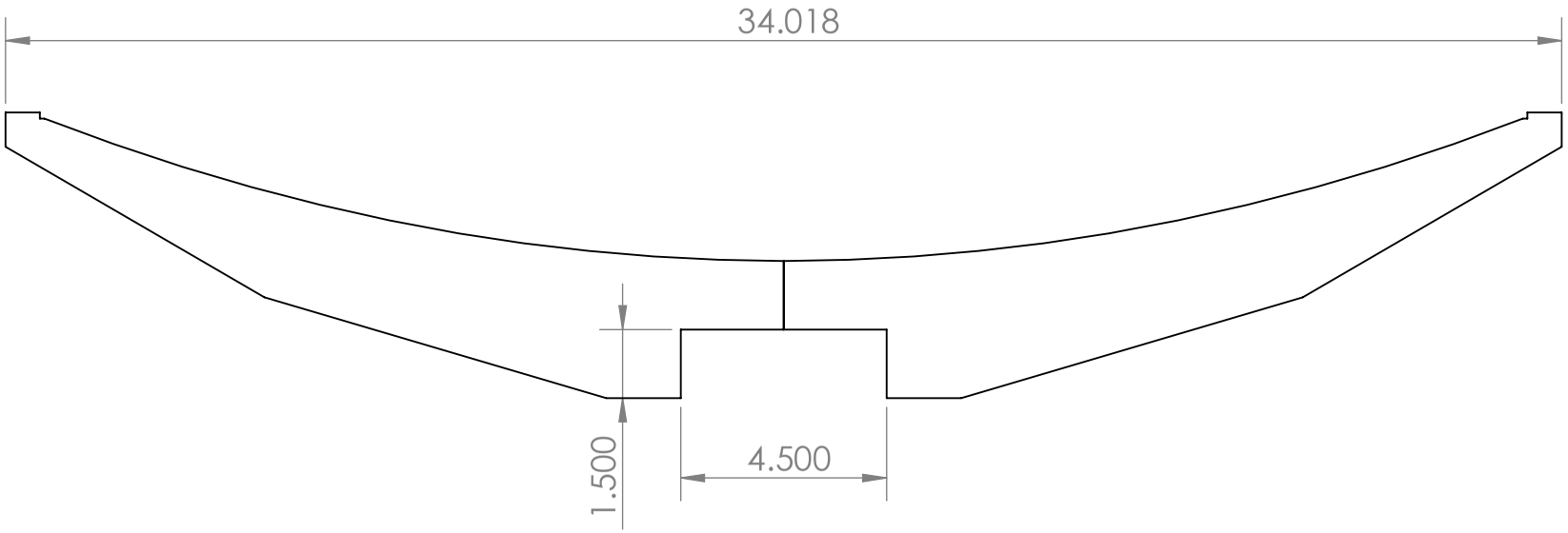

SolidWorks Student Edition.
For Academic Use Only.

TEAM HELIOS		
TITLE: MirrorTripodSupport2		
SANTA CLARA UNIVERSITY SCHOOL OF ENGINEERING		
DRAWN BY: Joseph Valdez		REV
SCALE:1:4	Date: 6/5/12	PART No: MHA-7

Sheet Notes:
-Material: Acrylic
-Parabolic Mirror Bought from greenpowerscience.com

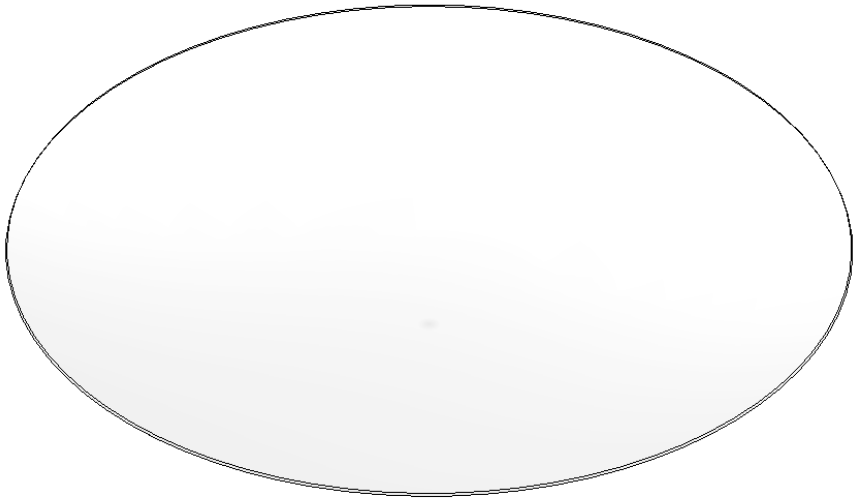

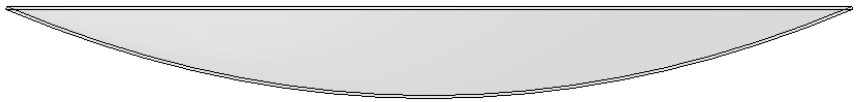

SolidWorks Student Edition.
For Academic Use Only.

TEAM HELIOS

TITLE: Mirror1

SANTA CLARA UNIVERSITY
SCHOOL OF ENGINEERING

DRAWN BY: Joseph Valdez

REV

SCALE: none | Date: 6/5/12 | Part No: MHA-6

Sheet Notes:
-Material: 20 guage sheet metal
~8" long
-Sheet metal will be bent to shape of solar receiver

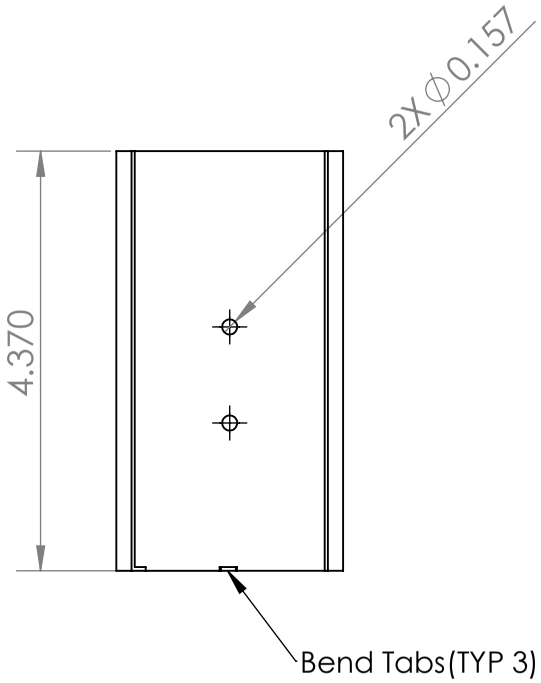

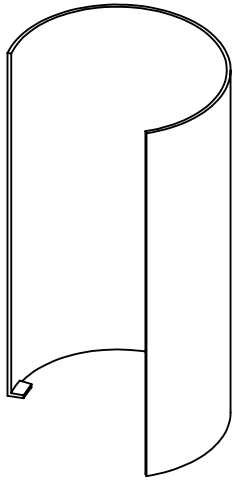

SolidWorks Student Edition.
For Academic Use Only.

TEAM HELIOS

TITLE: Sampleholder

SANTA CLARA UNIVERSITY
SCHOOL OF ENGINEERING

DRAWN BY: Joseph Valdez

REV

SCALE: 1:2 | Date: 6/5/12 | Part No: MHA-5

Sheet Notes:
-Units: inches
-Material:Aluminum
-Tolerance: +/- 0.005"

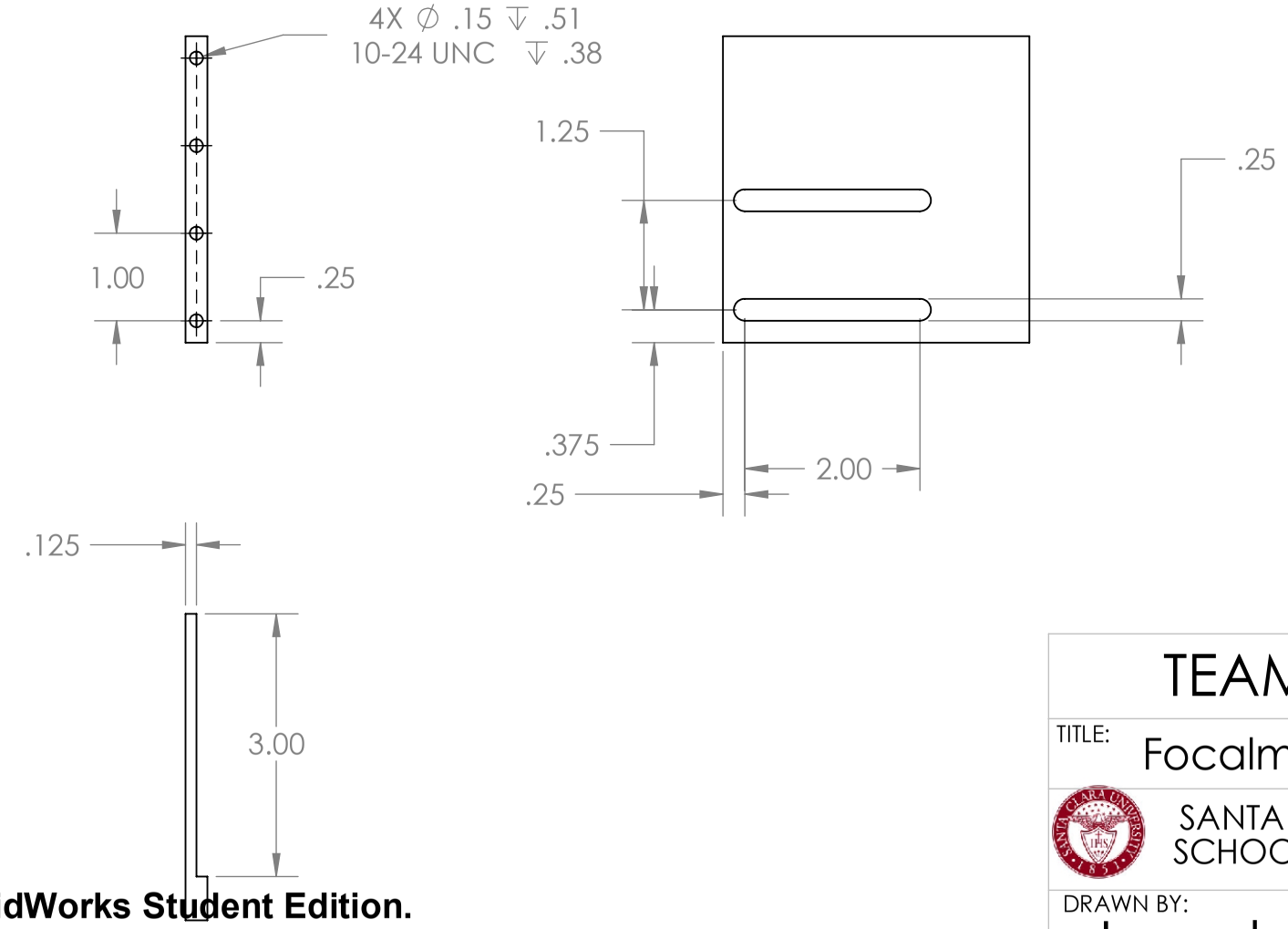

TEAM HELIOS

TITLE: Focalmountcouple

SANTA CLARA UNIVERSITY
SCHOOL OF ENGINEERING

DRAWN BY: Joseph Valdez

REV

SCALE: 1:2 | Date: 6/5/12 | PART No: MHA-4

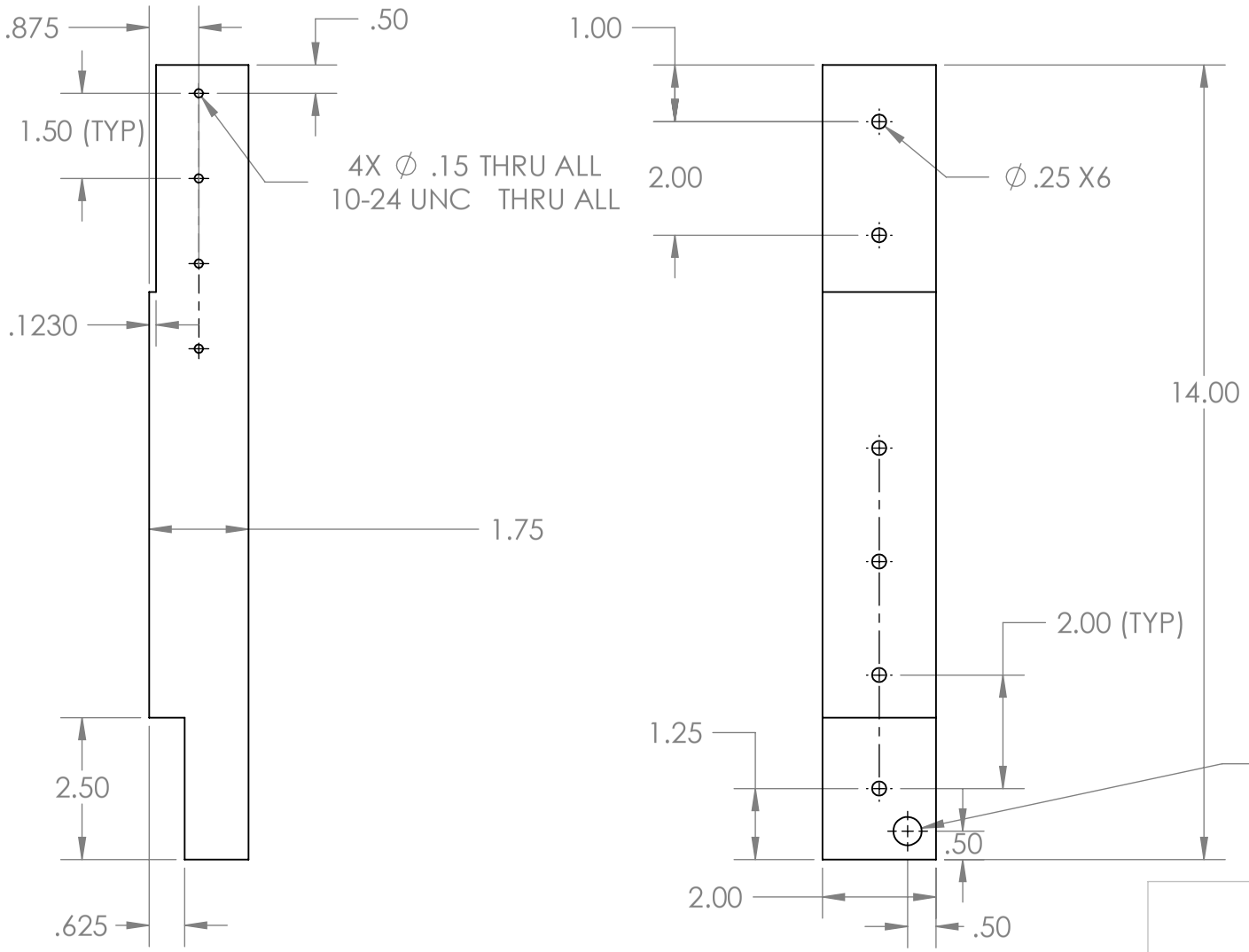

Sheet Notes:
-Units: inches
-Material: 6061T6 Aluminum
-Tolerance: +/- 0.005"
-Duplicate part has mirrored 0.5" Thru hole

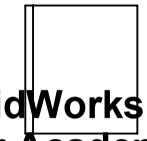

SolidWorks Student Edition.
For Academic Use Only.

TEAM HELIOS

TITLE: Base_couple

SANTA CLARA UNIVERSITY
SCHOOL OF ENGINEERING

DRAWN BY: Joseph Valdez

REV

SCALE: 1:3 | Date: 6/5/12 | PART No: MHA- 3

Sheet Notes:
-Units: inches
-Material: Wood
-1/4" and 3/16" drill bits for holes

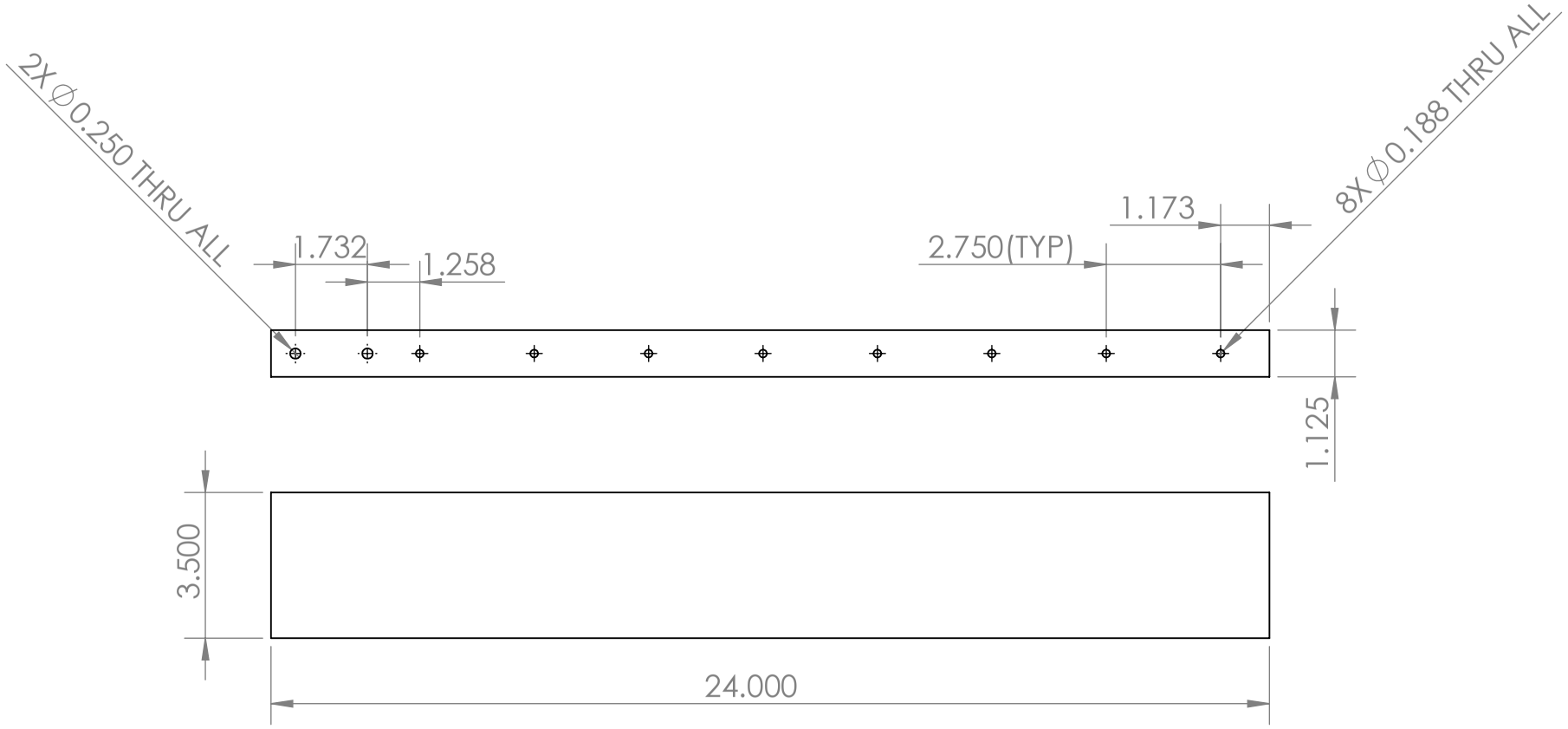

SolidWorks Student Edition.
For Academic Use Only.

TEAM HELIOS

TITLE: Beam

SANTA CLARA UNIVERSITY
SCHOOL OF ENGINEERING

DRAWN BY: Joseph Valdez

REV

SCALE: 1:8 | Date: 6/5/12 | PART No: MHA-8

Sheet Notes:
-units: inches
-Material: Steel
-Tolerance: 0.05"

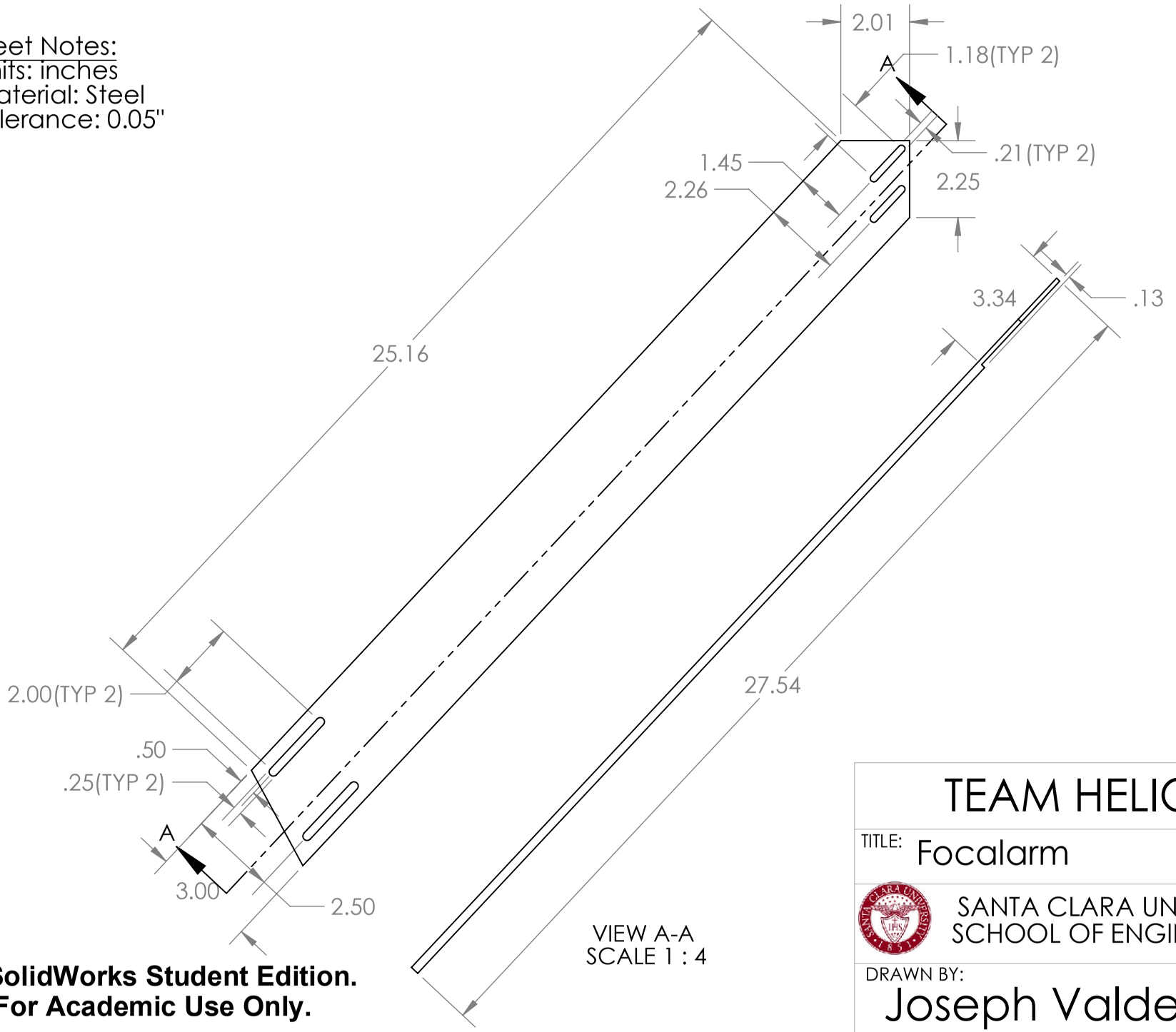

VIEW A-A
SCALE 1 : 4

SolidWorks Student Edition.
For Academic Use Only.

TEAM HELIOS

TITLE: Focalarm

SANTA CLARA UNIVERSITY
SCHOOL OF ENGINEERING

DRAWN BY: Joseph Valdez

REV

SCALE: 1:4 | Date: 6/5/12 | PART No: MHA-2

Sheet Notes
-Units Inches
-Material: Acrylic

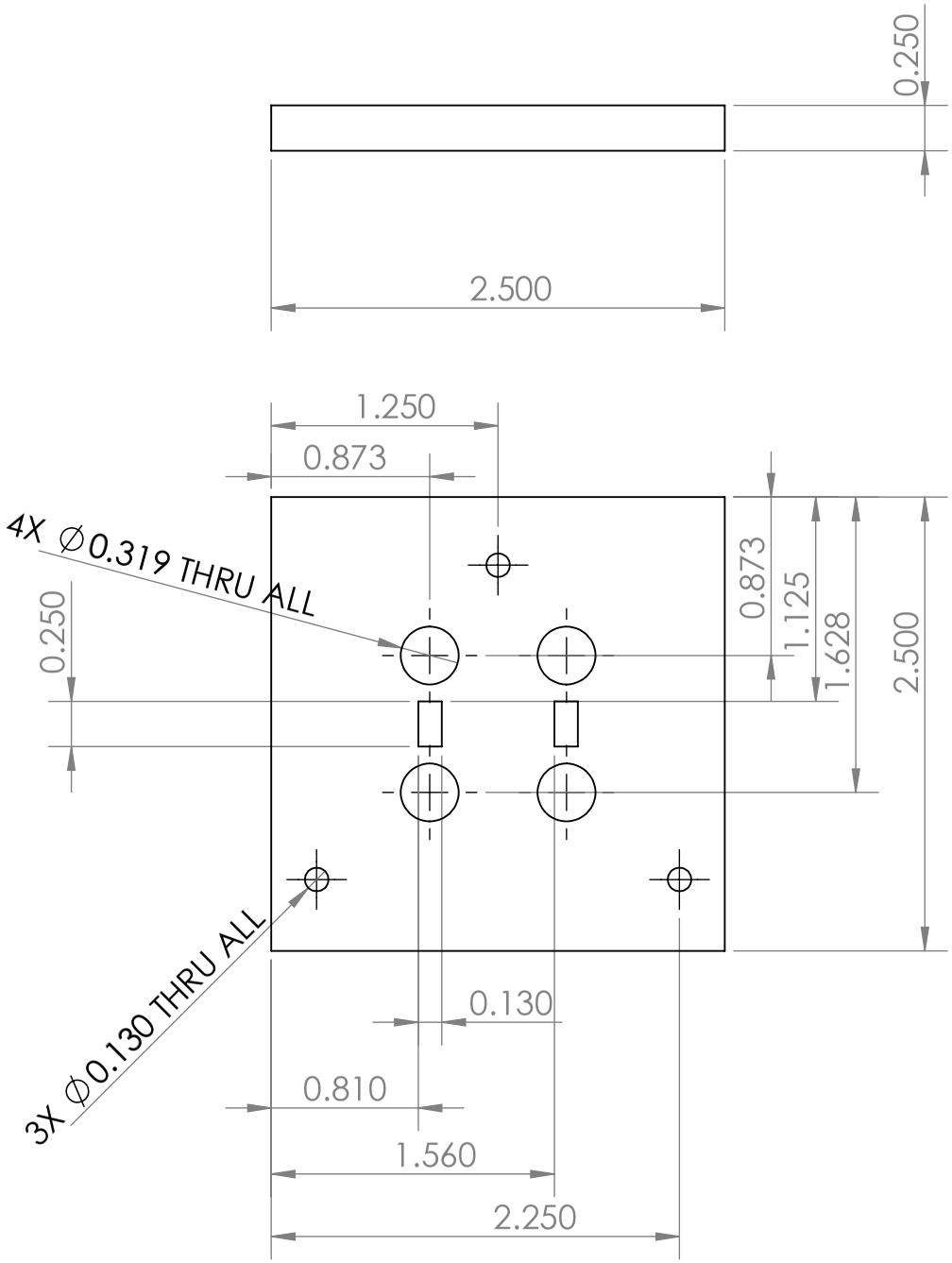

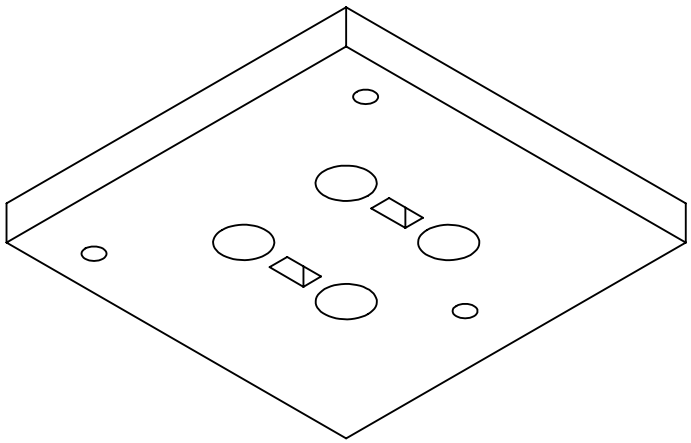

TEAM HELIOS

PROJECT:	Solar Tracker
TITLE:	Senor Base
	SANTA CLARA UNIVERSITY SCHOOL OF ENGINEERING
DRAWN BY:	Joseph Valdez
REV	
SCALE: 1:1	Date: 02-06-12
PART No: SEN-1	

Sheet Notes
-Units Inches
-Material: Acrylic

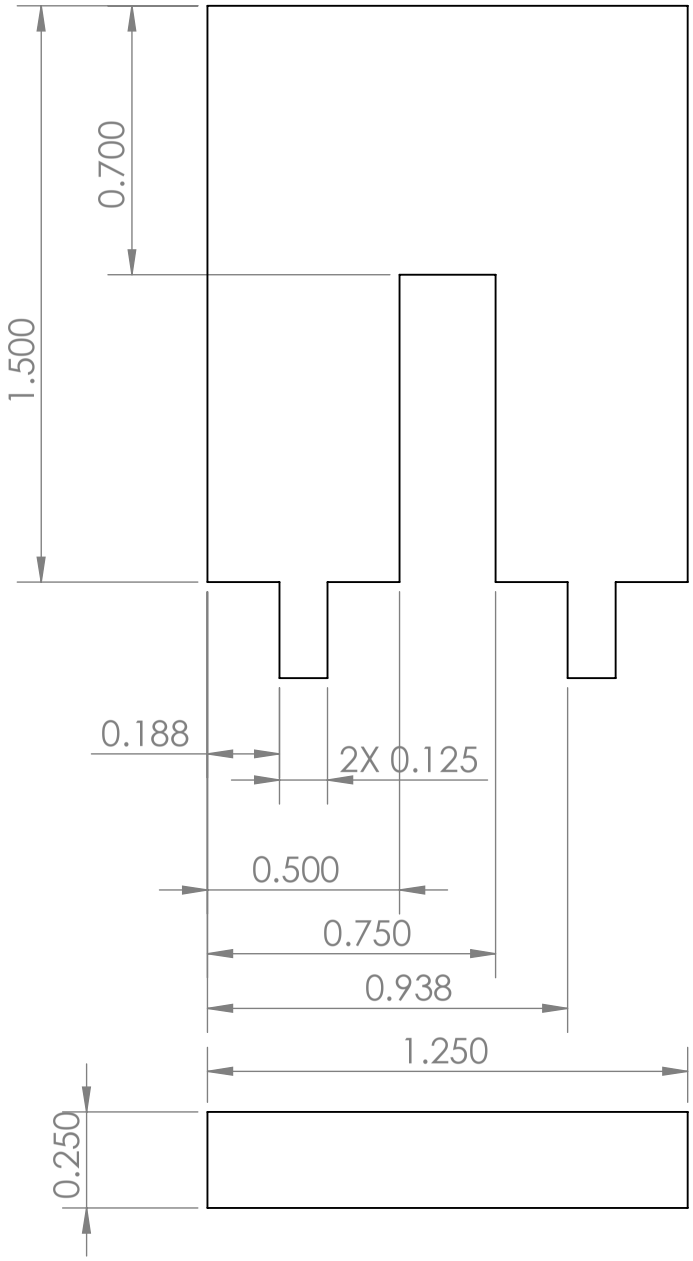

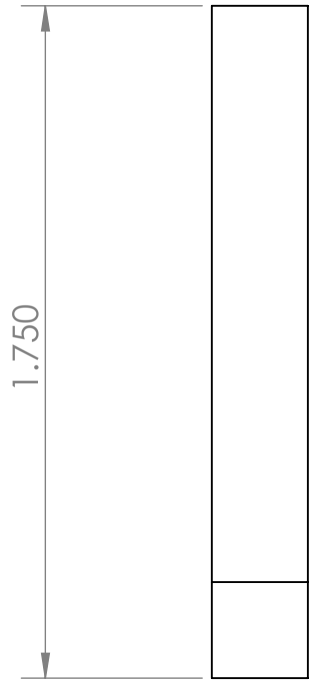

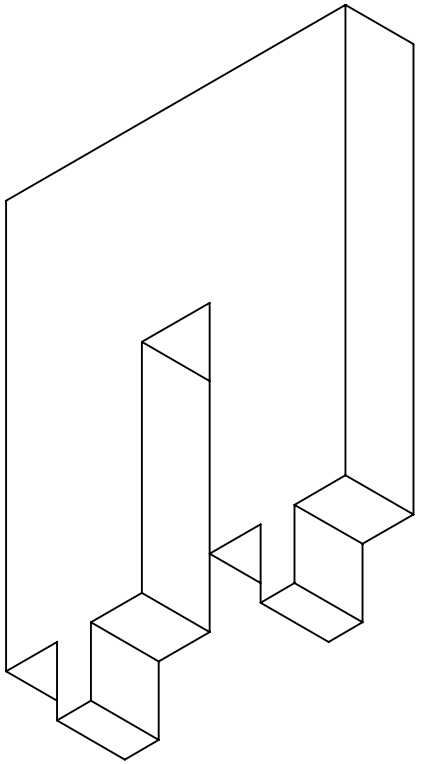

TEAM HELIOS

PROJECT: Solar Tracker

TITLE: Sensor Mast

SANTA CLARA UNIVERSITY
SCHOOL OF ENGINEERING

DRAWN BY: Joseph Valdez

REV

SCALE: 2:1	Date: 02-06-12	PART No: SEN-3

Sheet Notes
-Units Inches
-Material: Acrylic

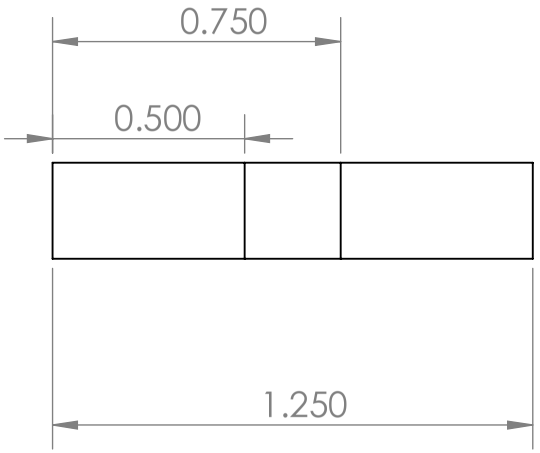

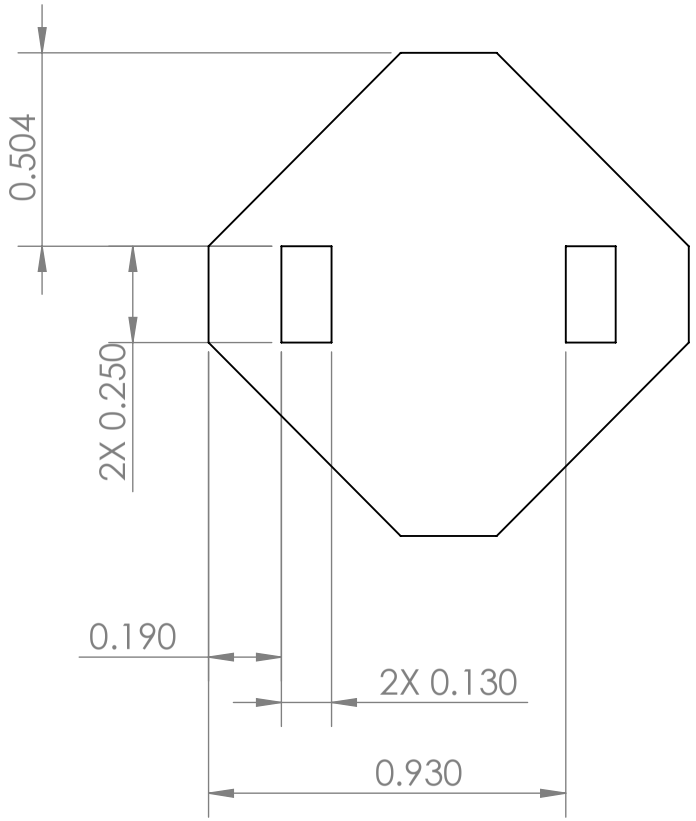

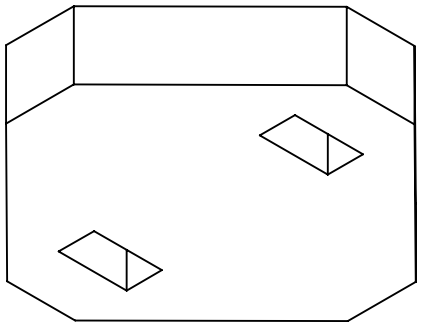

TEAM HELIOS

PROJECT: Solar Tracker

TITLE: Shade Hat

SANTA CLARA UNIVERSITY
SCHOOL OF ENGINEERING

DRAWN BY: Joseph Valdez

REV

SCALE: 2:1 | Date: 02-06-12 | PART No: SEN-2

Sheet Notes:
-units: inches
-Material: Steel
-Tolerance: 0.05"

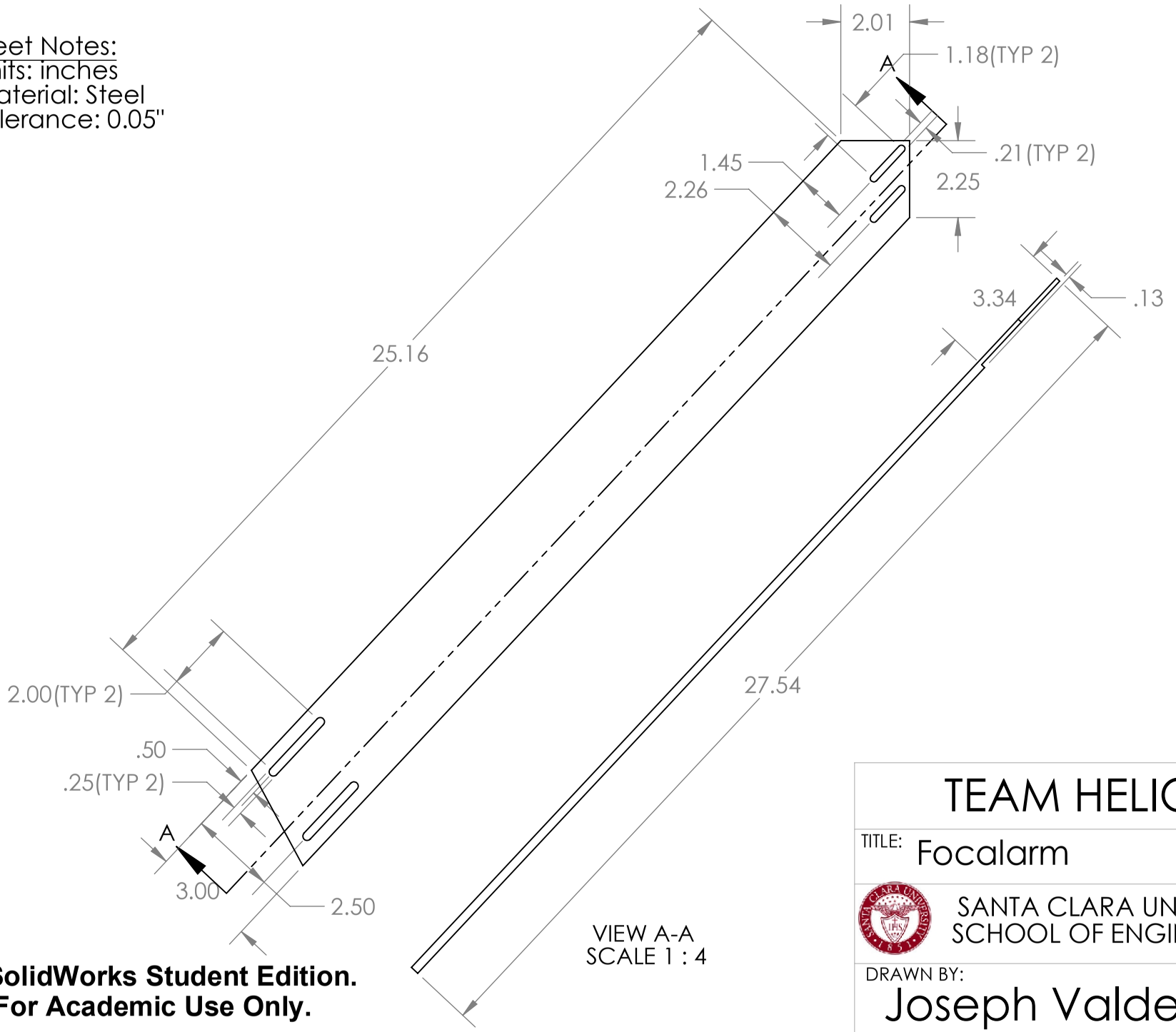

VIEW A-A
SCALE 1 : 4

SolidWorks Student Edition.
For Academic Use Only.

TEAM HELIOS

TITLE: Focalarm

SANTA CLARA UNIVERSITY
SCHOOL OF ENGINEERING

DRAWN BY: Joseph Valdez

REV

SCALE: 1:4 | Date: 6/5/12 | PART No: MHA-2

Sheet Notes:
-units: inches
-material: Aluminum 6061 T6
-tolerance: +/- 0.005"

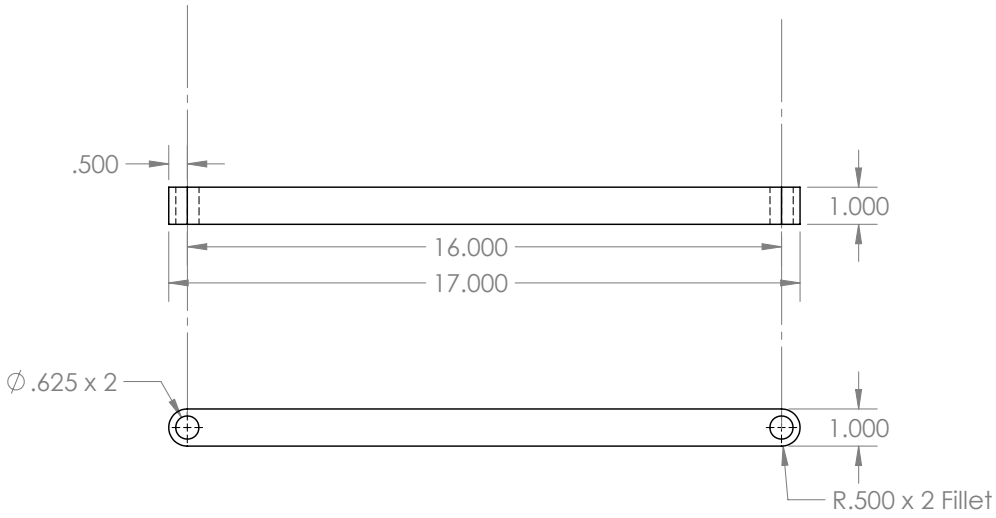

SolidWorks Student Edition.
For Academic Use Only.

TEAM HELIOS

TITLE: Riser

SANTA CLARA UNIVERSITY
SCHOOL OF ENGINEERING

DRAWN BY: Joseph Valdez

REV

SCALE: 1:4 | Date: 6/5/12 | Part No: MHA-10

Sheet Notes:
-units: inches
-material: Aluminum 6061 T6
-tolerance: ±0.005

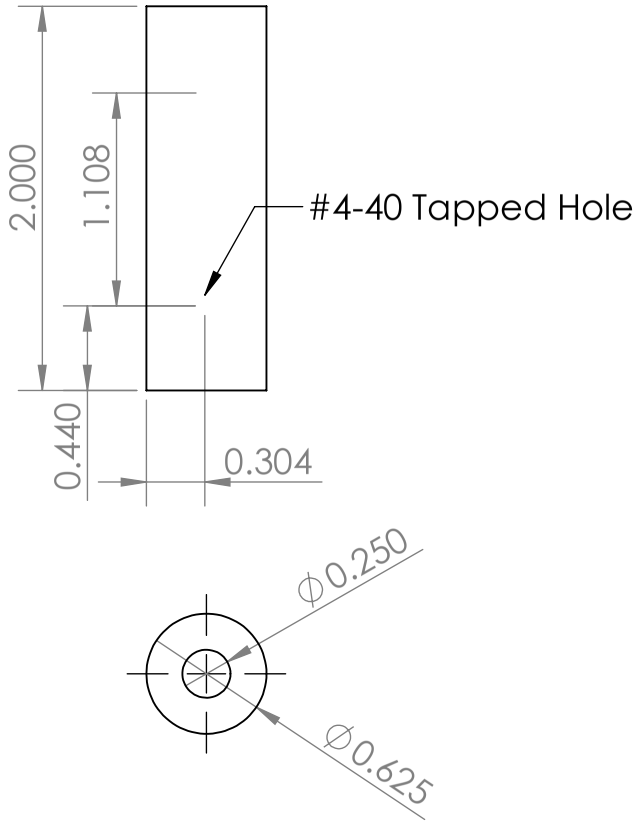

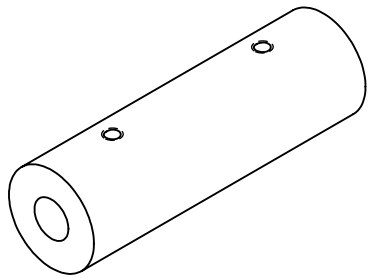

SolidWorks Student Edition.
For Academic Use Only.

TEAM HELIOS	
TITLE: shaft collar	
SANTA CLARA UNIVERSITY SCHOOL OF ENGINEERING	
DRAWN BY: Joseph Valdez	REV
SCALE: 1:1	Date: 6/8/12

Appendix E

Current Technologies - On the Market and Patents

E.1 MecaSolar MS-2 Tracker 10

meca solar

2-AXIS

High Tech Solar Trackers

MS-2 TRACKER 10 • MS-2 TRACKER 10 +

Products and Services

mecasolar is a company dedicated to the **design, manufacture and distribution of 2- axes, 1- axis seasonal solar trackers and fixed structures**, with cutting-edge technology, enabling solar photovoltaic energy production to be increased. World-leading **mecasolar** trackers and fixed structures are the securest, studiest, most efficient and profitable on the market.

MS-2 TRACKER 10

- V-shaped metal structure and grill for up to 13.16 kWp (Fifty-six 235 Wp modules) panels
- PLC tracking, in a fully equipped independent electric panel
- Three phase motors on both axes
- Hook-up/connection cabinet for storing protectors

The client can include as many inverters as they wish

MS-2 TRACKER 10 +

- V-shaped metal structure and grill for up to 13.16 kWp (Fifty-six 235 Wp modules) panels
- PLC tracking, in a fully equipped independent electric panel
- Three phase motors on both axes
- Hook-up/connection cabinet for storing protectors (magnetothermic (PIA), differential, power surge protection), fully wired
- Two 6.0 kWn single phase SMA Sunny Boy SB 6000 inverters for outdoors use, IP 65

Other SMA inverter models can be fitted

mecasolar makes a clear **commitment to its customers.** With the aim of satisfying the various and diverse needs of our clients, we offer a series of **complementary services** for all tracking systems:

- **Management and support** for everything related to **construction project execution, low voltage, medium voltage and module and inverter configuration**, with our entire Engineering Department at your disposal.
- Adapting to project management needs as required by the customer. **We schedule tracker system deliveries** to our customers in a timely manner and **fully manage and coordinate the logistics.**
- **Adjusting the tracker system to fit customer power requirements for photovoltaic panels and inverters.** Additionally, we can install **the inverter** at the clients' request.
- We provide electromechanical **corrective and preventative maintenance** yearly on the tracker systems based on the schedule and frequency defined by the client.

Production Capacity

mecasolar is one of the worldwide industry leaders with the greatest capacity in the market to manufacture solar trackers. Currently, in 2010, we have the **capacity to manufacture 1,272 solar trackers per month,** the equivalent to producing 14 MWp/month.

28,000 trackers/year **280 MW/year**

mecasolar holds at present the CE, ISO 9001:2008 and ISO 14001:2004 certifications, which makes it possible for it to achieve consistent, excellent fabrication quality with the best guarantees for our clients. Environmentally friendly and consistent with sustainable economic and social development. We also provide fast and flexible service. All components have been tested before being shipped to the client's construction site.

ISO 9001:2008 ISO 14001:2004

At present we have factories at the following sites:

- Fustiñana - Sede Central - Navarra - SPAIN
- Tesalonica - GREECE
- Turin - ITALY
- West Sacramento - USA
- Ontario - CANADA

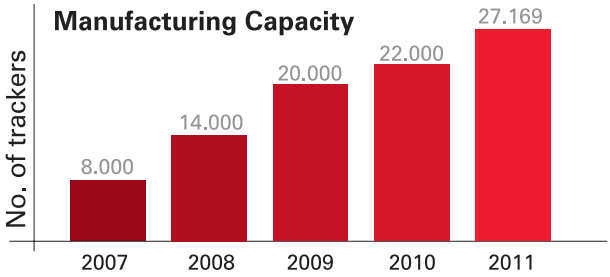

Experience

Advantages that make the difference

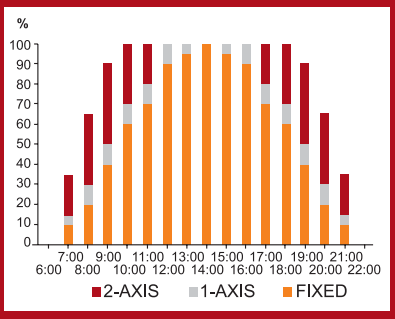

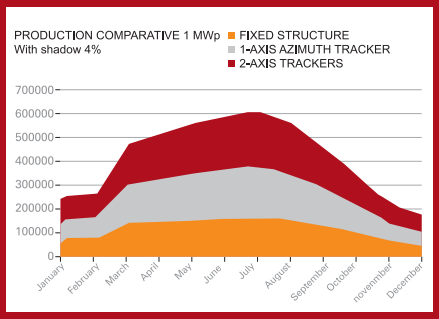

MULTI-POWER and MULTIPLE MANUFACTURER FLEXIBILITY

The design of the omega panel support structure provides the **mecasolar** tracker with incredible **FLEXIBILITY when it comes to installing different panels made by various manufacturers**.The system can handle a **maximum power of 13,16 kWp.**

OVER 35% INCREASE IN PRODUCTIVITY

The **mecasolar**tracking system is capable of increasing photovoltaic solar energy production by more than 35%, **when compared to a fixed installation.** This **maximizes profits by reducing the investment in solar panels.**

FOUNDATION

Foundation on surface footing - 10 cubic yards (7.5 m^3) - that does not require any excavation. It is only necessary to clean off the terrain, removing the top layer of vegetation and levelling the ground.

OUTPUT / THREE PHASE CONNECTION

Each of the three phases is connected to each one of the **3 inverters. This feature reduces losses due to wiring** and provides **a more balanced power output**. Upon any damage in any of the 3 phases, **2/3 of the installation is still productive.**

ADAPTABLE TO CHANGING WEATHER CONDITIONS

The **mecasolar** tracking system is connected to a **weather station** and works with a PLC controller. The solar tracking device uses this technology to orient the panels under a variety of climate conditions. The PLC programming permits the tracker to operate in **snow, electrical storms, fog, darkness and windy conditions**. It can withstand winds of up to 90 mph (145 Km/h), and is programmed to adjust the tracker to a horizontal position when wind speeds are in excess of 45 mph (75 km/h).

INDEPENDENT CONTROL

Each **mecasolar** solar tracker comes equipped with an **independent PLC** controller, which works to monitor solar movements, to handle the prevailing weather conditions and to perform remote operations.

STURDY, EASY TO INSTALL, REDUCED MAINTENANCE, AND LOW POWER USAGE

The **mecasolar** tracker motors **consume less energy per year (100 kWh/year)**, resulting in reduced **maintenance**. Likewise, the **robustness of their design and fabrication** guarantees the investment over the long term. Furthermore, the **easy installation reduces labour costs** and time spent on the construction project.

Simple and Fast Installation with Less Maintenance

1 Transport. 12 partially assembled trackers on 4 trucks.

The **mecasolar** trackers are partially assembled before being shipped. 10 fully assembled V-shaped structures are shipped on two trucks, and 10 grills are shipped on a third truck. It is not necessary to contract any special transportation.

2 Surface Footing. No excavation is necessary.

Foundation on surface footing that does not require any excavation. It is only necessary to clean off the terrain, removing the top layer of vegetation and levelling the ground. We provide our clients with the necessary mould.

3 Quick and simple tracker installation on the foundation footer:

With the same machine used to clean off the terrain, we install the V-shaped structure on the foundation footer. Then, the structure is aligned over the foundation bolts using a double nut system.

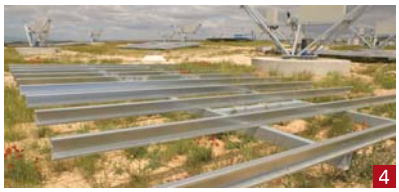

4 Flexible Installation of Modules Any module with any power rating.

The grill, the structure on which the modules are assembled, gives the **mecasolar** tracker great flexibility in that it permits mounting modules with different power ratings, made by different manufacturers. At this time, the **mecasolar** tracker is the market's most open option, which permits working with any type of module.

5 Quick Assembly on the Structure.

Given that one installation crew is able to work on the foundation and on mounting the V-shaped structure on the foundation on one side, while another crew is able to install the modules on the grills; the installation crew can be flexible and versatile and is able to meet reduced installation times.

6 Quick and Simple Tune-up

Our clients can count on the support of the **mecasolar** technical department at all times to guide them through all phases of their project including: project engineering; civil engineering, construction and installation; as well as in tune-ups and maintenance.

Technical Specifications MS-2 TRACKER 10 MS-2 TRACKER 10 +

Tracker axis	2-AXIS: Horizontal and Vertical
Maximum surface of modules	970 square feet (90m²)
Maximum Photovoltaic Power	13,16 kWp (depending on the efficiency of the modules)
Azimuth drive	By gearmotor and cogged crown wheel
Azimuth rotation angles	Vertical axis: -120 º to +120 º
Tilt drive	Electrically driven mechanical jack
Motorized Tilt	Adjustable from 0 º to 60 º
Tracker height at 60 °	22 feet (6.7 mts.) (from ground to top modules)
Motor consumption	100 kWh / year
Motor operating voltage	380 V Three Phase
Structure	Hot dipped galvanized steel structure
Structure design	"V" Structure on cogged crown wheel
Weight without modules, and without foundation	6600 lb (3000 Kg)
Electrical cabinets and PLC protection	Metal, weatherproof, fully wired, IP66 Includes PLC fully wired to motor with protection

Electrical supply cabinet	Metal, weather-tight, fully wired, IP66, includes AC surge protection and magnetothermic (PIA) differential (only for MS TRACKER +)
Tracking technology	independent Astronomical programming of PLC
Monitoring	On-site, Ethernet, Internet (OPTIONAL)
Inverters	2 SB SMA inverters 6.0 kWn IP65 1 SC 500 HE for 50 trackers and others combination
Modules to be installed	Any type of PV modules. Optional module holder profile
Module maximum weight	2750 lb (1250Kg)
Wind protection system	Programmable. Horizontal positioning at speeds over 43.5 mph (70 Km/h) (by gearmotor slipping)
Foundation	Surface circular foundation, 10 cubic yards (7,5m³) wire mesh concrete. Optional anchor bolts, direct bolt anchoring
Standard Compliant with	EUROCODE 0 EUROCODE 1 EUROCODE 3 CE
Maximum wind speed	87 mph (140Km/h)
Maintenance	Annual revision of electrical and mechanical parts to keep the guarantee in force

Structure diagram

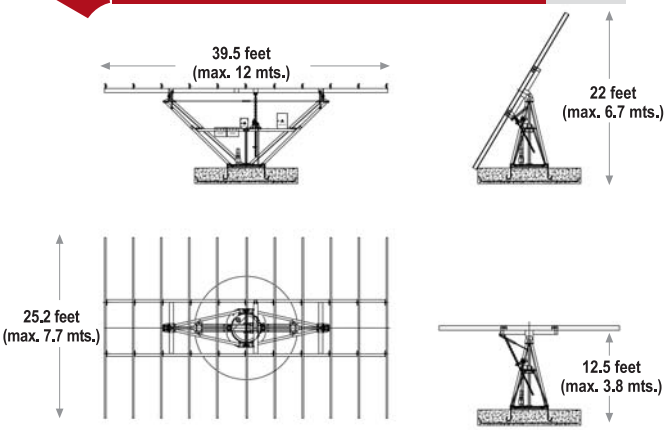

ISO 9001:2008 ISO 14001:2004

Checking of 2-axis tracker using finite element programme

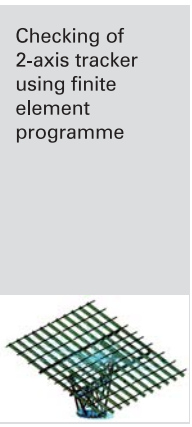

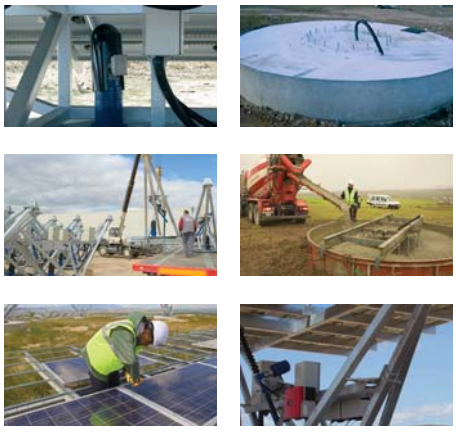

BI-672 / 2010 04/12 MECASOLAR - EN

MECASOLAR SPAIN
Pol. Ind. Santos Justo y Pastor, s/n,
31510 - Fustiñana, Navarra,
España
Phone : (+34) 948 840 993
(+34) 902 107 049
Fax: (+34) 948 840 702
mecasolar@mecasolar.com

MECASOLAR ITALY
Via Vittime di Piazza Fontana 1
10024 Moncalieri (TO)
Italia
Phone: (+39) 02 49 534 600
Fax: (+39) 02 49 534 634
italia@mecasolar.com

MECASOLAR HELLAS
Industrial Area of Thessaloniki
Building Block 40, DA 12a
P.O. Box: 1392 - 57022 Sindos,
Thessaloniki - Greece
Phone.: (+30) 2310 799 209
Fax: (+30) 23 10 570 597
hellas@mecasolar.com

MECASOLAR US
3410 Industrial BLVD
Suite 102,
West Sacramento, 95691CA
United States
Phone: (+1) 916 374 8722
Fax: (+1) 916 374 8063
usa@mecasolar.com

MECASOLAR CANADA
152 Duncan Street
Wallaceburg, ON N8A 4E2
Canada
Phone: (+1) 916 374 8722
Fax: (+1) 916 374 8063
canada@mecasolar.com

E.2 OPEL Solar SF-20 CPV

OPEL Solar™

Harnessing the sun
through concentration

FEiNA SF-20
Dual Axis Tracker

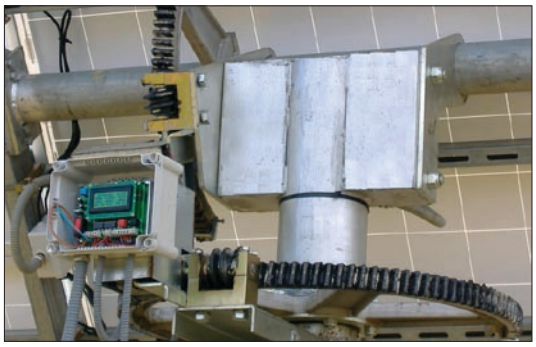

High Performance

The **SF-20** has a tracking accuracy of ±1° which can be improved by means of an optional solar probe down to ±0.1° to ensure that the panels produce at their full potential.

Versatile

The **SF-20** is a high performance tracker that can be customized to mount any size photovoltaic panel or solar thermal module.

Cost Effective Networking

The **SF-20** has networking capabilities which allow for the sharing of common resources in a solar field, such as a GPS unit, which provides accurate time and pin point location updates, and an Anemometer to protect the trackers in the event of extreme wind conditions.
The networking capabilities also allow for remote monitoring and programming, reducing the onsite maintenance costs.

Ease of Installation

The installation of the **SF-20** tracker can be completed by a two man team and does not require any field welding.
The **SF-20** utilizes a mono post mounting design that can be secured by a concrete poured foundation which can be installed on sloping terrain, reducing preconstruction landscaping costs.

Reliability

The **SF-20** has been in production for the past ten years and these trackers can be seen operating at high performance levels in installations around the world.

1. The estimate is based on data from NREL's PV Watts calculator comparing solar collectors on a fixed installation at Latitude Tilt and the same number of panels mounted on the dual axis tracker at a location in Southern California.

In a typical application, the high performance SF-20 dual axis tracker can increase the yield of silicon flat plate panels as much as 45% compared to fixed installations [1].

Physical Data

Type	2 axis
Height off ground	205 in (5.2 m)
Width	200 in (5.1 m)
Depth when horizontal	157 in (4 m)
Total weight	545 lbs (250 kg)
Frame weight	330 lbs (150 kg)
Wind resistance	90 mi/hr (145 km/hr)
Limited warranty	10 years [1]

Electrical Characteristics

Operating voltage	12 V
Consumption	14 Wh/day
Tracking Accuracy (open loop)	± 1°
Tracking accuracy (closed loop with sun sensor)	Typical: ± 0.1° Maximum [3]: ± 0.3°

Capacities

Module area	200 x 157 in (5.1 x 4 m)
Electrical yield (approx.) [2]	3150 W
Weight capacity	600 lb (272 kg)
Weight fully loaded	1150 lb (525 kg)
Rotation in azimuth	210°
Inclination angle range	85°

Shipping Dimensions

Volume	9.2 cu ft (0.26 m^3)
Length (max)	200 in (5.1 m)
Weight	545 lbs (250 kg)
Number per 40 ft container	60

1. Warranty: Ten Year Repair, Replacement Warranty. Freedom from defects in materials and workmanship under normal application, installation, use and service conditions. Please refer to our detailed limited warranty for additional details.
2. Based on installing eighteen 175 W PV panels (1.57 x 0.808 m)
3. Operating under wind conditions and cloudy skies

Diagram

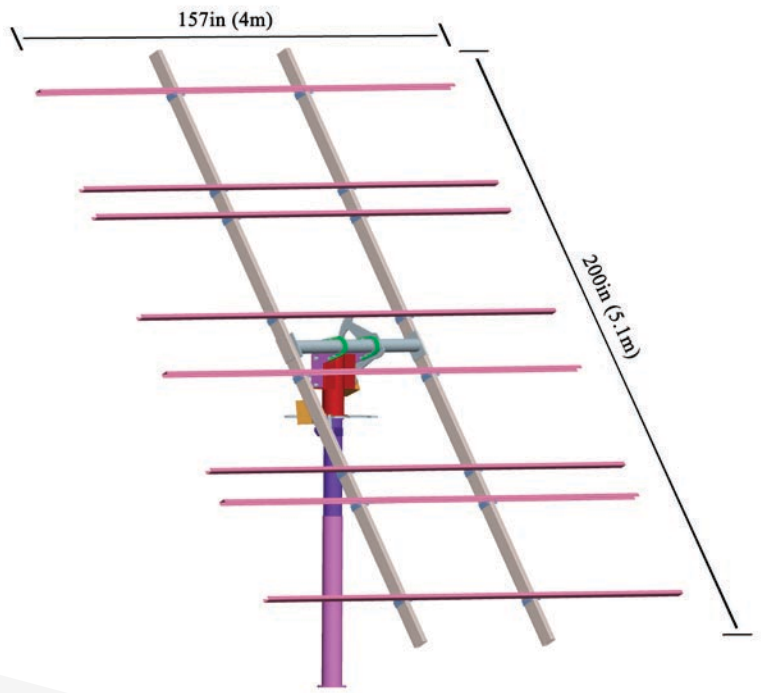

OPEL Solar™

OPEL Solar Inc. ◘ 3 Corporate Drive Suite 204, Shelton, CT 06484, U.S.A.
Telephone: +1 203-612-2366 ◘ E-mail: info@opelinc.com ◘ **www.opelinc.com**

11/16/09

E.3 PV Trackers PVT 7.2 DX

PVT 7.2DX DUAL-AXIS TRACKER

SPECIFICATIONS

PV Trackers develops innovative patented technology in the form of a dual-axis tracker that reduces the levelized cost of producing solar energy by 33%. Our technology combined with world-class design, easy installation and outstanding reliability are some of the reasons why we are the largest USA based dual axis-tracker company. We are also more than just a tracker company:

WE DESIGN POWER PLANTS

UPGRADES FROM THE 6.0DX INCLUDE:

• 20% MORE CAPACITY • LOWER PRICE/STC DC WATT • MORE EFFICIENT MOTORS • LOWER POWER USAGE • PATENTED STOW CAPABILITY • LONGER MTBF • SHORTER MTTR • ENVIROMENTALY SEALED DRIVES • ADDIONAL GEAR REDUCTION FOR BOTH N/S & E/W • UL LISTED POWER SUPPLY • OPTIONAL DC ARRAY CURRENT MONITORING • OPTIONAL WIRELESS

SPECIFICATION DATA

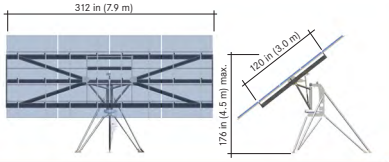

SOUTH ELEVATION EAST ELEVATION

ENERGY PERFORMANCE

Over fixed-tilt rack	≈ 40% annually (site dependent)
Photovoltaic Power / Tracker	6.0kW - 7.4kW (dependent on panel specifications)
String configuration	2 - 3 parallel strings operating within 250-600 volt window

PHYSICAL

Tracker axis	Dual-Axis
Azimuth rotation angle	+/-95° from South (software controlled)
Altitude tilt angle	0° to 60° (software controlled)
Tracking accuracy	+/- 0.5°
Height @ max. tilt (excluding panels)	14 feet 8 inches (4.5 m)
Width (excluding panels):	26 feet (7.9 m)
Weight (excluding panels)	Approx. 1700 lbs.

OPERATIONS

Azimuth drive	Worm Drive
Altitude drive	Ball Screw Linear Actuator
Drive consumption	0.16 kWh/day
Drive operating voltage	160-600 VDC and 277 watt AC (WYE)
Tracking technology	Calculation based tracking. Integrated shade avoidance
Communications	RS-485
Monitoring	On-site software, Internet
Temperature rating	-40° C to + 70° C
Standby power consumption	0.35 kWh/day
Wind protection system	Automatic feathering and stow algorithm
Wind load (max)	90 MPH

COMPONENTS

Structural material	Hot dipped galvanized steel
Structural design	Tripod legs / Tetrahedron support
Electrical cabinets	IP56 / Nema 4x

ENERGY

Panel surface area (max.)	500 s.f. (46.5 m²) - PVT to verify panel configurations
Panel types	Any type of PV module
Inverter types	Customer supplied inverters (1 or multiple trackers/inverter)

RELIABILITY

Complies with	N.E.C. 2008
Maintenance	Annual inspection, NO lubrication, panel cleaning as required
Guarantee	10 years fabricated parts & electronics Extended warranties available upon request

PVT 7.2DX DUAL-AXIS TRACKER

DESIGN GUIDELINES

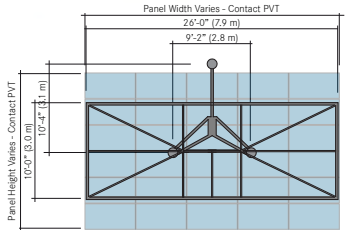

- Total panel/module area approx. 500 ft² (46.5 m²). Call PV Trackers to see how your panels fit.
- Typical panel configurations accomodate 24-33 units/tracker (6.0 to 7.4kW/tracker)

PLAN VIEW DIMENSIONS

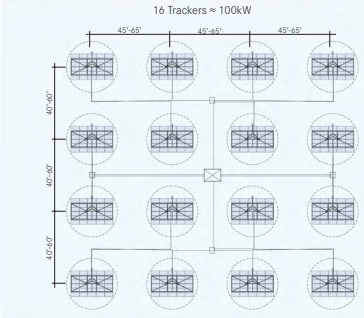

TRACKER SITE SPACING

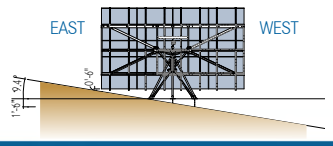

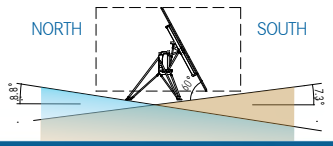

MAXIMUM SITE SLOPE

Preferred Option:

- Helical Piles (shown), ideal for 80% of soil conditions; require no site prep, concrete or reinforcing; and can be installed in 5 minutes

Other Options:

- Concrete Pier Footings
- Concrete Pad Foundation

GROUND ANCHORING OPTIONS

- Site Evaluation
- Feasibility Studies with Estimated Performance
- Installation Training
- Commissioning Support
- Remote Monitoring of Solar Power Plants
- 24/7 Security
- Extended Warranties Available

SERVICES PROVIDED

CAPTURING KILOWATT HOURS
2700 NE 4TH STREET, SUITE 200 BEND, OREGON 97701 541.389.1359 WWW.PVTRACKERS.COM PV TRACKERS

E.4 Patent Summary

E.5 US 7,884,279 B2

US007884279B2

(12) **United States Patent**
Dold et al.

(10) **Patent No.: US 7,884,279 B2**
(45) **Date of Patent: Feb. 8, 2011**

(54) **SOLAR TRACKER**

(75) Inventors: **Robert H. Dold**, Monson, MA (US); **Jeffrey J. Nieter**, Coventry, CT (US)

(73) Assignee: **United Technologies Corporation**, Hartford, CT (US)

(*) Notice: Subject to any disclaimer, the term of this patent is extended or adjusted under 35 U.S.C. 154(b) by 659 days.

(21) Appl. No.: **11/376,849**

(22) Filed: **Mar. 16, 2006**

(65) **Prior Publication Data**

US 2007/0215199 A1 Sep. 20, 2007

(51) **Int. Cl.**
H01L 31/045 (2006.01)

(52) **U.S. Cl.** **136/246**; 136/243; 136/244; 136/245

(58) **Field of Classification Search** 136/245, 136/246

See application file for complete search history.

(56) **References Cited**

U.S. PATENT DOCUMENTS

4,256,088	A	3/1981	Vindum	
4,404,565	A *	9/1983	Gurney et al.	343/881
4,830,678	A	5/1989	Todorof et al.	
4,930,493	A	6/1990	Sallis	
5,022,929	A *	6/1991	Gallois-Montbrun	136/246
5,269,851	A	12/1993	Horne	
5,317,145	A *	5/1994	Corio	250/203.4
5,986,203	A *	11/1999	Hanoka et al.	136/251
6,080,927	A	6/2000	Johnson	
6,284,968	B1 *	9/2001	Niesyn	136/246
6,662,801	B2 *	12/2003	Hayden et al.	126/571
6,780,365	B2 *	8/2004	Goldbach	264/251
2002/0074034	A1	6/2002	Fujisaki	
2002/0121298	A1	9/2002	Konold	
2003/0070705	A1	4/2003	Hayden et al.	
2004/0025931	A1	2/2004	Aguglia	
2004/0055631	A1	3/2004	Szymocha	
2005/0081908	A1	4/2005	Stewart	
2005/0133082	A1	6/2005	Konold	

FOREIGN PATENT DOCUMENTS

CN	85203323 U		8/1986
FR	2535033 A1		4/1984
WO	2004044502 A1		5/2004
WO	WO 2004/070281		8/2004
WO	WO 2004/099682		11/2004

OTHER PUBLICATIONS

Website http://www.newwavetruss.com/about.html.
First Office Action, Chinese Patent Office, Application No. 200780017811.0, mailed Feb. 5, 2010.

* cited by examiner

Primary Examiner—Jennifer K Michener
Assistant Examiner—Jayne Mershon
(74) *Attorney, Agent, or Firm*—Carlson Gaskey & Olds P.C.

(57) **ABSTRACT**

A two-axis solar tracker is capable of withstanding extreme weather conditions. The solar tracker includes a solar array, a frame, a base, a pivot frame, and a first and second actuator. The solar array is mounted to the frame and captures sunlight. The base is pivotally connected to the frame and defines a pivot axis for elevational movement of the solar array. The pivot frame is also pivotally connected to the frame and defines a pivot axis for azimuthal movement of the solar array. The first actuator controls elevational movement of the solar array and the second actuator controls azimuthal movement of the solar array. The solar tracker is pivotable between a raised position and a stowed position.

25 Claims, 11 Drawing Sheets

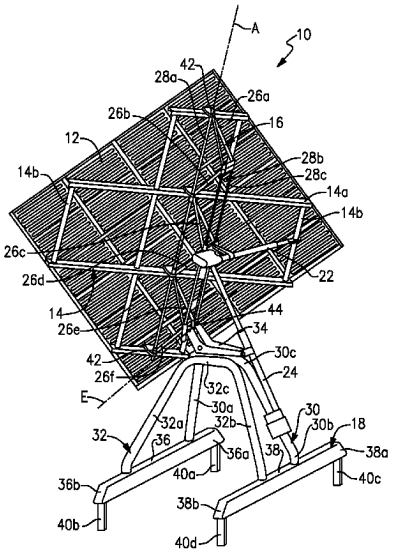

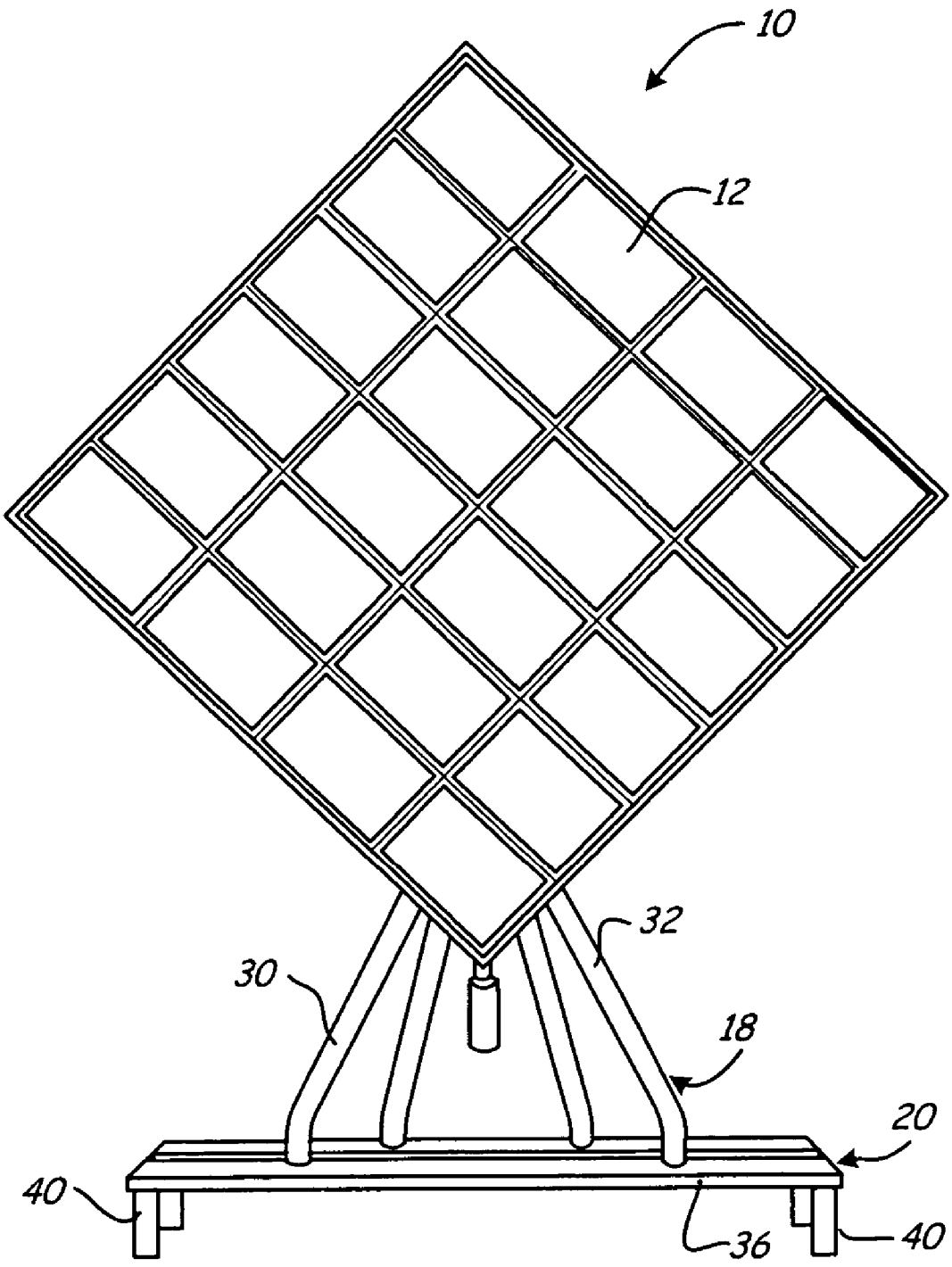

Fig. 1A

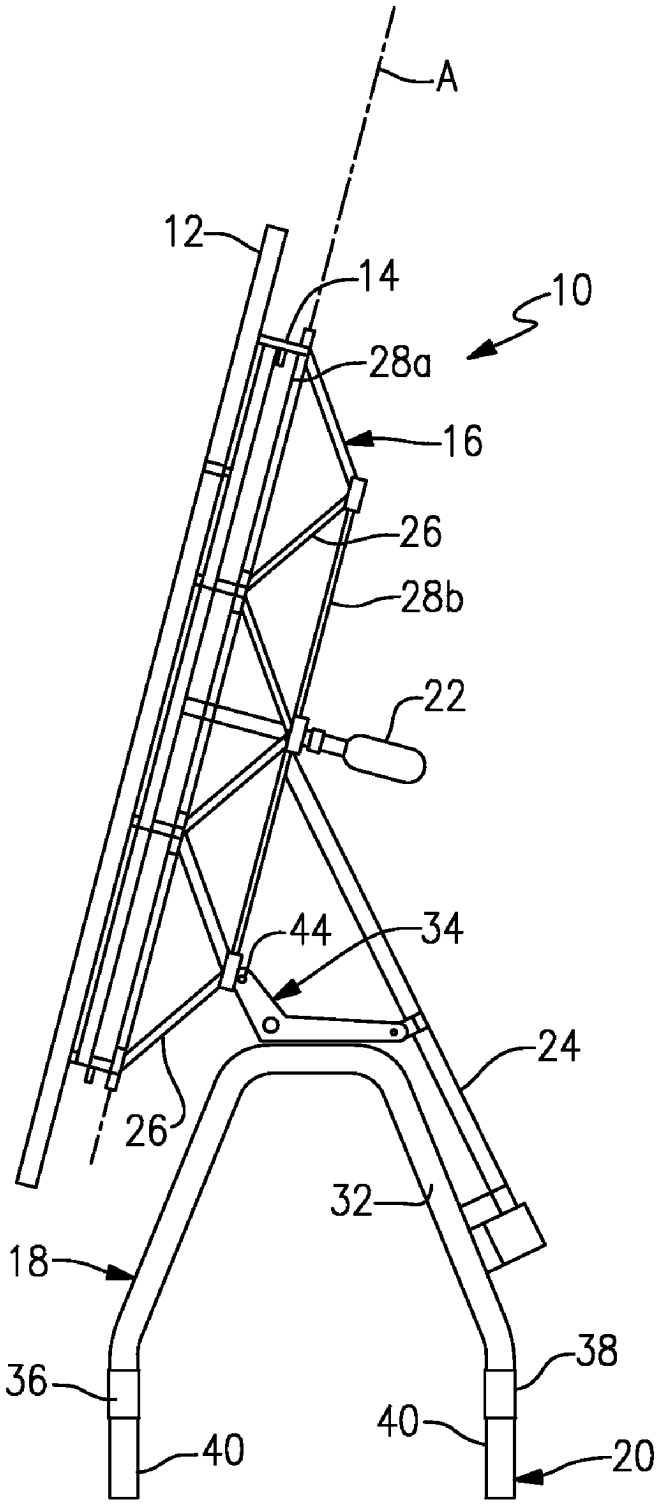

FIG.1B

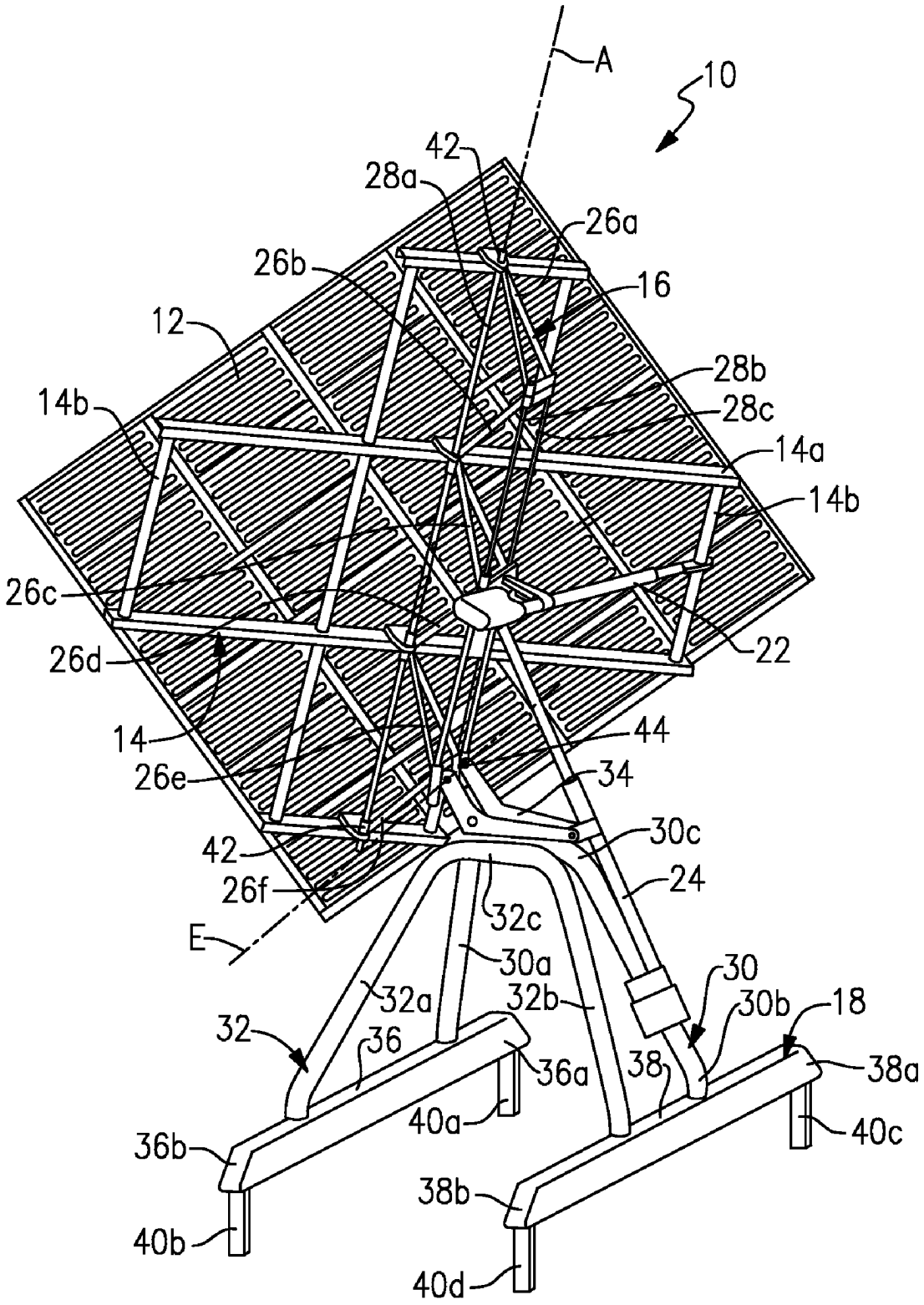
A
10
42
28a
26a
26b
16
12
28b
14b
28c
14a
14b
26c
22
26d
14
44
26e
34
30c
42
24
26f
32c
E
30a
30
32a
32b
30b
18
32
36
36a
38
38a
40a
40c
36b
38b
40b
40d

FIG.2

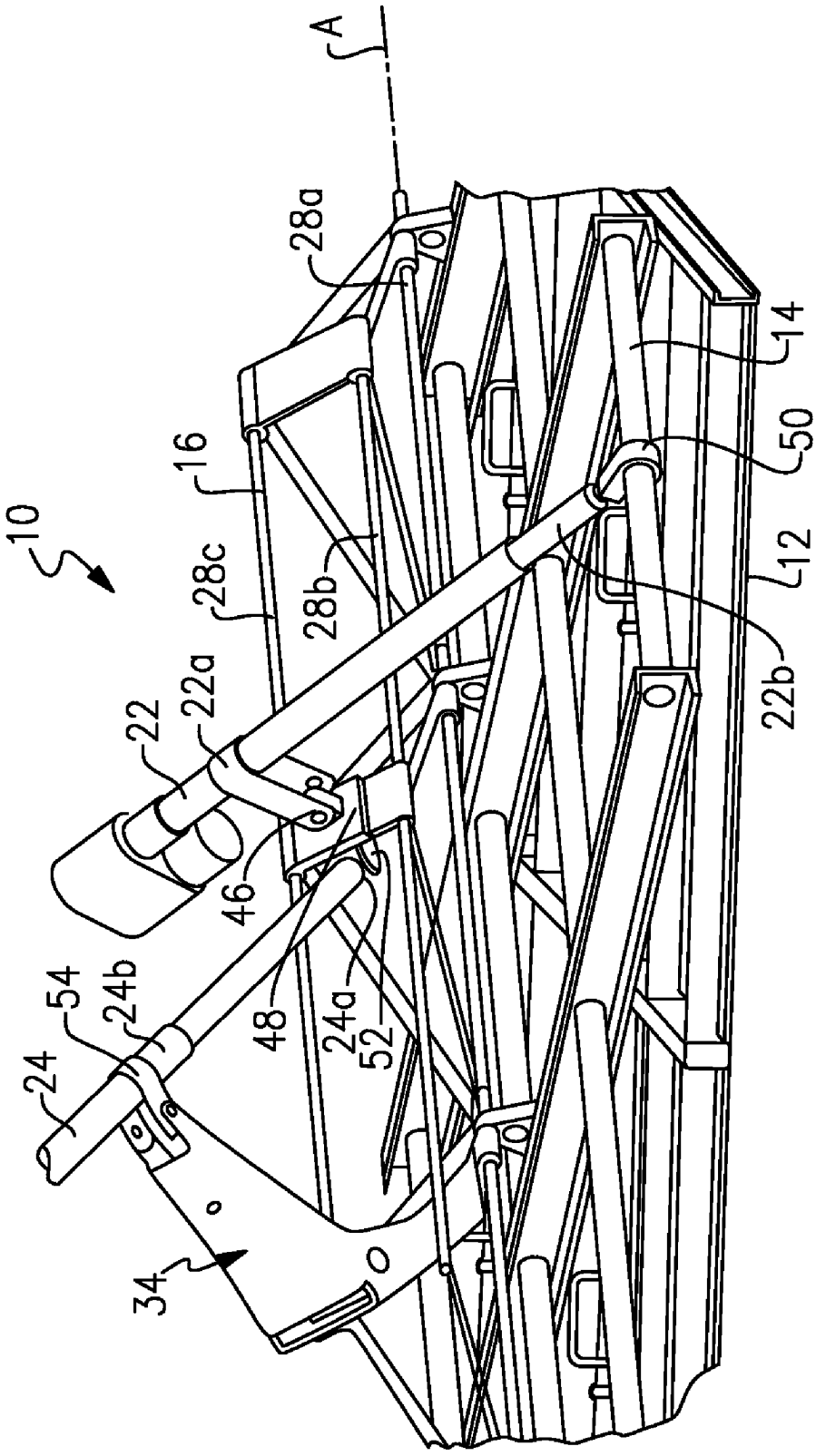

FIG.3

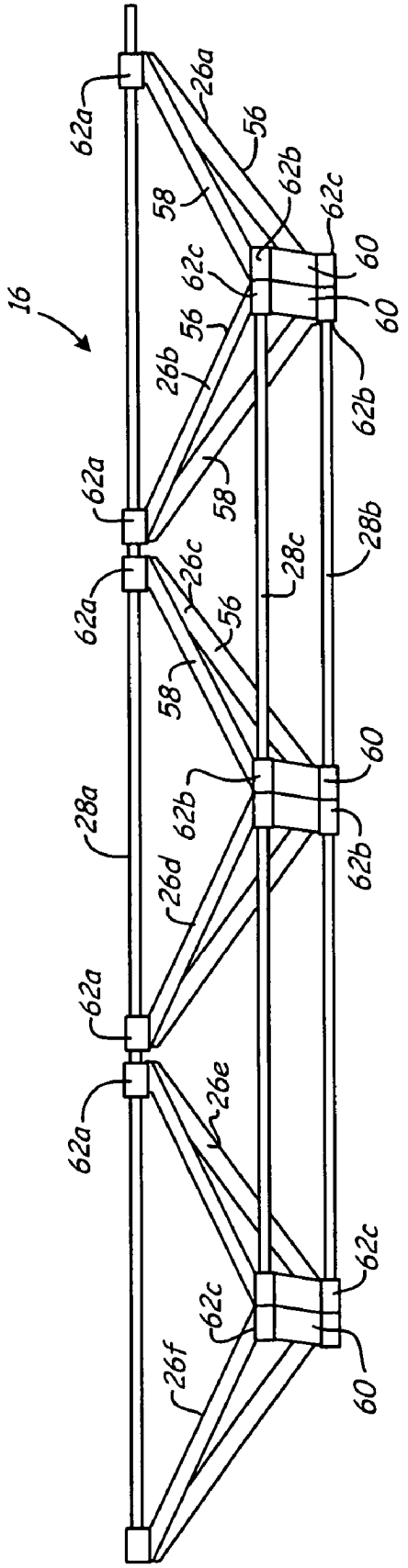
16
62a
26a
56
58
62b
62c
60
62c
56
26b
62a
58
28c
28b
26c
56
58
60
28a
62b
26d
62a
26e
62a
62c
62c
26f
60

Fig. 4

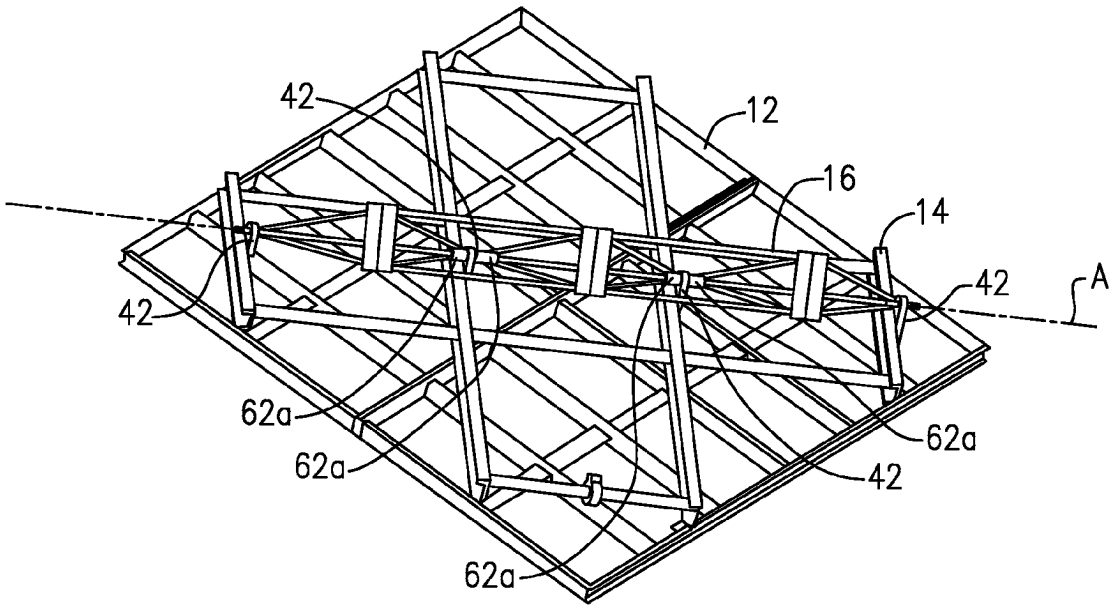

FIG.5

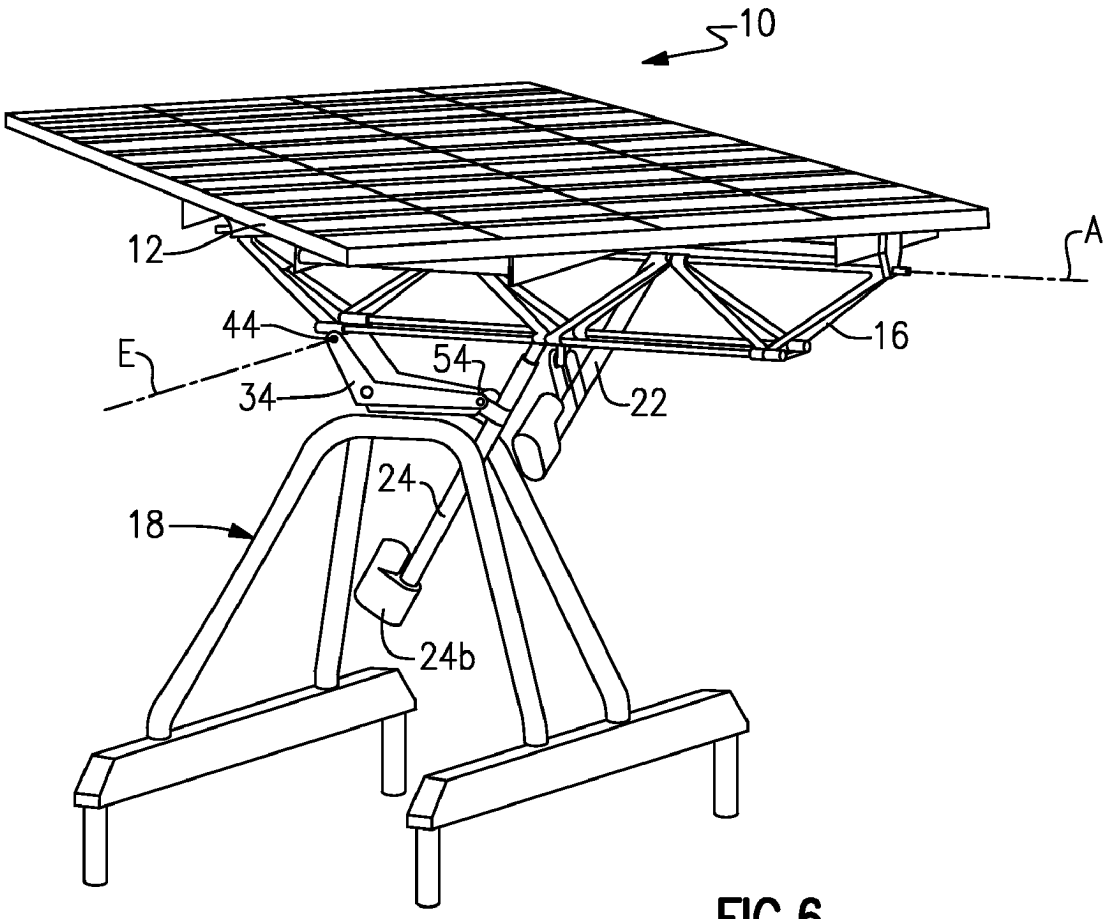

FIG.6

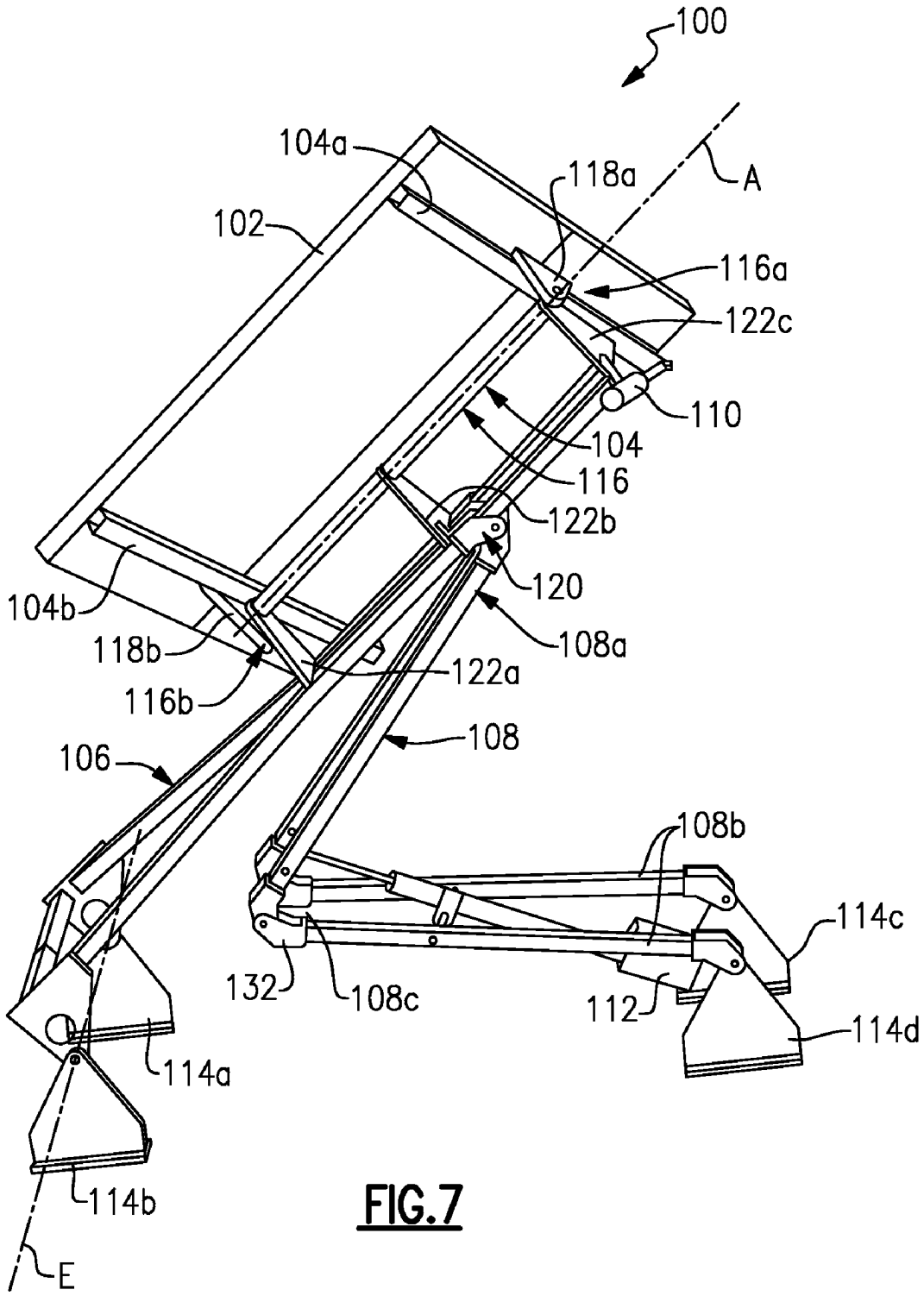
100
104a
118a
A
102
116a
122c
110
104
116
122b
120
104b
108a
118b
122a
116b
108
106
108b
114c
132
108c
112
114d
114a
114b
E

FIG.7

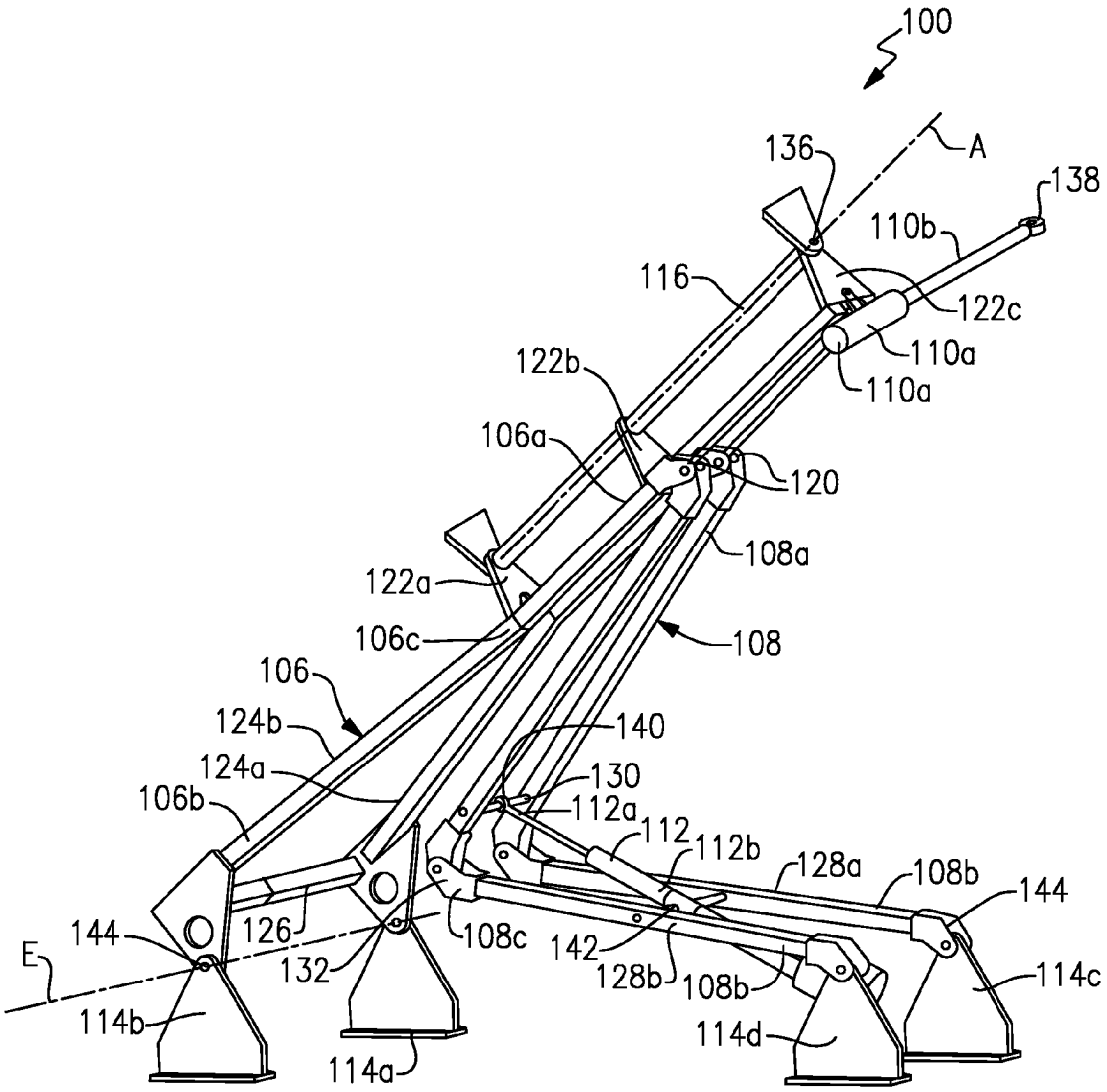
100
136
A
138
110b
116
122c
110a
122b
110a
106a
120
108a
122a
106c
108
106
124b
140
124a
130
106b
112a
112
112b
128a
108b
144
144
126
108c
142
E
132
128b
108b
114c
114b
114d
114a

FIG.8A

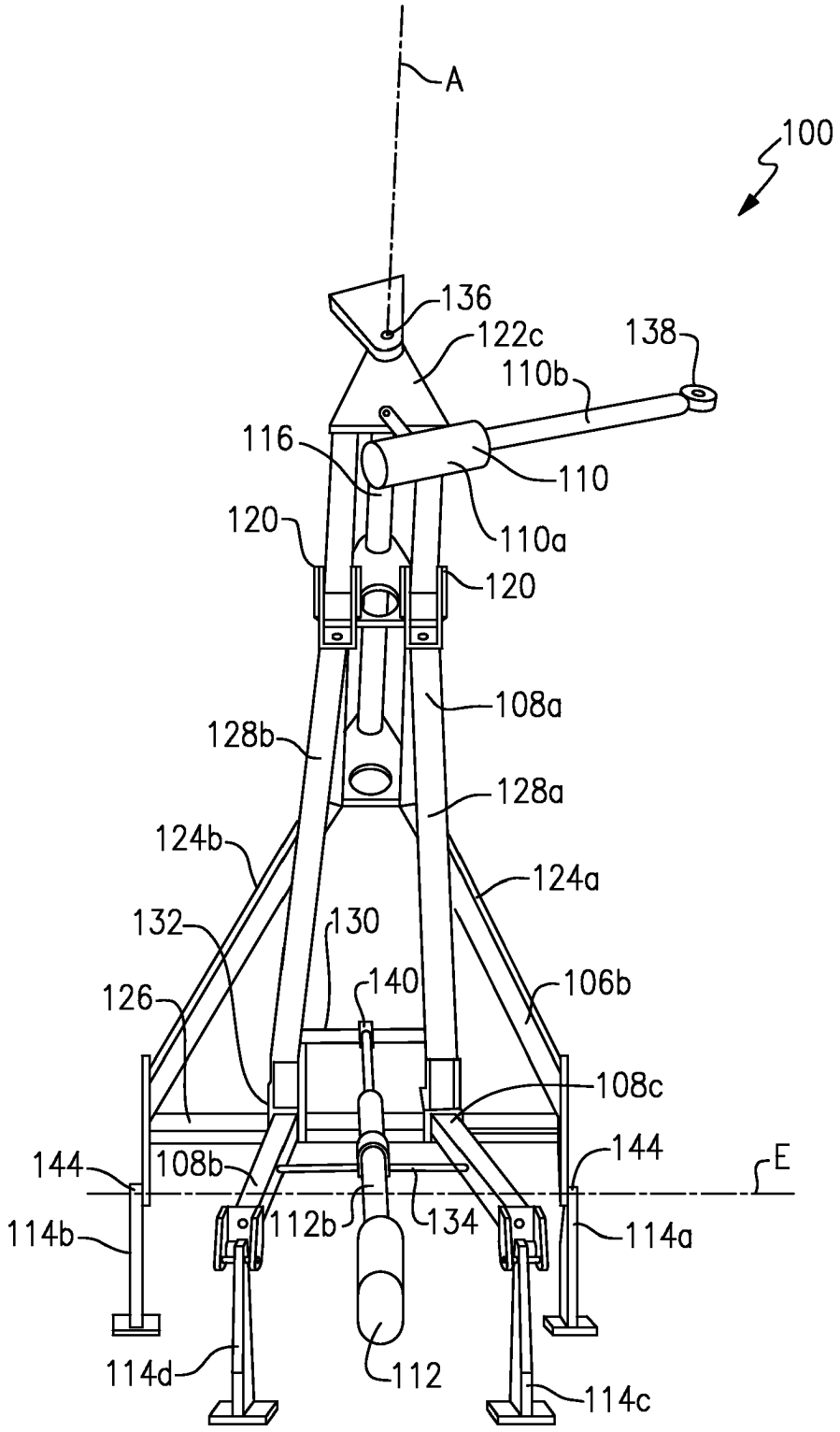
A
100
136
122c
138
110b
116
110
120
110a
120
108a
128b
128a
124b
124a
132
130
126
140
106b
108c
144
108b
144
E
114b
112b
134
114a
114d
112
114c

FIG.8B

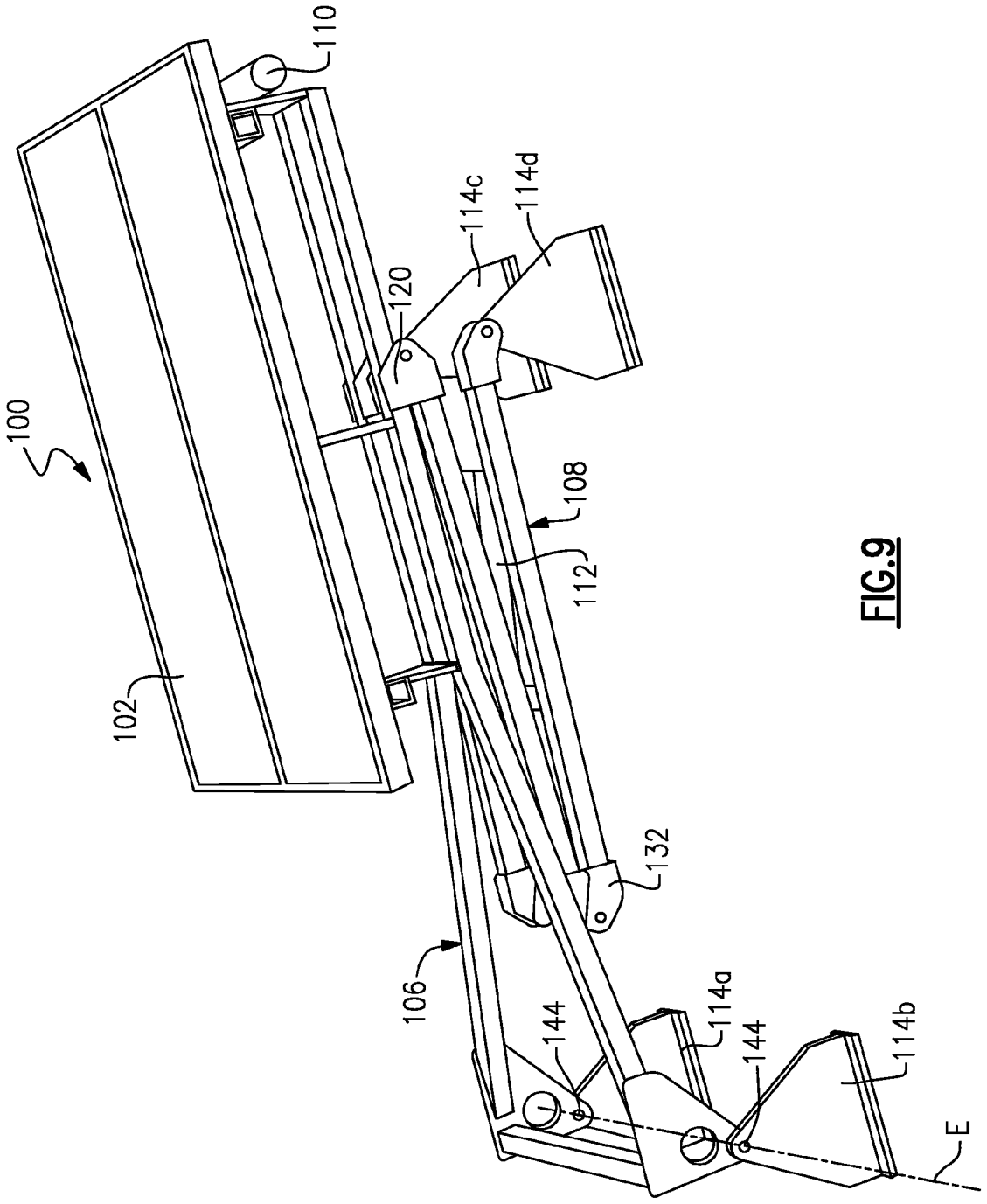

FIG.9

SOLAR TRACKER

BACKGROUND OF THE INVENTION

Solar cells, or photovoltaic cells, have the ability to convert sunlight directly into electricity. In order to capture the maximum amount of sunlight during the day, a tracker is connected to the cells and continuously aligns the light-absorbing panels of the cells in a direction perpendicular to rays from the sun so that the cells can absorb the highest amount of energy from the rays of sunlight. This is particularly important for high performance solar panels having concentrated cells. Current trackers are typically dual axis tracking systems having a linear actuator for elevational control and a geared or linear motor for azimuthal control. However, geared motors can be expensive and add to the cost of producing the tracker.

One problem with current tracker systems is that they are designed to mount on a post and have no means of stowing in extreme winds. Thus, the wind load resistance of the tracker system is low and can result in damage to the tracker or to the solar panels during extreme winds. It would thus be beneficial to be able to either increase the wind load resistance of the tracker or to fold the tracker into a stowed position during extreme weather conditions to reduce the potential of damage to the tracker or the solar panels. Additionally, because current tracker systems are designed to mount on a post, all of the loading is transferred to the base of the post, hindering the ability to integrate the solar tracker onto a building structure. In order to mount the solar trackers on a building structure, the mounting point for the tracker post must be designed to distribute the load of the tracker into the building structural members.

BRIEF SUMMARY OF THE INVENTION

A two-axis solar tracker is capable of withstanding extreme weather conditions. The solar tracker includes a solar array, a frame, a base, a pivot frame, and a first and second actuator. The solar array is mounted to the frame and captures sunlight. The pivot frame is pivotally connected to the frame and defines a pivot axis for azimuthal movement of the solar array. The base is pivotally connected to the pivot frame and defines a pivot axis for elevational movement of the solar array. The first actuator controls azimuthal movement of the solar array and the second actuator controls elevational movement of the solar array. The solar tracker is pivotable between a raised position and a stowed position.

BRIEF DESCRIPTION OF THE DRAWINGS

FIG. **1**A is a front perspective view of a first embodiment of a solar tracker.

FIG. **1**B is a side perspective view of the first embodiment of a solar tracker.

FIG. **2** is a rear perspective view of the first embodiment of a solar tracker in a raised position.

FIG. **3** is a magnified partial top and rear view of a solar array of the first embodiment of the solar tracker.

FIG. **4** is a magnified perspective view of a truss of the first embodiment of the solar tracker.

FIG. **5** is a magnified rear view of the first embodiment of the solar array with the truss mounted on the solar tracker.

FIG. **6** is a perspective view of the first embodiment of the solar tracker in a stowed position.

FIG. **7** is a perspective view of a second embodiment of the solar tracker in a raised position.

FIG. **8**A is a partial magnified view of the second embodiment of the solar tracker.

FIG. **8**B is a partial rear view of the second embodiment of the solar tracker.

FIG. **9** is a perspective view of the second embodiment of the solar tracker in a stowed position.

DETAILED DESCRIPTION

FIGS. **1**A and **1**B show a front view and a side view, respectively, of a first embodiment of two-axis solar tracker **10** in a raised position and will be discussed in conjunction with one another. Solar tracker **10** generally includes solar array **12** consisting of multiple panels, frame **14**, truss **16**, base **18**, leg mount **20**, first actuator **22**, and second actuator **24**. Truss **16** is a stiff, lightweight, and cost-effective support for solar array **12** and is pivotable relative to frame **14** and base **18**. In order to protect solar array **12** during extreme weather conditions, solar tracker **10** is pivotable between a raised position and a stowed position. Solar tracker **10** with truss **16** has increased wind load resistance and is adaptable to various building structures while using conventional linear actuators.

Solar tracker **10** is designed to align solar array **12** with respect to the sun so that it collects the maximum amount of solar energy. Solar energy is absorbed into solar array **12** where it is subsequently converted to useable energy. Solar array **12** absorbs the maximum amount of solar energy when solar array **12** is aligned normal to the rays of the sun. Solar array **12** is thus mounted to solar tracker **10**, which continually positions solar array **12** relative to the position of the sun. As can be seen in FIGS. **1**A and **1**B, solar array **12** can be formed from a plurality of smaller solar panels that are positioned proximate one another to form a large solar array. This allows solar array **12** to capture more sunlight. In one embodiment, the smaller solar panels are positioned relative to one another to form a diamond shaped array in order to provide less deflection as well as corner-to-corner support.

Truss **16** is mounted to frame **14** about an azimuthal axis A and is pivotally connected to base **18** about an elevation axis E. The triangular shape of truss **16** provides increased wind load resistance for solar tracker **10**. Truss **16** is formed from a plurality of truss sections **26** held together by a plurality of tubes **28**. In one embodiment, truss **16** is formed of a lightweight material, such as aluminum. Alternatively, truss **16** can be molded from a glass reinforced nylon or other thermoplastic.

Base **18** connects solar array **12** to leg mount **20** and generally includes first leg **30**, second leg **32**, and actuator mount **34**. First and second legs **30**, **32** of base **18** spread the load of solar tracker **10**. Actuator mount **34** is mounted to base **18** and pivotally connects truss **16** to base **18** so that solar array **12** can follow the elevation of the sun about elevation axis E, as well as pivot between a raised position and a stowed position.

Leg mount **20** generally includes horizontal first and second supports **36**, **38** that connect base **18** to leg mount **20**. Both first and second supports **36**, **38** have attachment posts **40** that allow installation of solar tracker **10** onto a building structure.

First and second actuators **22**, **24** provide two-axis tracking of solar tracker **10**. First actuator **22** controls azimuthal movement of solar array **12** and second actuator **24** controls elevational movement of solar array **12**. In one embodiment, first and second actuators **22**, **24** are linear actuators.

FIG. **2** shows a rear view of solar tracker **10** with truss **16** mounted on frame **14**. Frame **14** is mounted to the back of solar array **12** and extends across two dimensions of solar

array **12**. Frame **14** is formed from a plurality of supports **14***a*, **14***b* positioned relative to one another to form an array. If solar array **12** is formed from a plurality of smaller solar panels, frame **14** also maintains the plurality of smaller solar panels in position relative to one another. Truss **16** is attached to frame **14** and in combination with first and second actuators **22**, **24**, controls the alignment of solar array **12** relative to the sun. Although FIG. **2** depicts plurality of supports **14***a*, **14***b* positioned at intersecting right angles, supports **14***a*, **14***b* can be formed in any type of array as long as frame **14** can support truss **16** and maintain smaller solar panels relative to one another.

Truss **16** is mounted to frame **14** and connects solar array **12** to base **18**. Truss **16** is formed from a plurality of truss sections **26***a*, **26***b*, **26***c*, **26***d*, **26***e*, **26***f* (collectively truss sections **26**) held together by first tube **28***a*, second tube **28***b*, and third tube **28***c* (collectively tubes **28**). First tube **28***a* pivotally connects truss **16** to frame **14** at frame pivot joints **42** which defines azimuth axis A and allows truss **16** to support solar array **12**. Truss **16** is also pivotally connected to base **18** by actuator mount **34** at base pivot joint **44** in order to continually align solar array **12** with respect to the sun about the elevation axis E.

First leg **30** of base **18** has a first end **30***a*, a second end **30***b*, and a central portion **30***c*. First end **30***a* and second end **30***b* are spaced apart from each other and are connected by central portion **30***c*. Similarly, second leg **32** of base **18** has a first end **32***a*, a second end **32***b*, and a central portion **32***c*. First end **32***a* and second end **32***b* are also spaced apart from each other and are connected by central portion **32***c*. First and second legs **30** and **32** are connected to each other at central portions **30***c*, **32***c* with first ends **30***a*, **32***a* of first and second legs **30**, **32** spaced apart from each other in a V-shape and second ends **30***b*, **32***b* of first and second legs **30**, **32** spaced apart from each other in a V-shape. Actuator mount **34** is mounted to base **18** where central portions **30***c*, **32***c* of first and second legs **30**, **32** are connected.

First and second supports **36**, **38** of leg mount **20** stabilize base **18** and solar array **12**. First support **36** has a first end **36***a* and a second end **36***b* and second support **38** has a first end **38***a* and a second end **38***b*. First ends **30***a*, **32***a* of first and second legs **30**, **32** are attached to first support **36** between first and second ends **36***a*, **36***b* of first support **36**. Second ends **30***b*, **32***b* of first and second legs **30**, **32** are attached to second support **38** between first and second ends **38***a*, **38***b* of second support **38**. First and second supports **36**, **38** have attachment posts **40***a*, **40***b*, **40***c*, **40***d* (collectively attachment posts **40**) located at each of first and second ends **36***a*, **36***b* and **38***a*, **38***b* that allow installation of solar tracker **10** onto a building structure. Although FIG. **2** depicts leg mount **20** as having first and second supports **36**, **38**, solar panel **12** may be mounted on any support known in the art. Similarly, although FIG. **2** depicts attachment posts **40** as four separate posts, any means known in the art for mounting a device onto a structure can be used to mount solar tracker **10** to the building structure.

To better illustrate the attachment points of first and second actuators **22** and **24**, FIG. **3** shows a magnified partial top and rear view of solar array **12** with base **18** removed. First actuator **22** has a first end **22***a* pivotally connected to truss **16** at a first pivot joint **46** of a connector **48** positioned between second tube **28***b* and third tube **28***c*, and a second end **22***b* pivotally connected to frame **14** at pivot joint **50**. First actuator **22** thus pivots solar array **12** about axis A defined by first tube **28***a* of truss **16** as first actuator **22** telescopes in and out, controlling movement of solar array **12** in an azimuthal direction. First tube **28***a* therefore defines the azimuthal axis A for azimuthal movement of solar tracker **10**.

Second actuator **24** has a first end **24***a* pivotally connected to truss **16** at a second pivot joint **52** of connector **48** positioned between second tube **28***b* and third tube **28***c*, and a middle portion **24***b* pivotally connected to actuator mount **34** by pivot joint **54**. Second actuator **24** thus pivots solar array **12** about axis E defined by base pivot joint **44** as second actuator **22** telescopes in and out, controlling movement of solar array **12** in an elevational direction. Base **18** (through pivot joint **44**) therefore defines the elevation axis E for elevational movement of solar tracker **10**. First pivot joint **46** is generally transverse to second pivot joint **52**

FIG. **4** shows a magnified perspective view of truss **16**. Each of first, second, third, fourth, fifth, and sixth truss sections **26***a*, **26***b*, **26***c*, **26***d*, **26***e*, **26***f* (collectively, truss sections **26**) has a first side **56**, a second side **58**, and a third side **60** that together form a triangular shape. First, second, and third pivot holes **62***a*, **62***b*, **62***c* (collectively pivot holes **62**) are located between first, second, and third sides **56**, **58**, **60** and are sized to accept tubes **28**. First pivot hole **62***a* is located between first and second sides **26***a*, **26***b*, second pivot hole **62***b* is located between second and third sides **26***b*, **26***c*, and third pivot hole **62***c* is located between third and first sides **26***c*, **26***a*.

To form truss **16**, truss sections **26** are sliced at an angle from a truss extrusion and are subsequently assembled together with tubes **28**. First and second truss sections **26***a*, **26***b* are first aligned so that second pivot hole **62***b* of first truss section **26***a* abuts third pivot hole **62***c* of second truss section **26***b* and third pivot hole **62***c* of first truss section **26***a* abuts second pivot hole **62***b* of second truss section **26***b*. In this arrangement, first pivot holes **62***a* of first and second truss sections **26***a*, **26***b* are spaced apart. Third truss section **26***c* is then aligned with second truss section **26***b* such that first pivot holes **62***a* of second and third truss sections **26***b* and **26***c* are proximate each other but second and third pivot holes **62***b*, **62***c* are spaced apart. This pattern is repeated for the length of truss **16**.

After truss sections **26** have been properly positioned relative to one another, first tube **28***a* is passed through first pivot holes **62***a* of truss sections **26**. Second and third tubes **28***b*, **28***c* are then passed through alternating second and third pivot holes **62***b*, **62***c* of truss sections **26** on either side of truss **16**. After tubes **28** are positioned within pivot holes **62** of truss sections **26**, truss **16** is held together using epoxy. Other adhesive means or mechanical fasteners known in the art may also be used to hold truss **16** as a single unit. The triangular shape of truss **16** allows truss sections **26** to be spaced apart, resulting in increased resistance to side loads imparted to solar array **12** due to wind loading. Although FIG. **4** depicts truss **16** as having six truss sections **26***a*-**26***f* forming truss **16**, truss **16** may include as many truss sections as necessary to support solar array **12**.

FIG. **5** shows a magnified back view of solar array **12** with truss **16** mounted to frame **14**. After truss **16** has been assembled, truss **16** is mounted to frame **14** at intermediate points along first tube **28***a*. First tube **28***a* is connected to frame **14** by frame pivot joints **42** of frame **14** between first pivot holes **60***a*. Although FIG. **5** depicts truss **16** as extending diagonally across diamond-shaped solar array **12**, truss **16** may also extend down the center of the array, similar to a conventional tracking array. Positioning truss **16** diagonally across solar array **12** provides the maximum amount of support to solar array **12**.

FIG. **6** shows solar tracker **10** in a stowed position. In operation, solar tracker **10** can be in either a raised position (shown in FIGS. **1**A, **1**B, and **2**) or a stowed position. When it is desired that solar array **12** absorb solar energy, solar tracker **10** is in the raised position so that solar array **12** can capture as

much sunlight as possible. However, in extreme weather conditions, such as high winds, solar tracker **10** is moved into the stowed position in order to protect solar array **12** from damage. To move solar tracker **10** into the stowed position, second actuator **24** retracts and pivots at pivot joint **54** to cause solar array **12** to pivot about pivot joint **44** of actuator mount **34**. Solar array **12** pivots about pivot joint **44** until solar array **12** is substantially parallel to the ground. Truss **16** is capable of withstanding side load resistance and maintains solar array **12** stable relative to base **18** and leg mount **20**. In the stowed position, solar tracker **10** is better shielded from extreme weather conditions and flying debris that may damage solar array **12**. In one embodiment, solar array **12** includes a wind sensor and controller that align solar array **12** with the wind in order to minimize the wind loading of solar tracker **10**.

FIG. **7** shows a perspective view of a second embodiment of solar tracker **100** in a raised position. Solar tracker **100** generally includes solar array **102**, frame **104**, first linkage arm **106**, second linkage arm **108**, first actuator **110**, second actuator **112**, and leg mounts **114***a*-**114***d*. Linkage arms **106**, **108** of solar tracker **100** allow solar array **102** to be moved into a stowed position during high winds. Solar array **102** of solar tracker **100** functions in the same manner as solar array **12** of solar tracker **10**. Similar to solar tracker **10**, solar tracker **100** is also pivotable between a raised position and a stowed position, uses conventional linear actuators, and is adaptable to various building structures.

Frame **104** is attached to solar array **102** and connects solar array **102** to first and second linkage arms **106**, **108**. Frame **104** generally includes horizontal crossbars **104***a* and **104***b* and pivot frame **116**. Pivot frame **116** has a first end **116***a* and a second end **116***b*. First end **116***a* of pivot frame **116** is connected to crossbar **104***a* of frame **104** by first connector **118***a*. Second end **116***b* of pivot frame **116** is connected to crossbar **104***b* of frame **104** by second connector **118***b*. Although FIG. **7** depicts frame **104** of solar tracker **100** as including two crossbars **104***a*, **104***b* and a single pivot frame **116**, frame **104** can be any structure known in the art that allows pivotal connection of at least one of first and second linkage arms **106**, **108** to solar array **102**.

First and second linkage arms **106**, **108** are pivotally connected to each other by pivot joint **120**. First and second linkage arms **106**, **108** are also connected to frame **104** by first, second, and third connectors **122***a*, **122***b*, **122***c* connected to first linkage arm **106**. Although FIG. **7** depicts two linkage arms **106**, **108** pivotally connected to each other, solar tracker **100** may also be constructed with a scissor-type supporting structure or with a single actuator that provides the lift mechanism without departing from the intended scope of the present invention.

First and second actuators **110**, **112** provide two-axis tracking of solar tracker **100**. First actuator **110** controls azimuthal movement of solar array **102** about azimuthal axis A. Second actuator **112** controls elevational movement of solar array **102** about elevation axis E. In one embodiment, first and second actuators **110** and **112** are linear actuators.

Leg mounts **114***a*-**114***d* are pivotally attached to first and second linkage arms **106**, **108** and allow installation of solar tracker **100** to a range of locations, such as an existing roof support beam of a commercial building. Although FIG. **7** depicts leg mounts **114***a*-**114***d* as four separate attachment structures, any means known in the art for mounting a device onto a structure can be used to mount solar tracker **100** to the building structure.

FIGS. **8**A and **8**B show a magnified partial view of solar tracker **100** and a partial rear view of solar tracker **100**, respectively, and will be discussed in conjunction with one another. Solar array **102** has been removed in FIGS. **8**A and **8**B. First linkage arm **106** has a first end **106***a*, a second end **106***b*, and a center point **106***c* and includes first and second legs **124***a*, **124***b*. First and second legs **124***a*, **124***b* are parallel to each other from first end **106***a* to center point **106***c*. At center point **106***c*, first and second legs **124***a*, **124***b* branch out and extend away from each other to form a triangular shape so that first and second legs **124***a*, **124***b* are spaced from each other at second end **106***b*. First and second legs **124***a*, **124***b* are connected to each other at second section **106***b* by crossbar **126**.

Similarly, second linkage arm **108** also has a first section **108***a*, a second section **108***b*, and an intermediate section **108***c* and includes first and second legs **128***a*, **128***b*. First and second legs **128***a*, **128***b* extend away from each other slightly from first section **108***a* to the intermediate section **108***c*. First and second legs **128***a*, **128***b* are connected to each other at intermediate section **108***c* by intermediate crossbar **130**. Pivot joint **132** at intermediate section **108***c* facilitates elevational movement of solar tracker **100** about elevation axis E. At the intermediate section **108***c*, first and second legs **128***a*, **128***b* branch out and extend away from each other to form a triangular shape so that first and second legs **128***a*, **128***b* are spaced from each other at second section **108***b*. First and second legs **128***a*, **128***b* are connected to each other by stabilizing crossbar **134**.

First actuator **110** has a first end **110***a* and a middle portion **110***b*. First end **110***a* of first actuator **110** is pivotally connected to solar array **102** at pivot joint **136** and middle portion **110***b* of first actuator **110** is pivotally attached to frame **104** by pivot joint **138**. First actuator **110** thus pivots solar array **102** about pivot frame **116** as first actuator **110** telescopes in and out, to control movement of solar array **102** in an azimuthal direction about azimuthal axis A. Pivot frame **116** therefore defines the azimuthal axis A for azimuthal movement of solar tracker **100**.

Second actuator **112** has a first rod **112***a* and a middle cylinder **112***b*. First rod **112***a* of second actuator **112** is pivotally connected to second linkage arm **108** at intermediate crossbar **130** by pivot **140**. Middle cylinder **112***b* of second actuator **112** is pivotally attached to stabilizing crossbar **134** by pivot joint **142**. As second actuator **112** telescopes in and out, first linkage arm **106** pivots about first and second leg mounts **114***a* and **114***b*, pivoting solar array **102** about pivot joints **144** connecting first linkage arm **106** to first and second leg mounts **114***a* and **114***b*. This controls movement of solar array **102** in an elevational direction. The connection of first and second leg mounts **114***a*, **114***b* to second linkage arm **106** therefore defines a pivot axis for elevational movement of solar tracker **100**. In the embodiment shown, first and second actuators **110** and **112** are linear actuators.

Leg mounts **114***a*, **114***b* are pivotally attached to first and second legs **124***a*, **124***b* of first linkage arm **106**, respectively, at second section **106***b* of first linkage arm **106**. Leg mounts **114***c* and **114***d* are pivotally attached to first and second legs **128***a* and **128***b* of second linkage arm **108**, respectively, at second section **108***b* of second linkage arm **108**. Pivot joints **144** pivotally connect leg mounts **114***a*-**114***d* to first and second linkage arms **106**, **108**.

FIG. **9** shows a perspective view solar tracker **100** in a stowed position. Similar to solar tracker **10**, solar tracker **100** can be in either a raised position (FIG. **7**) or a stowed position. To move solar tracker **100** into the stowed position, second actuator **112** telescopes in and pivots second linkage arm **108** at pivot joints **132** so that the intermediate section **108***c* of second linkage arm **108** moves toward the ground. As the intermediate section **108***c* of second linkage arm **108** lowers,

second section **108***b* of second linkage arm **108** also pivots about third and fourth leg mounts **114***c*, **114***d*, which are attached to the ground. First section **108***a* of second linkage arm **108** also moves toward the ground as second linkage arm **108** pivots at pivot joint **132** and the intermediate section **108***c* lowers. This downward movement of second linkage arm **108** causes first end **106***a* of first linkage arm **106** to pivot about pivot joints **120** and also move toward the ground, with solar array **102**. As first end **106***a* of first linkage arm **106** moves toward the ground, second section **106***b* of first linkage arm **106** pivots about first and second leg mounts **114***a*, **114***b* until solar tracker **100** is in the fully stowed position. In the stowed position, solar tracker **100** is low to the ground and thus better shielded from extreme weather conditions and flying debris that may damage solar array **102**.

The solar tracker of the present invention is capable of withstanding extreme weather conditions and being moveable between a raised position and a stowed position. During normal operation, the solar tracker is in the raised position to capture a maximum amount of sunlight. During extreme weather, such as high winds, the solar tracker can retract the solar array into a stowed position. Two linear actuators control the elevational and azimuthal movement of the solar tracker in order to align a solar array with the sun during the day and to move the solar tracker between the raised and stowed positions. The solar tracker also spreads the load of the solar array such that the solar tracker can be mounted on a building structure.

In a first embodiment of the solar tracker, the solar array of the solar tracker is supported by a truss. The truss is designed to provide the solar tracker with increased side load resistance and is formed from a plurality of triangular truss sections that are connected to each other by a plurality of tubes. In a second embodiment of the solar tracker, the solar tracker includes a first and a second linkage arm that are pivotally connected to each other and to the solar array. The second linkage arm is also pivotable at a center point of the linkage arm to allow the solar tracker to retract toward the ground.

Although the present invention has been described with reference to preferred embodiments, workers skilled in the art will recognize that changes may be made in form and detail without departing from the spirit and scope of the invention.

The invention claimed is:

1. A two-axis solar tracker comprising:
- a solar array for capturing sunlight;
- a frame connected to the solar array;
- a pivot frame pivotally connected to the frame to define an azimuthal axis;
- a base pivotally connected to the pivot frame to define an elevation axis;
- a connector mounted to the pivot frame;
- a first actuator connected between the frame and the connector for controlling azimuthal movement of the solar array about the azimuthal axis; and
- a second actuator connected between the base and the connector for controlling elevational movement of the solar array about the elevation axis.

2. The solar tracker of claim **1**, wherein the pivot frame forms a truss.

3. The solar tracker of claim **2**, wherein the pivot frame is formed of glass reinforced thermoplastic.

4. The solar tracker of claim **2**, wherein the pivot frame is formed of extruded metal.

5. The solar tracker of claim **4**, wherein the extruded metal is aluminum.

6. The solar tracker of claim **2**, wherein the truss has a triangular shape.

7. The solar tracker of claim **1**, wherein the first and second actuators are linear actuators.

8. The solar tracker of claim **1**, wherein the pivot frame is a truss that supports the solar array.

9. The solar tracker of claim **8**, wherein said truss extends diagonally across said solar array.

10. The solar tracker of claim **9**, wherein said truss extends generally from a first corner of said solar array to a second opposite corner of said solar array.

11. The solar tracker of claim **8**, wherein the truss is formed from a plurality of truss sections connected to one another to form an elongated triangular shape.

12. The solar tracker of claim **8**, wherein the truss is formed of extruded metal or glass reinforced thermoplastic.

13. The solar tracker of claim **1**, wherein the solar tracker is pivotable between a raised position and a stowed position about the elevation axis.

14. The solar tracker of claim **13**, wherein said stowed position locates the solar array in a generally horizontal position.

15. The solar tracker of claim **14**, wherein said solar array is completely contained within a plane defined thereby.

16. The solar tracker of claim **1**, wherein the first actuator and the second actuator are attached to the connector in a transverse orientation.

17. The solar tracker of claim **1**, wherein said solar array is completely contained within a plane defined thereby.

18. The solar tracker of claim **1**, wherein the frame includes a plurality of supports, each support directly connected to at least one of the other supports.

19. A two-axis solar tracker comprising:
- a solar array for capturing sunlight;
- a frame connected to the solar array;
- a first leg mount;
- a first link arm pivotally connected to the first leg mount to define an elevation axis;
- a pivot frame pivotally connected between the frame and the first link arm to define an azimuthal axis;
- a first actuator connected between the frame and the first link arm for controlling azimuthal movement of the solar array about said azimuthal axis;
- a second leg mount;
- a second link arm pivotally connected to the second leg mount at a first section and pivotally connected to said first link arm at a second section, said second link arm includes a joint intermediate the first section and the second section; and
- a second actuator connected between the first section and the second section for controlling elevational movement of the solar array about said elevation axis.

20. The solar tracker of claim **19**, wherein the second actuator is pivotally mounted to the first section and pivotally mounted to the second section.

21. The solar tracker of claim **19**, wherein the first and second actuators are linear actuators.

22. The solar tracker of claim **19**, wherein the solar array captures sunlight.

23. The solar tracker of claim **19**, wherein the solar array is substantially planar.

24. The solar tracker of claim **19**, further including a third leg mount, wherein the first link arm is pivotally connected to the third leg mount.

25. The solar tracker of claim **24**, further including a fourth leg mount, wherein the second link arm is pivotally connected to the fourth leg mount.

* * * * *

E.6 US 7,779,987 B1

US007799987B1

(12) **United States Patent**
Hines

(10) **Patent No.: US 7,799,987 B1**
(45) **Date of Patent: Sep. 21, 2010**

(54) **SOLAR TRACKER**

(76) Inventor: **Stephen P. Hines**, 1540 Wabasso Way, Glendale, CA (US) 91208

(*) Notice: Subject to any disclaimer, the term of this patent is extended or adjusted under 35 U.S.C. 154(b) by 460 days.

(21) Appl. No.: **11/881,857**

(22) Filed: **Jul. 30, 2007**

(51) **Int. Cl.**
H02N 6/00 (2006.01)
H01L 31/00 (2006.01)
F24J 2/38 (2006.01)

(52) **U.S. Cl.** **136/246**; 136/243; 250/203.4; 126/600

(58) **Field of Classification Search** 136/246, 136/259; 250/203.4; 126/600, 604; 60/641.8–641.15
See application file for complete search history.

(56) **References Cited**

U.S. PATENT DOCUMENTS

4,046,462	A		9/1977	Fletcher et al.
4,055,161	A		10/1977	Jones
4,089,323	A		5/1978	Trihey
4,276,122	A		6/1981	Snyder
4,283,588	A	*	8/1981	Zitzelsberger 136/246
4,307,711	A		12/1981	Doundoulakis
4,315,500	A		2/1982	Gonder
4,360,004	A		11/1982	Testolini
4,467,787	A		8/1984	Ueda
4,762,298	A	*	8/1988	Wood 248/179.1
2003/0038022	A1		2/2003	Rogde
2004/0187907	A1		9/2004	Morgal
2009/0317442	A1	*	12/2009	Banister et al. 424/423

FOREIGN PATENT DOCUMENTS

GB	1552671	A *	9/1979
JP	60205151	A *	10/1985

OTHER PUBLICATIONS

"Portasol Solar Tracker continuously faces the sun", Engadget, Apr. 15, 2007, <http://www.engadget.com/2007/04/15/portasol-solar-tracker-continuously-faces-the-sun/>.*

* cited by examiner

Primary Examiner—Jessica L Ward
Assistant Examiner—Jacky Yuen
(74) *Attorney, Agent, or Firm*—Roy L. Anderson; Wagner, Anderson & Bright, LLP

(57) **ABSTRACT**

A solar tracker has a mounting surface to which a solar device is mounted and means for causing the mounting surface to change its orientation so as to be substantially perpendicular to the sun's rays as the sun travels through a useful arc relative to the solar tracker wherein change of orientation of the mounting surface is caused by bending of the solar tracker attributable. The bending can be caused by mechanical contraction or due to shrinkage caused by loss of water in which case capillary action causes the outer surface material to be saturated and grow when it is not exposed to sunlight. The bendable mounting surface support is an elongated tube held in a nominally vertical position in the absence of sunlight by a vertical support which can be a coiled compression spring, an extruded tube of closed-end structural foam, a vertical floating pole or an air-inflated tube.

17 Claims, 16 Drawing Sheets

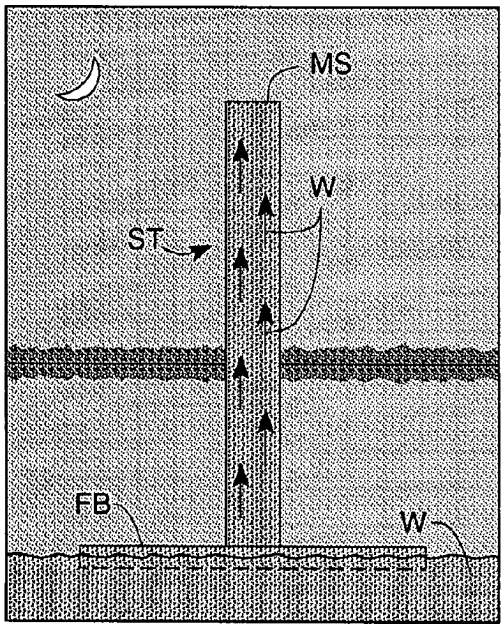

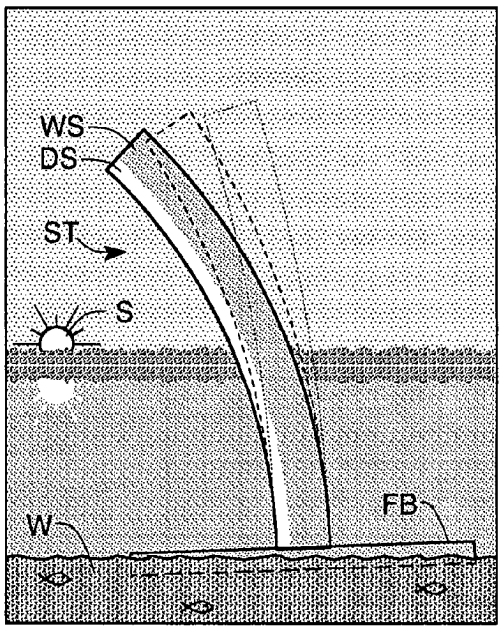

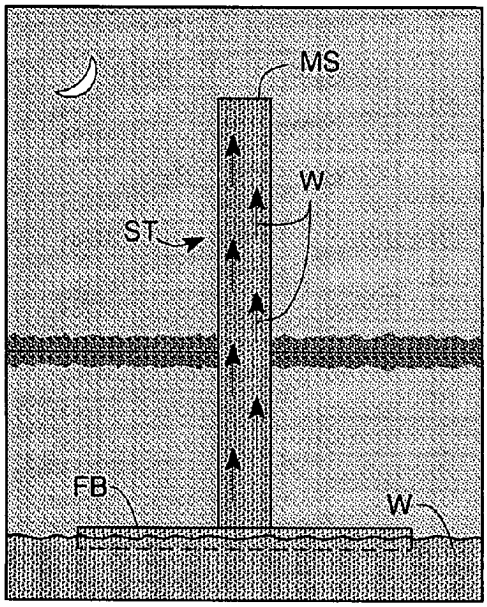

Fig. 1a

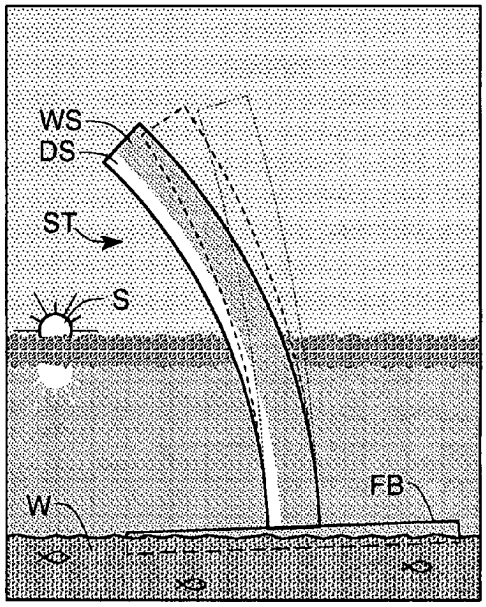

Fig. 1b

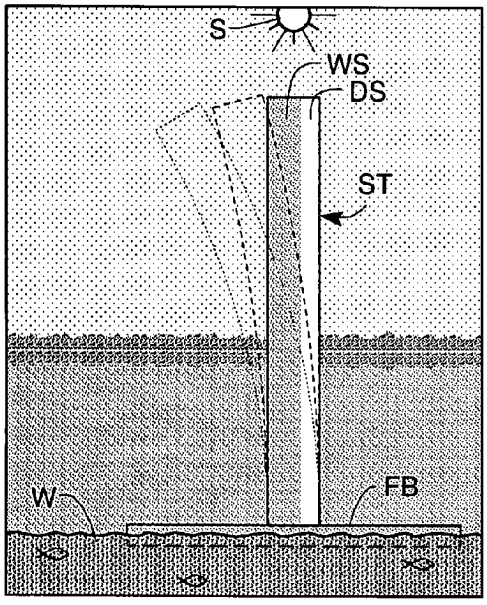

Fig. 1c

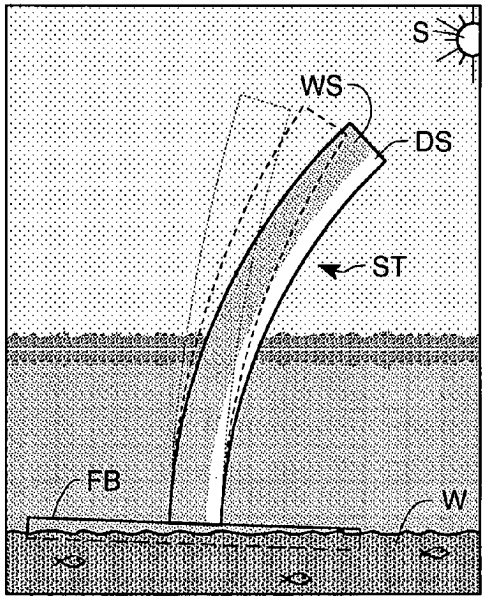

Fig. 1d

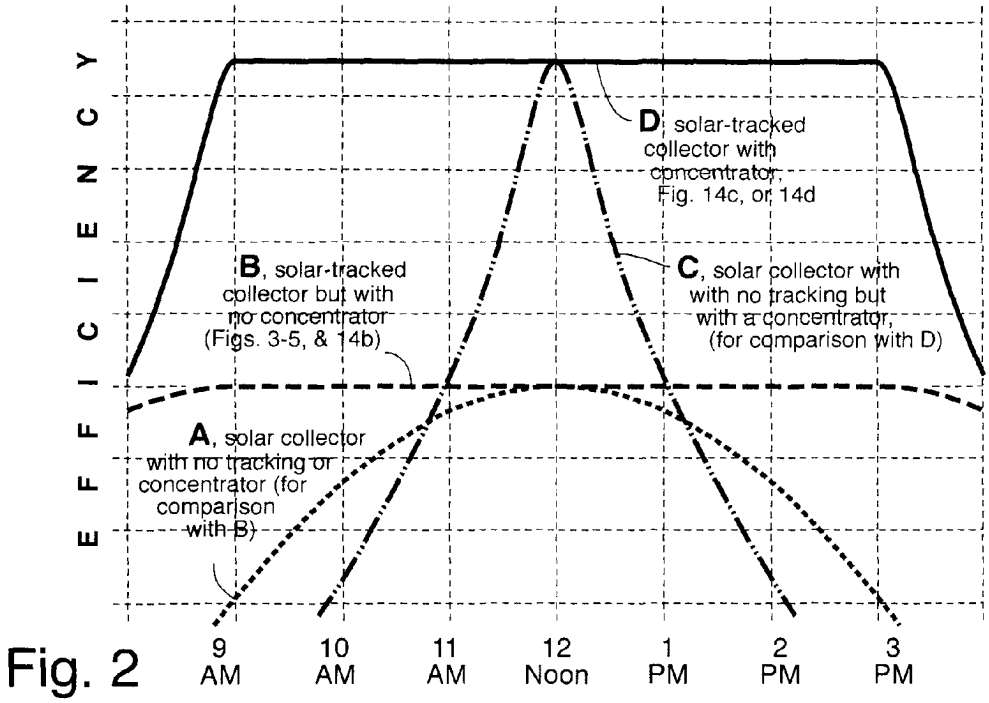
EFFICIENCY
D, solar-tracked collector with concentrator, Fig. 14c, or 14d
B, solar-tracked collector but with no concentrator (Figs. 3-5, & 14b)
C, solar collector with with no tracking but with a concentrator, (for comparison with D)
A, solar collector with no tracking or concentrator (for comparison with B)
9 AM
10 AM
11 AM
12 Noon
1 PM
2 PM
3 PM

Fig. 2

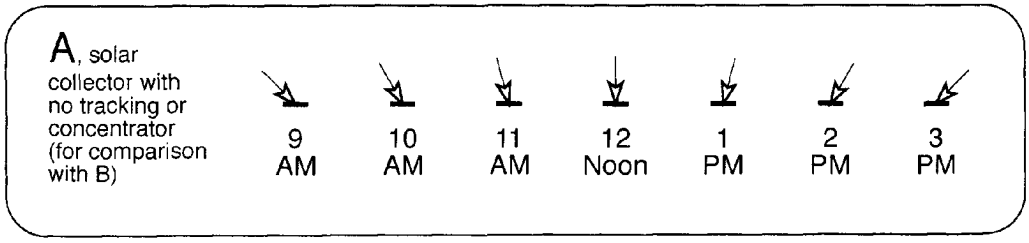
A, solar collector with no tracking or concentrator (for comparison with B)
9 AM
10 AM
11 AM
12 Noon
1 PM
2 PM
3 PM

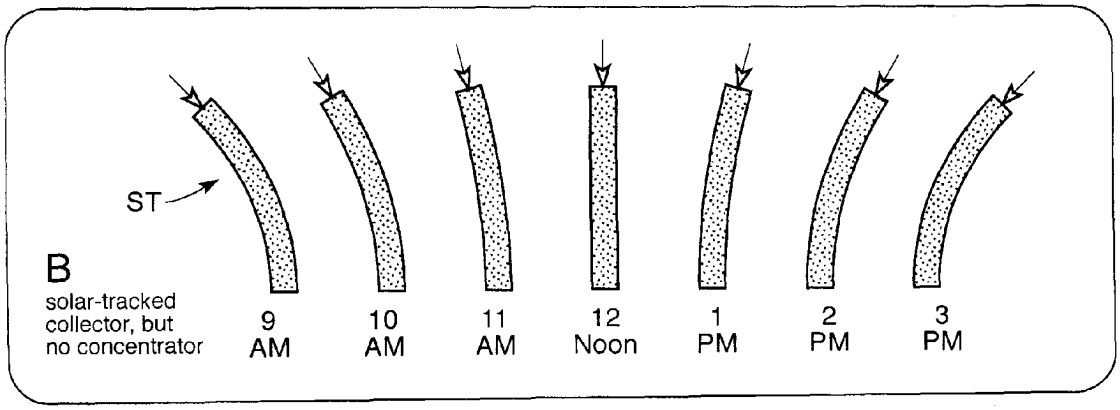
ST
B
solar-tracked collector, but no concentrator
9 AM
10 AM
11 AM
12 Noon
1 PM
2 PM
3 PM

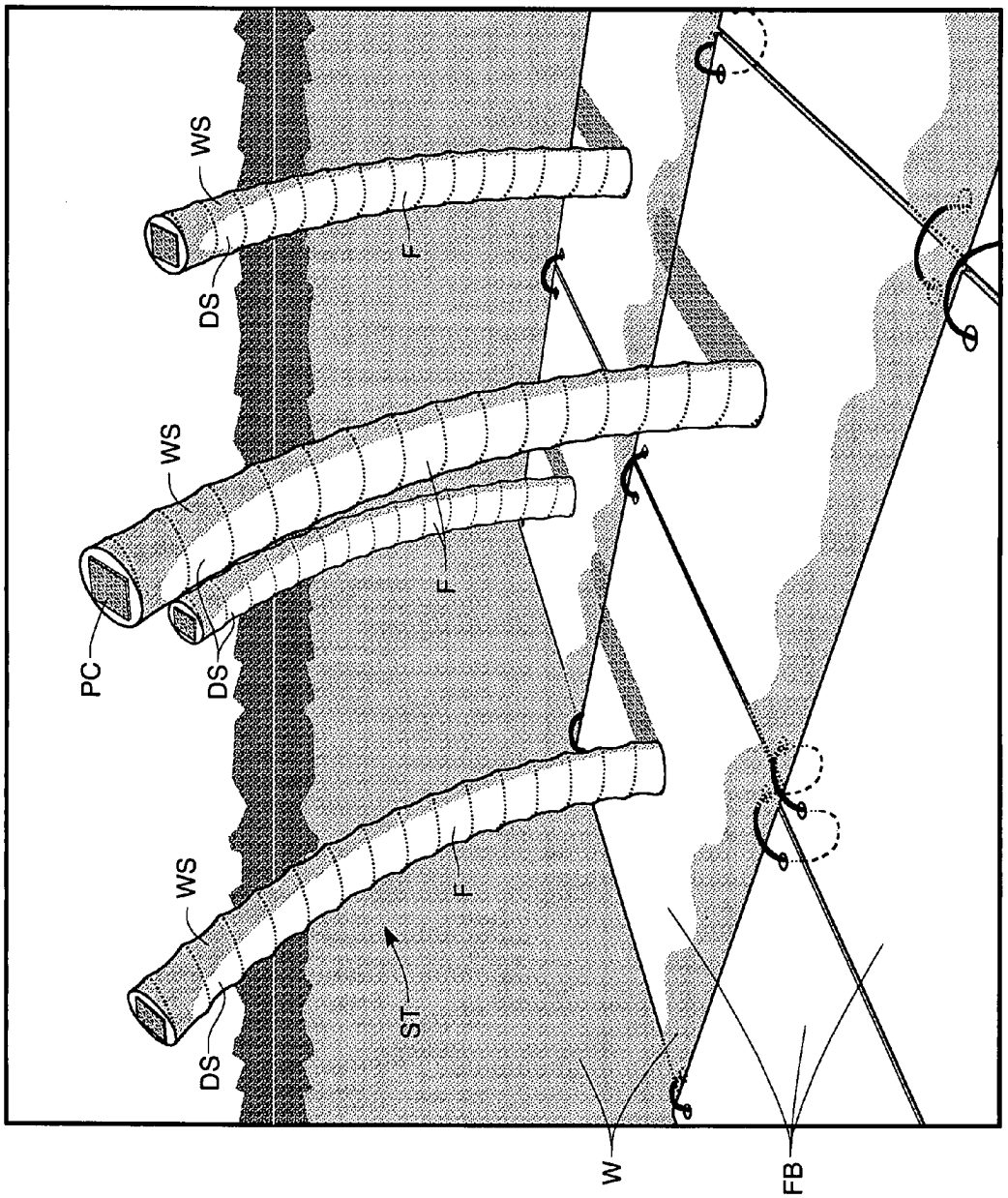

Fig. 3

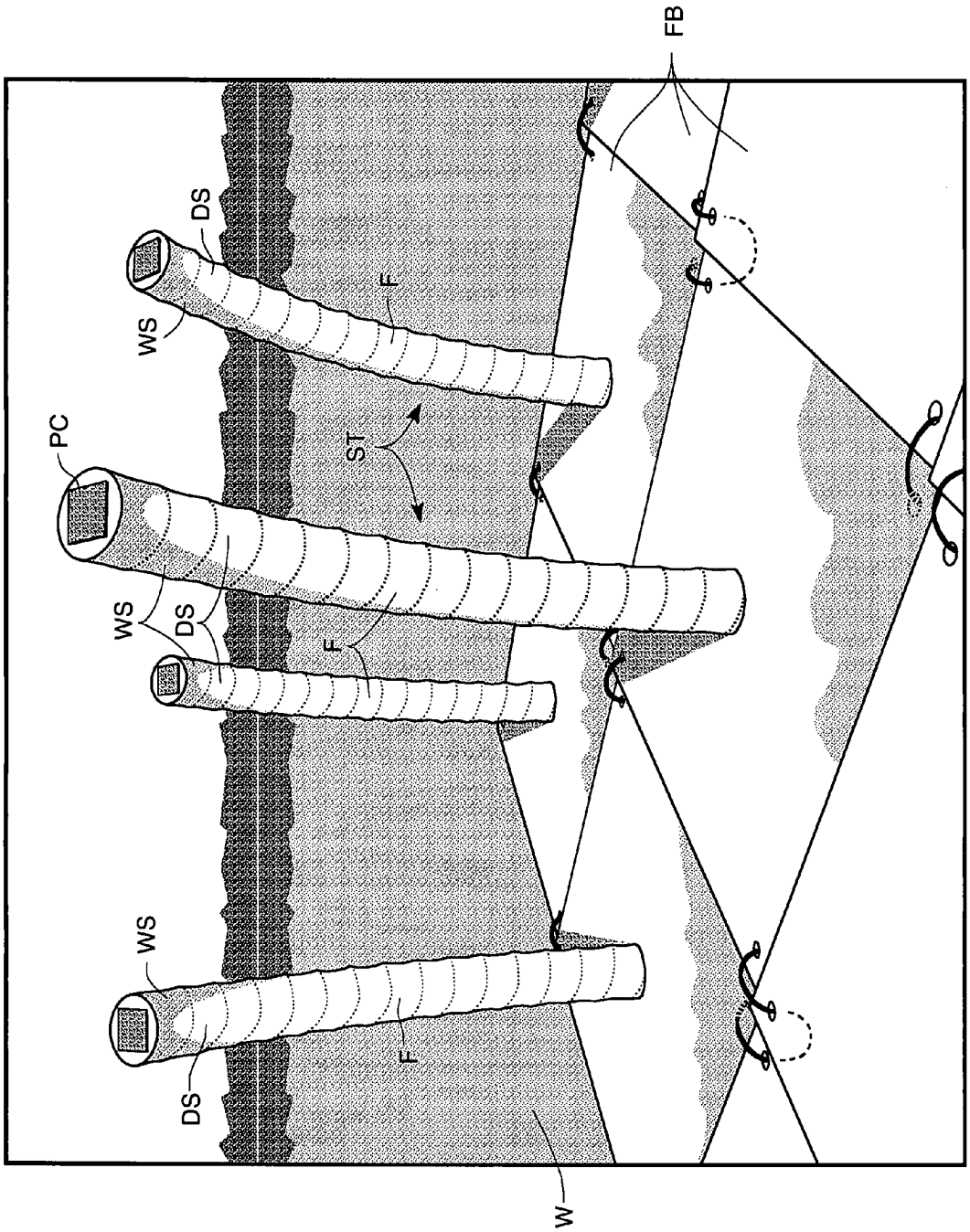

Fig. 4

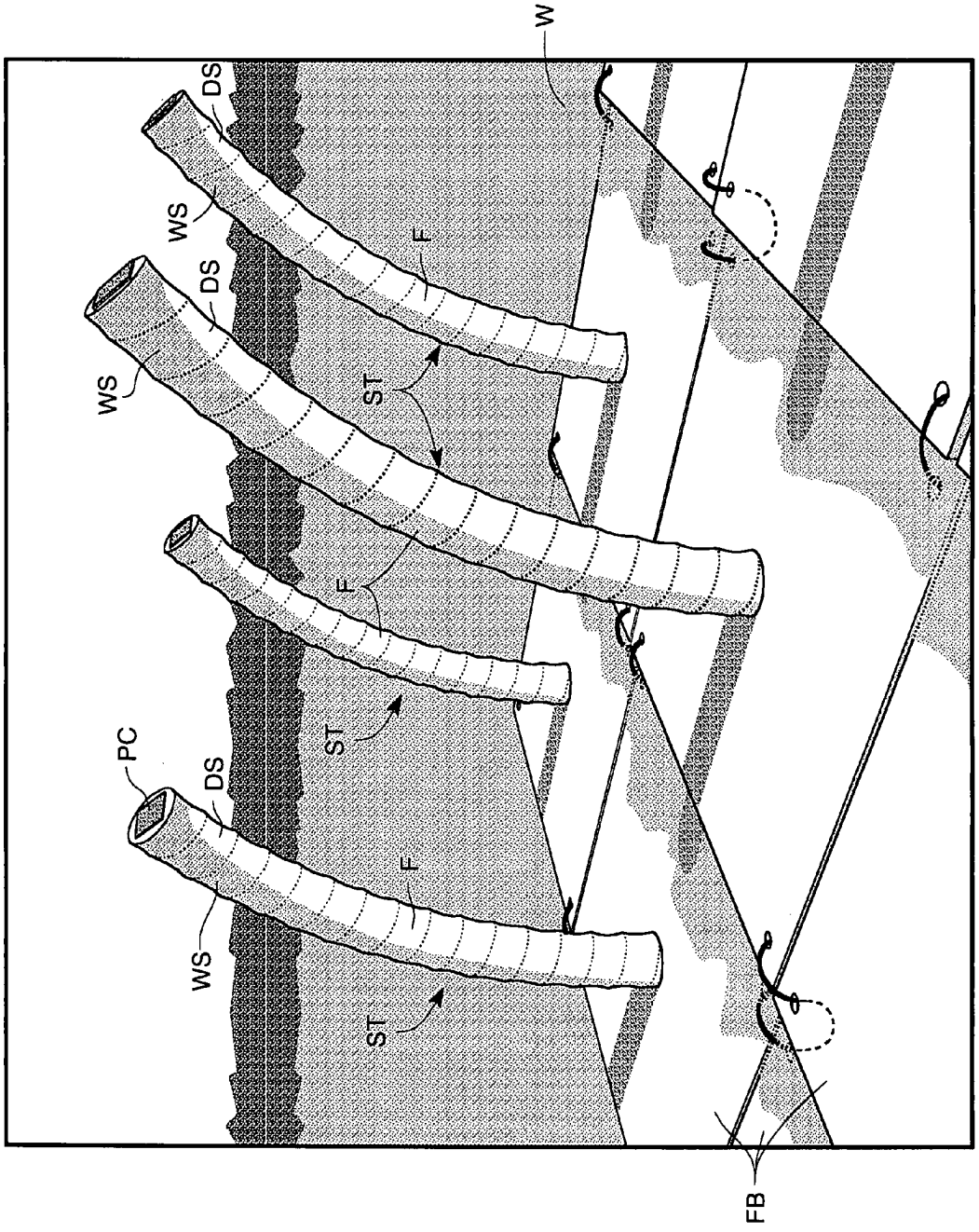

Fig. 5

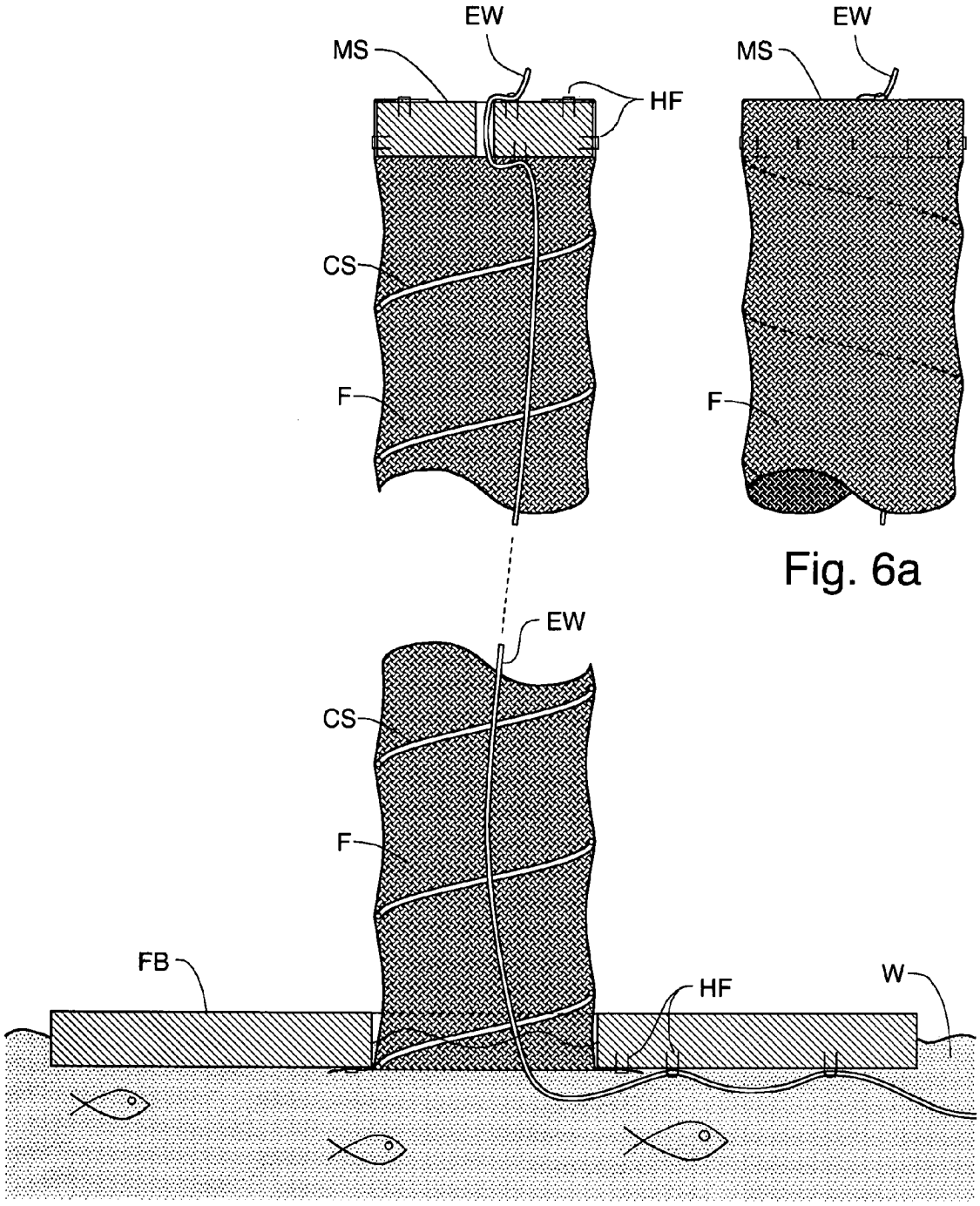

Fig. 6a

Fig. 6

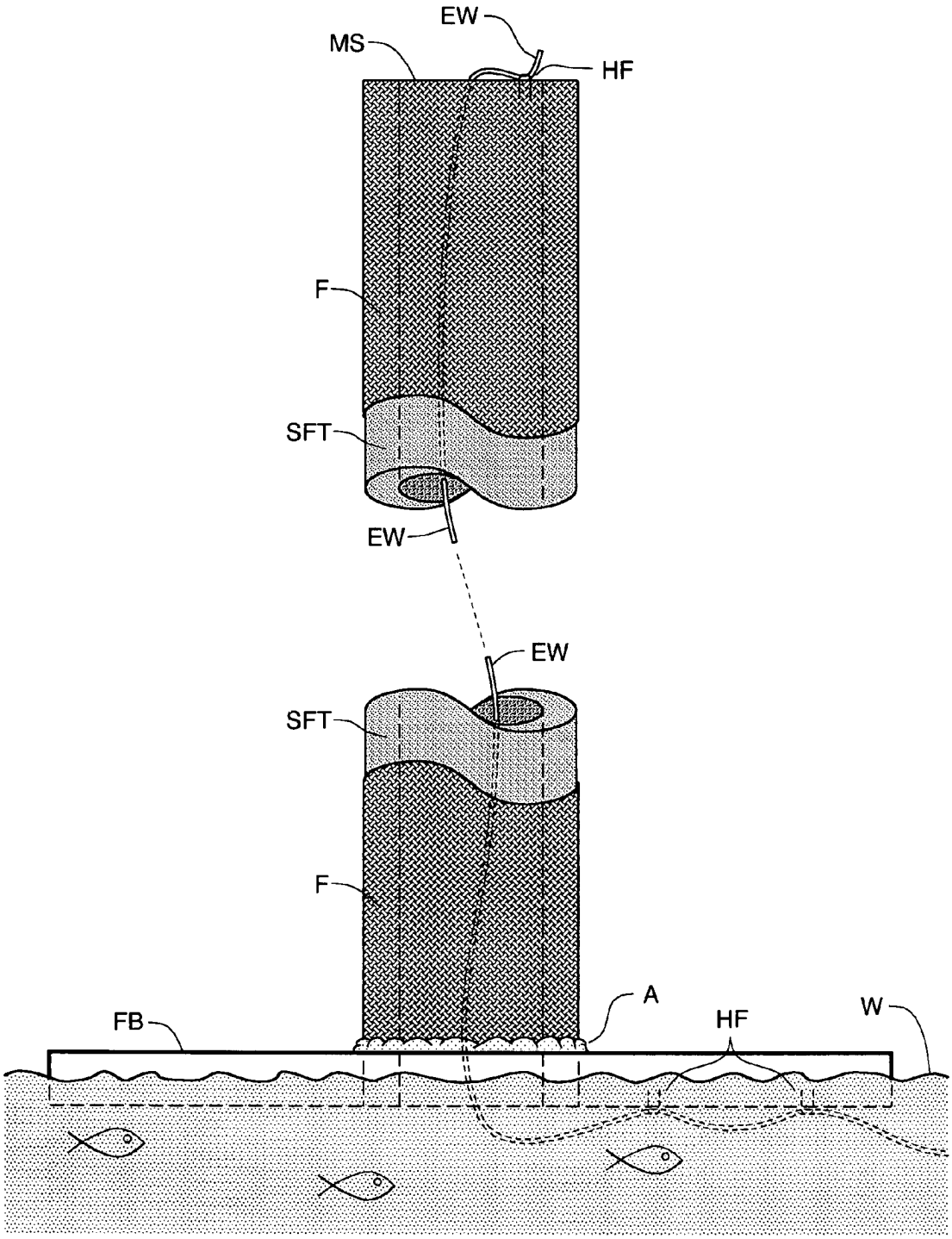

Fig. 7

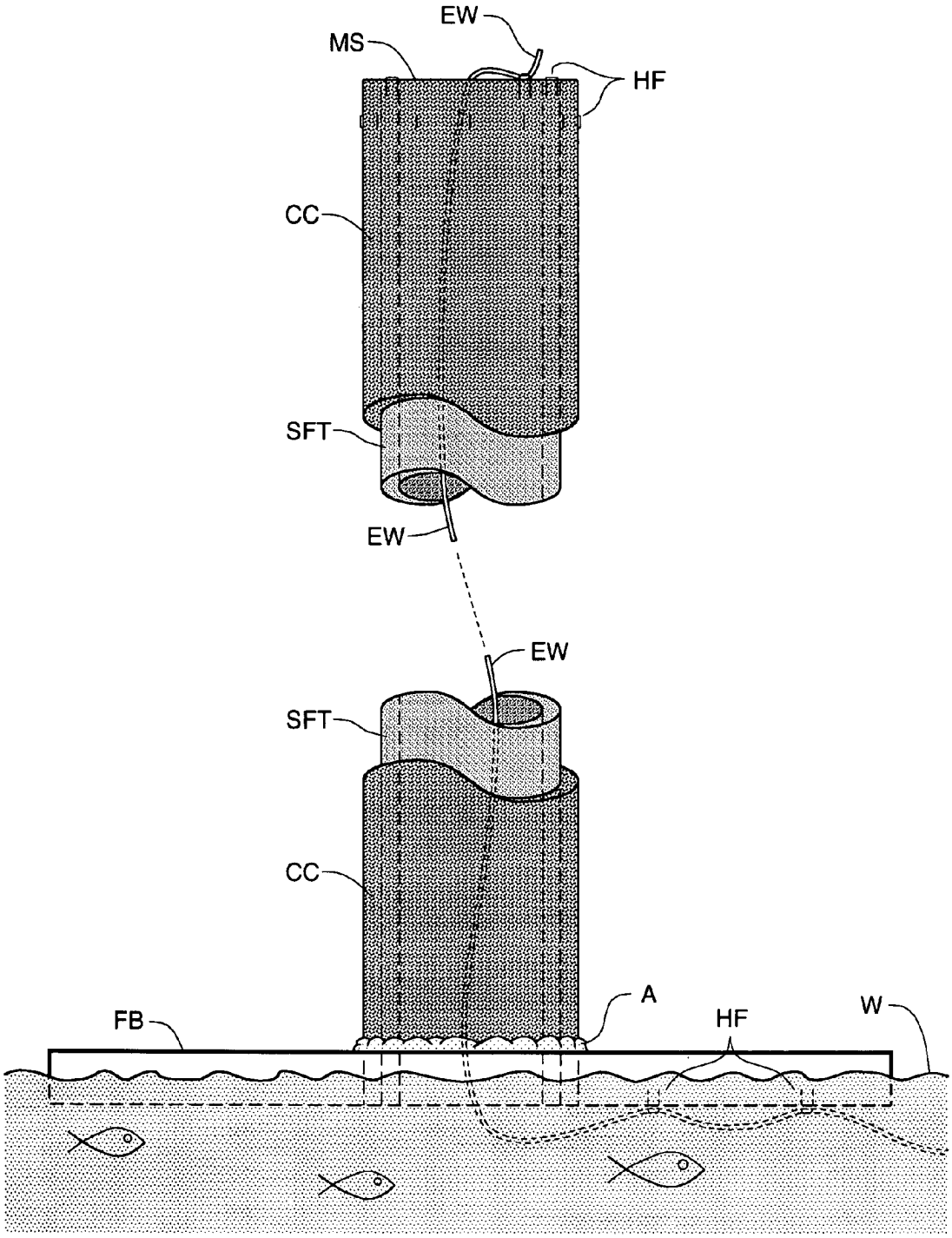

Fig. 8

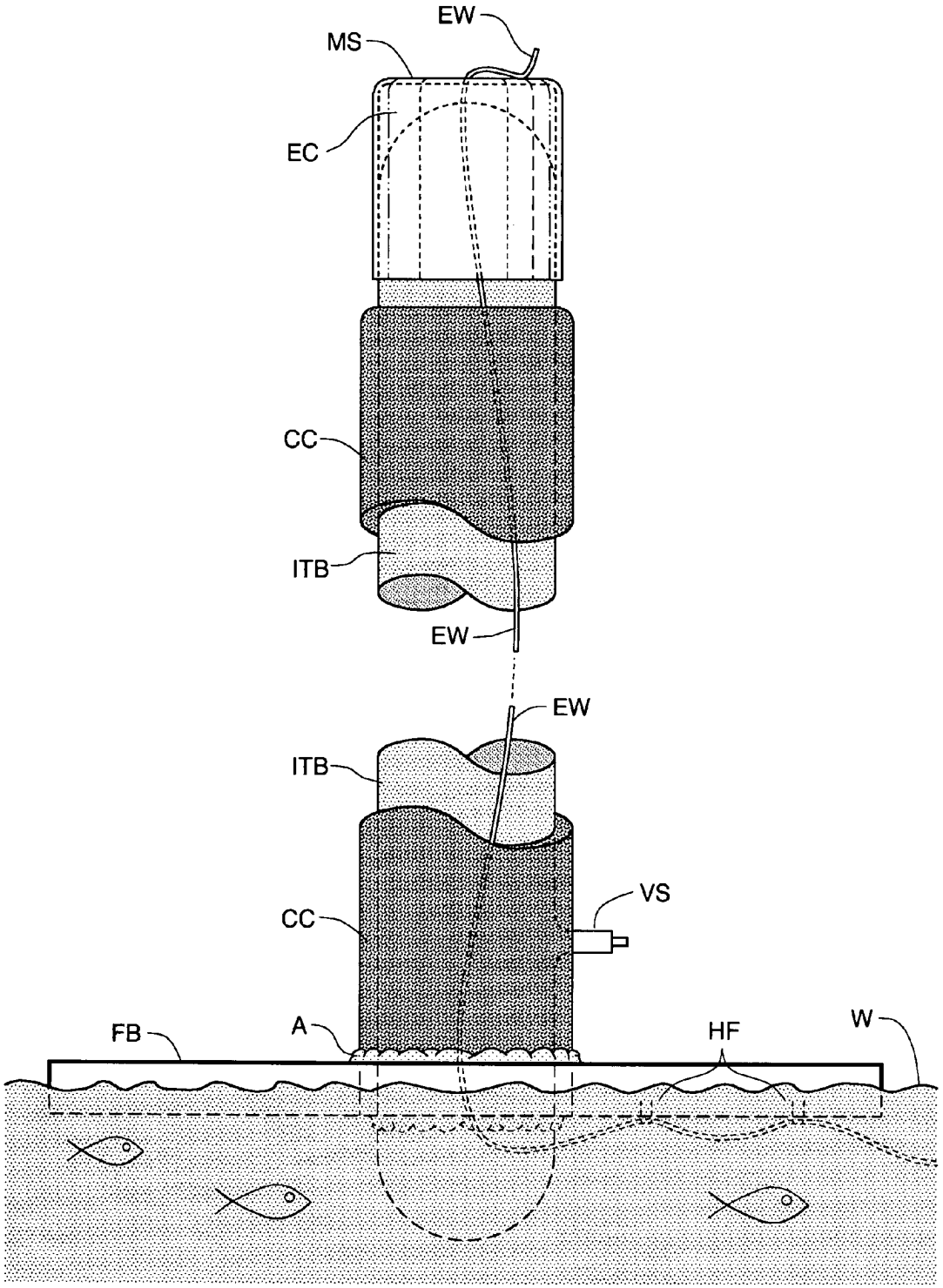

Fig. 9

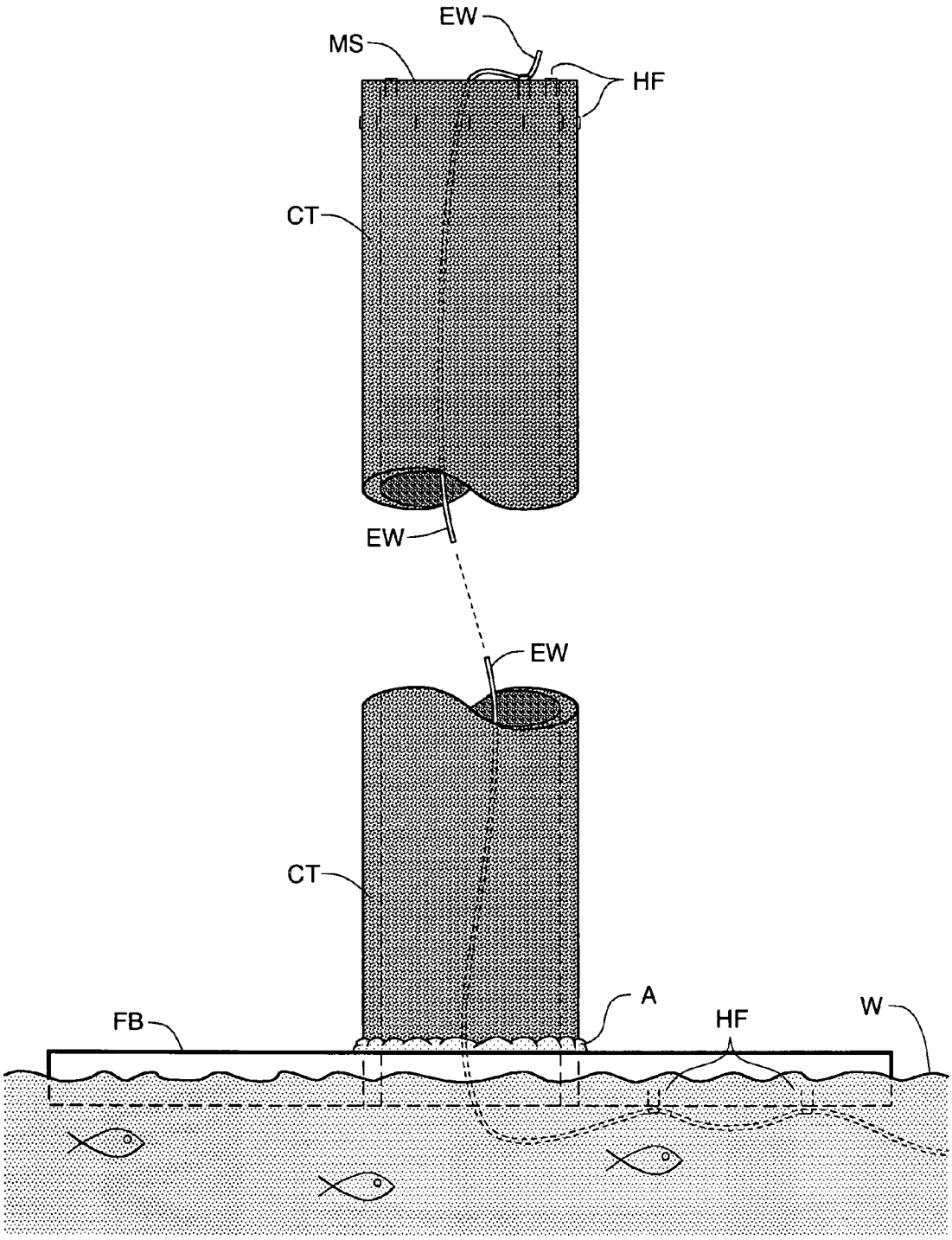

Fig. 10

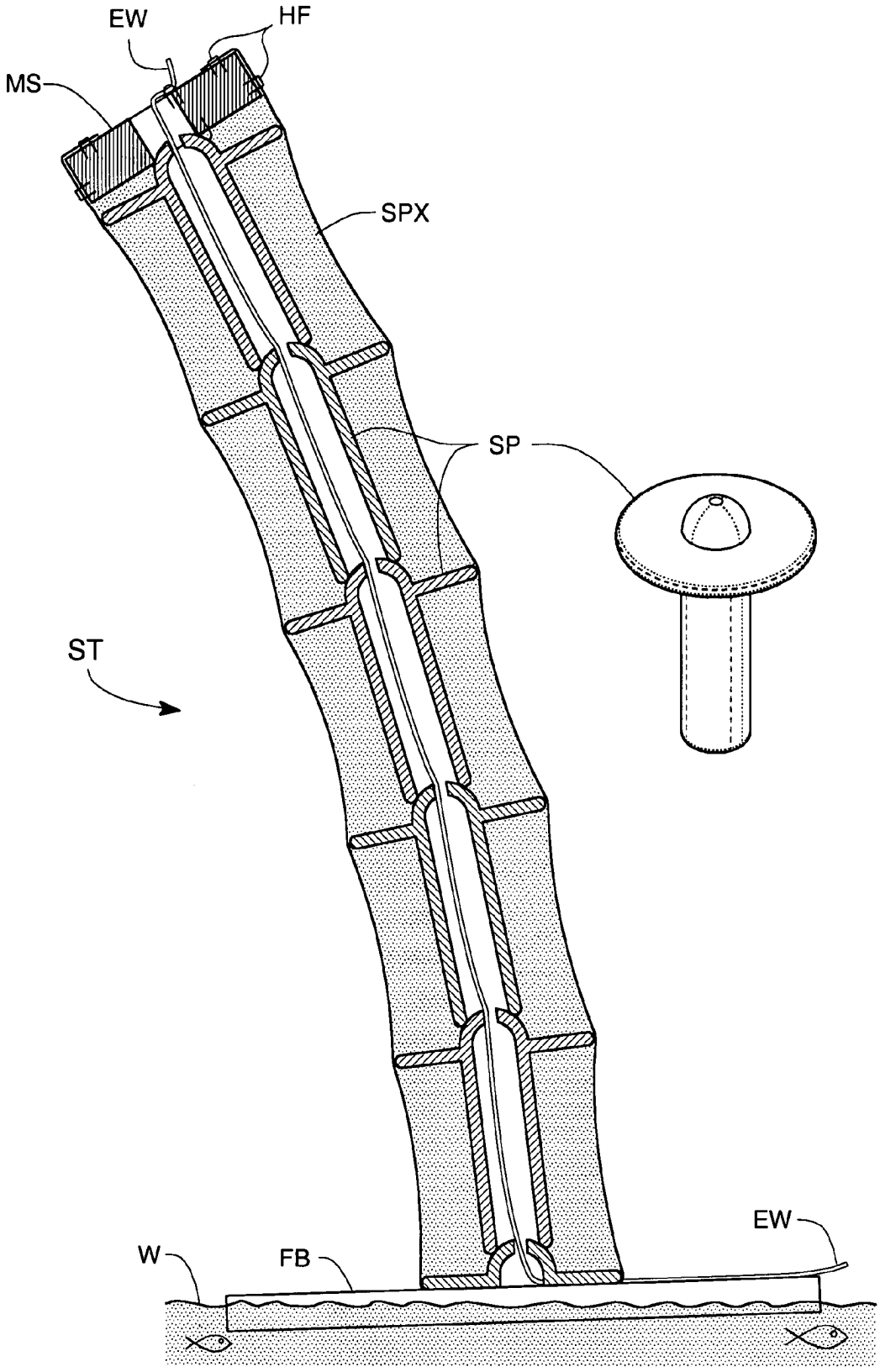

Fig. 11

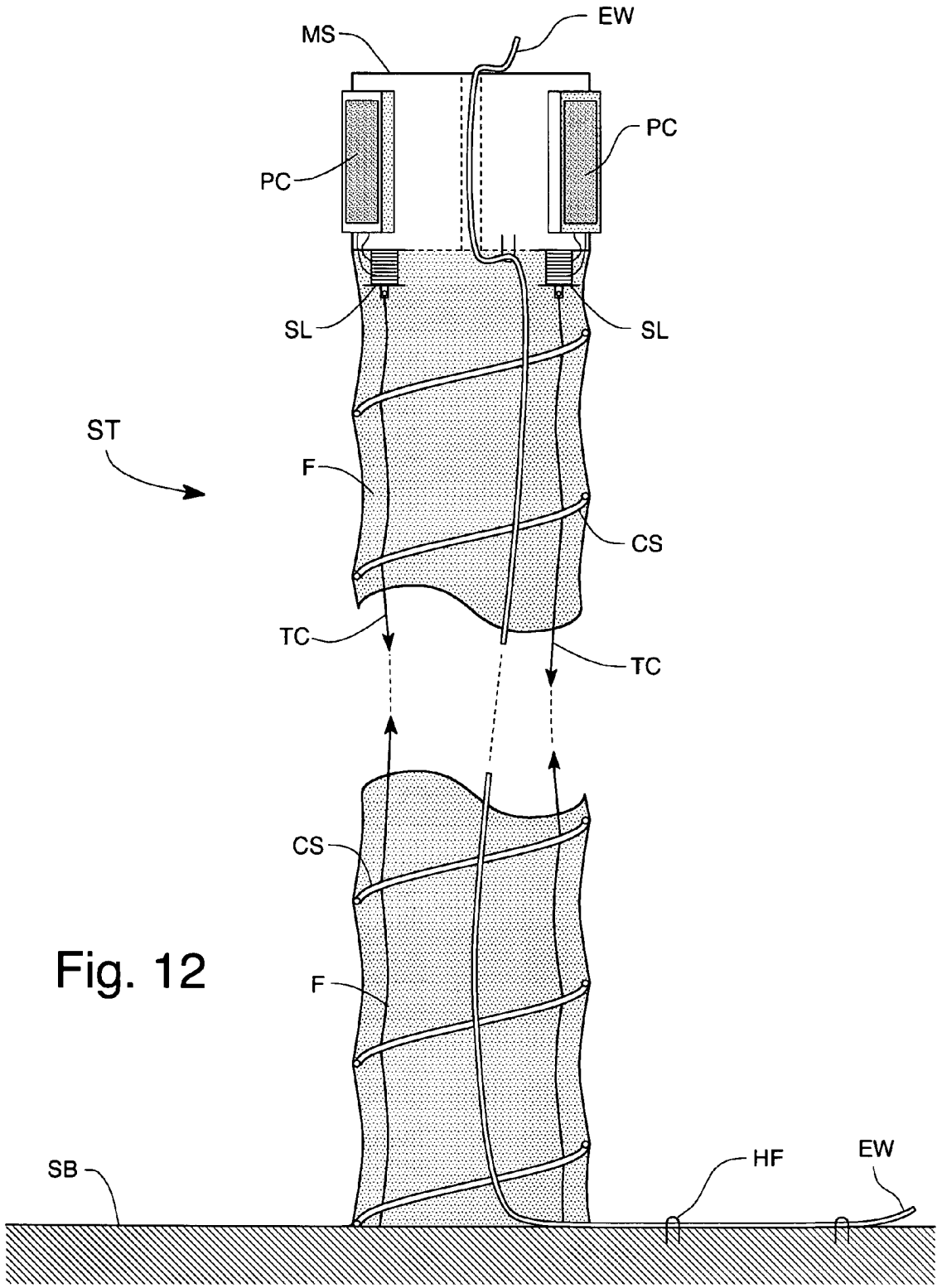

Fig. 12

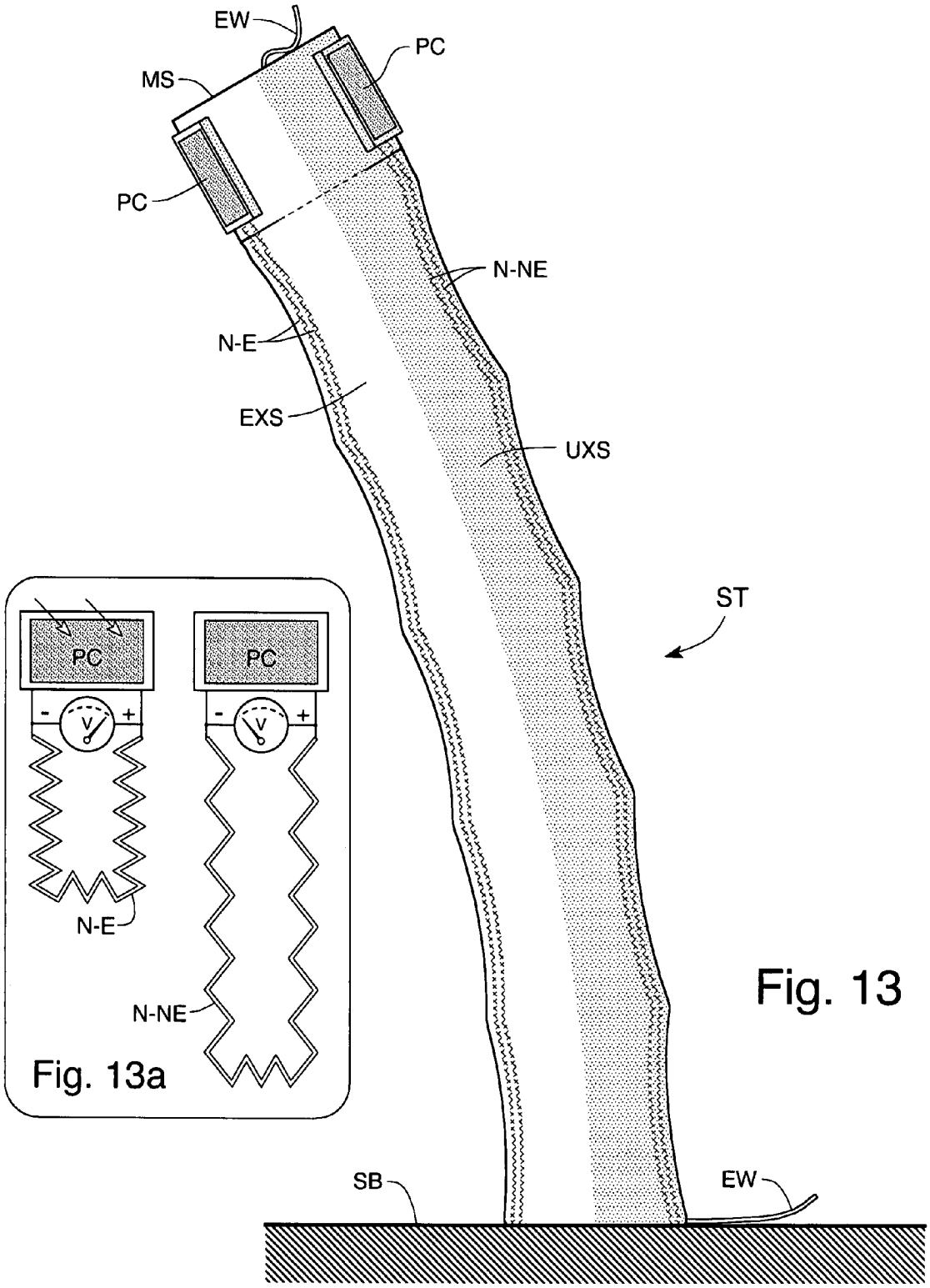

Fig. 13

Fig. 13a

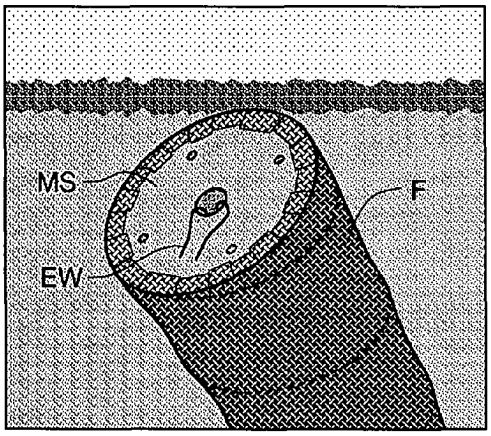

Fig. 14a

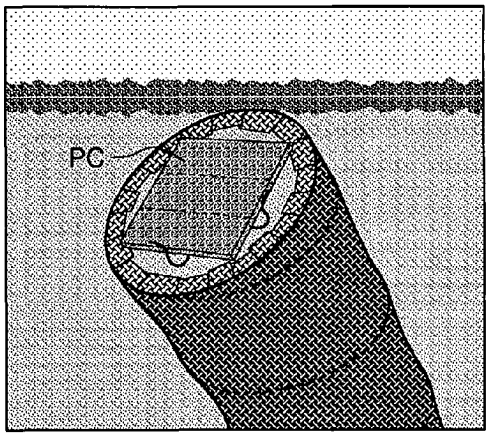

Fig. 14b

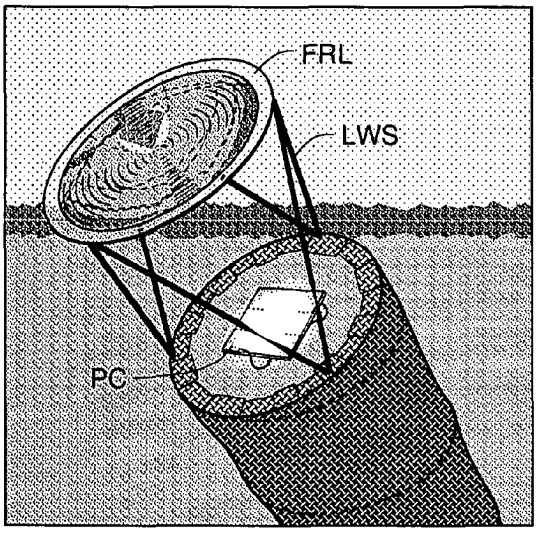

Fig. 14c

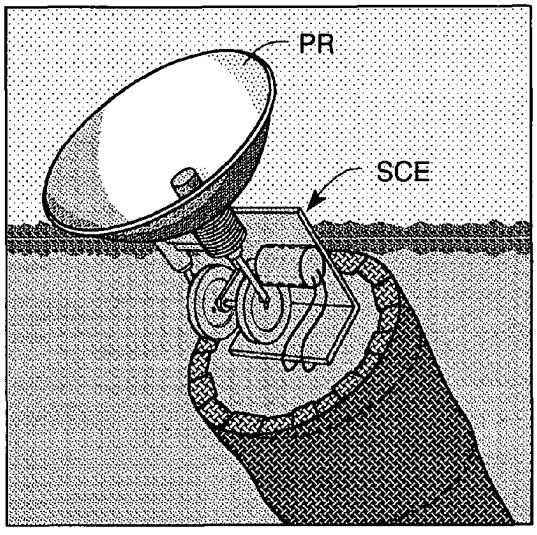

Fig. 14d

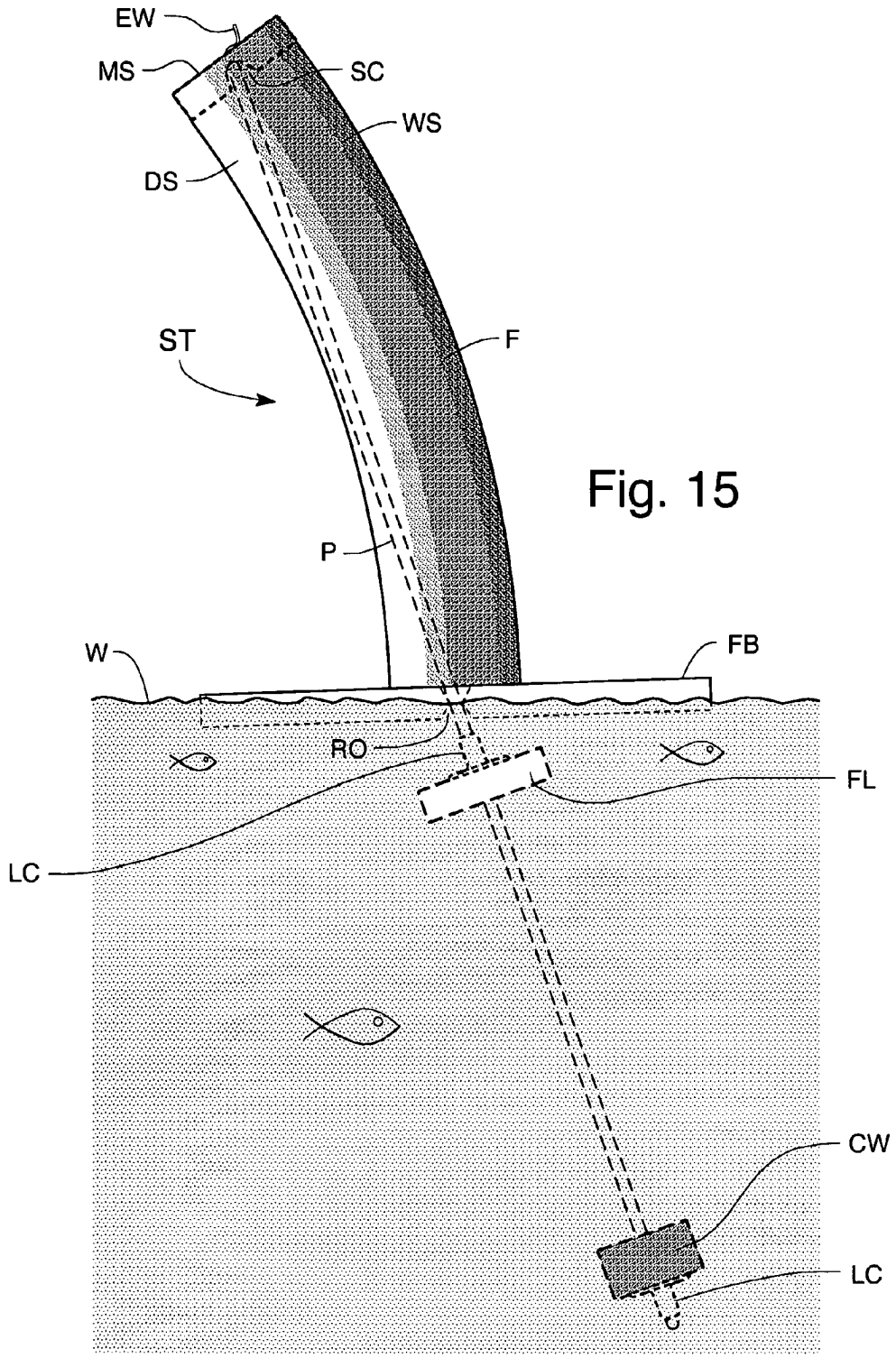

Fig. 15

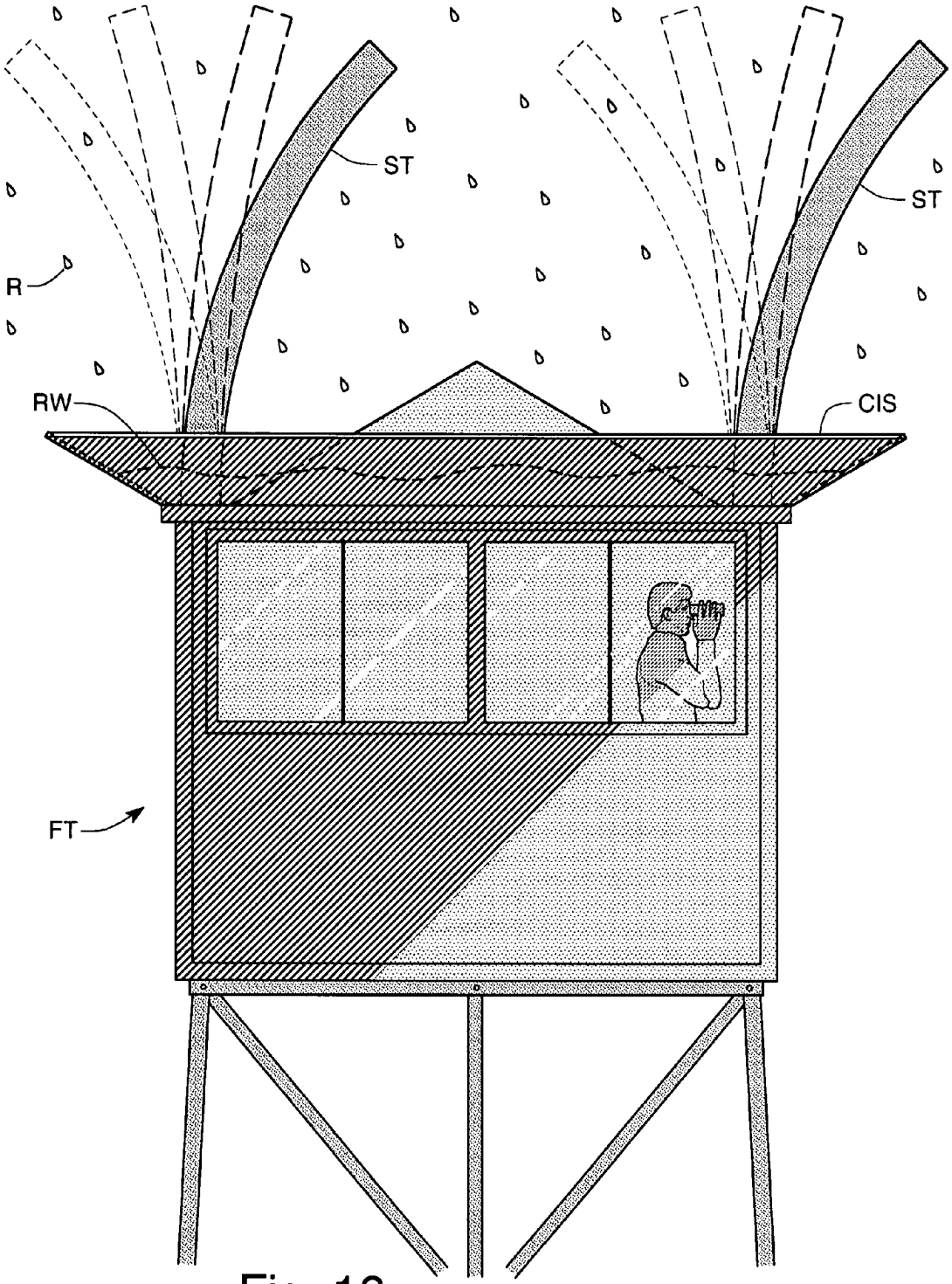

Fig. 16

SOLAR TRACKER

FIELD OF THE INVENTION

The present invention is in the field of platforms for increasing the efficiency of solar devices.

BACKGROUND OF THE INVENTION

Solar devices represent an important source of energy that is clean and non-polluting, especially as compared to energy derived from burning fossil fuels. Also, as concern continues to grow over greenhouse gasses and the topic of global warming gets more and more attention in the press and throughout the world, solar energy is a very timely subject.

The trouble with solar energy is efficiency and cost.

Although there has been enormous interest in solar energy, and vast amounts of money have been spent on its research and development, solar energy still does not represent as large a proportion of the world's energy as many would hope for, and continue to hope for.

Accordingly, anything that can increase the efficiency of solar energy, without prohibitively increasing its cost, will be welcome indeed. Thus, there exists a very real and long-felt need for ways to increase the efficiency of solar devices.

Moreover, even if solar devices can work efficiently and in a cost-effective manner, there are many different types of applications in which they might be used, if in fact suitable devices were available. Accordingly, another problem addressed by the present invention is increasing the efficiency of solar devices used in remote locations with relatively modest energy requirements, as well as for extremely low cost applications.

SUMMARY OF THE INVENTION

The present invention is generally directed to a solar tracker with a mounting surface to which a solar device is mounted and means for causing the mounting surface to change its orientation so as to be substantially perpendicular to the sun's rays as, the sun travels through a useful arc relative to the solar tracker wherein change of orientation of the mounting surface is caused by bending of the solar tracker.

In a first, separate group of aspects of the present invention, a bendable mounting surface support is provided with an outer surface material that shrinks (due to mechanical contraction or due to shrinkage caused by loss of water) when exposed to sunlight relative to a shaded side of the outer surface material not exposed to sunlight to keep the mounting surface substantially perpendicular to the direction of sunlight as the sun travels through a useful arc relative to the solar tracker.

In another, separate group of aspects of the present invention, the solar tracker is mounted to a platform that floats or sits atop a water source or is in contact with a water reservoir and water is in constant contact with the outer surface material of the bendable mounting surface support so that capillary action causes the outer surface material to be saturated and grow when it is not exposed to sunlight.

In still another, separate group of aspects of the present invention, the solar device (which may be a photovoltaic cell or a Stirling cycle engine coupled with a Fresnel lens or light concentrator) does not extend beyond the mounting surface relative to the bendable mounting surface support.

In yet another, separate group of aspects of the present invention, the bendable mounting surface support is an elongated tube held in a nominally vertical position in the absence of sunlight by a vertical support. The vertical support may be a coiled compression spring, an extruded tube of closed-cell structural foam, a vertical floating pole or an air-inflated tube (which may be maintained inflated by use of electricity generated by the solar device).

In a further, separate group of aspects of the present invention, a method for improving the efficiency of energy collection from a solar device is provided in which a solar device is mounted on a mounting surface of a solar tracker having a bendable mounting surface support with an outer surface material that expands when wet and contracts when dry and the outer surface material is placed in contact with a reservoir of water and then the outer surface material is exposed to the sun so the solar tracker bends in the direction of the sun as the sun travels through a useful arc relative to the solar tracker.

Accordingly, it is a primary object of the present invention to provide a solar tracker that improves the efficiency of energy collection.

This and further objects and advantages will be apparent to those skilled in the art in connection with the drawings and the detailed description of the preferred embodiment set forth below.

BRIEF DESCRIPTION OF THE DRAWINGS

FIGS. **1***a*-**1***d* generally illustrate a solar tracker according to the present invention showing its positions when there is no sun (FIG. **1***a*), at sunrise (FIG. **1***b*), at high noon (FIG. **1***c*) and in the afternoon (FIG. **1***d*).

FIG. **2** is a graph showing the efficiency of a solar collector which is stationary versus on a solar tracker.

FIGS. **3**-**5** illustrate a cluster of solar trackers following the sun during the day.

FIG. **6** illustrates a cross section of a solar tracker according to the present invention that uses a compression spring for support whereas FIG. **6***a* illustrates the exterior of the same solar tracker.

FIGS. **7**-**12** illustrate solar trackers according to the present invention with support mechanisms differing from that of FIG. **6**.

FIG. **13** illustrates a solar tracker according to the present invention that uses Nitinol wire as the shrinkage mechanism while FIG. **13***a* shows the Nitinol wire in electrified and non-electrified states.

FIGS. **14***a*-*d* illustrates alternative solar devices capable of being used with a solar tracker according to the present invention.

FIG. **15** illustrates a solar tracker according to the present invention that is mounted on a floating platform and where the top of the tube is supported by a separate float mechanism.

FIG. **16** illustrates a solar tracker according to the present invention designed into the roof of a forest tower.

DETAILED DESCRIPTION OF THE PRESENT INVENTION

The present invention provides a platform on which solar devices can be mounted to improve their performance in the presence of varying angles of sunlight.

The present invention is not directed to a solar collection device per se, nor to an energy conversion device, but to a platform on which solar devices can be mounted to make them more efficient. See FIGS. **14***a*-*d*. A benefit of the present invention is that it is passive, low tech, low cost and virtually maintenance free, making it ideal for third world countries and remote locations like oil drilling rigs and meteorological stations.

The present invention will now be discussed in connection with preferred embodiments illustrated in FIGS. **1-16**.

In the Figures and the following more detailed description, letter designations indicate various features relating to the invention, with like letter designations referring to like features throughout both the drawings and the description. Although the Figures are described in greater detail below, the following is a glossary of the elements identified in the Figures.

A adhesive (see FIGS. **7-10**)
CC open-cell cellulose covering (see FIGS. **8**, **9**)
CIS cistern (see FIG. **16**)
CS compression spring (see FIG. **6**)
CT open-cell cellulose sponge tube (see FIG. **10**)
CW counter weight (see FIG. **15**)
DS dry side (see FIGS. **1***b-d*, **3-5**, **15**)
EC end cap (see FIG. **9**)
EW electrical wire (see FIGS. **6-12**, **13**, **14***a*, **15**)
EXS exposed side (see FIG. **13**)
F fabric (see FIGS. **3-7**, **12**, **14***a*, **15**)
FB floating base (see FIGS. **1***a-d*, **3-11**, **15**)
FL float (see FIG. **15**)
FRL Fresnel lens (see FIG. **14***c*)
FT forest tower (see FIG. **16**)
HF hardware fasteners (see FIGS. **6-12**)
ITB inflated tubular balloon (see FIG. **9**)
LC locking collar (see FIG. **15**)
LWS light-weight struts (see FIG. **14***c*)
MS mounting surface (see FIGS. **1***a*, **6-14***a*, **15**)
N-E Nitinol electrified (see FIG. **13**, **13***a*)
N-NE Nitinol non-electrified (see FIG. **13**, **13***a*)
P pole (see FIG. **15**)
PC photovoltaic cell (see FIGS. **3-6**, **12**, **13**, **14***b-c*)
PR parabolic reflector (see FIG. **14***d*)
R rain (see FIG. **16**)
RO restricted opening (see FIG. **15**)
RW rain water (see FIG. **16**)
S sun (see FIGS. **1***b-d*)
SB stationary base (see FIGS. **12-13**)
SC socket cup (see FIG. **15**)
SCE Stirling cycle engine (see FIG. **14***d*)
SL solenoid (see FIG. **12**)
SFT structural foam tube (see FIGS. **7-8**)
SP spacer (see FIG. **11**)
SPX spandex (see FIG. **11**)
ST solar tracker (see FIGS. **1***a-d*, **2-5**, **11-13**, **15-16**)
TC tension cable (see FIG. **12**)
UXS unexposed surface (see FIG. **13**)
VS valve stem (see FIG. **9**)
W water (see FIGS. **1***a-d*, **3-11**, **15**)
WS wet side (see FIGS. **1***b-d*, **3-5**)

The present invention can use a variety of solar devices. Some examples of solar devices suitable for use with the present invention are photovoltaic cells PC (FIG. **14***b*) and a Stirling-cycle engine SCE (FIG. **14***d*). Either of these devices can be enhanced by a concentrating device like a Fresnel lens FRL (FIG. **14***c*) or a parabolic reflector PR (FIG. **14***d*).

The solar device that is used with a solar tracker ST is mounted on a mounting surface MS at the top of the solar tracker.

FIG. **14***a* shows the bare mounting surface MS with electrical wires EW that are available to be attached to a photovoltaic cell PC solar device.

FIG. **14***b* shows a photovoltaic cell PC mounted to the mounting surface MS at the top of the tube.

FIG. **14***c* shows a photovoltaic cell which is smaller and less expensive than in FIG. **14***b*, which is mounted to the mounting surface and sunlight is concentrated by a Fresnel lens FRL, supported by light-weight struts LWS. Without solar tracking, the smaller photovoltaic cell would produce little or no electrical energy. Further, with solar tracking this smaller photovoltaic cell produces much more energy than the larger cell without Fresnel lens.

FIG. **14***d* shows a parabolic reflector mounted to a Stirling cycle engine SCE and electrical generator mounted to the top of the tube. The Stirling cycle engine SCE works only when sunlight is focused on the tip and therefore the angular alignment with the sun is critical for its operation. A Stirling cycle engine would not work if on a stationary platform except in the rare cases that the sun aligned with the solar concentrator such as a parabolic reflector PR or lens (such as Fresnel lens FRL) for only a few hours a year.

The mounting surface can be supported vertically (relative to the ground) through any number of means so long as the support means has the flexibility to bend within a useful range to follow the sun during the peak hours from approximately 9 AM to 3 PM (6 hrs.×15°/hr.=90° bending (±45°)).

Generally speaking, the support means will have an elongated tube and a mechanism for causing movement of the tube in response to direct sunlight. The elongated tube of solar tracker ST is, in an especially preferred embodiment, cylindrical; however, the tube need not be of an exact cylindrical shape and need not necessarily be of uniform cross-section. For example, a tube with a nominally cylindrical shape or a variation from a cylindrical shape (such as a cylinder with serrated, scalloped, fluted or other longitudinal ridges) might also be used. What is important is that the tube be shaped so as to allow it to perform the function of providing support while still allowing the solar tracker to bend toward the path of the sun as the sun travels in an arc relative to the solar tracker over a useful period of time for collecting sunlight. Also, it is especially preferred that any solar collector mounted to the top mounting surface MS should be no larger than the diameter of the solar tracker tube so as to not shadow the solar tracker ST from the sun and interfere with its function.

A number of examples of means for keeping the tube substantially perpendicular to the sun's rays are set forth in the FIGS. **6-10** in which an outer surface of the tube needs to be made of, covered with, dipped in or coated with a material which expands when wet and contracts when dry. The mechanism for this action is that when water comes in contact with the tube covering, capillary action causes the material to become saturated and engorged with water molecules, pushing apart the material to make room for the water. This makes the wet side of the tube larger and longer. When the surface material dries out, as in the presence of sunlight, the material collapses or shrinks, pulling that side of the tube. Both the pushing on the wet side, and the collapsing on the dry side, bias the tube to bend in a curve toward the dry side. With the appropriate length-to-diameter ratio, the top surface, used for mounting solar devices, will angle over to be perpendicular to the sun's rays. FIGS. **1-5**, and **15-16**. The bending of the solar tracker ST stops automatically when the dry side DS falls into the shadow of the mounting surface MS, and when the wet side WS is exposed to the sunlight, thus providing a nulling to the bending that self-regulates the positioning of the mounting surface MS.

A first mechanism for vertically supporting a tube used in a solar tracker ST is to use a coiled compression spring CS inside a fabric covering F.

FIG. **6** illustrates an embodiment of the first mechanism. Compression spring CS is preferably made of a material that will resist rust and corrosion such as stainless steel, titanium

or fiberglass. The bottom of the fabric F is exposed to water W. FIG. **6***a* shows the exterior of the same top portion of the tube.

A second mechanism for vertically supporting a tube used in a solar tracker ST is to use an extruded closed-cell structural foam tube SFT (example: polyethylene plastic) that has enough inherent stiffness to hold itself vertically, but with enough flexibility to be bent by the shrinking of the drying outer covering. This material is currently used for boat bumpers.

FIGS. **7** and **8** illustrate embodiments of the second mechanism. The tube should have a hole through the center for an electrical wire to pass. (See FIGS. **6-10**, **14***a*.) FIGS. **7** and **8** also show an alternative mechanism for wetting fabric F (as compared to FIG. **6**) wherein water is supplied to fabric F due to sloshing of water over floating base FB.

A third mechanism for vertically supporting a tube used in a solar tracker ST is to use a vertical floating pole P that comes up through a loose hole, restricted opening RO, in a base.

FIG. **15** illustrates an embodiment of the third mechanism. The top of the pole P pushes upward on the socket cup SC on the underside of the top mounting surface MS, and is itself weighted at the bottom, under water, by counterweight CW to keep the bottom down (and the top up). The pole P fits loosely through a restricted opening RO in the floating base FB so that the solar tracker ST can bend through a useful range during daylight hours. The buoyancy of the float material FL, attached to the pole P underwater, is sufficient to overcome the total weight of (1) the pole P, (2) the counterweight at the bottom CW, (3) the top mounting surface MS, (4), the solar tracker fabric when wet, and (5) the solar collector device to be mounted to the top Mounting Surface MS, so that the mounting surface is raised in all conditions.

A fourth mechanism for vertically supporting a tube used in a solar tracker ST is to use an air-inflated tube.

FIG. **9** illustrates an embodiment of the fourth mechanism. Inflated tubular balloon ITB is coated with open-cell cellulose sponge covering CC, topped by end cap EC and mounting surface MS. In this case, to prevent puncturing the tubular balloon, the electrical wire EW is positioned between the inflated balloon and the walls of the end cap EC and inside the open-cell cellulose covering CC. Valve stem VS is used to inflate the balloon to keep it stiff enough to support itself and the chosen solar collector mounted on the mounting surface. The tube is mounted at floating base FB. The air can be sealed in the tube, FIG. **9**, like air in a balloon or car tire, or can be inflated continuously using a fan which draws energy from one or more dedicated photovoltaic cells PC. If the tube is open at the bottom, air can be supplied to the inside of the tube with a bubbler from below (not shown), or a fan (not shown) can blow air into the tube powered by one or more dedicated photovoltaic cells PC or a portion of the energy from photovoltaic cells PC mounted on the Mounting Surface MS can be bled off to provide power to the fan, the balance of the energy being routed by electrical wire EW to where it's needed, typically onshore to a home or business.

A fifth mechanism for vertically supporting a tube used in a solar tracker ST is to use a weight, cable, roller and push-rod assembly that can lift the Mounting Surface MS from inside (not shown).

In all of the foregoing five mechanisms, the surface of the tube can be any hydrophilic material, preferably black to absorb the maximum amount of light to dry out the sunny side of the covering. The surface material should have a high expansion to contraction ratio when wet or dry, such as cotton, or open-cell cellulose sponge. The expansion ratio (wet to dry) of fabrics can be enhanced by adding a material like Hydrogel to increase its absorbency. (Hydrogel is a network of polymer chains that are water-insoluble, sometimes found as a colloidal gel in which water is the dispersion medium. Hydrogels are superabsorbent (they can contain over 99% water) natural or synthetic polymers. Hydrogels also possess a degree of flexibility very similar to natural tissue, due to their significant water content.) Bulk materials that contain cellulosic fiber, like an open-cell cellulose kitchen sponge, also work well. See FIGS. **8-10**.

The curving mechanism of a cellulose kitchen sponge can be clearly seen as a damp sponge laying flat on a counter top dries out more on the top surface shrinking the top, pulling the top inward (leaving the bottom relatively damp and expanded) so that the ends lift up with the center in contact with the counter top. A solar tracker using a cellulosic fiber is essentially like a kitchen sponge standing on end, formed in a cylinder for it to have equal freedom to bend in any direction to follow the sun, and FIG. **10** is a simplified design using exclusively a cellulose sponge tube CT whose diameter and wall thickness are chosen to be flexible to bend over the desired angular range but stiff enough to support itself and a solar collector mounted to the mounting surface MS.

Each combination of solar tracker construction materials will provide a certain amount of bending between the shaded and sunny state of the tube. The length, diameter and material of the tube need to be chosen to yield the desired amount of bending. For example, as in FIG. **8**, if a 1" thick covering of cellulose sponge over a 10" diameter polyethylene tube with 1" thick wall yielded 2° of bending per linear foot of the tube, the tube would need to be 22.5 ft. long to provide 45° of bending.

Movement of a solar tracker ST of the present invention in accordance with movement of the sun S is illustrated in FIGS. **1***a-d*.

In FIG. **1***a*, a solar tracker ST with a vertical cylinder is mounted to floating base FB. Fabric F covering of tube comes in contact with water W. Before the sun S is up, capillary action pulls water up the sides of the cylinder. Fabric is saturated and engorged with water, causing it to elongate. Because all sides of the cylinder are wet, the cylinder expands uniformly on all sides and grows upward and straight.

In FIG. **1***b*, sunlight shines on an exposed surface of the cylinder, drying out the sunny side allowing the fabric to shrink, collapsing the dry side DS down but leaving the wet side WS expanded. This makes the cylinder curve toward the sun so that the top is substantially perpendicular to the sun.

In FIGS. **1***c* & *d*, during the day, as the sun's position changes the drying is shifted to different positions on the cylinder, pulling the cylinder in different directions. Any areas which were sunny and dry but are now shady become wet with capillary action. This change causes the cylinder to bend in a different direction, but always making the top mounting surface MS substantially perpendicular to the sun.

The greatly increased efficiency of a solar device obtained by use of a solar tracker in accordance with the present invention is demonstrated in FIG. **2**. FIG. **2** graphs the efficiency of solar collectors which are stationary (see box A in FIG. **2**) and on a solar-tracker (see box B in FIG. **2**) which has the ability to be effective over a 6 hour period, ±3 hours to high noon. At 3 hours from noon (either 9 AM or 3 PM) when the sun is at 45° from overhead, a stationary collector collects only 70.7% of the energy compared to when at noon, calculated as cos α (where α=sun's angle from high noon).

Graph A in FIG. **2** is the efficiency of energy collected on a stationary photovoltaic cell, face up at 0° (not shown but of the type shown in FIG. **14***b*), for a base-line reference. Graph B in FIG. **2** shows the improvement when that same photo-

voltaic cell is mounted to a solar tracker ST. The solar-tracked photovoltaic cell operates at 100% efficiency during the entire 6-hour tracking period.

Graphs C and D in FIG. **2** show a much more dramatic improvement in efficiency when using solar collectors with concentrators as in FIGS. **14***c* and **14***d*. Graph C is included only for reference since it shows that the efficiency of a non-tracked photovoltaic cell mounted face up under a Fresnel lens is only effective when the sun passes over at high noon. The sun does not reach high noon (directly overhead) except for a few hours a year (and even then, only if located within 23.5° latitude of the equator), so even a solar device with a Fresnel lens as in FIG. **14***c*, would not be effective unless aimed directly at the sun. Graph D shows the efficiency of the same photovoltaic cell with Fresnel lens on a solar tracker, as shown in FIG. **14***c* which operates at peak efficiency for the entire 6 hour period of the solar tracker, every day, for the whole year.

A very real advantage of the solar tracker ST is in applications when concentrators are used. FIG. **14***d* shows a configuration using a parabolic mirror PR and Stirling cycle engine SCE which operate efficiently only when accurately aimed at the sun; however, for weight consideration, the preferred embodiment of this invention is shown in FIG. **14***c* with a thin Fresnel lens FRL and light-weight struts LWS.

FIGS. **3-5** show a cluster of solar trackers ST following the sun during the day. As sunlight shines on the wet side WS of each solar tracker, the fabric F dries out and shrinks. These same Figures also illustrate how floating bases of multiple solar trackers can be loosely lashed together into a solar tracker "farm" floating on a lake or ocean or other body of water. A farm of solar trackers, fixed or floating on a shallow pond like a rice patty, can be electrically wired together to supply electrical needs. Buoys with warning lights, remote weather transmitters and deep-sea oil-drilling rigs, which are difficult to reach, can also benefit from the increased energy from this solar tracker.

However, the solar trackers ST of the present invention need not only be used on large bodies of water; instead, they can also be placed on the roof of a building (or other locations) as long as the bottoms of the tubes are supplied with water. FIG. **13** illustrates the use of solar trackers ST in a forest tower FT which typically has little or no access to a traditional electrical utility. The roof of this tower incorporates a cistern CIS which collects rainwater RW and which supports four solar trackers ST, one at each corner. The rainwater is collected in a perimeter trench in which the bases of the solar trackers are immersed. Collected water is pulled with capillary action up the absorbent surface of the solar trackers. Photovoltaic collectors supply electricity to the tower for radio communications, lights, etc.

Up until now, each of the embodiments of solar tracker described has utilized bending of the solar tracker caused by a mechanism involving capillary action; however, other methods of mechanically shrinking a surface of the solar track exposed to sunlight can also be used, and FIGS. **11-13** illustrate additional such embodiments of the present invention.

In FIG. **12** three tension cables TC are pulled by solenoids SL powered by photovoltaic cells PC. Because a tension cable TC is only pulled when its photovoltaic cells PC receives sunlight, solar tracker ST is tilted toward sunlight by use of a different mechanism, but in the same fashion, as the solar trackers shown in FIGS. **3-5**. If three tension cables TC are used (which is especially preferred, additional cables although not needed, could perform the same function), they should be spaced 120° apart from each other. The solar trackers of FIGS. **11** and **12** have an outer stretchable fabric such as Spandex SPX and the tube is supported by spacers SP that sit on top of one another but allow the tube to bend in whatever direction is caused by tension cables being unevenly tensioned relative to one another about the tube. Whether or not a tension cable is tensioned or not is determined by whether it is on a sunlit surface of the solar tracker associated with a photovoltaic cell PC receiving direct sunlight or a shaded surface of the solar tracker associated with a photovoltaic cell not receiving direct sunlight. The amount a tension cable is tensioned will depend upon the amount of sunlight reaching its photovoltaic cell PC; accordingly, the photovoltaic cell PC must be positioned so that it properly tensions its associated tension cable, and the best location to do this is at the top of the tube support, although this increases the weight that must be supported.

In FIG. **13** the tension cables and solenoids used in FIG. **12** are replaced by Nitinol wires, attached to or woven into the fabric, which are used to bend the tube of solar tracker ST. Nitinol is a shape memory alloy, "SMA" (also known as a smart alloy or memory metal), that "remembers" its geometry. After a sample of SMA has been deformed from its original crystallographic configuration, it regains its original geometry by itself during heating (one-way effect) or, at higher ambient temperatures, simply during unloading (pseudo-elasticity or superelasticity). A photovoltaic cell PC can be used to electrify Nitinol wires so that they get hot and contract and then when they are no longer fed with an electrical current they will resume their non-electrified extended state. FIG. **13***a* illustrates a Nitinol wire in both an electrified state N-E and in a non-electrified state N-NE. Nitinol wires can be incorporated into a suitable fabric F that stretches by using the zig zag pattern shown.

Although it is believed that the embodiments of FIGS. **11-13** will cost more than embodiments that utilize capillary action to cause bending of the solar tracker, they may be more suitable for use in environments where water is not plentiful, such as arid regions.

While the invention has been described herein with reference to certain preferred embodiments, those embodiments have been presented by way of example only, and not to limit the scope of the invention. Additional embodiments and further modifications are also possible in alternative embodiments that will be obvious to those skilled in the art having the benefit of this detailed description. For example, many of the vertical support mechanisms can be adapted for use in other embodiments, such as using the spacers of FIG. **11** in a solar tracker utilizing capillary action to cause bending of the solar tracker.

Accordingly, still further changes and modifications in the actual concepts described herein can readily be made without departing from the spirit and scope of the disclosed inventions as defined by the following claims.

What is claimed is:

1. A solar tracker, comprising:

a mounting surface to which a solar device is mounted;

a bendable mounting surface support with an outer surface material that expands when exposed to water but not exposed to sunlight and contracts when exposed to sunlight that supports the mounting surface; and

a device for collecting electrical energy from the solar device;

wherein the outer surface material expands and grows due to absorption of water when it is without sunlight and sunlight shining on the outer surface material causes a sunlit side of the outer surface material to shrink relative to a shaded side of the outer surface material not exposed to sunlight due to drying of the sunlit side thus causing

the bendable mounting surface support to bend toward the direction of sunlight so that the mounting surface is substantially perpendicular to said direction of sunlight as the sun travels through a useful arc relative to the solar tracker.

2. The solar tracker of claim **1**, wherein the solar tracker is mounted to a platform.

3. The solar tracker of claim **2**, wherein the platform sits atop a water source and the water is in constant contact with the outer surface material so that capillary action causes the outer surface material to be saturated when it is not exposed to sunlight.

4. The solar tracker of claim **3**, wherein the platform floats atop the water source.

5. The solar tracker of claim **2**, further comprising:

a water reservoir in constant contact with the outer surface material so that the capillary action causes the outer surface material to be saturated when it is not exposed to sunlight.

6. The solar tracker of claim **1**, wherein the solar device does not extend beyond the mounting surface relative to the bendable mounting surface support.

7. The solar tracker of claim **1**, wherein the solar device is comprised of a photovoltaic cell and a Fresnel lens held in a fixed position relative to the photovoltaic cell for concentrating sunlight on the photovoltaic cell.

8. The solar tracker of claim **1**, wherein the solar device is comprised of a Stirling cycle engine.

9. The solar tracker of claim **8**, wherein the solar device is further comprised of a concentrator for concentrating sunlight to the Stirling cycle engine and an electrical generator connected to the Stirling cycle engine.

10. The solar tracker of claim **1**, wherein the bendable mounting surface support is an elongated tube.

11. The solar tracker of claim **10**, wherein the elongated tube is held in a nominally vertical position in the absence of sunlight by a vertical support.

12. The solar tracker of claim **11**, wherein the vertical support is comprised of a coiled compression spring.

13. The solar tracker of claim **11**, wherein the vertical support is comprised of an extruded tube of closed-cell structural foam.

14. The solar tracker of claim **11**, wherein the vertical support is comprised of a nominally vertical floating pole.

15. The solar tracker of claim **11**, wherein the vertical support is comprised of an air-inflated tube.

16. The solar tracker of claim **15**, wherein the air-inflated tube is maintained inflated by use of electricity generated by the solar device.

17. The solar tracker of claim **1**, wherein the device for collecting electrical energy is an electrical wire.

* * * * *

E.7 US 2010/0024861 A1

US 20100024861A1

(19) United States

(12) Patent Application Publication

(10) Pub. No.: US 2010/0024861 A1

(43) Pub. Date: Feb. 4, 2010

Cabanillas Saldaña

(54) **DUAL-AXIS SOLAR TRACKER**

(75) Inventor: **Juan Pablo Cabanillas Saldaña**, Toledo (ES)

Correspondence Address:
SUGHRUE MION, PLLC
2100 PENNSYLVANIA AVENUE, N.W., SUITE 800
WASHINGTON, DC 20037 (US)

(73) Assignee: **CABANILLAS INGENIEROS, S.L.**, Torrijos, Toledo (ES)

(21) Appl. No.: **12/444,824**

(22) PCT Filed: **Oct. 9, 2007**

(86) PCT No.: **PCT/ES2007/000574**

§ 371 (c)(1),
(2), (4) Date: **May 12, 2009**

(30) **Foreign Application Priority Data**

Oct. 9, 2006 (ES) U200602226
Oct. 25, 2006 (ES) U200602371
Dec. 22, 2006 (ES) U200602756

Publication Classification

(51) **Int. Cl.**
H01L 31/042 (2006.01)

(52) **U.S. Cl.** **136/244**

(57) **ABSTRACT**

The invention relates to a two-axle solar tracker, consisting of a moving supporting system for solar panels, which maximises the energy production of said panels and which is formed by a vertical axle and a horizontal axle in relation to which the system rotates in order to track the sun's path. The aforementioned axles are components of a structure supported at the centre and supported peripherally on wheels positioned on a running track or surface. The structure rotates about a fixed central point supporting the vertical axle of the tracker. At least one board is positioned on the horizontal axle of the structure in order to receive the solar modules or panels and said board(s) can rotate about the horizontal axle so that the solar panels are maintained perpendicular to the sun's rays.

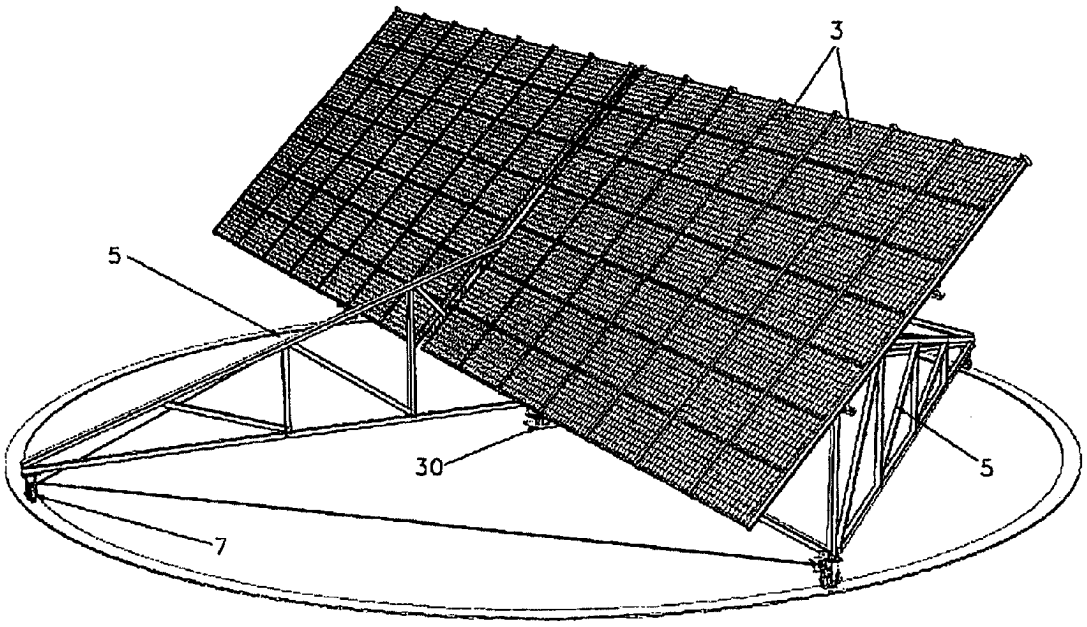

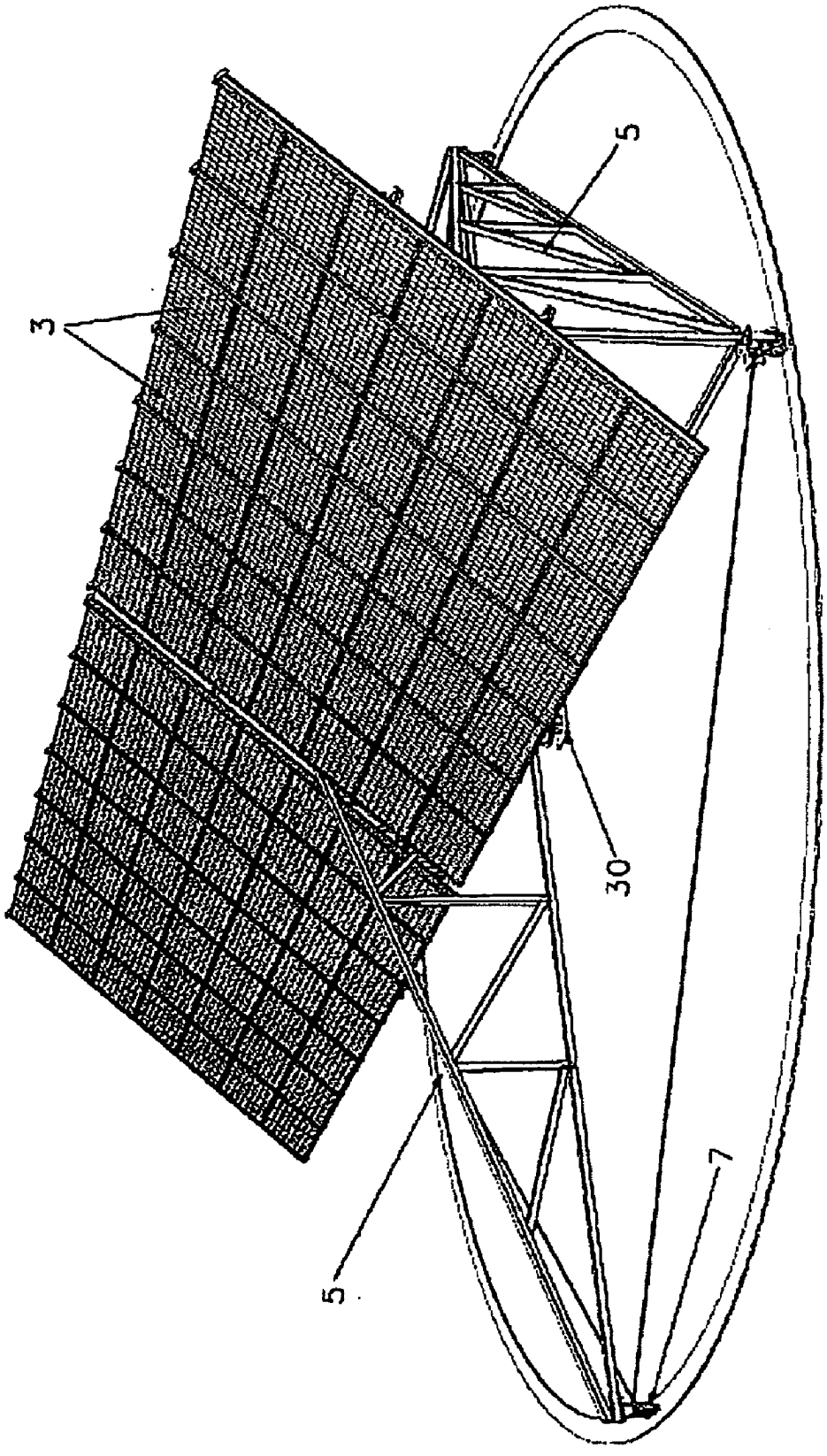

FIG. 1a

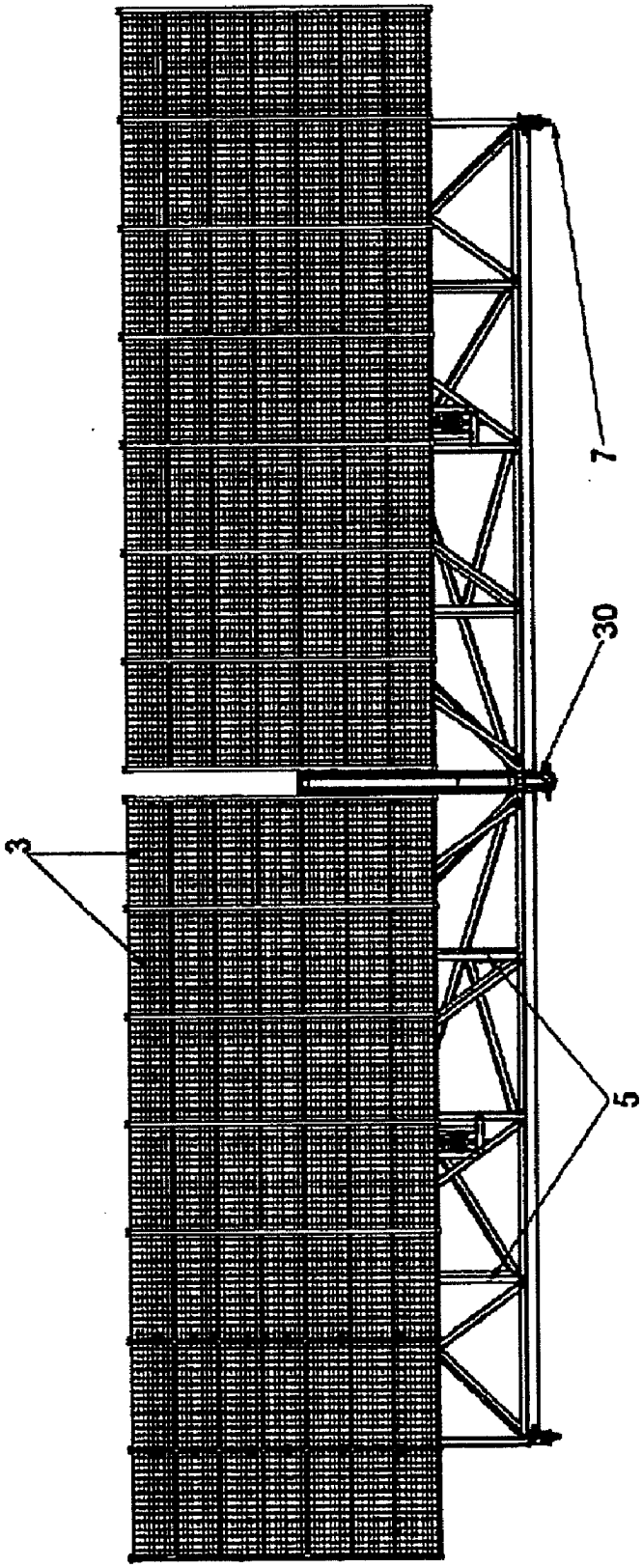

FIG. 1b

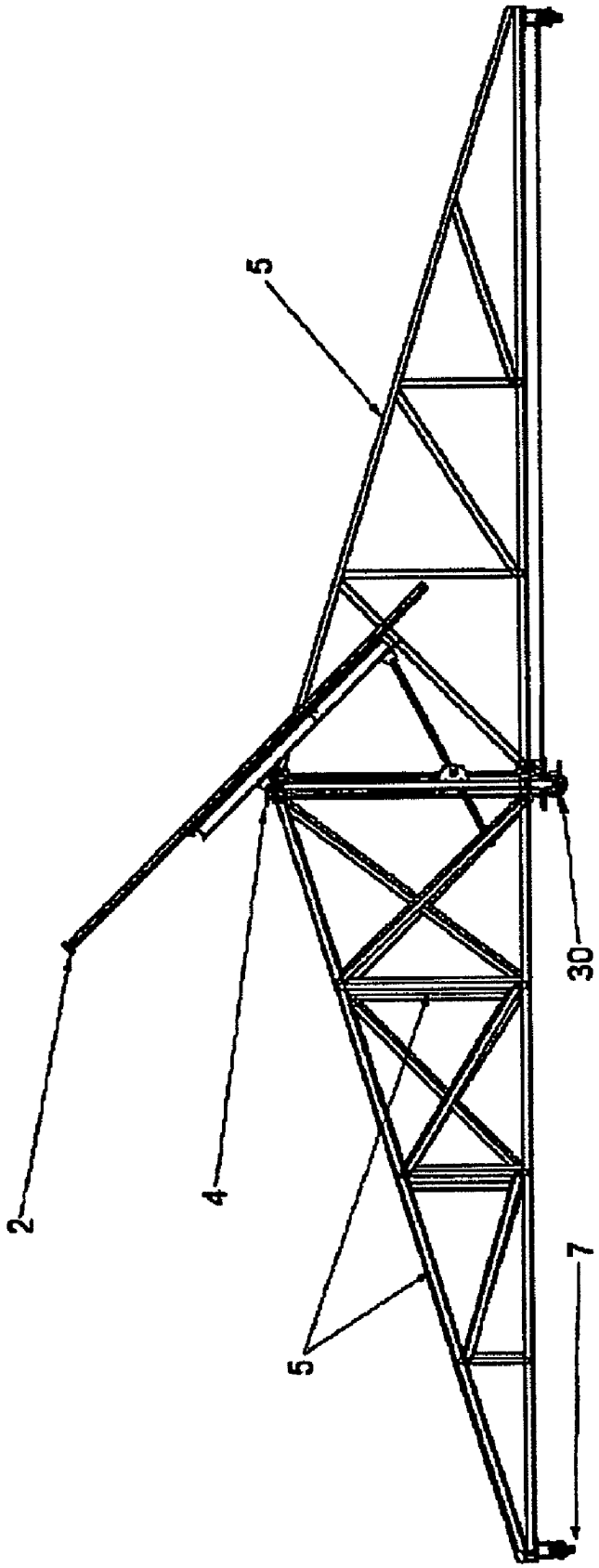

FIG.1c

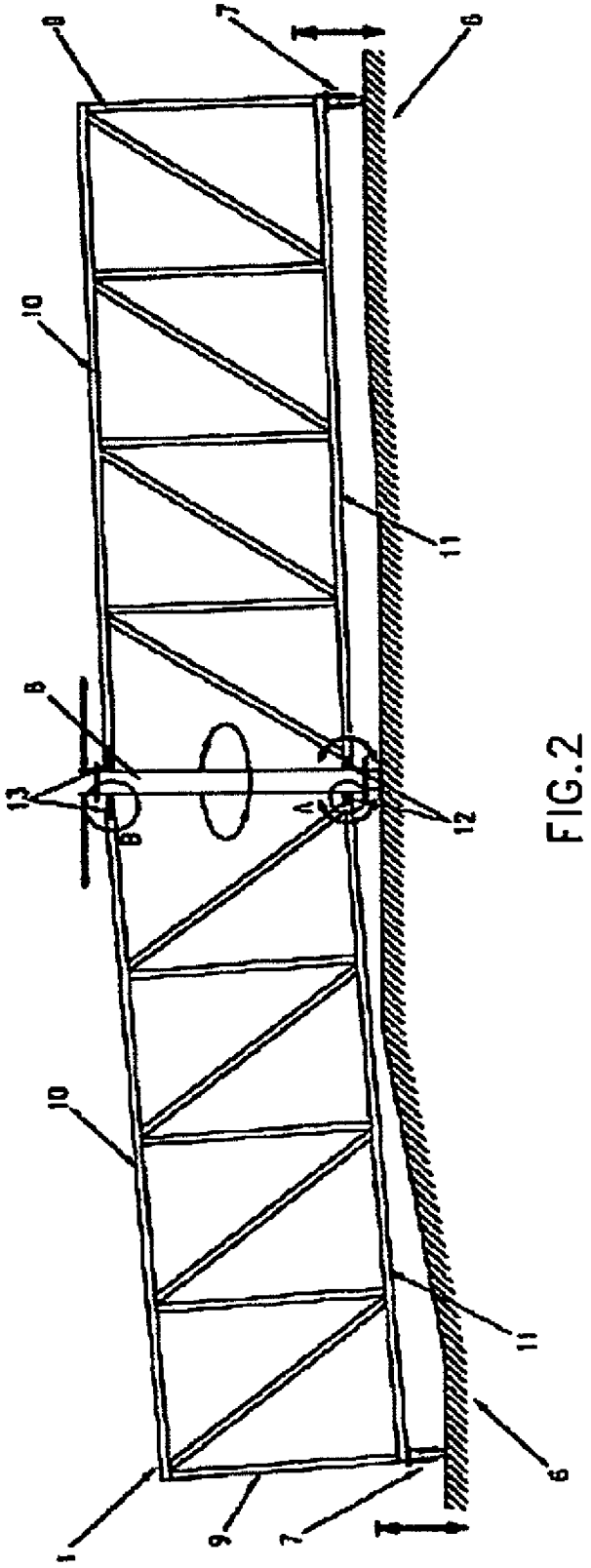

FIG.2

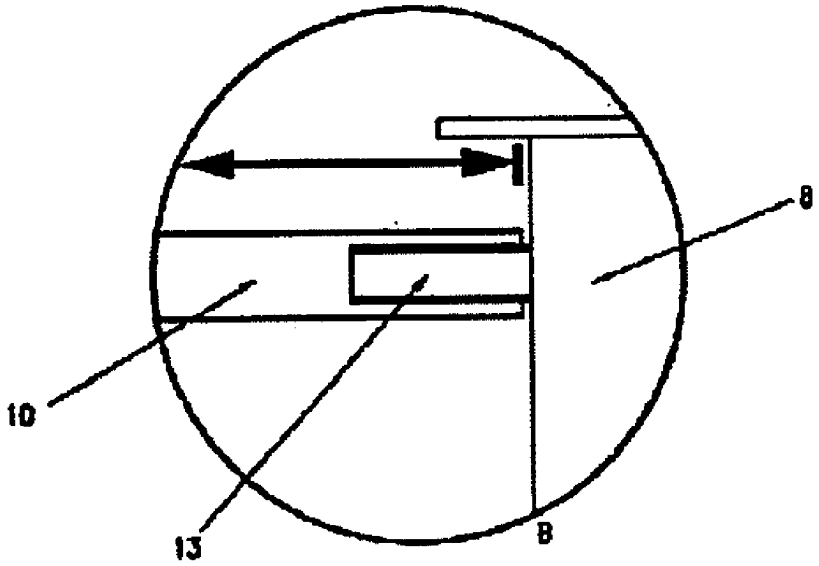

FIG. 4

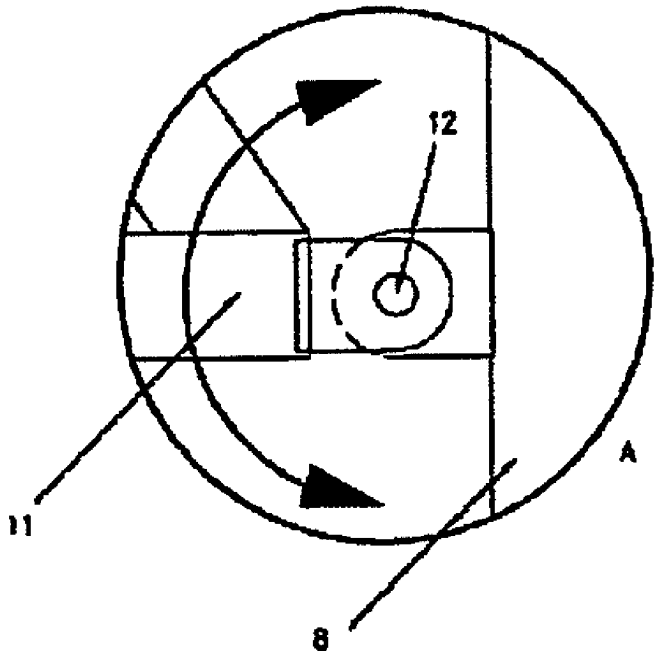

FIG. 3

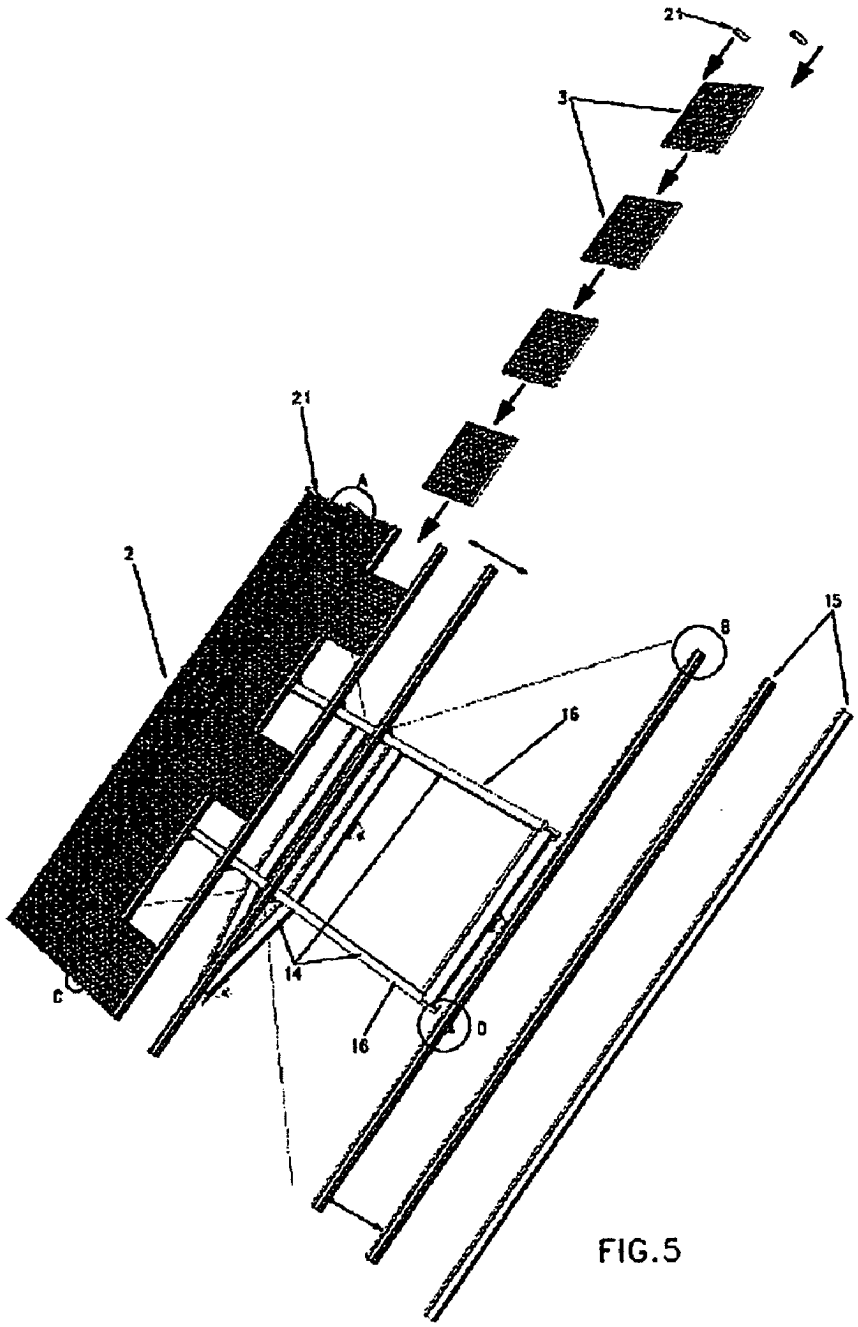

FIG.5

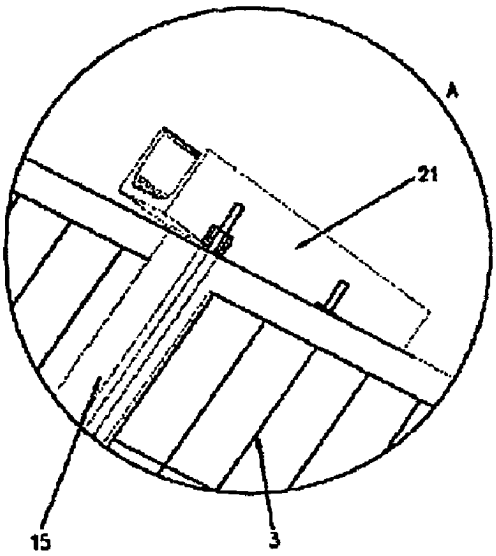

FIG.6

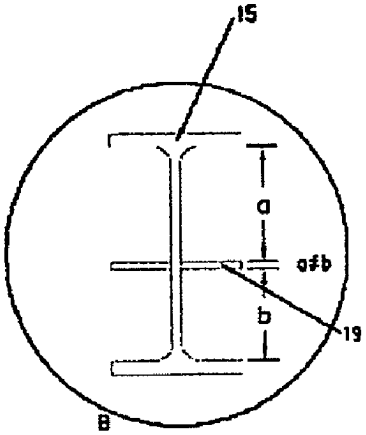

FIG.7

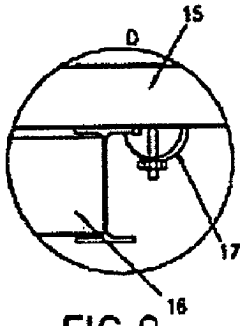

FIG.9

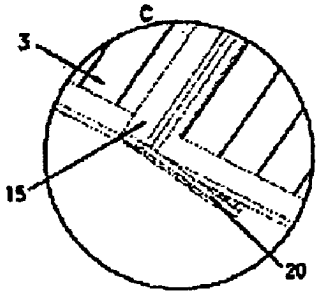

FIG.8

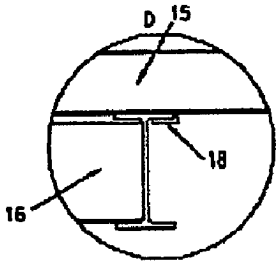

FIG.10

FIG. 11

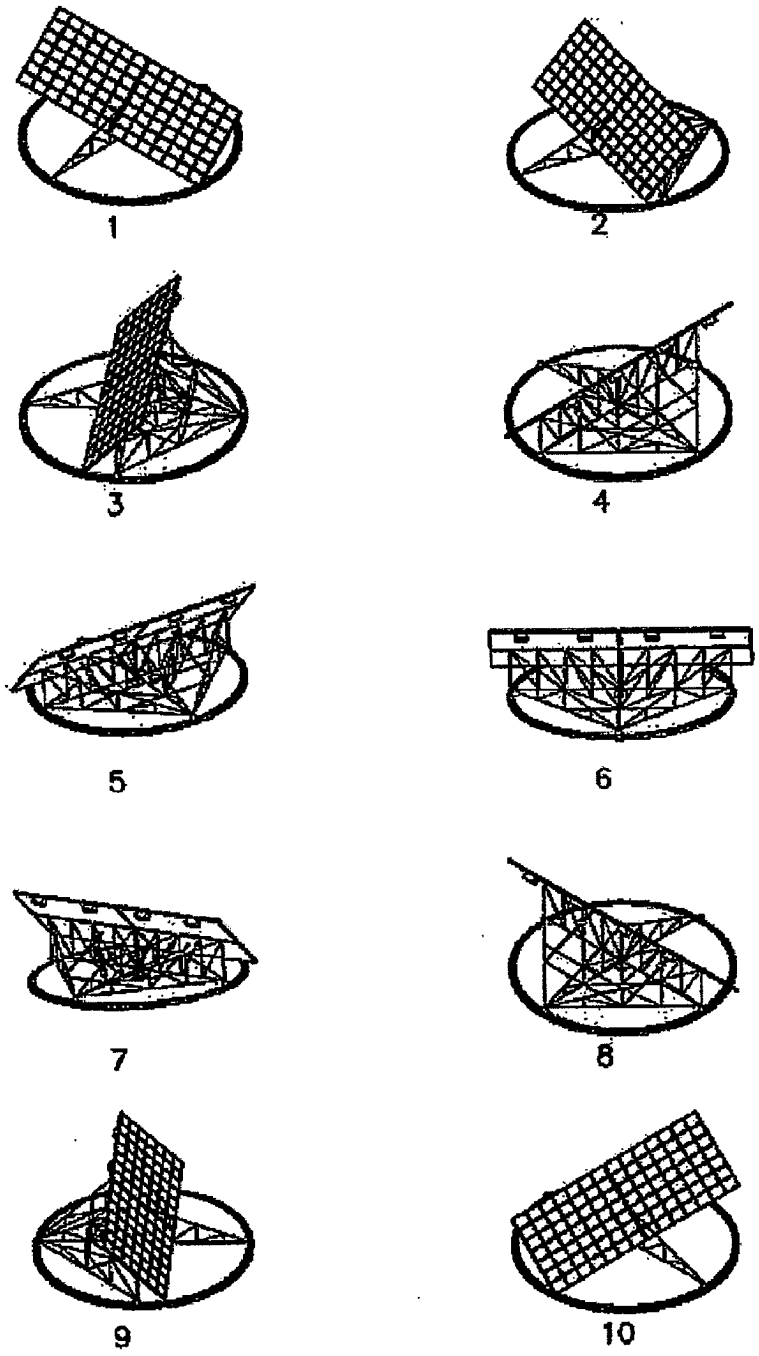

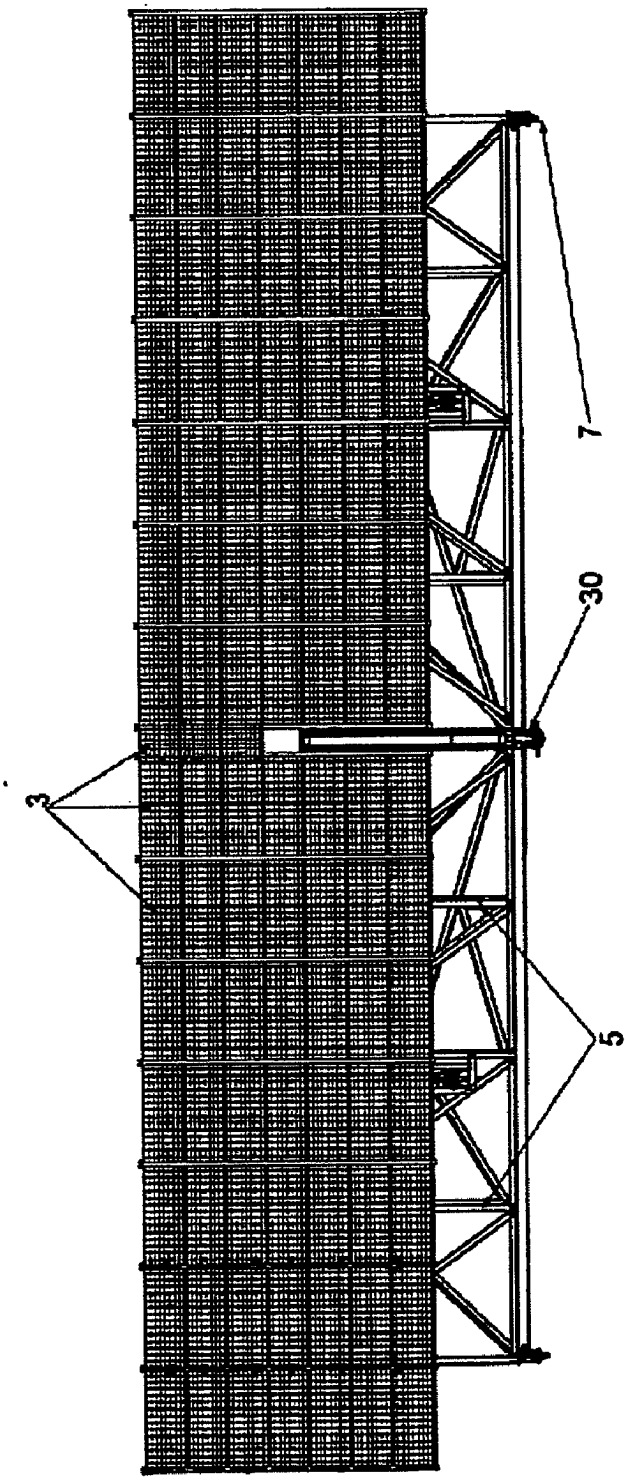

FIG.12a

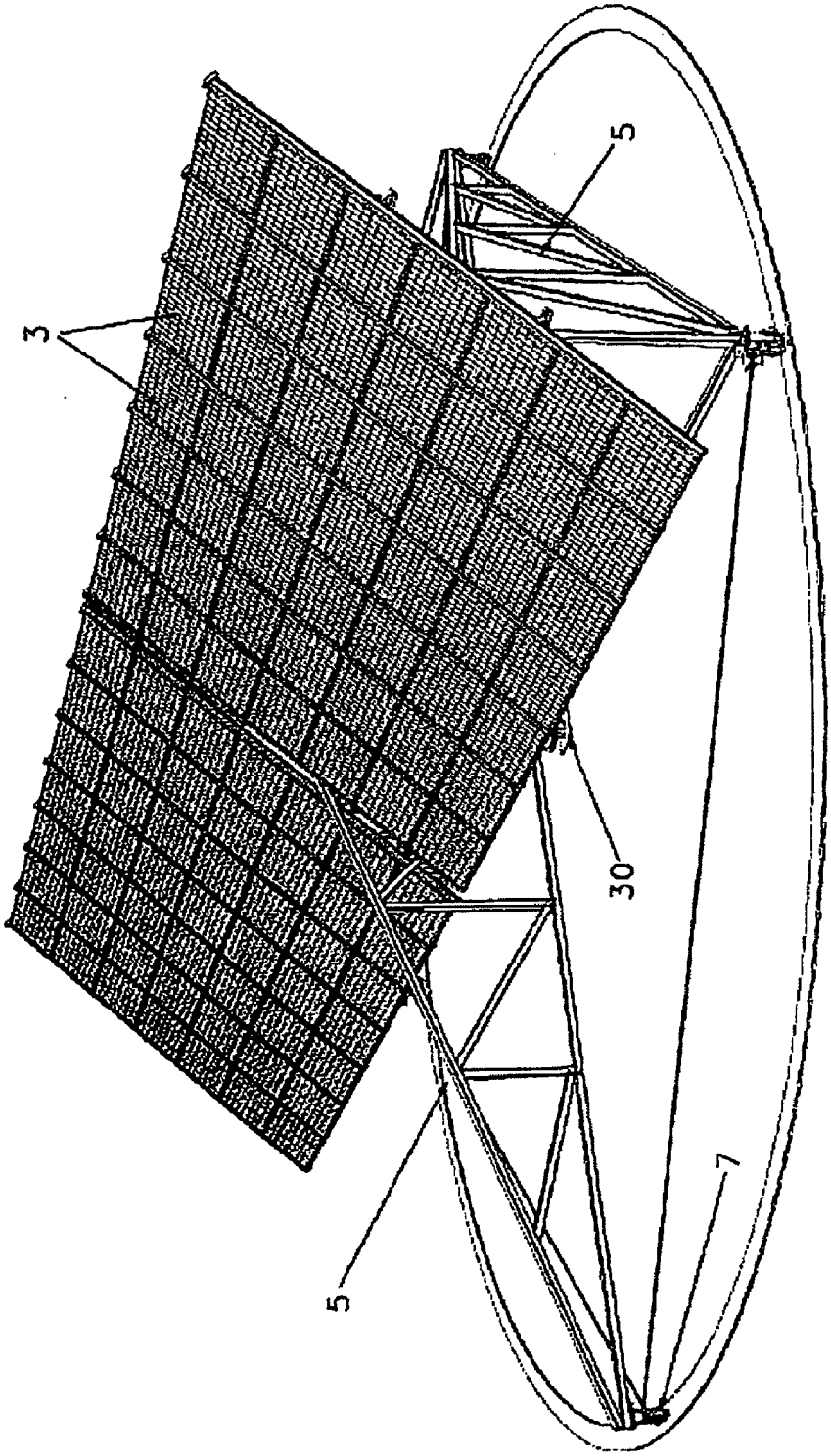

FIG. 12b

DUAL-AXIS SOLAR TRACKER

FIELD OF THE ART

[0001] The dual-axis solar tracker, object of the present patent application, relates to a moving support system for solar panels favoring as much as possible the energy production thereof, upon allowing the positioning of the plane of the solar panels in the perpendicular to the rays of sunlight during the entire day.

[0002] The main application of the present invention is the solar energy sector, and particularly, solar trackers or devices.

PRIOR STATE OF THE ART

[0003] Solar trackers such as that object of the present invention are not known in the state of the art, however other solar trackers are known which can be grouped in:

[0004] Panels in a plane on a fixed monopost or the like, with a single central support,

[0005] Panels in a plane on a lower non-rolling rotating frame, and

[0006] Panels in multiple planes with multiple horizontal axes on an inclined structure (stands) with a lower rolling platform.

[0007] These types of trackers have their advantages and drawbacks but on the whole, considering that relating to manufacture, maintenance, reliability etc., the proposed invention provides a number of advantages since:

[0008] it minimizes particular components involving a high price,

[0009] it requires very little labor and materials in its manufacture and assembly, and

[0010] it is a simple and efficient device.

[0011] Likewise, an additional problem of the known solar trackers rolling on a running surface or track, is that they require a perfect horizontalness of said running surface or track since due to their high rigidity and in the case that said surface or track was not perfectly horizontal, the passage of a wheel on a lower point thereof would cause said wheel to be suspended without touching the surface, and therefore when the wheel losing contact with the support surface or track is a tractor wheel a lack of traction would occur and would consequently make the rotation of the assembly difficult.

[0012] In addition, the solar panels to be assembled on the boards of the solar trackers of the state of the art are not standardized, therefore different solar panels would require boards with different dimensions. In the current state of the art said solar panels are usually arranged screwed to the profile forming the plane or board of panels, its main drawback being the requirements in its execution, such as the making of boreholes, precision in construction, the need to check the screws in the event of galvanization, accessibility to the board by the two sides thereof, etc., although without a doubt, the most important factor is time and therefore the labor necessary for assembling the panels with screws since it will be necessary to place them on one face of the board and screw them on the other face. This action is made very difficult due to the large dimensions of the planes formed by the panels. Likewise, the fact of using screws as a fixing of the panels makes it easy to steal them.

[0013] U.S. Pat. No. 4,256,088-A, describes a solar concentrator which includes a modularized point focusing solar concentrating panel which is movably mounted to track the sun. This panel has an overall parabolic reflecting surface and a triangular or approximately triangular configuration which improves structural integrity, minimizes wind resistance and permits rapid and easy stowing.

[0014] US application number U.S. Pat. No. 2,001,036024-A1, describes a matrix solar dish concentrator with flexed glass mirrors is patterned from orthogonal planes parallel to the axis of symmetry of a paraboloid and intersecting the paraboloid, this pattern making all parabolic trusses uniform. The solar dish tracks the solar azimuth with a bicycle wheel and tracks the solar zenith with a television satellite dish actuator. A solar receiver is supported with a low shade structure outside a cone of concentrated sunlight.

DESCRIPTION OF THE INVENTION

[0015] As has already been mentioned, the present invention relates to a dual-axis solar tracker, specifically a vertical axis and another horizontal axis with respect to which it will rotate in order to track the path traced by the sun. Said axes are included as components of a metal profile structure supported at its center and on wheels in its periphery, in turn being supported on a running surface or track. The solar tracker, and therefore the mentioned structure, rotates on a fixed central point on which the vertical axis of the tracker is supported, said structure incorporating the horizontal axis on which at least one board is located for receiving the solar modules or panels, said board or boards being able to rotate on said horizontal axis so that the solar panels are maintained perpendicular to the rays of sunlight.

[0016] The solar panel or panels used for capturing solar energy are incorporated or assembled in the preferably metal solar tracker structure, specifically in one or more boards forming said structure. Said board or boards in turn form a plane which is maintained perpendicular to the rays of sunlight, i.e. the solar panels incorporated in the boards are maintained perpendicular for the purpose of achieving a better and greater capture of solar energy.

[0017] The board or board of the structure, and therefore the plane of solar modules or panels, is provided with two movements, a movement of rotation with respect to a vertical axis and a movement of rotation with respect to a horizontal axis, both axes being perpendicular to one another. The lower point of the vertical axis is fixed to the ground, such that the tracker rotates with respect to said fixed point, whereas the horizontal axis, perpendicular to the vertical axis, enables the rotation of the board or boards possible with respect to it. In the case of more than one board of panels, the rotation thereof in a synchronized manner, forming a single plane, is recommendable although such panels can evidently rotate in an asynchronous manner, i.e. independently, for example in those cases in which the means of the traction elements of any of the boards does not operate correctly.

[0018] The object of the present invention is therefore a dual-axis solar tracker which allows maintaining the perpendicularity of the solar modules or panels with respect to the rays of sunlight, independently of the position of the sun which changes throughout the day.

[0019] As has been mentioned the plane of panels is formed by at least one board, integrating the solar tracker structure and supporting the solar panels, said boards being supported on the mentioned rolling structure rotating with respect to the central point fixed to a footing for locking the entire assembly. The rolling structure, supported on the vertical axis at its center and on wheels in its periphery, some wheels being drive wheels and other wheels being support wheels, rotates

due to the action of said drive wheels (motor-driven wheels with automated geared motors) on a running track or horizontal surface (ground, planar bed plate, concrete girder, metal profile, etc.).

[0020] The horizontal axis, which in the event that the tracker has two boards will be divided into two horizontal axes, is integrated in the rolling structure and determines and controls the rotation of the board or boards, and therefore of the plane of solar modules or panels, preferably by means of automated drives, for example worm screw mechanism geared motors. The rotation of the board or boards with respect to the horizontal axis or axes, and therefore of the solar panels with respect to the horizontal axis or axes is thus achieved with an easy automation for each day and time of the year. Said automated drives can be common for more than one board or be independent for each of the boards if these boards are independent, thus allowing the boards to be able to rotate in a synchronized manner but independently driven.

[0021] Both the rotation with respect to the vertical axis or point as well as with respect to the horizontal axis or axes is controlled by means of a control unit (of the optical type or programmable automaton type), being able to incorporate different sensors facilitating the position of the solar panels of the tracker depending on the position of the sun and of the meteorological conditions.

[0022] The rolling structure is formed by a structural assembly of lattice girders and as has already been mentioned, it is supported on the running surface through wheels and on a single, central and fixed vertical rotation point. The board or boards on which the solar panels are assembled form part of said structure as does the horizontal rotation axes. Said structure in turn has a projection at its front part by way of a nose providing great stability to the structural assembly and therefore to the solar device.

[0023] The solar tracker proposed by the invention likewise has a device allowing the correct operation thereof on a running surface which is not perfectly horizontal, thus adapting to the level variations of said surface.

[0024] Another object of the present invention is therefore a solar tracker which is able to prevent the level variations of its running and support surface, preventing the requirement of perfect horizontalness of the running surface on which the tracker is supported.

[0025] In order to achieve the foregoing, and more specifically in order to prevent the malfunction in the solar tracker due to the non-horizontalness of the running surface, the solar tracker object of the present invention will have its plane of panels formed by two boards of solar modules or panels.

[0026] Said two boards are anchored on a lattice girder which is part of the rolling support structure. The lattice girder forming the solar device is horizontally divided into two equal parts connected to the vertical axis given that each of the parts has an upper bar and a lower bar attached to the vertical axis by means of moving couplings. On the side opposite that of the coupling and at its lower part, i.e. at the outer lower ends of the lattice girder, there is at least a support and traction wheel on the running surface. The upper or lower side of the lattice girder defines a single imaginary horizontal axis in the event that the running surface is perfectly planar.

[0027] The need for the running surface on which the solar tracker rotates to be perfectly horizontal is prevented by means of the moving coupling mechanism which is detailed, since said mechanism allows the wheels to always make contact with the running surface or track regardless of the horizontalness thereof by means of the action of the actual weight of the wheels, therefore not losing traction and support.

[0028] Said moving couplings are formed, for example, by means of a hinge between the lower bars of the lattice girder and the vertical axis, said hinge transmitting all the stresses, except the rotating bending moment according to the hinge axis, generated between the girder and the central vertical axis. Meanwhile, in the coupling between the upper bars and the central axis, a tongue and groove joint transmitting all the stresses between the upper bar and the vertical axis is used, the tongue and groove joint being of the type allowing the axial stress in the upper bars of the lattice girder to be only transmitted in a direction approaching the central vertical axis.

[0029] Not transmitting this stress in the direction of moving away from the central vertical axis is what allows the wheel to be supported on the surface or track even though it is not horizontal and has level differences.

[0030] The maximum raising and lowering limitations of the wheels are determined by:

[0031] Maximum raising: the wheels can not be raised above the position in which the upper bar makes contact with the vertical axis in the tongue and groove joint.

[0032] Maximum lowering: the wheels have the length of the tongue and groove joint located between the upper bars and central vertical axis as a lowering limit.

[0033] A final object of the invention is allowing the use of different dimensions in the tracker of solar panels, as well as the fixing thereof in the boards, solving the drawbacks of the non-standardization of the width, height and thickness of the solar panels or modules, allowing the use of different solar panels on the board or boards of the tracker according to the requirements of the final installer.

[0034] The system for fixing the solar modules or panels in the board or boards of the solar tracker requires the board or boards to be formed by a preferably rectangular frame inside which the girders having a metal profile slide, spacing them apart the width of the required panel. Said metal profiles form rails in which the solar panels will be housed and subsequently fixed without such solar panels needing to be screwed to the profiles of the boards. The flanges of said profiles must be equal to or less than the dimension of the framing of the panel for the purpose of not reducing the radiation emitted on the active surface of the panels. These profile girders can have any U-, I-shaped section etc.

[0035] Once the board incorporating a certain profile according to the measurement of the panel to be used in the rails of its profiles has been formed and assembled, the solar panels are introduced and slid therein, and if there are clearances it is then possible to use silicone points for preventing the movement of said panels in the rails due to the possible excessive clearance of the rail.

[0036] As has already been mentioned, each board is formed by a preferably metal frame with a UPN profile or the like and with guides or runners therein and preferably IPE or UPN profiles or the like, perpendicular to the main girders demarcating the perimeter of said frame and therefore of the board, said guides being coupled to the frame by means of attachments allowing the sliding thereof on the frame. With this arrangement the width between two guides can be adapted to the width of the solar modules or panels which must be slid between said guides.

[0037] The guides likewise have an eccentric flat bar dividing the height of said guide in its entire length into two parts, and as it is eccentric said two heights son different, also allowing the introduction of solar panels with different thicknesses. The guides have at their lower part a permanent closure or plug for preventing the solar panels from sliding and coming out of the rail when they are introduced between two guides. An opening and closing system is arranged at the upper part and in order to prevent the unwanted removal of the solar panels introduced in the rails.

[0038] In order to ensure the stiffening of each panel, steel cables with their corresponding tensioners are diagonally used, which cables attach the corners or edges of the board or boards with the central area of their frame, such that the cables structurally contribute to the maintenance of the "frame—guides—panel" assembly, providing a convenient and necessary securing (Saint Andrew's cross) in a simple manner.

DESCRIPTION OF THE DRAWINGS

[0039] The following drawings accompanying the description in a non-limiting manner are referred to below for the purpose of facilitating the understanding of the invention:

[0040] FIG. **1** shows a perspective view (**1***a*), a front elevational view (**1***b*) and a side elevational view (**1***c*) of the solar tracker object of the present invention.

[0041] FIG. **2** shows the side elevational view of the lattice girder, central axis and running assembly.

[0042] FIG. **3** shows detail A of FIG. **2**.

[0043] FIG. **4** shows detail B of FIG. **2**.

[0044] FIG. **5** shows an exploded view of the assembly of the solar panels in a board according to the present invention.

[0045] FIG. **6** shows a possible solution of detail A of FIG. **5**.

[0046] FIG. **7** shows detail B of FIG. **5**.

[0047] FIG. **8** shows detail C of FIG. **5**.

[0048] FIG. **9** shows detail D of FIG. **5**.

[0049] FIG. **10** shows an alternative to detail D of FIG. **5**.

[0050] FIG. **11** shows the rotation sequence of the dual-axis solar tracker with respect to its vertical axis in ten of its positions.

[0051] FIG. **12** shows a front elevational view (**12***a*) and a perspective view (**12***b*) of the solar tracker object of the present invention with a single board of solar panels.

DESCRIPTION OF A PREFERRED EMBODIMENT

[0052] The solar tracker object of the present invention is supported on a running surface or track, for example the ground, planar bed plate, or circular rail **6** and rotates with respect to its axis **8** and central point **30**, which is fixed to the ground through a footing for locking the assembly. The solar tracker is formed by a rolling support structure **5** rotating with respect to said central point **30** and axis **8**, said support structure **5** of the solar tracker being formed by a structural assembly **9**, **10**, **11** of metal lattice girders. As can be seen in the figures, particularly in FIG. **11**, sequences A, B, C, D, H, I, J, the support structure **5** has a projection at its front part by way of a nose providing great stability to the structural assembly and therefore to the solar device.

[0053] The rotation of the solar tracker with respect to the vertical axis and therefore with respect to its central anchoring point **30** is achieved by means of using support wheels **7**, at least two of which will be motor-driven. The fact of placing geared motors or rotation drives in the wheels, i.e. in the edge of the structure instead of in the vertical rotation axis, allows reducing the size of said geared motors upon requiring less power due to the large action arm.

[0054] The support structure **5** is likewise useful as a support for the horizontal axis **4** of each board **2** of the solar tracker. The solar panels **3** forming the plane of panels of the tracker and which are responsible for capturing rays of sunlight are fixed in said boards **2**.

[0055] Worm screw drive geared motors, for example, are used for the movement of the boards **2**, and therefore of the panels **3**, with respect to the horizontal axis **4**. The fact of being able to have a drive device for each board **2** allows the movement of each board **2** with respect to the horizontal axis **4** to be able to be synchronized but independent.

[0056] The boards **2** likewise have weighting elements in order to minimize the compression work of the drive as well as their buckling.

[0057] As has already been described, the dual-axis solar tracker **1** is formed by two support boards **2** of solar panels **3** and each board is integrated with a horizontal rotation axis **4**, each board rotating with respect to its corresponding horizontal axis **4**, said axes **4** being fixed on the rolling support structure **5** of the solar tracker.

[0058] Said structure **5** is formed by a structural assembly of lattice girders and is supported on the running surface **6** through wheels **7** as well as on a rotation point **30**.

[0059] The two boards **2** are supported on a lattice girder **9**, perpendicular to the running surface **6** and which is divided into two equal parts by the vertical axis **8**. Each of the parts of said lattice girder **9** has an upper bar **10** and a lower bar **11** which are secured by means of moving couplings to the vertical axis **8**, a tongue and groove joint **13** and a hinge **12** respectively. It likewise has, at its outer lower ends, support wheels **7** which are preferably motor-driven and drive the tracker **1**, making it rotate with respect to the central point **30**.

[0060] In the event that the running surface **6** is not perfectly horizontal, see FIG. **2**, and in order to prevent one of the wheels **7** from being in midair without making contact with the surface **6** and therefore making the traction impossible and affecting the rotating movement of the tracker **1**, the tongue and groove joint **13** of the upper bar **10** and the hinge **12** of the lower bar **11** allow the wheel **7** to keep making contact with the running surface **6** regardless of the level changes thereof. The hinge **12** allows the lower bar **11** to rotate lowering its end such that the tongue and groove joint **13** of the upper bar **10** slides the necessary distance. The maximum lowering limit of the wheel **7** is determined by the length of the tongue and groove joint **13**.

[0061] The system is equally functional when the running surface **6** is raised, but in this case the hinge **12** allows the lower bar **10** to rotate lifting its end and the tongue and groove joint **13** is shortened. The maximum raising limit of the wheel **7** is determined by the contact between the upper bar **10** and the vertical axis **8**.

[0062] If the horizontalness of the running surface is ensured it is possible for the solar tracker to have a single horizontal axis **4** with two boards **2** on each side of the vertical axis **8** instead of a horizontal axis for each board.

[0063] The objective of the solar tracker **1** is, as its own name indicates, to track the path traced by the sun attempting to capture the greatest amount of rays of sunlight. In order to do this, in addition to describing a rotating movement on the vertical axis **8**, it has the mentioned solar panels **3** in the two

boards **2** located on a frame **14** so that by means of the rotating movement with respect to the horizontal axis **4** the panels remain perpendicular to the rays of sunlight.

[0064] Each of said boards **2** has a preferably rectangular frame **14** with its two main bars **16** parallel to the upper bar **10** of the lattice girder **9**. The sides of the frame **14** are formed by an IPN profile or the like. For supporting the panels **3** on said frame **14**, the tracker **1** has guides or runners **15** which are located on the frame **14** perpendicular to the main bars **16**. Said guides **15** are coupled and slide on the frame **14**, specifically on the main bars **16** of the frame **14**.

[0065] Said sliding and securing is achieved by means of sliding attachments **18**, of the folded sheet type sliding along the flanges of the frame, or screwed clamps **17**. Specifically, the clamps are formed by a semicircular shaped element which is screwed at its center to the sliding guide **15**, is connected to said guide **15** at one of its ends and is free at the opposite end. There is thus a space between the free end of the clamp and the guide **16**, a space in which a flange of the IPN profile of the longest side of the frame **16** is housed, and after sliding along said frame **14** until achieving the width of the solar panel **3** to be introduced between two consecutive guides **15** forming a rail, the inviolable screw of the clamp **17** is tightened, thus ensuring the position of the guide **15** on the frame **14**.

[0066] The sliding attachment, the folded sheet **18** sliding along the flanges of the frame, is connected to the sliding guides or runners **15**, determining a space between one side of the folded sheet **18** and the guide or runner **15** intended to partially house, as occurs with the previous example of the clamp, the main bar **16**, the longest bar of said frame **14**.

[0067] The foregoing are two preferred embodiments of the adaptation system for adapting the boards in order to house solar panels with different dimensions according to the needs or preferences of the installer, said adaptation and securing system being able to use other components both for facilitating the sliding of the guides and their subsequent securing and for securing the panels to said guides.

[0068] The guides **15**, preferably with an IPE profile, have an eccentric flat bar **19** dividing the height of said guide **15** in its entire length into two parts, and as it is eccentric said two heights (a, b) are different, which also allows using the solar tracker **1** not only with solar panels **3** with different widths but also with different thicknesses.

[0069] The assembly of the solar panels **3** in the solar tracker **1** through the boards **2** formed by the frame **14** and the guides **15** is simple and is carried out as is detailed below.

[0070] The guides **15** are first fitted to the width of the solar panels **3** which will be used in the tracker **1** by means of the sliding thereof along the sides **16** of the frame and the fixing of the clamps **17**. Once the rails for housing the panels **3** are ready, the panels **3** start to be introduced between the guides and according to their thickness supported on the flat bar **19** of the guide **15** or below said flat bar **19**.

[0071] The solar panels **3** are closed when they reach the end part of the guide **15**, thus preventing them from coming out of the rail, by a permanent closure **20**, and once all the panels have been introduced in the corresponding rail, said rail is closed by means of a UPN profile **21** or the like, which is fixed to the corresponding end by way of a lid by means of a nut which can be an inviolable or antitheft nut.

[0072] Finally, and once the panels **3** have been introduced into both boards **2** of the solar tracker **1** and in order to ensure the stiffening of each board **2**, steel cables **22** with their corresponding tensioners are used, which cables attach the corners and edges of each board with the central area of their frame, such that the cables structurally contribute to the maintenance of the "frame—guides—panel" assembly, providing a convenient and necessary securing in the form of a Saint Andrew's cross in a simple manner.

[0073] Another embodiment, shown in FIG. **12**, shows a solar tracker which only includes a single board of solar panels rotating with respect to a horizontal axis.

1. A solar tracker (**1**), of the type allowing the solar panels (**3**) to be maintained perpendicular to the rays of sunlight, characterized in that it comprises:

- A plane determined by at least one board (**2**) incorporating the solar panels (**3**), fixed on a rolling support structure (**5**), formed by a structural assembly of lattice girders, with a horizontal rotation axis (**4**),
- a central point (**30**) on which there is arranged a single fixed vertical rotation axis (**8**), centered with respect to the rolling support structure (**5**) and supporting said rolling support structure (**5**) with at least one board (**2**),
- a projection at the front part of the rolling support structure (**5**) by way of a nose, and
- automated systems driving the rotation with respect to both axes (**4**, **8**), a first rotation of at least said one board (**2**) with respect to said horizontal axis (**4**) and a second rotation of the vertical axis (**8**) of the structure (**5**) with respect to the central point (**30**) on a running surface or track (**6**).

2. The solar tracker according to claim **1**, characterized in that it has wheels (**7**) located at the lower part of the rolling support structure (**5**) for the rotation with respect to the vertical rotation axis (**8**), and support on the running surface (**6**).

3. The solar tracker according to claim **2**, characterized in that the horizontal rotation axis (**4**) is located on a lattice girder (**9**) which is part of the support structure (**5**) and perpendicular to the running surface (**6**), said lattice girder (**9**) being horizontally divided into two equal parts by the vertical axis (**8**) and each of these parts has an upper bar (**10**) and a lower bar (**11**) connected to the vertical axis by means of moving couplings (**12**, **13**), each of the outer lower ends of the lattice girder (**9**) having at least one of the mentioned wheels (**7**) on the running surface (**6**).

4. The solar tracker according to claim **3**, characterized in that the lower bars (**11**) of the lattice girder (**9**) are connected to the vertical axis (**8**) by means of a hinge (**12**) transmitting the stresses generated between the lattice girder (**9**) and the central vertical axis (**8**).

5. The solar tracker according to claim **3**, characterized in that the upper bars (**10**) of the lattice girder are connected to the vertical axis (**8**) by means of a tongue and groove joint (**13**) transmitting the stresses between the lattice girder (**9**) and the central vertical axis (**8**), allowing the axial stress in the upper bars (**10**) of the lattice girder (**9**) to only be transmitted in the direction approaching the central vertical axis (**8**) of the bar (**10**).

6. The solar tracker according to claim **3**, characterized in that the contact between the upper bar (**10**) and the vertical axis (**8**) limits the maximum raising position of the support wheels (**7**) located at the outer lower ends of the lattice girder (**9**).

7. The solar tracker according to claim **5**, characterized in that the maximum lowering position of the support wheels (**7**) is determined by the length of the tongue and groove joint (**13**).

8. The solar tracker according to claim **3**, characterized in that each of the two parts of the lattice girder (**9**) determines a horizontal axis (**4**) so that each of them supports a support board (**2**) of the solar panels (**3**), rotating or turning with respect to said horizontal axes (**4**).

9. The solar tracker according to claim **2**, characterized in that at least two of said wheels are motor-driven and the rest are support wheels.

10. (canceled)

11. The solar tracker according to claim **1**, characterized in that each board has at least one worm screw driven by a geared motor for rotating each board with respect to the horizontal axis.

12. The solar tracker according to claim **1**, characterized in that the boards rotate with respect to the horizontal axis in a manner synchronized with one another.

13. The solar tracker according to claim **1**, characterized in that the boards rotate with respect to the horizontal axis in a manner independent from one another.

14. (canceled)

15. (canceled)

16. The solar tracker according to claim **1**, characterized in that the support boards (**2**) of the solar panels (**3**) comprise a rectangular metal frame (**14**) with guides or runners (**15**) for introducing the solar panels (**3**) between two of said guides or runners (**15**) that are perpendicular to the longest side (**16**) of the frame (**14**) and sliding along such frame, such guides or runners being coupled to said frame (**14**) by means of attachments (**17**, **18**) allowing the sliding of said guides or runners (**15**) on said frame (**14**, **16**).

17. (canceled)

18. The solar tracker according to claim **13**, characterized in that said sliding attachment is a semicircular shaped clamp (**17**) screwed at its center to the sliding guides or runners (**15**) and integral at one of its ends with the guide or runner (**15**) and free at the opposite end, determining a space between said free end and the base of the guide or runner (**15**) intended to partially house the longest side (**16**) of said frame (**14**).

19. The solar tracker according to claim **13**, characterized in that said sliding attachment is a folded sheet (**18**) integral with the sliding guides or runners (**15**), determining a space between one side of the folded sheet (**18**) and the guide or runner (**15**) intended to partially house the longest side (**16**) of said frame (**14**).

20. (canceled)

21. (canceled)

22. (canceled)

23. (canceled)

24. (canceled)

25. (canceled)

26. (canceled)

27. (canceled)

28. (canceled)

29. (canceled)

* * * * *

E.8 US 2010/0282243 A1

US 20100282243A1

(19) United States

(12) Patent Application Publication

(10) Pub. No.: US 2010/0282243 A1

(43) Pub. Date: Nov. 11, 2010

Meyer

(54) **SOLAR TRACKING**

(75) Inventor: **Steven M. Meyer**, Georgetown, TX (US)

Correspondence Address:
TEXAS INSTRUMENTS INCORPORATED
P O BOX 655474, M/S 3999
DALLAS, TX 75265

(73) Assignee: **Texas Instruments Incorporated**, Dallas, TX (US)

(21) Appl. No.: **12/613,853**

(22) Filed: **Nov. 6, 2009**

Related U.S. Application Data

(60) Provisional application No. 61/112,738, filed on Nov. 8, 2008.

Publication Classification

(51) **Int. Cl.**
F24J 2/40 (2006.01)
F24J 2/38 (2006.01)

(52) **U.S. Cl.** **126/601**; 126/605

(57) **ABSTRACT**

The disclosed invention is a solar tracker that is a simple 2 axis system that can be powered with integrated stepping motors and lead screw actuators that provides the necessary structural support and 2 degrees of freedom in the motion of the solar collector, to increase the electrical output of the system. Since the solution is designed for use with only one solar panel the mechanical forces such as wind load are much lower and easier to manage. The disclosed invention is also a solar tracker that is a single axis version where the base is fixed and the elevation is set at an average value for the location and pivoting mechanism operates the azimuth axis. Since the dominant energy improvement comes from tracking the azimuth, this would be a likely solution where a lower cost or less complex system is desired.

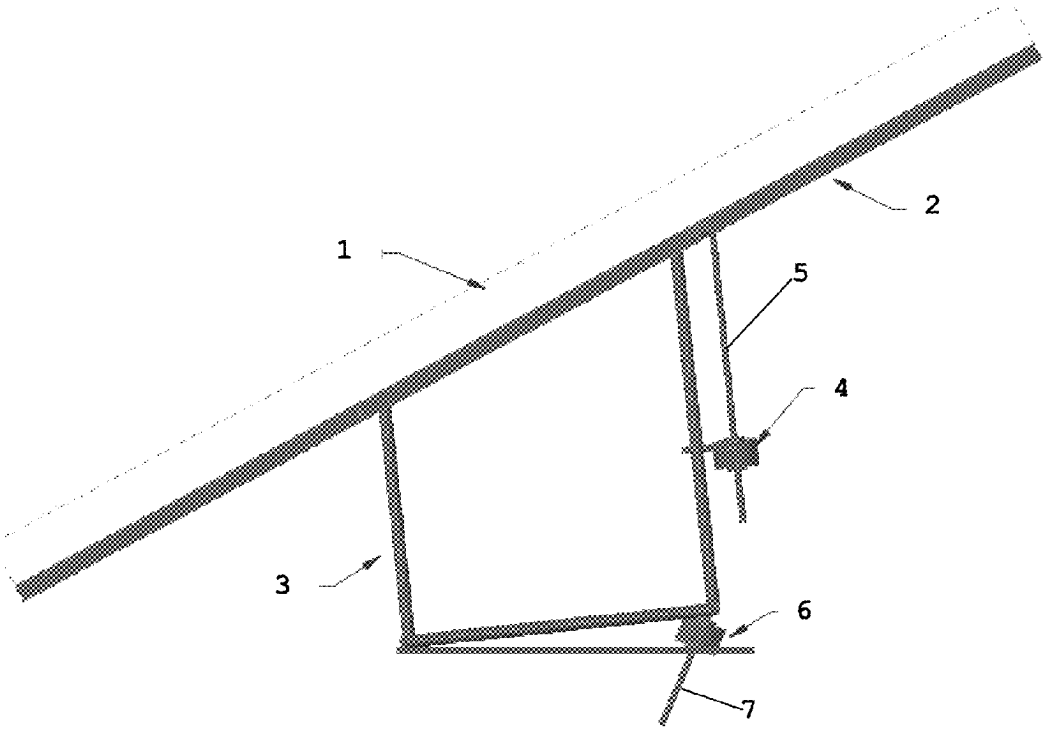

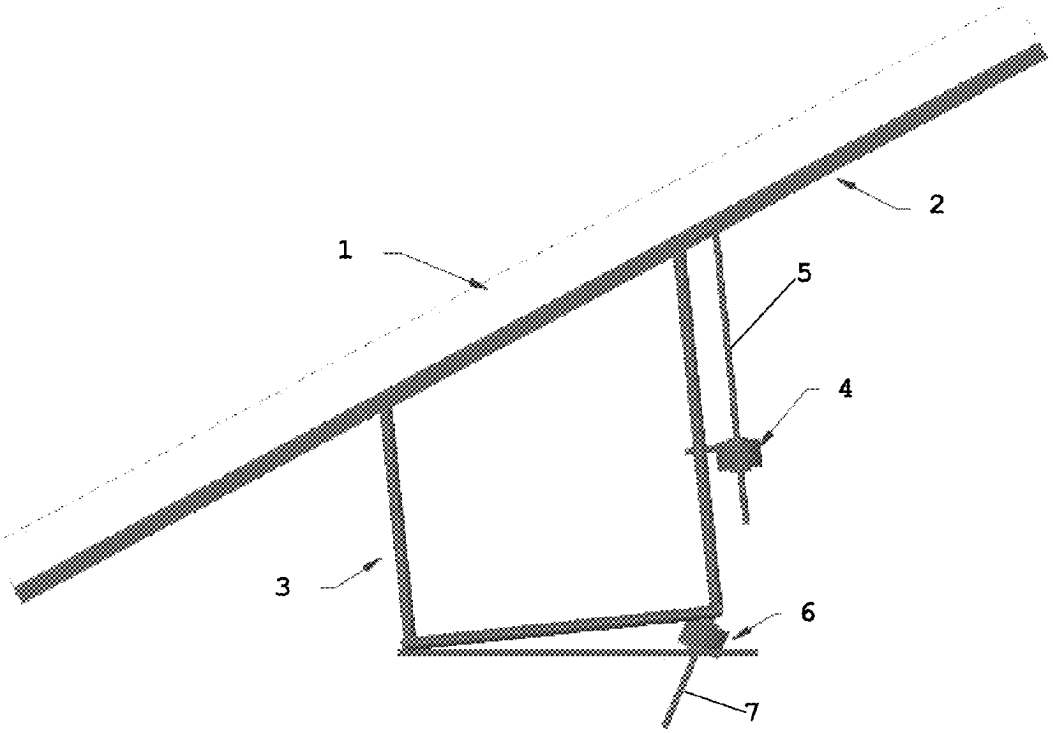

FIG. 1

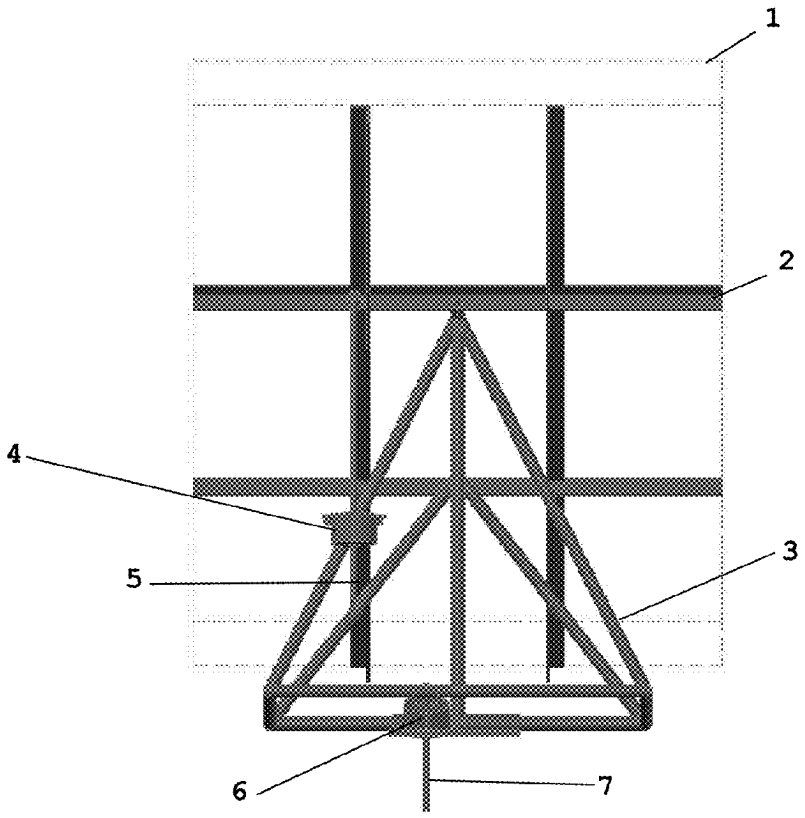
1
2
4
5
3
6
7

FIG. 2

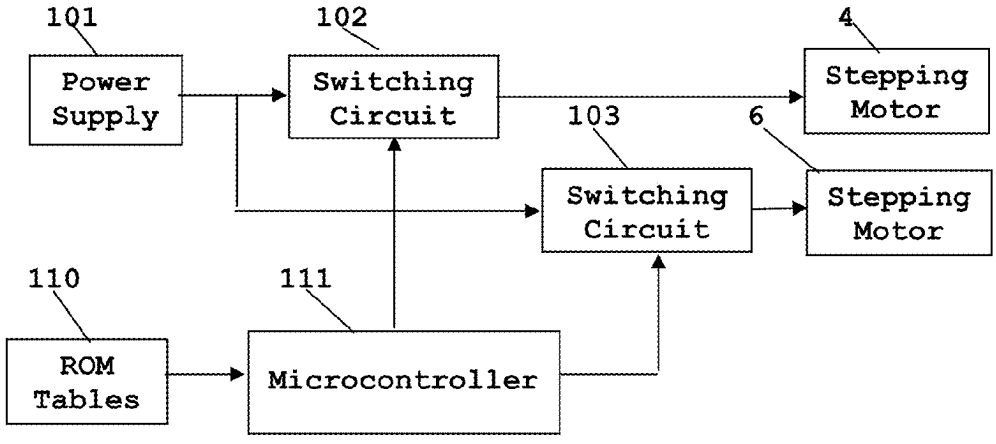
101
Power Supply
102
Switching Circuit
4
Stepping Motor
103
6
Switching Circuit
Stepping Motor
110
ROM Tables
111
Microcontroller

FIG. 3

SOLAR TRACKING

CLAIM OF PRIORITY

[0001] This application claims priority under 35 U.S.C. 119(e)(1) to U.S. Provisional Application No. 61/112,738 filed Nov. 8, 2008.

TECHNICAL FIELD OF THE INVENTION

[0002] The technical field of this invention is solar tracking and more specifically solar tracking for a single solar panel.

BACKGROUND OF THE INVENTION

[0003] Conversion of light from the sun into electricity depends on the orientation of the solar panel to sun. By following the sun's daily change of azimuth and annual variations in elevation as a result of the location with respect to the Earth's curvature, the total output of the solar panel can be increased substantially. Some solar trackers report greater than 40% increase in total power output.

[0004] Implementing a solar tracker for a single solar panel is not popular because they are not cost effective. Existing tracking systems are designed for groups of solar panels typically from 10 to 20 at a time. This makes the cost of the system more acceptable. While solar tracker systems are readily available, they are usually designed on a steel pipe mast and must be mounted on a poured concrete block on the ground. These systems are typically not suited to integration with a residential roof.

SUMMARY OF THE INVENTION

[0005] This invention is a solar tracker with a simple two axis system operated with integrated stepping motors and lead screw actuators that provides the necessary structural support and two degrees of freedom in the motion of the solar collector, to increase the electrical output of the system. Because this invention is designed for use with only one solar panel, the mechanical forces such as wind load are much lower than seen in systems for groups of solar panels and easier to manage. The invention may also be practiced in a single axis version where the base is fixed and the elevation is set at an average value for the location and the pivoting mechanism operates the azimuth axis. Since the dominant energy improvement using solar tracking comes from tracking the azimuth, such a single axis systems provides a lower cost and less complexity than two axis systems.

BRIEF DESCRIPTION OF THE DRAWINGS

[0006] These and other aspects of this invention are illustrated in the drawings, in which:

[0007] FIG. **1** is a side view of the invention;

[0008] FIG. **2** is a rear view of the invention; and

[0009] FIG. **3** is a block diagram of the control circuit for the stepper motors.

DETAILED DESCRIPTION OF PREFERRED EMBODIMENTS

[0010] This invention is a method and apparatus for solar tracking. This application describes numerous specific details in order to provide a thorough understanding of the present invention. One skilled in the art will appreciate that one may practice the present invention without these specific details. Additionally, this disclosure does not describe some well known items in detail to not obscure the present invention.

[0011] The invention is a simple 2 axis solar panel tracking system. This solar panel tracking system is operated using integrated stepping motors and lead screw actuators. These components provide structural support and two degrees of freedom in the motion of the solar panel. This solar panel tracking increases the electrical output of the system. This invention is designed for use with only one solar panel. Therefore the mechanical forces such as wind load are much lower and easier to manage than prior art tracking systems which control groups of solar panels.

[0012] An alternative embodiment includes a single axis where the base is fixed and the elevation is set at an average value for the location. In this alternative embodiment a pivoting mechanism operates the azimuth axis. Since the dominant energy improvement comes from tracking azimuth, this alternative embodiment would be useful where a lower cost or less complex system is desired.

[0013] FIG. **1** is a side view of the invention. FIG. **2** is a rear view of the invention. Solar panel **1** is mounted to sub frame **2** to provide a means of attachment and support to the actuation system. Stepping motor **4** having a concentric lead screw **5** is mounted to base frame **3** on a pivoting bracket and terminates as a tie rod end on a pin fixed to sub frame **2**. Sub frame **2** is attached to base frame **3** by two pivot shafts at the midline. This arrangement permits simple motion of solar panel **1** in azimuth.

[0014] Base frame **3** is mounted to a plate with simple hinge type bearings at one end and a second stepping motor **6** and concentric lead screw **7** to allow elevation of the assembly. Base frame **3** should be designed taking into account the maximum winter solar angle of elevation to reduce the total range of motion required for seasonal adjustment. The known combination of integrated lead screw and stepping motor can easily achieve 0.001" accuracy. Thus this arrangement enables precise control of the azimuth and elevation.

[0015] The second embodiment of the invention eliminates stepper motor **6** and lead screw **7**. Sub frame **2** is mounted on base frame **5** at a fixed elevation. This fixed elevation is selected having an angle corresponding to the average solar elevation at the location of the installation. Because azimuth solar tracking provides most of the benefit of solar tracking, this single axis embodiment provides substantial benefit at reduced cost.

[0016] FIG. **3** is a circuit diagram of the control circuit for stepper motors **4** and **6**. Power supply **101** supplies electric power to switching circuits **102** and **103**. Switching circuit **102** supplies switched power to stepping motor **4**. Switching circuit **103** supplies switched power to stepping motor. Microcontroller **111** controls the switching of both switching circuits **102** and **103**. Microcontroller **111** consults data stores in ROM tables **110** regarding the solar azimuth and elevation for the current time. Microcontroller **111** causes switching circuits **102** to supply electric power to stepping motor **4** and switching circuits **103** to supply electric power to stepping motor **6** to control the orientation of solar panel **1**. For the alternate embodiment having only one axis, the circuit of FIG. **3** is modified to eliminate switching circuit **103** and stepping motor **6**.

[0017] Other embodiments of the present invention will be apparent to those skilled in the art after considering this disclosure or practicing the disclosed invention. The specifi-

cation and examples above are exemplary only, with the true scope of the present invention being determined by the following claims.

What is claimed is:

1. A solar tracker for a solar panel, comprising:

a subframe having a solar panel mounted thereon;

a base frame;

a first stepping motor, a corresponding first lead screw and a corresponding first tie rod mounted between said subframe and said base frame disposed for movement of said subframe in azimuth relative to said base frame; and

a second stepping motor, a corresponding second lead screw and a corresponding second tie rod mounted between said subframe and said base frame disposed for movement of said subframe in elevation relative to said base frame.

2. The solar tracker of claim **1**, wherein:

said base frame and said second stepping motor, said corresponding second lead screw and said corresponding second tie rod mounted corresponding to a maximum winter solar angle of elevation for a installation location to reduce the total range of motion required for seasonal adjustment.

3. The solar tracker of claim **1**, further comprising:

a electronic controller connected to said first stepping motor and said second stepping motor, said electronic controller controlling said first stepping motor and said second stepping motor to cause said solar panel to track daily sun movement.

4. A solar tracker for a solar panel, comprising:

a subframe having a solar panel mounted thereon;

a base frame, said subframe mounted on said base frame at a fixed elevation corresponding to an average solar elevation for a installation location; and

a stepping motor, a corresponding lead screw and a first tie rod mounted between said subframe and said base frame disposed for movement of said subframe in azimuth relative to said base frame.

5. The solar tracker of claim **1**, further comprising:

a electronic controller connected to said stepping motor, said electronic controller controlling said stepping motor to cause said solar panel to track daily solar movement.

* * * * *

Title	Patent/Publication Number	Date	PV or CSP?	Actuation Type	Innovation
Solar Tracker	US 7,884,279 B2	Feb. 8, 2011	PV	Tip-Tilt --- 2 linear actuators	Tracker can fold up in high wind to minimize damage, folding action is also what controls elevation angle.
Solar Tracker	US 7,799,987 B1	Sept. 21, 2010	PV	Tip-Tilt	Works like a sunflower thing bends around by shrinking/extending some side of the column. Claims it ca be done with capillary action.
1 and 2 axis solar tracker	US 2010/0326427 A1	Dec. 30, 2010	Not Specified	Tip-Tilt Hybrid	Interesting design, severely limited in elevation tilt angle, more for azimuthal tracking.
2 Axis Solar Tracking System	US 2010/0288062 A1	Nov. 18, 2010	More PV	Tip-Tilt	Designed for single solar panel, uses 3 points to define plane
Low Profile Solar Tracking Module	US 2009/0250095 A1	Oct. 9, 2009	PV	Tip-Tilt	basically a stacked Gimble. Single point of control for tip, many control for tilts.
Solar Tracking	US 2010/0282243 A1	Nov. 11, 2010	Either	Tip-Tilt	Tip entire structure, not just panels. Uses 2 linear actuators, the second on being used for standard tilt in azmuth direction.
Solar Tracking Mechanism	4,628,142	Dec. 9, 1986	Either		Solar receiver at bottom of base on rotating shaft. Sun concentrated on shape memmory alloy coil or solar cell
Solar Tracker with 2 Axes	US 2010/0012113 A1	Jan. 21, 2010	PV	rotation in two directions	Rotate in two directions in either direction around vertical axis
Solar Tracking Device for Solar Cells	US 2011/0017270 A1	Jan. 27, 2011	CSP		One support (support and rotate) unit and one moving (XY) unit no concrete base
Dual-Axis Solar Tracker	US 2010/0024861 A1	Feb. 4, 2010	PV	rotation in two directions	Moving support system that rotates using wheels

Figure E.1: Table of Related Patents

Appendix F

Preliminary Designs

F.1 Initial Brainstorm

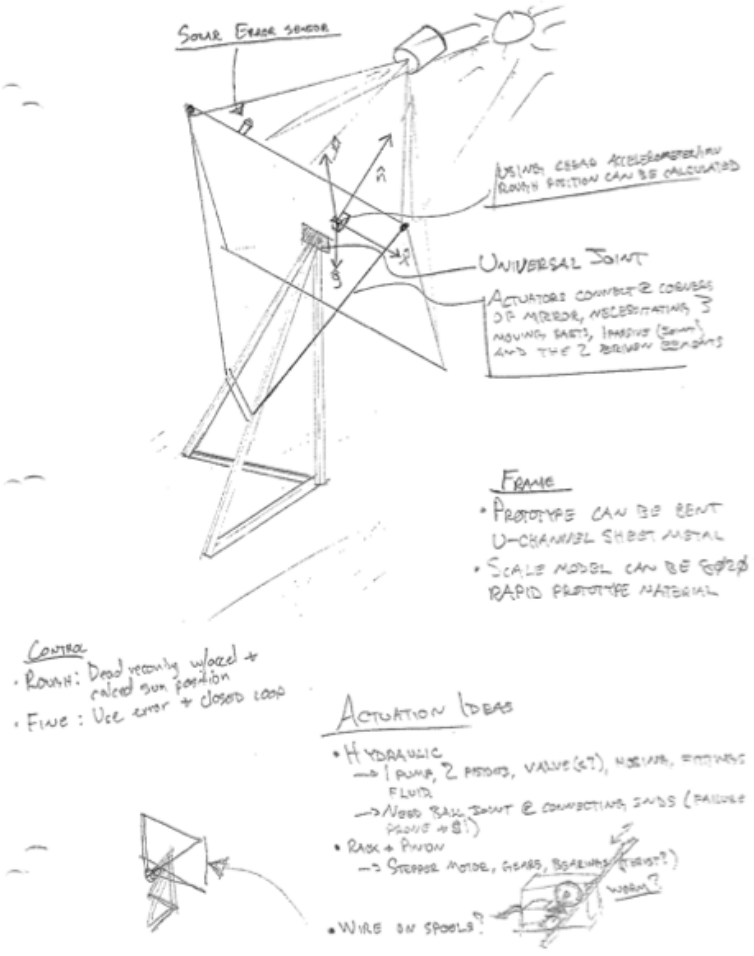

Figure F.1: Design 1

Figure F.2 represents two independently rotated planes. One on the bottom to provide azimuthal control, the other to provide elevation control. For small models, this design lends itself well to use of servos but at larger scales, motors will need to be used. A Lazy Susan-type of bearing plate can be used to provide a rotating base platform if gears are used to provide rotation of the bottom plate.

Figure F.3 represents a modified actuation idea for design 1. In this idea, opposite corners of the mirror are connected with tensioned wire, and wound about a spool that can be turned

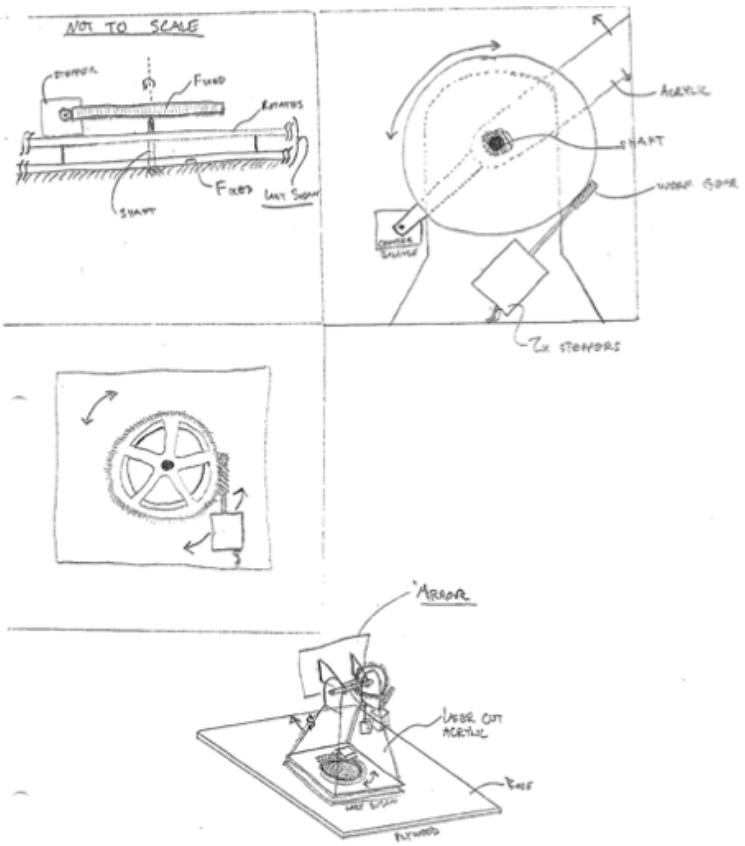

Figure F.2: Design 2

with a motor. When the spool rotates, the relative lengths of the two wires will natrually change the distance of the spool to the plane (think of it as a triangle). We believe there are several ways to compensate for this. One example would be to use adjustable cable tensioners which allow extra slack to be introduced into the system, while keeping the cables taught.

Figure F.7 represents the basis of this design is to move like a joystick. This movement is achieved by controlling the shaft that the dish sits on from the bottom with two hydraulic cylinders. The actuation allows the shaft to pivot on a ball joint, allowing it to sweep and track the sun across the sky.

Figure F.8 is essentially the same design as design 7 except magnets attract the metal shaft to particular positions. It is similar in concept to a stepper motor. At the base there are several magnets that have electrical current pass through their coils in order to attract the metal rod. These are arranged along a spherical bowl in which the rod sweeps along.

Figure F.9 is a design which utilizes the principle that one needs three points to define a plane. The actuators the dish is attached to move up and down in order to control the tilt of the dish.

Figure F.10 is a design which controls the elevation angle through the use of two linear actuators that move either up or down in order to adjust the tilt of the dish. These actuators

are attached to a lazy susan base that rotates in order to adjust the azimuth angle. The lazy susan rotates using a DC motor and spur gears, which are cheap and simple to utilize.

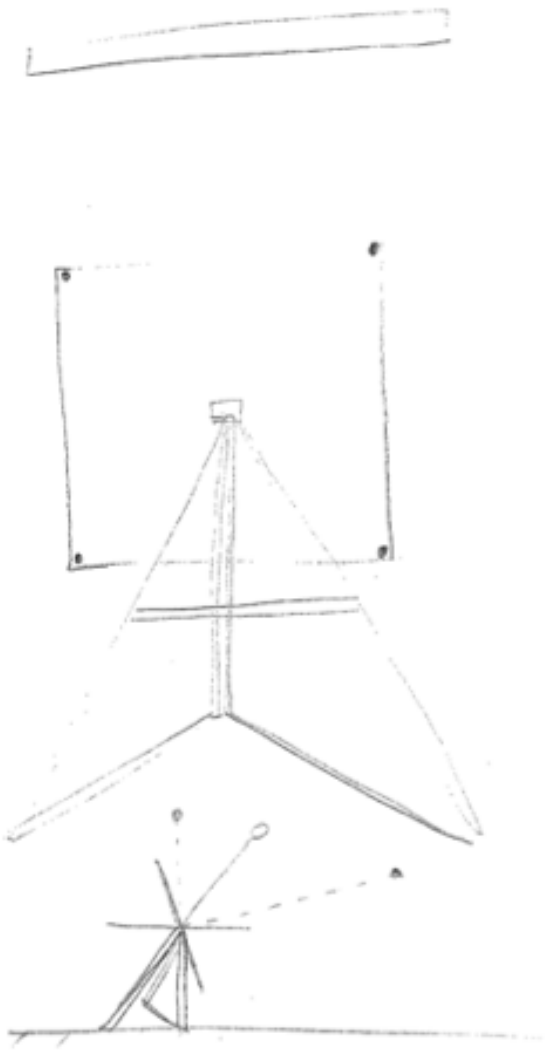

Figure F.3: Design 3

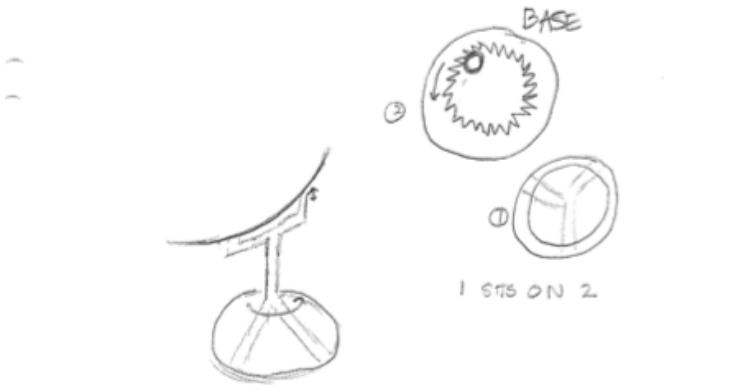

THREE LEG SUPPORTS ROTATE ON CIRCULAR BASE TO CHANGE POSITION IN AZIMUTHAL DIRECTION THEN TIP TILT BY LINEAR ACTUATORS BASED ON THE SUNS LOCATION. THE BASE SPINS BY A GEAR BASED ON THE STEPPER MOTOR. THERE IS ONLY ONE LINEAR ACTUATOR BECAUSE ONLY ONE SIDE NEEDS TO CHANGE THE ANGLE OF THE DISK

Figure F.4: Design 4

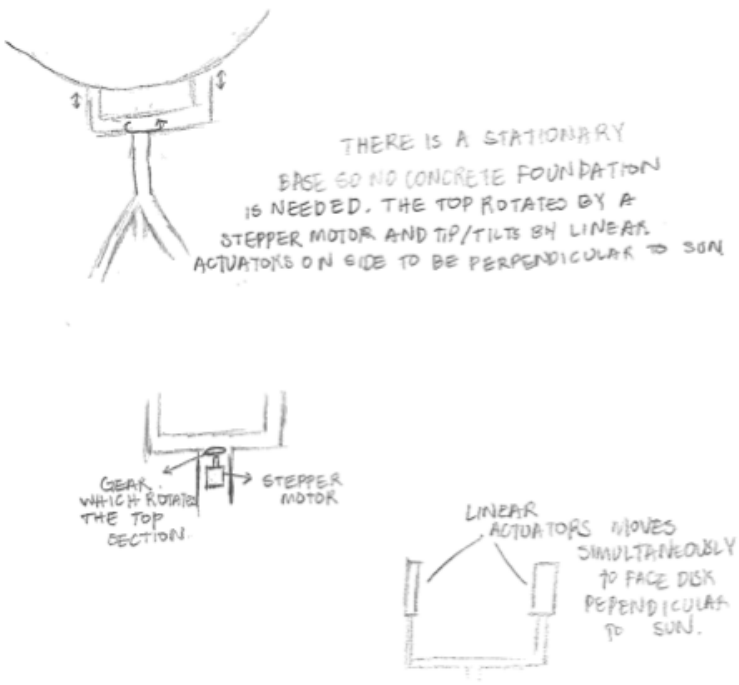

Figure F.5: Design 5

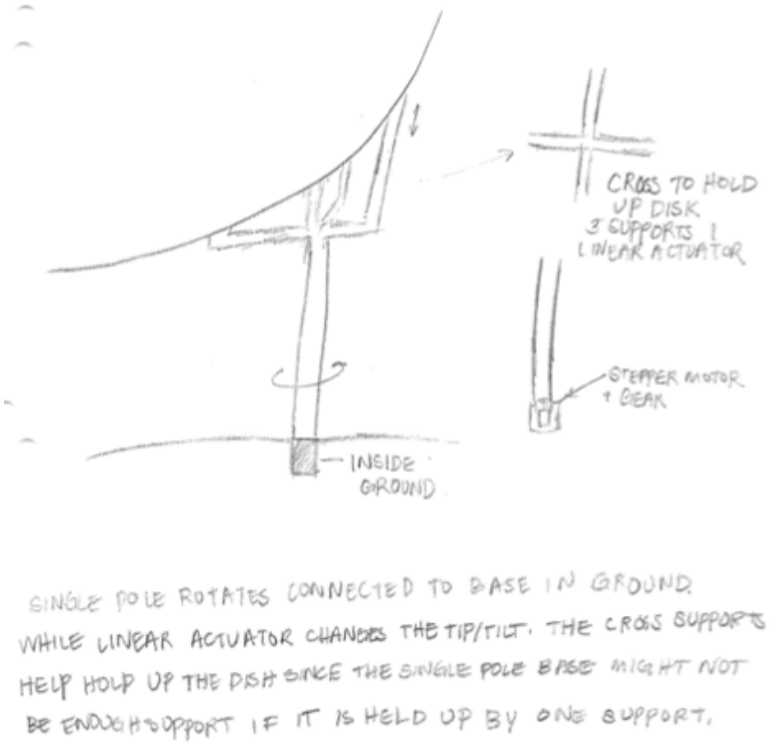

Figure F.6: Design 6

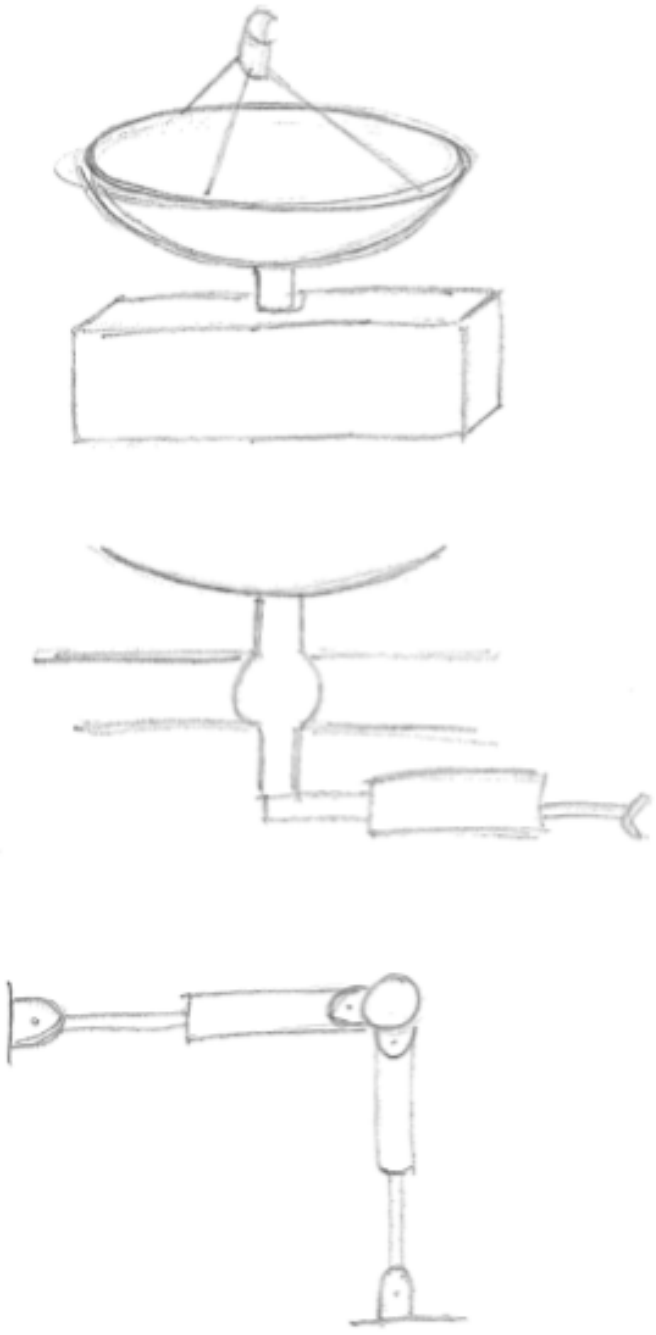

Figure F.7: Design 7

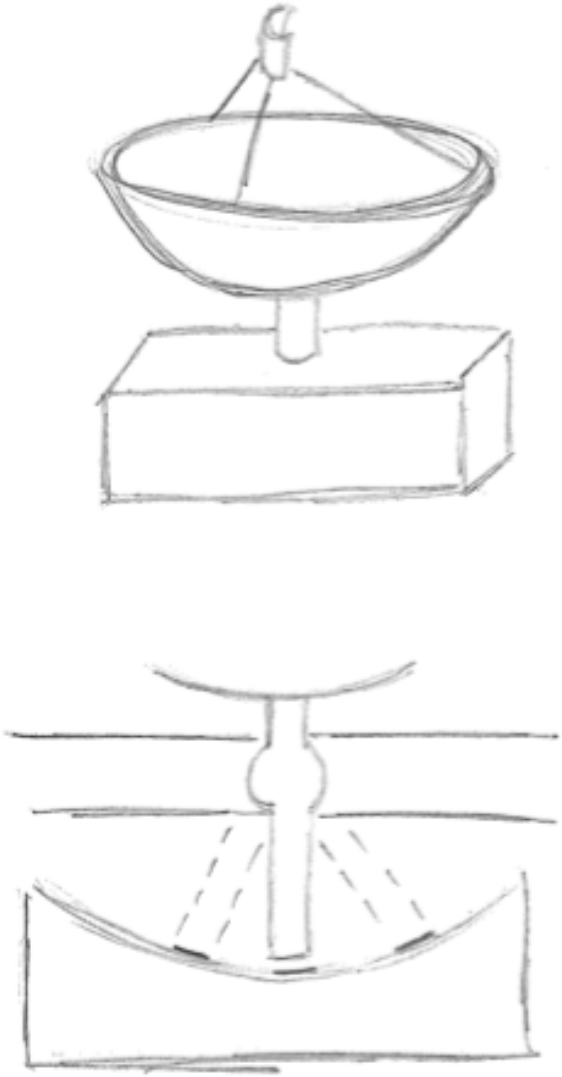

Figure F.8: Design 8

Figure F.9: Design 9

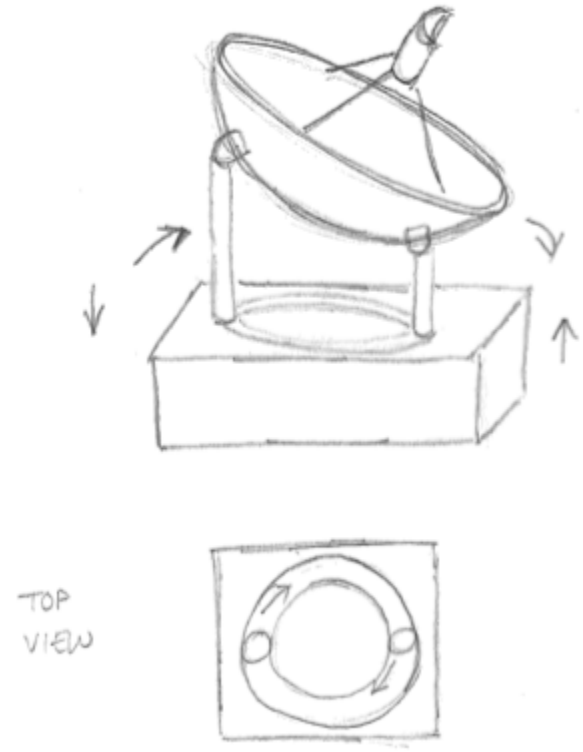

Figure F.10: Design 10

F.2 Design Scoring

F.3 Performance Design Specifications

ELEMENTS/	PARAMETERS			
REQUIREMENTS	UNITS	DATUM	TARGET - RANGE	AS_BUILT
SPECS				
Azimuth rotation angle	Degrees	+/-90	+/-90	+/-70
Elevation tilt angle	Degrees	0-90	0-90	5-90
Tracking accuracy	Degrees	+/-0.5	0.1-0.5	0.5
Height @ max. titlt (excluding panels)	Feet	21	5 (SCALED)	3.5
Width (excluding panels)	Feet	15.4	3 (SCALED)	6
Weight (excluding panels)	Pounds	1900	60 (SCALED)	60
OPERATIONS				
Drive consumption	Kilowatt hour/day	0.16	0.16	0.11
Drive operating voltage	Volts	240 VAC 1ϕ/ 208 VAC 3ϕ	24	24
Temperature rating	Celsius	-40 to +55	-40 to +55	-40 to +55
Wind load (max operation)	miles/hour	31	40-50	40
ENERGY PERFORMANCE				
Improvement over fixed-tilt rack (for photovoltaic power generation)	Percentage	40	40-45	N/A

	TARGET or	DESIGN IDEAS																	
CRITERIA	FACTOR	1 = Baseline		two		three		four		five		six		seven		eight		nine		ten	
Time – Design	90	90		70		90		60		70		60		40		60		60		40	
Time – Build	60	60		40		50		60		60		60		50		80		60		50	
Time – Test	30	30		30		30		30		30		30		30		30		30		30	
Time Score	3.5		3.5		2.85		3.11		3.11		3.24		3.11		2.66		3.50		3.11		2.66
Cost – Prototype	$ 500	$ 500		$ 600		$ 600		$ 600		$ 550		$ 600		$ 700		$ 900		$ 650		$ 600	
Cost – Production	$ 2,500	$ 2,500		$ 3,000		$ 3,000		$ 3,000		$ 2,750		$ 3,000		$ 3,500		$ 4,500		$ 3,250		$ 3,000	
Cost Score	3		3		3.60		3.60		3.60		3.30		3.60		4.20		5.40		3.90		3.60
Machining	0.5	5	1.5	4	2	2	1	2	1	2	1	2	1	4	2	1	0.5	2	1	2	1
Range of Motion	5.5	5	16.5	5	27.5	3	16.5	4	22	4	22	4	22	2	11	2	11	4	22	4	22
Mounting Hardware	1.5	3	4.5	1	1.5	3	4.5	2	3	3	4.5	1	1.5	7	3	2	3	2	3	2	3
Control Mechanism	2	3	6	4	8	2	4	4	8	4	8	4	8	5	10	2	4	4	8	4	8
Sweep Volume	5	3	15	2	10	3	15	2	10	3	15	3	15	2	10	2	10	3	15	3	15
Actuator Force	3.5	3	10.5	2	7	4	14	3	7	3	10.5	1	3.5	2	7	1	3.5	2	7	3	10.5
	TOTAL		54.0		56.0		54.6		51		61.0		50.8		42.6		29.6		55.5		59.7
	RANK																				
	% MAX		88.6%		91.9%		89.6%		83.7%		100.0%		83.3%		70.0%		48.6%		91.0%		98.0%
	MAX	61.0																			

NOTE: User fills in Yellow areas, gold areas are calculated or fixed

BASELINE = first design

Timescore(i)=Timescore(B)*(TD(i)/TD(B) + TB(i)/TB(B) + TT(i)/TT(B))/3

Costscore(i)=Costscore(B)*(Cprot(i)/Cprot(B) + Cpro(i)/Cpro(B))/2

Total(i) = SUM(Factor(j)*Comparison(i,j)) + (Timescore(B)-Timescore(i)) + (Costscore(B) - Costscore(i))

Design Idea Descriptions

two	follows the design sketches found in the Appendix
three	
four	
five	
six	
seven	
eight	
nine	
ten	

Comparison(i,j) = 5 if idea "i" is much better than baseline for criteria "j"

Comparison(i,j) = 4 if idea "i" is better than baseline for criteria "j"

Comparison(i,j) = 3 if idea "i" is same as baseline for criteria "j"

Comparison(i,j) = 2 if idea "i" is worse than baseline for criteria "j"

Comparison(i,j) = 1 if idea "i" is much worse than baseline for criteria "j"

Appendix G

Customer Interviews

G.1 Interview Questions

1. How would you describe the market for solar trackers? What is the biggest issue with tracking solutions today?
2. What are the most common complaints you have or receive from customers?
3. How often is maintenance needed on a solar tracking system and which parts are the usual causes of breakdown?
4. What is the average return rate of investment for a solar tracker versus a fixed PV array system? If the ROI is shorter for tracking systems than fixed, is this point heavily communicated to customers?
5. What would constitute an ideal solar tracker in order to get the best performance out of solar energy systems

Customer: Joe Sugg	**Interviewer:** Darcy Marumoto
Address: 500 El Camino Real, Santa Clara, CA 95053	**Date:** October 21, 2011
Telephone: (408) 551-1606	**Product Used:** Chromosun
Willing to do follow-up?: Yes	**Type of User:** Facilities Manager

Table G.1: Contact information for Joe Sugg.

G.2 Interview Responses

Question/Prompt	Customer Statement	Interpreted Need
Current Market	Don't know.	Don't know much about the product and its uses. The technology isn't well-known.
Current Issue	Cost and maintenance.	The price of the product needs to be significantly lower and maintenance on the product is too frequent.
Customer Complaint	The system currently in use is not very reliable.	Solar tracking system need to be very reliable with minimal monitoring.
Maintenance of System	N/A	Maintenance isn't completed by the user but rather than the company and should be more interactive for the user.
Average ROI of Tracker vs. Fixed Array	No capital investment so the energy costs for the school is 5% less than before.	The return on cost should be higher for the amount of power being installed.
Ideal tracker	What our product should be when the project is complete.	Looking for something which works well, compact and has a low cost.

Table G.2: Response and interpreted need gathered from Joe Sugg's interview.

Customer: Mark Freeman	**Interviewer:** Joseph Valdez
Address:1430 Enterprise Blvd., West, Sacramento, CA 95691	**Date:** October 21, 2011
Telephone: (916) 374-8722 ext. 114	**Product Used:** Dual Axis Solar Trackers
Willing to do follow-up?: Yes	**Type of User:** Solar Contractor

Table G.3: Contact information for Mark Freeman.

Question/Prompt	Customer Statement	Interpreted Need
Current Market	There are many solutions today with the industry growing base upon the politics and economy	The customer changes what the product looks and does and has to meet the standards the government puts forth.
Current Issue	Size and scale of the application. Also weather is a big factor to whether or no solar trackers are used.	The product needs to be scaled down for residential use to open the market and needs to be able to harvest energy under different conditions.
Customer Complaints	Too expensive because of shipment and training for electricians are needed to transition to work from AC to DC.	Trackers require a different conversion of energy into electricity, which causes installation problems. Also price is driven mainly due to shipping cost which is a large overhead to the customer.
Maintenance of System	Minimal maintenance to grease bearings and gears.	Maintenance shouldn't be frequent and should be something the users can do themselves.
Average ROI of Tracker vs. Fixed Array	Not determined by the installer of the product.	Every aspect of the process should be involved with costs just in case the user has any questions about the product.
Ideal tracker	Something that increases the power production of the system and gets more from the money spent.	The tracker needs to harvest more energy than a fixed system. Also the customer needs to see their money spent is toward a good investment.

Table G.4: Response and interpreted need gathered from Mark Freeman's interview.

Customer: Carlos Garcia	**Interviewer:** Joseph Valdez
Address: N/A	**Date:** October 21, 2011
Telephone: 34 608232550	**Product Used:** Manufactures dual-axis trackers.
Willing to do follow-up?: Yes	**Type of User:** Solar Contractor

Table G.5: Contact information for Carlos Garcia.

Question/Prompt	**Customer Statement**	**Interpreted Need**
Current Market	For PV or CSP solar systems.	Trackers have a wide range of uses on any type of solar energy system.
Current Issue	Pole mounted systems and the wind load the system can handle.	Current systems have very expensive and permanent foundations and mainly mounted with poles. Also, the wind tolerance of trackers need to increase.
Customer Complaints	No comment.	N/A
Maintenance of System	Structure and driving system is completely separate so there is long-term reliability. Also many of the parts can be found in store and an easy to do fix.	If there is any maintenance that needs to be done, the user should be able to do it quickly without a specialized crew.
Average ROI of Tracker vs. Fixed Array	Tracker systems gain approximately 45% more energy than fixe systems and thus should have the same rate of return on investment.	Trackers should have about the same or only slightly longer return rate of investment.
Ideal tracker	A system that is reliable, a high energy yield, low cost and minimal maintenance.	The ideal tracker is one that would be the most effective and user friendly.

Table G.6: Response and interpreted need gathered from Carlos Garcia's interview.

Appendix H

Project Management Data

H.1 Timeline

	Task Mode	Task Name	Duration	Start	Finish	Predecessors
1		**Design Tracker**	**31 days**	**Mon 9/19/11**	**Mon 10/31/11**	
2		Research Exisiting Solutions	25 days	Mon 9/19/11	Fri 10/21/11	
3		Patent Search	25 days	Mon 9/19/11	Fri 10/21/11	
4		Preliminary Designs	6 days	Mon 10/24/11	Mon 10/31/11	2,3
5		**Prototype I**	**34 days**	**Tue 11/1/11**	**Fri 12/16/11**	
6		Solidworks Design	12 days	Tue 11/1/11	Wed 11/16/11	4
7		Control Algorithm	14 days	Tue 11/1/11	Fri 11/18/11	4
8		Machine Parts and Assemble	10 days	Mon 11/21/11	Fri 12/2/11	6,7
9		Testing	10 days	Mon 12/5/11	Fri 12/16/11	8
10		**Final Design**	**193 days**	**Mon 9/19/11**	**Wed 6/13/12**	
11		**Prototype II**	**45 days**	**Mon 12/19/11**	**Fri 2/17/12**	
12		Design Changes from Prototype I	16 days	Mon 12/19/11	Mon 1/9/12	9
13		Solidworks Design	11 days	Tue 1/10/12	Tue 1/24/12	12
14		Control Algorithm Modification	11 days	Tue 1/10/12	Tue 1/24/12	12
15		Machine Parts and Assemble	10 days	Wed 1/25/12	Tue 2/7/12	13
16		Testing	8 days	Wed 2/8/12	Fri 2/17/12	15
17		**Scaled Proof of Concept**	**55 days**	**Mon 2/20/12**	**Sun 5/6/12**	
18		Design Changes from Prototype II	5 days	Mon 2/20/12	Fri 2/24/12	16
19		Solidworks Design	6 days	Mon 2/27/12	Mon 3/5/12	18
20		Force Analysis	5 days	Mon 2/27/12	Fri 3/2/12	18
21		Order Parts	6 days	Tue 3/6/12	Tue 3/13/12	19,20
22		Machine Parts	14 days	Tue 3/6/12	Fri 3/23/12	19,20
23		Assemble	8 days	Mon 3/26/12	Wed 4/4/12	21,22
24		Testing	23 days	Thu 4/5/12	Sun 5/6/12	23
25		**Papers**	**193 days**	**Mon 9/19/11**	**Wed 6/13/12**	
26		Conceptual Design Review	51 days	Mon 9/19/11	Mon 11/28/11	
27		P3 Phase II Report	31 days	Mon 1/9/12	Mon 2/20/12	
28		Senior Thesis	53 days	Mon 4/2/12	Wed 6/13/12	
29		**Presentations**	**138 days**	**Mon 11/28/11**	**Wed 6/6/12**	
30		Conceptual Design Review	1 day	Mon 11/28/11	Mon 11/28/11	
31		School of Engineering	1 day	Sun 4/15/12	Sun 4/15/12	
32		EPA P3 Conference	2 days	Sat 4/21/12	Mon 4/23/12	
33		Senior Design Conference	1 day	Thu 5/10/12	Thu 5/10/12	
34		Center for Science, Technology and Society	1 day	Mon 5/14/12	Mon 5/14/12	
35		Hardware	1 day	Wed 6/6/12	Wed 6/6/12	

Figure H.1: Timeline of the project over the course of a year.

To keep track of important deadlines and project milestones a Gantt chart was used. The chart summarized each important goal and deadline from the 2011–2012 school year.

H.2 Budget

Figure H.2 is an itemized income and expense report for the project. It helped monitor the cash flow to ensure that the the team did not overspend. As seen in the figure, the budget is divided up into estimated, spent and pending sections. The estimated section helped determine how much the team needed to fundraise to complete the project. When the components were bought (orders placed), it would go into the spent column whereas items waiting to be ordered were placed in the pending column. Finally, the chart shows the net reserve of funds after the project was completed.

TEAM	Helios
DATE	11-Jun-12

INCOME				
Category	**Source**	**Sought**	**Committed**	
Grant	EPA P3	$3,000.00	$3,000.00	
	CSTS	$3,000.00	$3,000.00	
	SCU Engineering	$1,650.00	$1,650.00	
	SCU Undergraduate Travel	$3,132.00	$2,000.00	
	TOTAL	$10,782.00	$9,650.00	**$9,650.00**

EXPENSES					
Category	**Description**	**Estimated**	**Spent**	**Pending**	
Prototypes	Acrylic	$30.00	$21.43		
	Acrylic Adhesive	$5.00	$4.93		
	Mounting Hardware	$20.00	$10.05		
	Servo Motors	$200.00	$40.97		
Base	Acrylic	$30.00	$30.08		
	Acrylic Adhesive	$5.00			
	Mounting Hardware	$20.00	$18.93		
	80/20 Aluminum	$50.00	FREE		
	Lead Screw	$20.00	$20.00		
	Actuator Stops	$60.00	$50.00		
Actuators	Arduino	$40.00	$88.54		
	Stepper Motors	$80.00	$43.19		
	Motor Controller	$150.00	$114.97		
	Linear Actuators	$400.00	$1,981.39		
	Electronic Connections + Sensor	$100.00	$133.83		
Structure	Ply Wood	$30.00	$20.00		
	Aluminum	$200.00	$168.32		
	Sheet Metal	$5.00	FREE		
	Parabolic Mirror	$1,200.00	$309.99		
	Bearings and Couplings	$40.00	$78.91		
Travel	Flight to and from D.C.	$3,132.00	$1,338.80		
	Housing/Meals	$3,000.00	$1,807.88		
	Shipping	$500.00	$2,000.00		
Misc.	Copying/Materials	$100.00	$129.00	$40.00	
	T-shirts	$200.00	$400.00		
	TOTAL	$9,617.00	$8,411.21	$40.00	**$8,451.21**

Net Reserve	$1,198.79

Figure H.2: Itemized expense report.

Note: The budget is an up to date list of all expenses known.

Appendix I

Provisional Patent

Provisional *e*Docket Data Sheet

*e*Docket™ generated 5/1/2012 **Case Reference and Status**

Lumen Ref. No.: **SCU-108/PROV** Case Status: **Filed**

Client Ref. No.: **S12-S01**

Assoc. Ref. No.:

Title: **New Two-Axis Solar Tracker Design for Low Cost Deployment and Profile for Reduced Loading Moments**

Filing Data

Application No.: **61/635239** Assignment No.:

Filing Date: **4/18/2012** Recordation Date:

Applicant(s)

Assignee(s): Santa Clara University

Licensee(s):

Associate:

Gov. Agency:

Contract No.:

Inventor(s)

Matthew Neber
Hohyun Lee
Laughlin Barker
Criselle G. Olaes
Darcy Marumoto
Joseph Valdez

Prosecution History

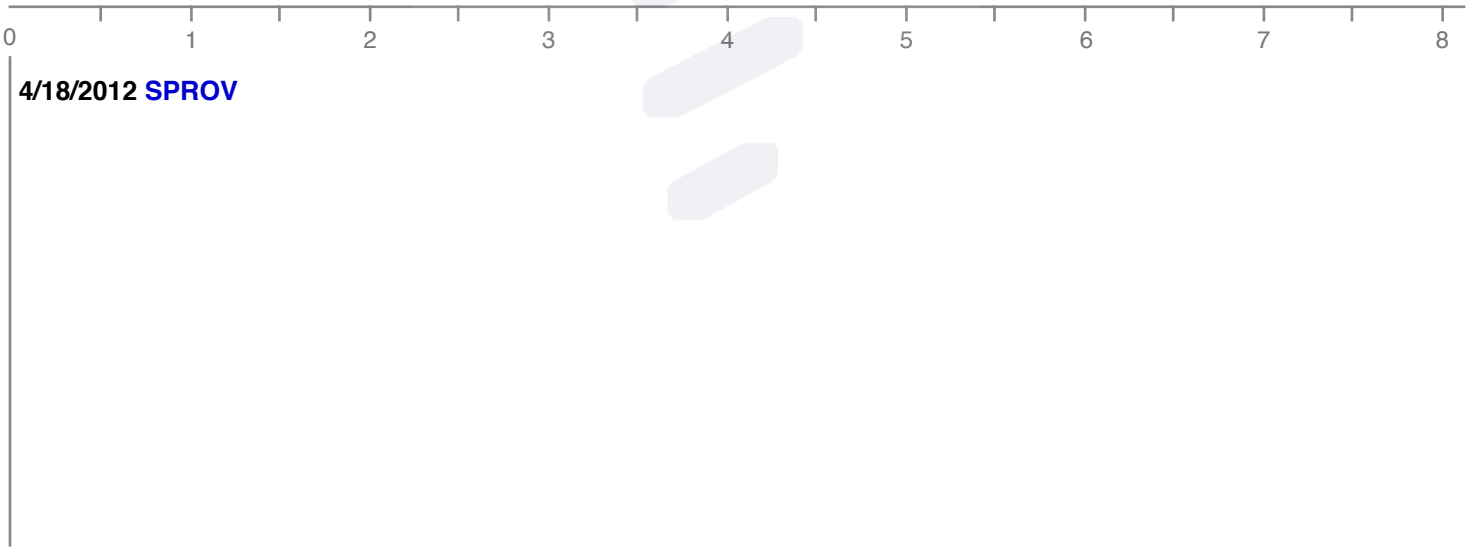

US Provisional Patent Application

for

New Two-Axis Solar Tracker Design for Low Cost Deployment and Profile for Reduced Loading Moments

by

Matthew Neber, Hohyun Lee, Laughlin Barker, Criselle G. Olaes, Darcy Marumoto, and Joseph Valdez

SUMMARY

The solar tracker is a well known device which is essential for any concentrated solar power application, and also greatly improves performance of photovoltaic devices. Representative examples of the state of the art for existing two axis trackers include US 7,884,279, US 7,910,870, US 2006/0054162, and US 2010/0024861. One problem that can arise in connection with solar power is destruction of solar power systems by severe weather. Wind forces are currently an issue with mounting a tracking dish or PV panel atop a pole driven into the ground. Conventional PV tracking systems cannot be regressed for self preservation without disassembly and storage. Another disadvantage of conventional trackers is that they must be mounted atop a tall structure to allow the tracking device to have sufficient ground clearance when tracking the sun at elevations relatively close to the horizon.

The present approach addresses these problems by providing easily produced parts and fewer parts, and a wide base which does not require an augered and cemented post for installation. Systems according to these principles can autonomously lay down flat to weather strong winds. For photovoltaics specifically, this presents an opportunity to have roof mount panels which track the sun without adding any risk to the roof itself in adverse weather conditions. The present approach fixes the base of the tracking device close to the ground for added stability and support in a lower cost and more easily deployable package.

A low cost easily deployable solar tracking unit was conceived for concentrated solar power applications where a large and heavy dish concentrator must articulate to follow the sun's path throughout the sky. The benefits of the design were soon recognized to be applicable to photovoltaic panels as well with the unique feature that the panel may be positioned in a flat, low profile orientation.

In one embodiment, the system includes two perpendicular coplanar linear actuators. Together these two actuators control the azimuth and elevation of whatever device is mounted to the two moving pivot points. This configuration is believed to be new and previously unused. The advantage of this design is the ability to use off the shelf and low fidelity parts instead of manufacturing specifically to the application.

The tracker supports the device tracking the sun at two points for added structural stability over most other trackers, which typically attach at a single pivot point.

However, a large moving base is not necessary as with other trackers which employ a two mount point scheme. Figure 1 and Figure 2 illustrate the tracking system with a concentrated solar power apparatus mounted. The solar collector may easily be replaced by a flat panel supporting a photovoltaic array. Hence the versatility of this system. Note from Figure 2 that by extending the actuator attached to the base to its full length, the solar collector will lay down flat. This proves extremely useful for a solar panel array because of the ability to lay flat in adverse weather conditions, and the possibility to be applied to a roof mounting system for home power generation.

The most common two axis tracking systems currently in use have a single pole driven into the ground combined with a drive unit coupling the pole to the tracking unit. To install the pole an auger must be used, and this can only be installed in climates where the soils will support a heavy post set in with cement. Installation requires considerable work from a civil engineering standpoint because the pressure distribution for a pole in the earth is complex even for simple lateral and axial loads from wind [1]. The single drive unit operates the azimuth and elevation by rotating about vertical and horizontal axes. These drive units contain multiple sets of gears that must be designed to handle very large moments and loads, therefore making them heavy duty pieces of equipment. Also, they often are fitted with heavy counter balances. In contrast, the present approach requires only light anchoring into the ground due to its wide base, and efficiently deals with moment loading from the geometry of the design.

The design geometry is based on triangle manipulation, where two of the triangle’s sides are fixed lengths. By manipulating the position of the two points where the fixed-length sides intersect the base, the angle and orientation of the fixed length sides relative to the plane of the actuators is controlled. The angle between the plane and the fixed length legs is limited to normal, determined by the length ratio of the two fixed-length sides. The orientation of either fixed-length leg in the plane is unconstrained if the two points where the legs intersect the base of the triangle can be positioned at any point along the two principle axes. The described angle and orientation translates to the elevation and azimuth when one of the fixed-length sides is the tracking plane.

In order to orient the tracking plane to any azimuth and elevation in the hemisphere above the actuator plane would require that both actuators be able to move their carriages equally in both directions from the intersection point. With modification of the length ratio the two fixed-length sides, the tracker can cover the sun's path in any part of the world. Between the Tropic of Cancer and Tropic of Capricorn, the actuator paths must cross one another to capture the entire path of the sun, detailed in figure 1 and figure 2.

Figure 3 illustrates the sun's path at Santa Clara University — latitude 37.3414 — at summer and winter solstices. They are the highest and lowest path the sun takes for that location in a year. All other paths lie in between these two lines. The shaded area is the tracker coverage area. Although the details of Figure 3 will depend on location, the general shape of the curves will be

similar, and sufficient coverage can be obtained with the tracker detailed in figure 1 and figure 2 at any location.

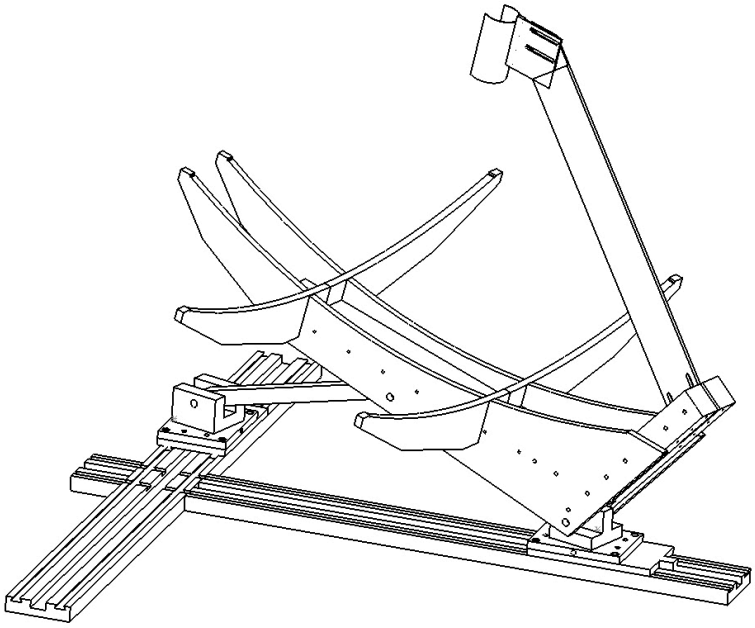

Figure 1. Overview of concentrated solar power tracking unit.

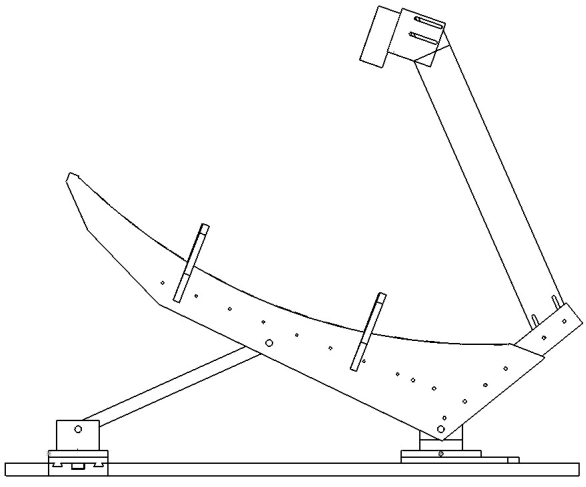

Figure 2. Side view of concentrated solar power unit

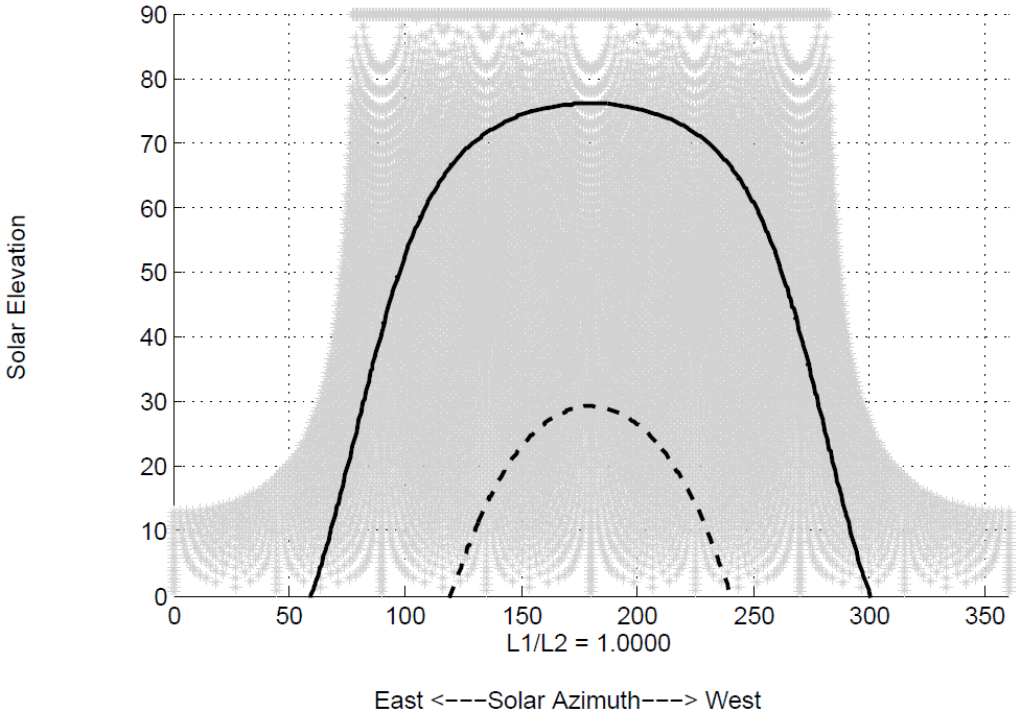

Figure 3. Coverage area of solar tracker. Shaded area represents all possible combinations of elevation and azimuths for a particular geometry. Solid line and dashed line represent sun's path at summer and winter solstices respectively.

One possible variation is mounting multiple panels on a single unified grid system to be driven with a single pair of drive units. The arrays would then be considered a single modular deployable unit driven by only one central location. This would reduce cost by reducing the total number of components and save on power requirements to drive the system by reducing redundancies. The scale of this variation can be as large as megawatt size photovoltaic arrays for utility scale power production. Figure 4 shows a schematic of this concept as it could be applied to a roof mount photovoltaic system. The total number of panels may be decreased by incorporating a tracking system. The panels are also spaced so that they

shade other panels as little as possible during early and late hours.

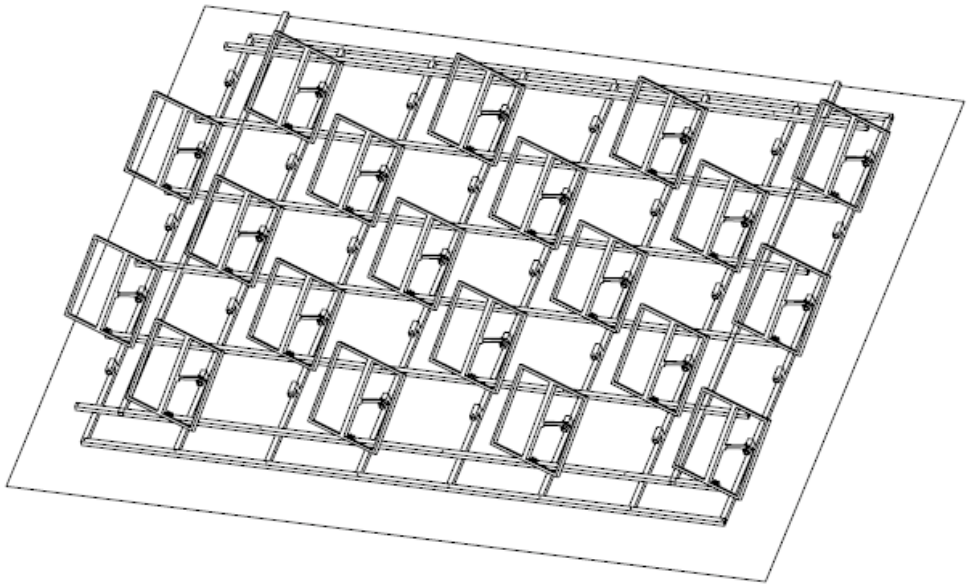

Figure 4. Possible roof array of solar panels on a unified grid system.

Various applications are possible. For concentrated solar power applications this system can be used on large scale commercial and residential units as well as small scale (lab scale) units. Large scale units include dish collectors up to 100 square meters in collector area and are used primarily for renewable power generation. Small scale (lab scale) units are solar collectors that can be easily stored in a room and transported to test sites. For photovoltaic applications the system offers the possibility to roof mount solar panels which may track the sun. The system also provides more support to a photovoltaic module than any currently produced system and offers the ability to retract to a low profile flat position for adverse weather conditions.

[1] J. Anderson and C. Gay, "Solar and Photovoltaic Systems: A short, Basic Course," A. Materials, Ed., ed.

UNITED STATES PATENT AND TRADEMARK OFFICE

UNITED STATES DEPARTMENT OF COMMERCE
United States Patent and Trademark Office
Address: COMMISSIONER FOR PATENTS
P.O. Box 1450
Alexandria, Virginia 22313-1450
www.uspto.gov

APPLICATION NUMBER	FILING or 371(c) DATE	GRP ART UNIT	FIL FEE REC'D	ATTY.DOCKET.NO	TOT CLAIMS	IND CLAIMS
61/635,239	04/18/2012		125	SCU-108/PROV		

CONFIRMATION NO. 9594

30869
LUMEN PATENT FIRM
350 Cambridge Avenue
Suite 100
PALO ALTO, CA 94306

FILING RECEIPT

Date Mailed: 04/27/2012

Receipt is acknowledged of this provisional patent application. It will not be examined for patentability and will become abandoned not later than twelve months after its filing date. Any correspondence concerning the application must include the following identification information: the U.S. APPLICATION NUMBER, FILING DATE, NAME OF APPLICANT, and TITLE OF INVENTION. Fees transmitted by check or draft are subject to collection. Please verify the accuracy of the data presented on this receipt. **If an error is noted on this Filing Receipt, please submit a written request for a Filing Receipt Correction. Please provide a copy of this Filing Receipt with the changes noted thereon. If you received a "Notice to File Missing Parts" for this application, please submit any corrections to this Filing Receipt with your reply to the Notice. When the USPTO processes the reply to the Notice, the USPTO will generate another Filing Receipt incorporating the requested corrections**

Applicant(s)

Matthew Neber, Santa Clara, CA;
Hohyun Lee, Santa Clara, CA;
Laughlin Barker, Santa Clara, CA;
Criselle G. Olaes, Santa Clara, CA;
Darcy Marumoto, Pearl City, HI;
Joseph Valdez, Folsom, CA;

Power of Attorney:
Robert Lodenkamper--55399

If Required, Foreign Filing License Granted: 04/25/2012
The country code and number of your priority application, to be used for filing abroad under the Paris Convention, is **US 61/635,239**
Projected Publication Date: None, application is not eligible for pre-grant publication
Non-Publication Request: No
Early Publication Request: No
** **SMALL ENTITY** **
Title

Two-Axis Solar Tracker Design for Low Cost Deployment and Profile for Reduced Loading Moments

PROTECTING YOUR INVENTION OUTSIDE THE UNITED STATES

Since the rights granted by a U.S. patent extend only throughout the territory of the United States and have no effect in a foreign country, an inventor who wishes patent protection in another country must apply for a patent

in a specific country or in regional patent offices. Applicants may wish to consider the filing of an international application under the Patent Cooperation Treaty (PCT). An international (PCT) application generally has the same effect as a regular national patent application in each PCT-member country. The PCT process **simplifies** the filing of patent applications on the same invention in member countries, but **does not result** in a grant of "an international patent" and does not eliminate the need of applicants to file additional documents and fees in countries where patent protection is desired.

Almost every country has its own patent law, and a person desiring a patent in a particular country must make an application for patent in that country in accordance with its particular laws. Since the laws of many countries differ in various respects from the patent law of the United States, applicants are advised to seek guidance from specific foreign countries to ensure that patent rights are not lost prematurely.

Applicants also are advised that in the case of inventions made in the United States, the Director of the USPTO must issue a license before applicants can apply for a patent in a foreign country. The filing of a U.S. patent application serves as a request for a foreign filing license. The application's filing receipt contains further information and guidance as to the status of applicant's license for foreign filing.

Applicants may wish to consult the USPTO booklet, "General Information Concerning Patents" (specifically, the section entitled "Treaties and Foreign Patents") for more information on timeframes and deadlines for filing foreign patent applications. The guide is available either by contacting the USPTO Contact Center at 800-786-9199, or it can be viewed on the USPTO website at http://www.uspto.gov/web/offices/pac/doc/general/index.html.

For information on preventing theft of your intellectual property (patents, trademarks and copyrights), you may wish to consult the U.S. Government website, http://www.stopfakes.gov. Part of a Department of Commerce initiative, this website includes self-help "toolkits" giving innovators guidance on how to protect intellectual property in specific countries such as China, Korea and Mexico. For questions regarding patent enforcement issues, applicants may call the U.S. Government hotline at 1-866-999-HALT (1-866-999-4158).

LICENSE FOR FOREIGN FILING UNDER

Title 35, United States Code, Section 184

Title 37, Code of Federal Regulations, 5.11 & 5.15

GRANTED

The applicant has been granted a license under 35 U.S.C. 184, if the phrase "IF REQUIRED, FOREIGN FILING LICENSE GRANTED" followed by a date appears on this form. Such licenses are issued in all applications where the conditions for issuance of a license have been met, regardless of whether or not a license may be required as set forth in 37 CFR 5.15. The scope and limitations of this license are set forth in 37 CFR 5.15(a) unless an earlier license has been issued under 37 CFR 5.15(b). The license is subject to revocation upon written notification. The date indicated is the effective date of the license, unless an earlier license of similar scope has been granted under 37 CFR 5.13 or 5.14.

This license is to be retained by the licensee and may be used at any time on or after the effective date thereof unless it is revoked. This license is automatically transferred to any related applications(s) filed under 37 CFR 1.53(d). This license is not retroactive.

The grant of a license does not in any way lessen the responsibility of a licensee for the security of the subject matter as imposed by any Government contract or the provisions of existing laws relating to espionage and the national security or the export of technical data. Licensees should apprise themselves of current regulations especially with respect to certain countries, of other agencies, particularly the Office of Defense Trade Controls, Department of State (with respect to Arms, Munitions and Implements of War (22 CFR 121-128)); the Bureau of Industry and Security, Department of Commerce (15 CFR parts 730-774); the Office of Foreign AssetsControl, Department of Treasury (31 CFR Parts 500+) and the Department of Energy.

NOT GRANTED

No license under 35 U.S.C. 184 has been granted at this time, if the phrase "IF REQUIRED, FOREIGN FILING LICENSE GRANTED" DOES NOT appear on this form. Applicant may still petition for a license under 37 CFR 5.12, if a license is desired before the expiration of 6 months from the filing date of the application. If 6 months has lapsed from the filing date of this application and the licensee has not received any indication of a secrecy order under 35 U.S.C. 181, the licensee may foreign file the application pursuant to 37 CFR 5.15(b).

SelectUSA

The United States represents the largest, most dynamic marketplace in the world and is an unparalleled location for business investment, innovation and commercialization of new technologies. The USA offers tremendous resources and advantages for those who invest and manufacture goods here. Through SelectUSA, our nation works to encourage, facilitate, and accelerate business investment. To learn more about why the USA is the best country in the world to develop technology, manufacture products, and grow your business, visit SelectUSA.gov.

Appendix J

References

J.1 Senior Design Conference Presentation

SANTA CLARA UNIVERSITY 1912-2012 SCHOOL OF ENGINEERING — A Century of Engineering Excellence

DESIGN OF A LOW-PROFILE SOLAR TRACKER WITH HYBRIDIZED CONTROL

LAUGHLIN BARKER, DARCY MARUMOTO, CRISELLE G. OLAES, JOSEPH VALDEZ
BUSINESS STUDENT: OLIVER GLENN

Santa Clara University
Mechanical Engineering
2012

Why Renewable Energy?

Energy Consumption in the United States, 2010

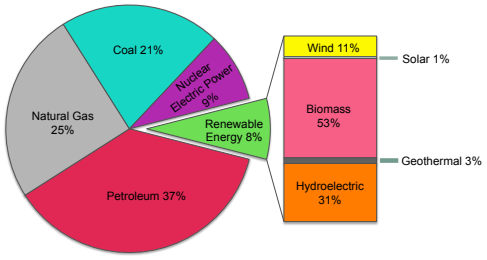

Source: http://205.254.135.7/totalenergy/data/annual/perspectives.cfm

Why Solar?

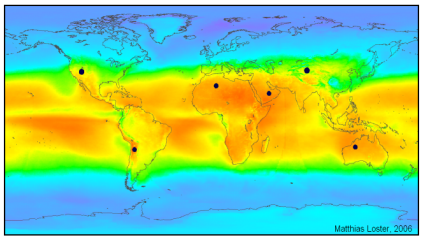

0 50 100 150 200 250 300 350 W/m²

Σ● = 18 TWe

Source: http://physics.ucsd.edu/do-the-math/wp-content/uploads/2011/09/Solar_land_area.png

Existing Technology: PV

Source: http://www.solarpanelcostreview.com/solarpanel cost/sun-tracker-solar-tracker-30/

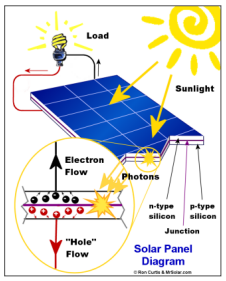

Source: http://save-our-planet-earth-now.blogspot.com/2010/08/how-does-solar-energy-work.html

Existing Technology: CSP

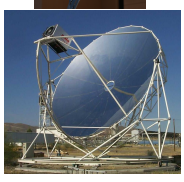

Source: http://www.wikinfo.org/index.php/Solar_tracker

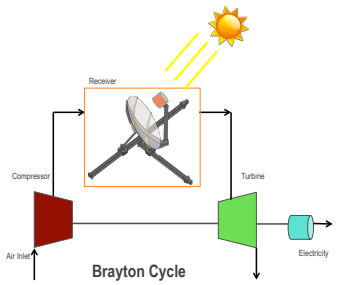

Problem Definition

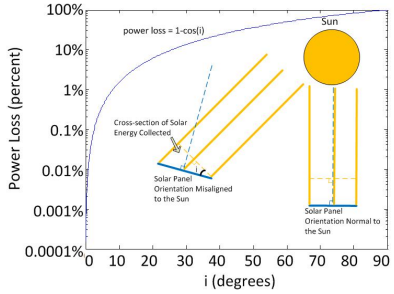

Why Solar Trackers?

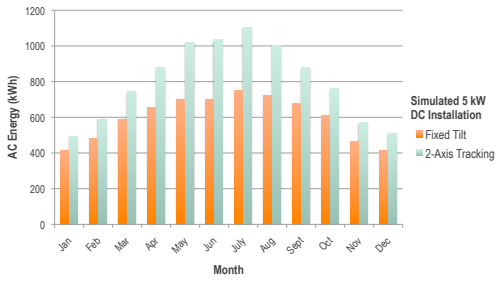

Source: http://rredc.nrel.gov/solar/calculators/PVWATTS

Project Goals

Objectives

- Residential scale
- Affordable price

Technical Challenges

- Reduce forces on parts
- Low sweep volume
- Reduce installation & shipping costs
- Accurate & precise 2 DOF orientation

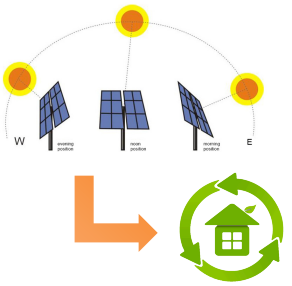

Source: http://www.qldwindmillandsolar.com.au/solar-trackers

Approach

- T-configuration → Low profile
- Off the shelf parts → Low cost
- Hybrid Control → Pointing Precision
- Unique Design → Reduced Install Costs

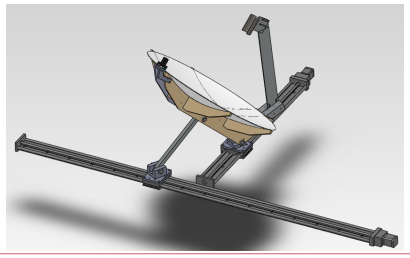

Tracker Range Analysis

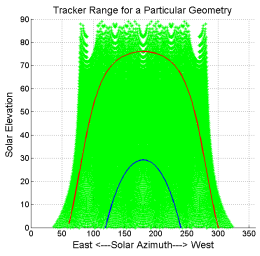

--- Summer solstice June 21st
--- Winter solstice December 21st

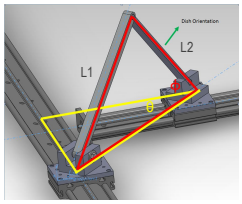

L1 = Length 1
L2 = Length 2
θ = 180 +/- azimuth angle
ϕ = 90 - elevation angle

Sweep Volume

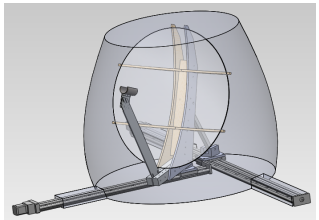

VOLUME = 0.95 m³
SURFACE AREA = 5.67 m²

VOLUME = 0.41 m³
SURFACE AREA = 2.75 m²
+ DEAD VOLUME = 0.69 m³

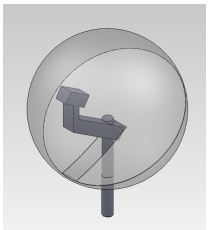

Force Analysis

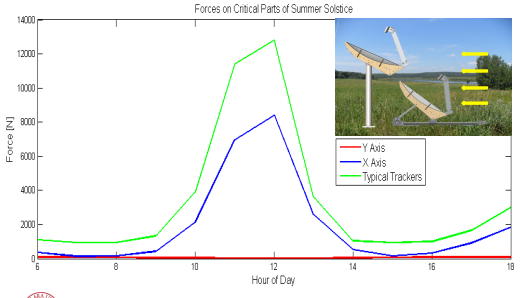

Prototype Tracker

Testing: Precision & Accuracy

How *precise* is positioning?

Hysteresis Test Results n=8	
MEAN	0.05°
MAX	0.14°
STDEV	0.05°

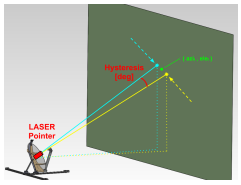

Conclusion

- Tracker is *precise*, but how *accurate*?

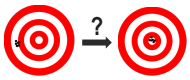

Hybridized Control

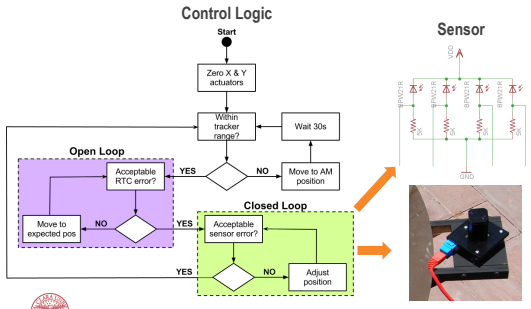

Testing: Hybrid Control

Setup

- Parabolic Mirror
- Receiving cavity + thermocouple

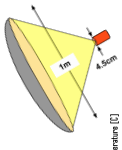

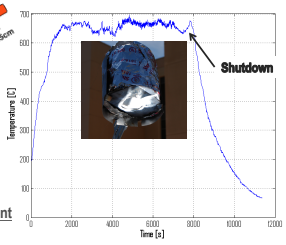

Conclusion

- Maintains focal point inside cavity
- Corrects for installation misalignment

Business Perspective

- Market and Cost Analysis
- Viability of the Business
- Keys to Success

Business Plan

Cost Per 6 Meters^2

Fixed Costs (per unit) 6 meters^2 dish tracker	*Scaled Model*	2012	2013
Parts			
Structure	$150.00	$50.00	$50.00
Motors	$300.00	$100.00	$100.00
Electronics (Actuators*2)	$1,500.00	$500.00	$500.00
Raw Materials	$1,500.00	$500.00	$500.00
Total/unit	$3,450.00	$1,150.00	$1,150.00

Fixed Costs

Fix Cost (per year)	2012	2013
Total	$238,000.00	$204,000.00

Selling Price = $3,500 per 6m^2
Market Average = $2,000 per 6m^2

Breakeven Point = 87 6m^2 units

Cost Comparison

Installation Costs

Average Installation Expense	
Other Trackers	$4,000
Helios Tracker	$1,000

Difference= $3,000

True Price Comparison

Total Price	
Other Trackers	$6,000
Helios Tracker	$4,500

Difference= $1,500

Conclusion

Low Profile

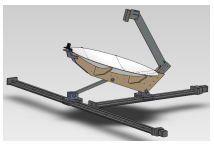

Control

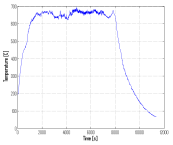

Force Reduction

Cost

Acknowledgements

- Dr. Hohyun Lee
- Matthew Neber
- Dr. Timothy Hight
- Don MacCubbin, Calvin Sellers, & Ursula Uys
- EPA P3
- Willem P. Roelandts & Maria Constantino-Roelandts Grant
- Undergraduate Programs Senior Design Project Funds
- Undergraduate Research Office
- KEEN Foundation

Kern Entrepreneurship Education Network

Questions

helios

Next Steps

Challenges and Improvements

- New mirror holder using less material (lighter weight)
- Design of overhang to achieve larger range
- Reduce Cost
- Ground screw/mount system
- Wind analysis for non-normal loading
- DC motor/worm gear (power consumption)

Source: http://www.kemper-solar.eu/gb/tracker-technology/foundation/

Appendix – Current Range

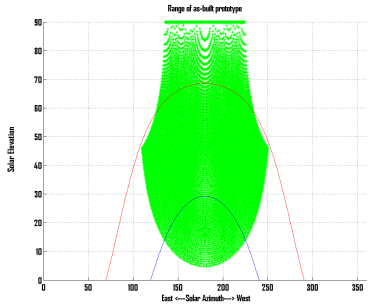

Appendix – Range of Different L1/L2

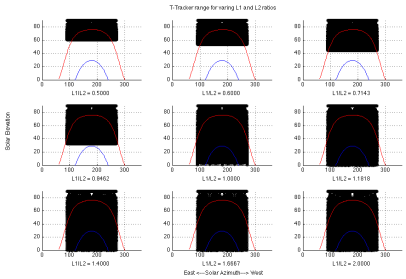

Appendix – Range Added with 22.2% Overhang

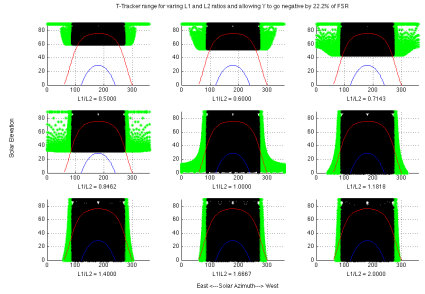

Appendix – Sensor Structure

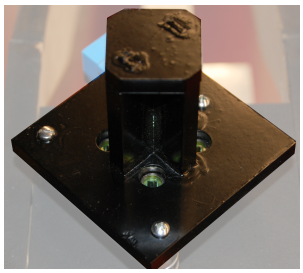

Appendix – Maths…

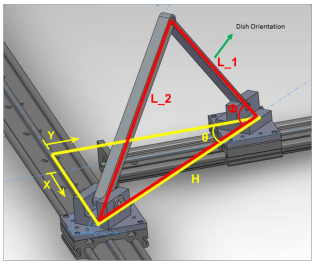

(x,y)→ (azi,ele)

$azimuth = 180 \pm \theta$

$elevation = 90 - \phi$

$$\sec^2(\theta)y^2 - 2L_2\sec(\theta)\cos(\phi)y + (L_2^2 - L_1^2) = 0$$

$$x = y\tan(\theta)$$

(azi,ele)→ (x,y)

$$\theta = \tan^{-1}\left(\frac{X}{Y}\right)$$

$$\phi = \cos^{-1}\left(\frac{L_1^2 - H^2 - L_2^2}{-2HL_2}\right)$$

$$H = \sqrt{x^2 + y^2}$$

Appendix – Electronics

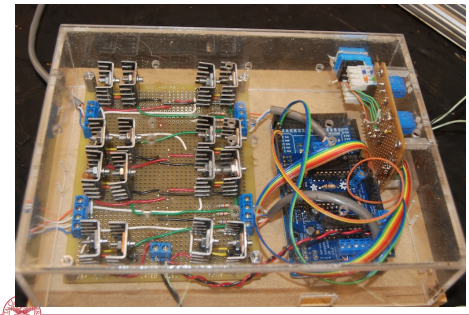

Appendix – Zeroing Actuators

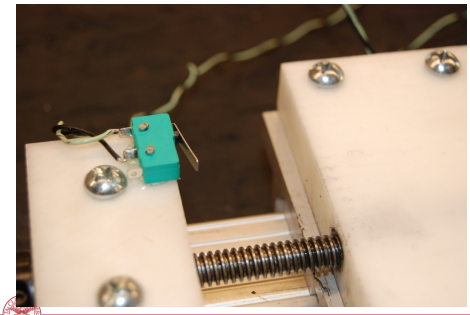

Appendix – CAD: mirror mounts

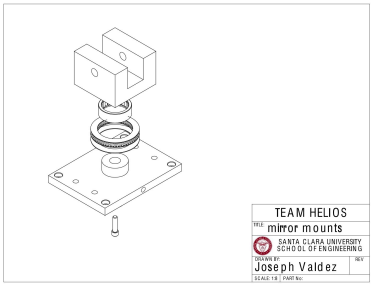

Appendix – Free Body Diagram

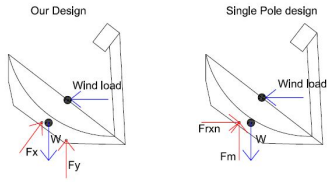

J.2 EPA P3 Conference Poster

Brighten Up Solar Energy

Enhanced Solar Thermal Energy Harvest for Power Generation from Brayton Cycle

Laughlin Barker, Hohyun Lee, Darcy Marumoto, Matthew Neber, Criselle Olaes & Joseph Valdez
Santa Clara University, California

Background, Problem Definition and Objective

Energy Consumption in the United States, 2010

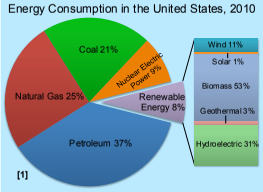

Energy Use in Homes, 2005

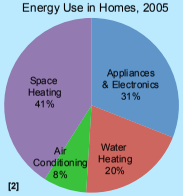

Combined heat and power (CHP) will supply the home with electricity and heat for space heating, cooling and water purification.

Current concentrated solar power receivers are expensive and contain too many parts. Also trackers, a necessary component of CSP systems, are expensive and need expensive supports to withstand wind loads. By designing an absorber integrated with a heat exchanger and a cheap low-profile tracker using two linear actuators, CSP can be an economical viable solution at the residential scale.

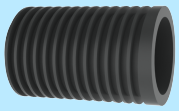

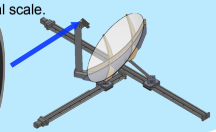

Data Findings, Outputs & Outcomes

Necessary Concentration for Efficiency

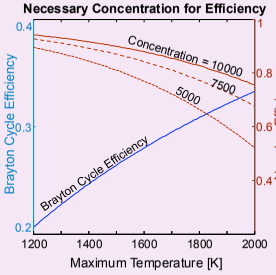

Smaller Dish Requires Higher Temperatures

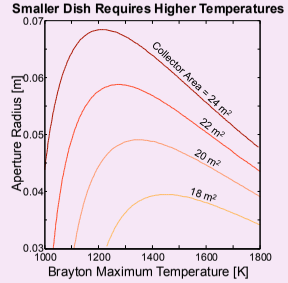

Tracking Range of Particular Geometry

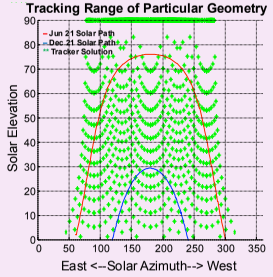

Blackbody Cavity Performance

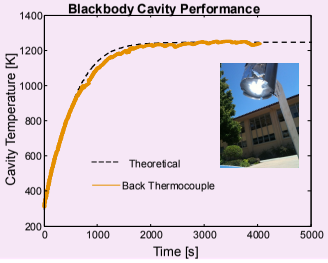

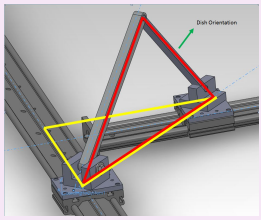

Discussion, Conclusion and Phase II Plan

-30,000 lb CO_2/yr [6]

As of 2009, the United States emits 17.9% [7] of the world's carbon dioxide output, second to China.

Operating Conditions of Receiver

Operating Temperature	1700 K
Temperature of Air	1500 K
Brayton Cycle Efficiency	26%
Exit Air Temperature	1100 K
Mass Flow Rate	10 g/s
Compression Ratio	7.6

$10K System
(10-30 yrs no maintenance)

Estimated energy consumption of a average for single family detached homes in a year is 31,769 kWh [8] ($3.685.20). The payoff of the system will be about 3 years. This involves tracker modifications and incorporating the receiver. A complete business plan through the five key areas listed to the right needs to analyze how to bring the product to the market in the next few years.

Integrate the Absorber with a Heat Exchanger

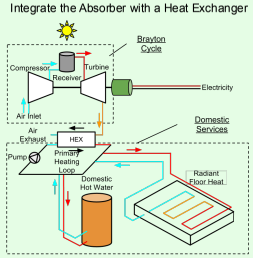

Key Areas for a Business Plan

References:
[1] http://205.254.135.7/totalenergy/data/annual/perspectives.cfm
[2] http://205.254.135.7/consumption/residential/reports/electronics.cfm
[3] http://www.arb.ca.gov/cosprod/geninfo/cpsmog.htm
[4] http://www.rgbstock.com/photo/mlLQWua/Summer
[5] http://www.seco.cpa.state.tx.us/publications/renewenergy/solarenergy.php
[6] EIA, "Carbon Dioxide Emissions from the Generation of Electric Power in the United States," D. o. Energy, Ed., ed, 2000.
[7] http://www.eia.gov/cfapps/ipdbproject/IEDIndex3.cfm?tid=90&pid=44&aid=8
[8] USA, "Table US14. Average Consumption by Energy End Uses," EIA, Ed., ed, 2005

For More Information: http://helios.engr.scu.edu/wordpress/

J.3 CSTS Poster Session

Low Profile Solar Tracker with Hybridized Control

Laughlin Barker, Darcy Marumoto, Criselle Olaes, Joseph Valdez and Hohuyn Lee
Mechanical Engineering, Santa Clara University, CA 95053

Motivation

- To counter rising energy prices, energy insecurity, and global climate change, we must embrace a green energy economy.
- Solar energy is the most abundant and capable renewable resource.
- Solar trackers can improve photovoltaic (PV) power generation by up to 40%
- While advantageous to PV systems, trackers are 100% necessary for Concentrating Solar Power (CSP) systems.

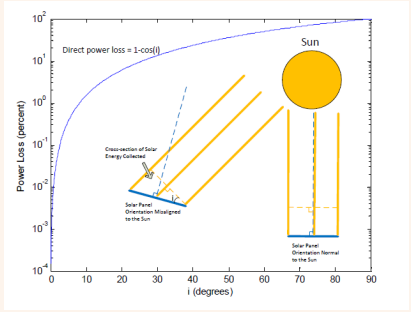

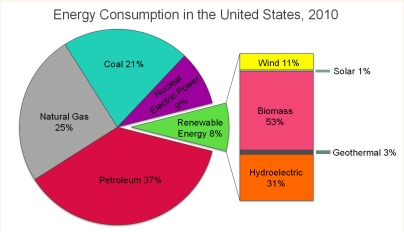

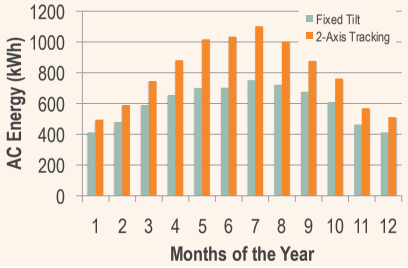

Technical Approach

- Unique "T" design allows normal orientation of panels/mirror to the Sun.
- Capable of following Sun throughout daily and annual trajectories.
- Design allows for inexpensive and off the shelf parts, reducing cost.
- Ability to store the tracker in a low-profile configuration reduces dangerous wind loads to protect the device.

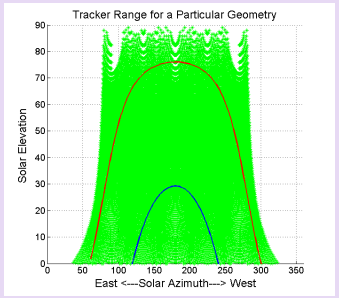

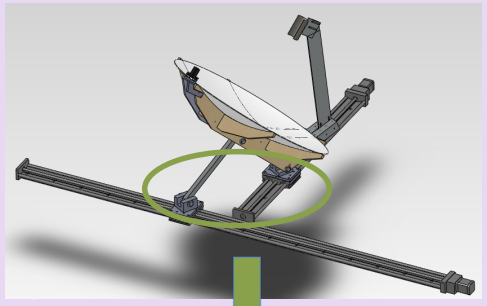

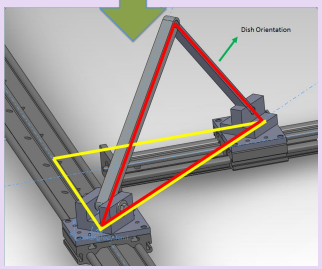

Design and Results

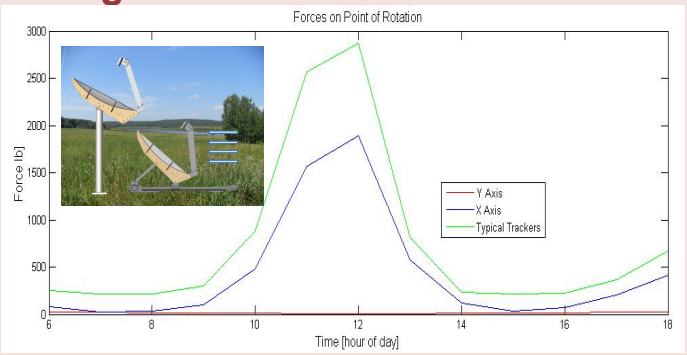

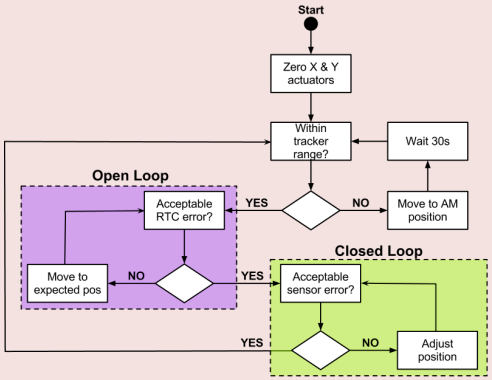

- Wind loads – calculated the maximum reaction force on both actuators and compared reaction force on the base of the single pole design.
- Mechanical hysteresis – preformed tests on the precision of the system.
- Hybridized control – performed tests on the control system's performance for correcting error
- Open loop – acceptable error of +/-7°.
- Closed loop: Engages when open loop has acceptable error. Adjustments made in 0.25° increments

Conclusion

- Patent application filed!
- Achieved low profile to reduce wind loading.
- Successful hybrid control strategy to improve accuracy and reduce installation costs.

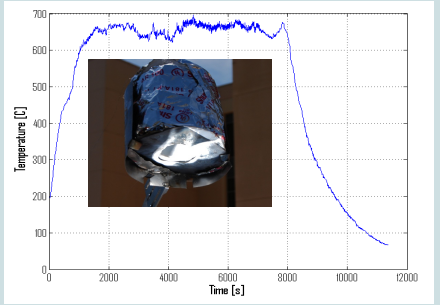

Acknowledgments: School of Engineering, Office of Undergraduate Research, Wilem and Maria Roelants Fellowship Center of Science, Technology and Society, & EPA P3 Program